NASA CR-159867

National Aeronautics and
Space Administration

ENGINE DIAGNOSTICS PROGRAM CF6-50 ENGINE PERFORMANCE DETERIORATION

by

Ray H. Wulf

General Electric Company
Aircraft Engine Business Group
Evendale, Ohio 45215

November 1980

Prepared For

National Aeronautics and Space Administration

NASA-20631

NASA-Lewis Research Center
21000 Brookpark Road
Cleveland, Ohio 44135

PREFACE

The work was performed by the General Electric Aircraft Engine Business Group located in Evendale, Ohio. The program was conducted by the National Aeronautics and Space Administration Lewis Research Center, Cleveland, Ohio, under Contract NAS3-20631, "CF6 Jet Engine Diagnostics Program." The NASA project engineers for this program are Robert Dengler and Charles Mehalic.

The requirements of NASA Policy Directive NPD 2220.4 (September 4, 1970) requiring the use of SI Units have been waived in accordance with the provisions of paragraph 5d of that Directive by the Director of Lewis Research Center.

TABLE OF CONTENTS

Section		Page
1.0	SUMMARY	1
2.0	INTRODUCTION	3
3.0	APPROACH	4
4.0	QUANTIFICATION OF DETERIORATION	6
	Performance Results	6
	Short-Term Deterioration	6
	Long-Term Deterioration	11
	Summary of Performance Studies	47
	Hardware Inspection Results	50
	Deteriorated Engine	52
	Refurbished Engine	118
	Summary - Performance Deterioration Models	124
	Initial Installation Engine	125
	Refurbished Engine	127
	Multiple-Build Engine	128
5.0	RECOMMENDATIONS	130
	Study Criteria	130
	Studies	131
6.0	CONCLUDING REMARKS	136
	APPENDICES	139
	APPENDIX A - Cruise Trending Procedure	140
	B - Cruise Performance Data	141
	C - List of References	170
	D - Symbols and Acronyms	171
	E - Special Terminology	177
	F - Quality Assurance Report	180
	DISTRIBUTION LIST	196

LIST OF ILLUSTRATIONS

Figure		Page
3-1.	Definition of Long-Term Deterioration.	5
4-1.	DC-10-30 Airplane Checkout Sequence for a Typical Initial Flight.	7
4-2.	Fuel Flow Deterioration - Initial Installation DC-10-30.	13
4-3.	EGT Deterioration - Initial Installation DC-10-30.	13
4-4.	Fuel Flow Deterioration - Initial Installation A300-B.	14
4-5.	EGT Deterioration - Initial Installation A300-B.	14
4-6.	Fuel Flow Deterioration - Initial Installation B747.	15
4-7.	EGT Deterioration - Initial Installation B747.	15
4-8.	Fuel Flow Deterioration - Initial Installation DC-10-30.	16
4-9.	EGT Deterioration - Initial Installation DC-10-30.	16
4-10.	Fuel Flow Deterioration - Initial Installation A300-B.	17
4-11.	EGT Deterioration - Initial Installation A300-B.	17
4-12.	Fuel Flow Deterioration - Initial Installation B747.	18
4-13.	EGT Deterioration - Initial Installation B747.	18
4-14.	Test Cell Data - Typical Engines (Hours).	23
4-15.	Test Cell Data - Typical Engines (Cycles).	23
4-16.	Test Cell Data - Nontypical Refurbished Engines (Hours).	25
4-17.	Test Cell Data - Nontypical Refurbished Engines (Cycles).	25
4-18.	Distribution for Multiple-Build Engines.	27
4-19.	Multiple-Build Engine Deterioration - Hours.	29
4-20.	Multiple-Build Engine Deterioration - Cycles.	30

LIST OF ILLUSTRATIONS (Continued)

Figure		Page
4-21.	Composite/Multiple-Build Deterioration Characteristics Vs. Time and Cycles.	31
4-22.	Comparison of Multiple-Build Engine Deterioration Rates (DC-10-30) - Hours.	34
4-23.	Comparison of Multiple-Build Engine Deterioration Rates (A300-B) - Hours.	35
4-24.	Comparison of Multiple-Build Engine Deterioration Rates (B747) - Hours.	36
4-25.	Comparison of Multiple-Build Engine Deterioration Rates (DC-10-30) - Cycles.	37
4-26.	Comparison of Multiple-Build Engine Deterioration Rates (B747) - Cycles.	38
4-27.	Effect of Flight Length on Deterioration at Removal.	43
4-28.	Effect of Flight Length on Time to Removal.	43
4-29.	Flight Length Vs. Cycles Times Hours at Removal.	44
4-30.	EGT Deterioration for Flight Length/Derate.	45
4-31.	Fuel Flow Deterioration for Flight Length/Derate.	45
4-32.	EGT Deterioration for Flight Length and Derate.	46
4-33.	Fuel Flow Deterioration for Flight Length and Derate.	46
4-34.	Typical Deterioration for DC-10-30 Installation.	49
4-35.	Typical Deterioration for A300-B Installation.	49
4-36.	Typical Deterioration for B747 Installation.	49
4-37.	CF6-50 Deterioration Modes - Fan Section.	53
4-38.	Dial Gage Shown Measuring Fan Blade Tip Clearance Near Leading Edge of the Blade.	55

LIST OF ILLUSTRATIONS (Continued)

Figure		Page
4-39.	Epoxy Microballoon Fan Shroud Material Showing Typical Erosion Effects After Revenue Service.	56
4-40.	Epoxy Microballoon Fan Shroud Material with Open Cells After Repair.	56
4-41.	Fan Outlet Guide Vanes with Repaired Nylon Spacers.	58
4-42.	Erosion Pattern on Stage 1 Fan Blade.	59
4-43.	Fan Section - Estimated Deterioration Characteristics at 6000 Hours.	62
4-44.	CF6-50 Deterioration Modes - HP Compressor Section.	64
4-45.	CF6-50 Flowpath Coatings - HP Compressor Section.	65
4-46.	Examples of Spalled Coatings in HPC.	66
4-47.	Abradable Rub Coating Deterioration.	67
4-48.	Flange Growth/Casing Eccentricity.	69
4-49.	Effect of Casing Distortion.	70
4-50.	Casing Out of Roundness.	71
4-51.	Clearance Difference from Nominal Versus Stage - Short Vanes Result of Assembly Rework.	72
4-52.	Types of Deterioration Modes: Casing Out of Roundness and Hand Grinding of Blade Tips.	74
4-53.	HP Compressor Tip Clearance Increase After 4000 Hours.	75
4-54.	Example of Airfoil Tip Erosion.	77
4-55.	Degradation of Rotor Blade Surface Finish.	78
4-56.	Degradation of Stator Vane Surface Finish.	79
4-57.	Loose Blades and Vanes.	80
4-58.	Blade and Vane Dovetail Looseness (4000 Hours).	82

LIST OF ILLUSTRATIONS (Continued)

Figure		Page
4-59.	Stage 5 VSV Bushing Life.	83
4-60.	HP Compressor Section - Estimated Deterioration Characteristics at 4000 Hours.	84
4-61.	CF6-50 Deterioration Modes - HP Turbine Section.	86
4-62.	HP Turbine Blade Tip Notches (Concave Side Only).	87
4-63.	Stage 1 Blade Δ Tip Clearance Versus Time.	88
4-64.	Stage 2 Blade Δ Tip Clearance Versus Time.	89
4-65.	Trend of Stage 1 HP Turbine Blade Tip Clearance.	90
4-66.	Trend in Changes of Stage 2 HP Turbine Tip Clearance.	91
4-67.	CF6-50C HPT Stage 1 Shroud Distortion at 10 Seconds into a Takeoff Transient.	93
4-68.	CF6-50C HPT Stage 1 Shroud Distortion at 80 Seconds into a Takeoff Transient.	94
4-69.	CF6-50C HPT Stage 1 Shroud Distortion at 120 Seconds into a Takeoff Transient.	95
4-70.	CF6-50C HPT Stage 1 Shroud Distortion at Steady-State Takeoff.	96
4-71.	CF6-50C HPT Shroud Distortion at Steady-State Cruise.	97
4-72.	CF6-50C HPT Stage 1 Shroud Rub Histogram.	98
4-73.	CF6-50C HPT Stage 2 Shroud Rub Histogram.	99
4-74.	HPT Stage 1 Blade Tip Clearances During Transient Operation.	100
4-75.	CF6-50 HPT Airfoil Surface Finish Range.	102
4-76.	HPT Vane Surface Roughness Average.	104
4-77.	HPT Blade Surface Roughness Average.	105
4-78.	Stage 1 HPT Nozzle Distortion - HPT Internal Leakage.	106

LIST OF ILLUSTRATIONS (Continued)

Figure		Page
4-79.	HP Turbine Section - Estimated Deterioration Characteristics.	107
4-80.	CF6-50 LP Turbine Section Deterioration Modes.	109
4-81.	Effect of LPT Blade Tip/Shroud Clearance on Efficiency at Cruise.	110
4-82.	Effect of LPT Interstage Seal Clearance on Efficiency at Cruise.	111
4-83.	Degradation of LP Turbine Vane Surface Finish (Convex Side).	113
4-84.	Degradation of LP Turbine Blade Surface Finish (Convex Side).	114
4-85.	LPT Vane Surface Finish - Efficiency Effects at Cruise.	115
4-86.	LPT Blade Surface Finish - Efficiency Effects at Cruise.	116
4-87.	LPT Section - Estimated Deterioration Characteristics at 6000 Hours.	117
4-88.	Initial Installation Engine at 4000 Hours.	126
4-89.	Unrestored Losses for Typical Engine.	127
4-90.	Multiple Build Engine at Removal.	129
5-1.	Cost Effective Factors.	132
B-1. Through B-28.	CF6-50 Cruise Trend Data.	142 Through 169
C-1.	Engine Assembly Build Up Record Card.	184
C-2.	Engine Assembly Configuration Record Card.	186
C-3.	Test Operating Requirements Document.	189
C-4.	Prep-to-Test and Test Check-Off Sheet.	191

LIST OF ILLUSTRATIONS (Concluded)

Figure		Page
C-5.	Instrumentation Check Sheet.	192
C-6.	Inspection Check List.	193
C-7.	Work Order Sample.	194
C-8.	HPTR Blade Inspection Sheet.	195

LIST OF TABLES

Table		Page
4-I.	Short-Term EGT Loss.	8
4-II.	Short-Term SFC Loss.	9
4-III.	Early Revenue Service EGT Loss.	10
4-IV.	EGT Margin Comparison.	10
4-V.	Initial Installation Long-Term Losses.	12
4-VI.	Initial Installation Deterioration Rates.	19
4-VII.	Inbound Test Cell Performance Data.	20
4-VIII.	Initial Installation - Long-Term Deterioration.	21
4-IX.	Unrestored Performance Loss.	24
4-X.	Composite CF6-50 Deterioration Rates.	32
4-XI.	Comparison of Deterioration Rates by Airlines.	39
4-XII.	Performance Deterioration at 2,000 Hours (Airline E).	40
4-XIII.	Performance Deterioration by Aircrft Types (Airline F).	41
4-XIV.	Estimated Deterioration in Fan Section After 6000 Hours.	62
4-XV.	Casing Out of Roundness.	73
4-XVI.	HP Compressor Section - Estimated Deterioration at 4000 Hours.	84
4-XVII.	HP Turbine Section - Estimated Deterioration at 4000 Hours.	107
4-XVIII.	LP Turbine Section - Estimated Deterioration at 4000 Hours.	117
4-XIX.	Average Refurbished Fan Module.	119
4-XX.	Average Refurbished HP Compressor Module.	120

LIST OF TABLES (Concluded)

Table		Page
4-XXI.	Average Refurbished HPT Module.	121
4-XXII.	Average Refurbished LPT Module.	12
4-XXIII.	Average Refurbished Engine Module.	123
5-I.	Cost Reduction Studies.	133
5-II.	Cost Effective Study Results.	135

1.0 SUMMARY

A program was initiated with the General Electric Company to conduct performance deterioration studies for the CF6-50 high bypass turbofan engine. The basic objectives were to determine the specific causes of deterioration which result in increased fuel consumption (performance loss), and to identify potential ways for minimizing or eliminating these effects. Normal flight recordings and test cell performance data were analyzed, as well as data from hardware inspections at airline overhaul shops, in order to define the extent and magnitude of engine deterioration.

These studies indicated that the rates of deterioration differed markedly between that of operation during aircraft checkout procedures (short term) and revenue service (long term). The short-term losses occurred rapidly, whereas the long-term losses exhibited a gradual rate. The level of short-term losses was determined to be equivalent to 0.7 percent in cruise fuel burn (cruise sfc) for all three aircraft types (DC-10-30, A300-B, and B747) currently powered by CF6-50 engines. An assessment of performance deterioration with respect to individual modules was not possible for the short-term aspect, since hardware inspections are not conducted following the checkout flights.

Because operational conditions vary, and since the airlines practice an "on-condition" engine maintenance concept, the average period of revenue service for an engine's initial installation varies somewhat with respect to individual aircraft type. The average long-term performance deterioration occurring from the time of an engine's first revenue service flight until it is returned to a maintenance facility for refurbishment is presented below for each of the three aircraft types.

Aircraft Type	Hours	Δ Cruise SFC, %
DC-10-30	30[illegible]	1.5
A300-B	[illegible]	1.1
B747	[illegible]	1.6

The values listed are in addition to the prior 0.7 percent Δ sfc deterioration that occurs during aircraft acceptance checkout flights.

Engines returned for repair are subsequently reassembled from the airlines' supply of available serviceable modules which are acceptable for operation, but may have varying degrees of unrestored performance. The unrestored performance losses for the average airline refurbished engine when reinstalled for additional revenue service operation has been found to be equivalent to a cruise fuel burn of 1.8 percent. Exclusive of the unrestored performance losses existing following refurbishment, the amount of long-term performance deterioration occurring during typical revenue service periods for engines having multiple installations and refurbishments is presented below for the three aircraft types.

Aircraft Type	Revenue Service Period, Hours	Δ Cruise SFC, %
DC-10-30	3030	0.8
A300-B	2000	0.7
B747	3850	0.9

Based on estimated labor and fuel costs at the end of 1979, it was determined from studies that it is potentially cost effective to restore 71 percent of the unrestored losses noted for the average refurbished engine. For 1980, this represents a potential reduction in fuel consumption of 26 million gallons and savings to the airlines of 16.6 million dollars based on projected flight hours for all CF6-50 model engines.

The potential for making a notable impact toward energy conservation in the 1980's has been demonstrated.

2.0 INTRODUCTION

A program was initiated for the CF6 family of turbofan engines to identify and quantify the causes of performance deterioration which increase fuel consumption. The recent energy demand has outpaced domestic fuel supplies creating an increased United States dependence on foreign oil. This increased dependence was accentuated by the OPEC embargo in the winter of 1973-1974 which triggered a rapid rise in the price of fuel. This price rise, along with the potential for further increases, brought about a set of changing economic circumstances with regard to the use of energy. These events were felt in all sectors of the transportation industry. As a result, the Government with the support of the aviation industry, initiated programs aimed at both the supply and demand aspects of the problem. The supply aspect is being investigated by determining the fuel availability from new sources such as coal and oil shale, with concurrent programs in progress to develop engine combustors and fuel systems to accept these broader based fuels.

Reduced fuel consumption is the approach being employed to deal with the demand aspect of the problem. Accordingly, NASA is sponsoring the Aircraft Energy Efficiency (ACEE) program which is directed toward reducing fuel consumption for commercial air transports. The long-range effort to reduce fuel consumption is expected to evolve new technology which will permit development of a more energy efficient turbofan, or an improved propulsion cycle such as that for turboprops. Studies have indicated large reductions in fuel usage are possible (e.g., 15 to 40 percent); from this approach, however, a significant impact in fuel usage is considered to be 15 or more years away. In the near term, the only practical propulsion approach is to improve the fuel efficiency of current engines since these engines will continue to be the significant fuel users for the next 15 to 20 years.

The Engine Component Improvement (ECI) program is the element of the ACEE program directed at improving the fuel efficiency of current engines. The ECI program consists of two parts: (1) Performance Improvement and (2) Engine Diagnostics. The Performance Improvement program is directed at developing engine performance improvement and retention concepts for new production and retrofit engines. The Engine Diagnostics effort is to provide information related to determining the sources and magnitudes of performance deterioration for the high bypass ratio turbofan engines utilized on wide-body aircraft.

As part of the Engine Diagnostics effort, NASA-Lewis initiated a program with the General Electric Company to conduct performance deterioration studies for the CF6-6D and CF6-50 model engine. The basic objectives of the program were (1) to determine the specific causes for engine deterioration which increase fuel burn, (2) to isolate short-term losses from the longer term losses and, (3) to identify potential ways to minimize the deterioration effects. This report covers the investigation of the CF6-50 engine model; a prior report (Reference 1) summarizes the findings for the CF6-6D model engine.

3.0 APPROACH

Figure 3-1 provides a graphical representation of performance deterioration for a typical engine's life cycle. It indicates the major elements of performance deterioration and also introduces terminology that will be used throughout this report. As illustrated, deterioration can be conveniently divided into two main categories: that which occurs in the short-term, and that which occurs over the long-term. The short-term losses are indicated by a rapid rate of deterioration as illustrated by the vertical line in the figure. These losses occur at the aircraft manufacturer's facility during the airplane flight acceptance checkout which is prior to any revenue service operation. The long-term losses occur only during revenue service operation and are indicated by the more gradual rate of deterioration. Three major elements of long-term deterioration are classified as Initial Installation (first period of revenue service and prior to any refurbishment), Unrestored Performance (losses remaining after typical refurbishment), and Multiple Installation also called Multiple Build (revenue service periods subsequent to Initial Installation).

The basic approach employed for the CF6-50 diagnostics efforts was to accumulate sufficient performance and hardware inspection data to establish performance deterioration trends for the entire life cycle of the engine. Performance data were obtained from test cell recordings at the General Electric Company's and airlines' facilities, from aircraft manufacturers' acceptance flights, and from cockpit cruise recordings for revenue service operation of several airlines. Hardware data were obtained from airline and General Electric records, and these were supplemented with on-site inspection of hardware conditions at specific airline facilities. The performance data were used to establish the magnitude and characteristic trend of deterioration. An evaluation with respect to operational variables such as user airline, aircraft type, and amount of takeoff derate was also conducted for the long-term performance deterioration data. The hardware inspection data were used to isolate the deterioration mechanisms and then this information was used in conjunction with previously derived influence coefficients to assign a magnitude of loss to each mechanism. Comparison of an overall loss assessed independently from both hardware and performance data was then made to determine the validity of the results.

Based on the results emanating from the analysis of all data, a cost effectiveness feasibility study aimed at eliminating or minimizing the effects of the deterioration mechanisms identified was then conducted. The recommendations generated from this study are also presented herein.

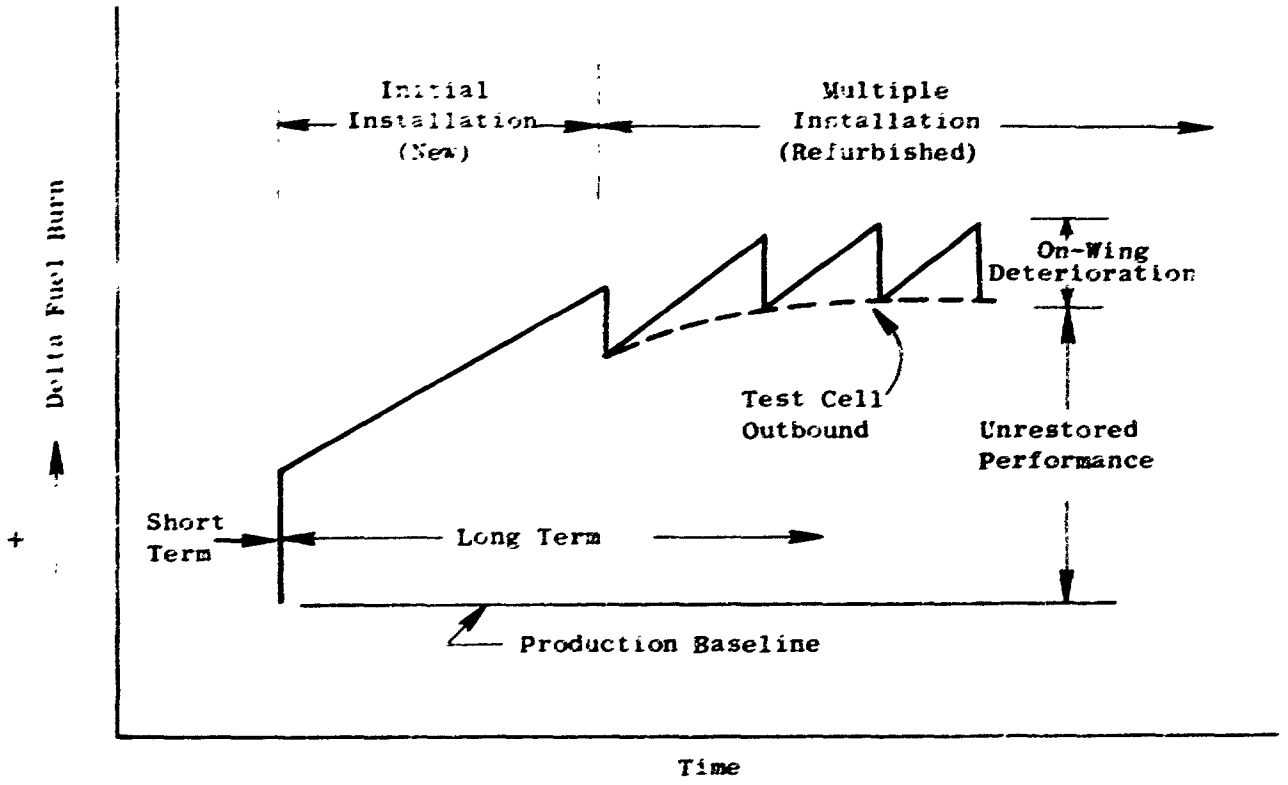

Figure 3-1. Definition of Long-Term Deterioration.

4.0 QUANTIFICATION OF DETERIORATION

This section presents the major results from the studies conducted for the purpose of identifying the magnitude and characteristic trend of performance deterioration for the life cycle of the engine.

PERFORMANCE RESULTS

The performance studies were designed to permit the determination of the magnitude of short-term losses, and to isolate the long-term losses into classifications which were similar to the divisions used to define the life cycle of the engine (Figure 3-1). These classifications include the on-wing loss for the initial installation of the production new engine, the unrestored losses remaining after a shop visit based on test cell calibrations, and the subsequent on-wing losses after engine re-installation (termed multiple-build loss). The results from the analyses of performance data are presented for each classification in the following sections of this report.

Short-Term Deterioration

An objective of the CF6-50 deterioration studies was to define the magnitude and sources for the short-term losses. While hardware data required to assign the losses to the individual damage mechanisms or sources were not available, sufficient performance data were available to define the magnitude of the loss for this aspect of performance deterioration.

Short-term losses could conceivably include those accrued during the first few hundred hours of revenue service, as well as those losses which occur at the aircraft manufacturer during airplane acceptance checks prior to revenue service. However, General Electric has elected to identify short-term losses as only those losses which occur at the aircraft manufacturer. This decision was made initially during the studies completed as part of this program for the CF6-6D model engine. The CF6-6D results (Reference 2) indicated that this selection was the most appropriate; therefore, the same criterion was used for these studies.

The procedure used by the Douglas Aircraft Company for acceptance of the DC-10-30 aircraft is typical of that also employed by The Boeing Company and Airbus Industrie for the B747 and A300-B aircraft. After extensive ground tests, aircraft/engine overall performance and system operations are reviewed during the initial flight. The short-term loss is determined from steady state cruise performance measurements taken at high altitude during the initial flight. Additional flights are conducted, as required, for corrective actions and formal customer acceptance.

A representative DC-10-30 airplane checkout sequence for a typical initial flight during the acceptance flight program is presented schematically in Figure 4-1.

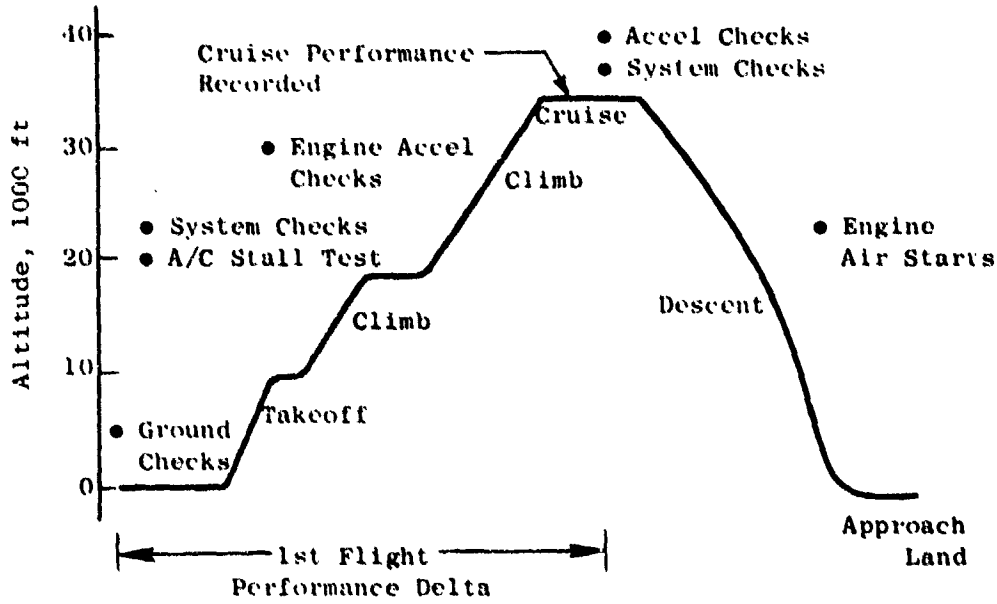

Figure 4-1. DC-10-30 Airplane Checkout Sequence for a Typical Initial Flight.

After normal takeoff and climb to medium altitude, a number of system checks are conducted, including an airplane stall check which produces large excursions in engine power. These checks are followed by a climb to high altitude, during which acceleration checks from flight idle to maximum climb power are conducted on each engine, one at a time. (These acceleration checks can result in "hot rotor reburst" which will be discussed later.) Performance data obtained at stabilized conditions to establish short-term deterioration are obtained upon reaching cruise altitude; actual altitudes differ for each aircraft type. Additional acceleration and system checks are then performed at cruise, and are followed by a shutdown and relight for each engine during aircraft descent. Approach operation during the initial flight generally includes several go-arounds, and the flight is terminated with a landing utilizing full reverser power.

Cockpit cruise performance data recorded during the first checkout flight of each aircraft included both stabilized engine parameters and airplane conditions. Significant engine performance parameters recorded during the cruise setting consisted of fuel flow (WFM), exhaust gas temperature (EGT), fan speed (N_1), and core speed (N_2), while airplane conditions included altitude, Mach number, and ambient temperature. In order to assess performance deterioration, it was necessary to compare these cruise measurements at altitude with the uninstalled, sea level static performance data baseline obtained during the engine production acceptance testing.

Prior efforts have produced a reliable procedure to correlate sea level static measurements of EGT with those obtained during cruise operation. The correlation procedure was based on engine cycle data supplemented with comparisons of EGT levels recorded during takeoff and cruise operation for a number of revenue service engines. The procedure permits the calculation of EGT margin from an equivalent certified maximum EGT level for cruise conditions. Since EGT margin can be obtained in the test cell, a direct comparison between the equivalent EGT margins produces the delta change. This procedure was developed because of the historic interest in EGT as an indicator of engine health; experience dictates that the procedure produces acceptable results.

On the other hand, comparisons of test cell fuel flow levels with those obtained during cruise have been characterized by large unexplainable variations, and a suitable adjustment procedure has not yet been developed. Experience has shown that cruise fuel flow levels have been useful primarily to trend delta changes with time; actual levels have been less consistent than EGT measurements. Several conditions are known to contribute to greater inconsistencies in fuel flow measurements as compared with those of EGT. First, small differences in exhaust nozzle area which occur between individual turbine reversers or fixed nozzles can produce large changes in fuel flow, but only small changes in EGT. Similarly, changes in thrust produce relatively large changes in fuel flow with smaller changes in EGT. In addition, fuel flow is not required to be monitored for safe operation, and need not be established to the same degree of accuracy as EGT.

Based on these considerations, the procedure used to establish short-term fuel burn deterioration was to determine the change in EGT margin from measured temperatures and; then, with the aid of computer cycle decks, engine derivatives and component models, to calculate the corresponding changes in fuel flows. This fuel flow calculation procedure has been previously substantiated with inbound test cell engines where deterioration in both EGT and fuel flow can be properly assessed.

Cruise performance data recorded during the initial checkout flight at the three aircraft manufacturers' facilities were analyzed for representative engines. These data describing the short-term EGT loss for the CF6-50 engine are summarized by aircraft type in Table 4-I.

Table 4-I. Short-Term EGT Loss.

Aircraft Type	No. of Engines	Δ EGT Margin (° C)	Standard Deviation (° C)
DC-10-30	51	9.8	± 9.5
A300-B	51	8.3	± 8.7
B747	7	6.5	± 4.6

Although there is considerable spread for the individual engines, the distribution is considered normal, and the standard deviations are very similar to the level measured for production new engines. The lower EGT loss measured for the B747 aircraft could conceivably be the result of less abusive testing during the airplane checkout. However, the small data sample size (seven engines) lowers confidence in the results, and a firm determination for the B747 aircraft requires additional study.

The short-term loss experienced on the 53 individual DC-10-30 engines was plotted versus production engine margin to determine if a correlation was evident. That analysis indicated that engines with better test cell margin did not tend to sustain a larger short-term loss, and a correlation or trend was not evident.

As discussed earlier, the measured loss in cruise EGT was used to predict the short-term fuel burn increase. Using the appropriate procedure and adjustment factors, the equivalent short-term cruise sfc losses (fuel burn) for the measured EGT losses are summarized in Table 4-II.

Table 4-II. Short-Term SFC Loss.

Aircraft Type	Δ EGT Margin (° C)	Δ Cruise SFC (%)
DC-10-30	9.8	0.78
A300-B	8.3	0.66
B747	6.5	0.52

The small sample size of data for the B747 warrants caution even though the change appears realistic compared with the other two aircraft types.

The airplane checkout typically consists of three to four different flights including a final acceptance flight prior to delivery. Available data from the aircraft manufacturers were reviewed to determine if additional losses occurred during subsequent flights. Unfortunately, very little data were available and it was not possible to make a thorough assessment. However, early revenue service data were reviewed for the three types of aircraft to make a cursory determination of the deterioration characteristics following the initial checkout flights. (Note: prior studies for the CF6-6D engine model indicated very little deterioration occurs after the initial checkout flight during at least the first several hundred hours of engine operation.)

The cruise data available from early revenue service operation are summarized in Table 4-III.

Table 4-III. Early Revenue Service EGT Loss.

Aircraft Type	No. of Engines	Time		Δ EGT Margin (° C)	Standard Deviation (° C)
		Hours	Cycles		
DC-10-30	16	200	60	10.8	± 8.9
A300-B	21	200	153	15.3	± 5.2
B747	20	340	65	14.8	± 8.1

Comparisons of these data with the short-term losses assessed from initia' checkout flights (Table 4-I) produced the changes in EGT margin as presented in Table 4-IV.

Table 4-IV. EGT Margin Comparison.

Aircraft Type	Short Term (° C)	Early Revenue (° C)	Difference (°C)
DC-10-30	9.8	10.8	1.0
A300-B	8.3	15.3	7.0
B747	6.5	14.8	8.3

These early revenue service data indicate very little change in the deterioration for the DC-10-30, a result which is in agreement with data obtained for CF6-6D engines installed on the DC-10-10 aircraft. The large change for the A300-B during early revenue service could be attributed to the high number of accumulated cycles (153), however, the EGT change is larger than expected based on the long-term studies which are discussed later. The change for the B747 aircraft is also larger than expected based on the long-term studies, but does confirm the belief that the small data sample size (seven engines) available to describe the short-term losses for the B747 aircraft may have produced inaccurate results.

Based on these studies, short-term deterioration for the CF6-50 engine is best summarized by the following statements:

- There is not a significant difference in short-term losses for the CF6-50 engine when utilized on the DC-10-30, A300-B, or B747 aircraft.
- The average short-term loss for the CF6-50 model engine is approximately 9° C loss in EGT margin and 0.7% increase in cruise fuel burn.

Long-Term Deterioration

Initial Installation - The performance deterioration characteristics for the initial installation of the engine is of primary concern to the engine manufacturer, since it is only during this period that an engine is tested with all new components. As such, the deterioration characteristics provide considerable insight into the durability capabilities of the engine, which identifies any need or needs for specific product improvements. On the other hand, since the initial installation engine represents only a small percentage of the entire fleet, these data are less meaningful to the airlines.

Two general types of performance data were utilized to determine the long-term deterioration characteristics for the production new engine. First cockpit cruise recordings obtained by the airlines during revenue service were accumulated and analyzed to produce deterioration trends. These cruise data which were generally obtained from in-house General Electric files are in various formats, but all are expressed in delta deviations. The baseline in all cases is the applicable aircraft manufacturer's flight manual which includes expected engine parameters for various flight conditions. The second source of available performance data was from a limited number of test cell recalibrations of deteriorated engines prior to refurbishment.

Cruise Trend Data:

There was a large quantity of revenue service cockpit recordings from which to statistically derive the magnitude and trends of cruise performance deterioration. The airlines currently use cruise data to derive monthly trends for the average of all engines in their fleets. While this procedure produces a statistical fuel burn trend for the fleet (information of major economic concern), it provides very little insight into the deterioration characteristics of the individual engines. Therefore, for the benefit of this program, the revenue service cruise data were analyzed by tracking the performance level from installation to removal for specific individual engines on a regular basis (monthly, or as regularly as feasible). This method not only permitted assessment of engine performance deterioration characteristics as required to satisfy program objectives, but also produced the necessary comparative data required to identify potential effects from operational variables. Because each engine was being trended on the same basis of Δ cruise sfc since installation (baseline earliest cruise data available), it was possible to group the individual trends to derive a statistical average by adjusting the initial starting points to a zero or common reference.

The airlines trend fuel flow and other cruise performance parameters at constant fan speed, not thrust. This provides a convenient and effective method for trending performance changes for condition monitoring purposes. However, the actual fuel burn increase (cruise sfc) caused by deterioration is different than actually measured by changes in fuel flow at fan speed based on cycle deck and other analytical models used to compare sea level with cruise operation. Therefore, it is necessary to calculate these changes in cruise

sfc, since installed thrust, required to calculate cruise sfc, cannot be measured in flight. Based on previous experiences using the mathematical model of a thermodynamic cycle for a deteriorated CF6-50 engine, the change in cruise sfc is equivalent to approximately 0.9 percent of the cruise fuel flow delta at constant fan speed. The cruise sfc levels discussed in this report were derived using this factor.

Cruise performance trend data were collected and analyzed for the initial installation of CF6-50 engines installed on the three different aircraft. Statistical curve fits of these data were studied using least-square polynomial curve fit techniques for polynomials to the third degree of the form:

$$Y = A_0 + A_1X + A_2X^2 + A_3X^3$$

Stepwise regression techniques were used to identify the "best fit" curves for the normalized data, and the resultant fits for all three aircraft types was linear for both hours and cycles. There is a wide spread in the individual data points; however, the confidence levels associated with the average trends are over 99 percent.

The fuel flow and EGT trends are summarized for a representative group of engines for the DC-10-30, A300-B, and B747 aircraft in Figures 4-2 through 4-13. These data are shown as a loss at constant fan speed and as a function of both accumulated hours (Time Since Installation - TSI) and cycles (Cycles Since Installation - CSI). The losses are represented by a linear rate with time as dictated by the best statistical fit of the data.

Data obtained from Figures 4-2 through 4-7, using the appropriate adjustment factors to obtain equivalent cruise sfc levels, produce the deterioration levels for the three different aircraft types as shown in Table 4-V.

Table 4-V. Initial Installation Long-Term Losses.

Aircraft Type	Hours/Cycles	Takeoff Δ EGT (° C)	Δ Cruise Fuel Flow (%)	Δ Cruise sfc (%)
DC-10-30	3,000/877	15	1.6	1.5
A300-B	2,000/1,334	14	1.2	1.1
B747	4,000/772	12	1.8	1.6

These data cover the period from initiation of revenue service and do not include the short-term losses which occurred during aircraft acceptance flights. The hours presented in this chart are considered representative times for the available data, and the hours-to-cycles relationships as shown are typical for the three aircraft types.

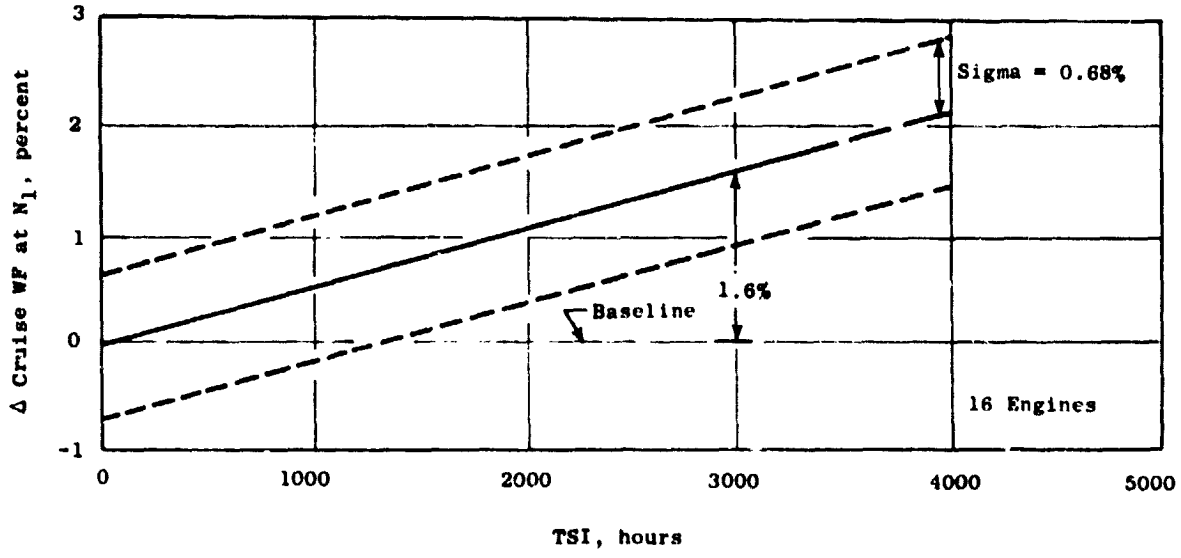

Figure 4-2. Fuel Flow Deterioration - Initial Installation DC-10-30.

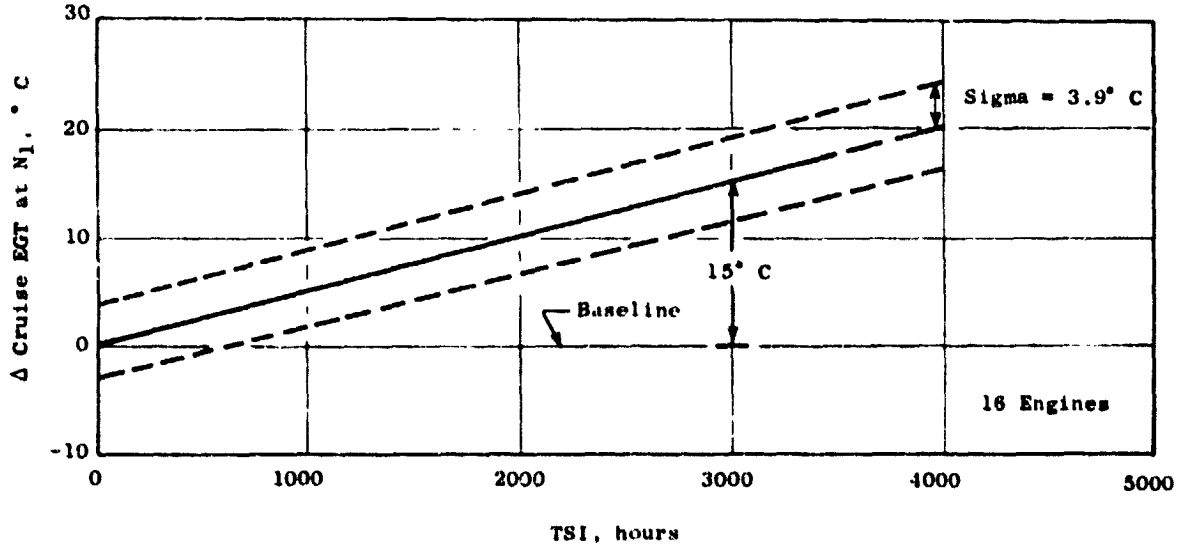

Figure 4-3. EGT Deterioration - Initial Installation DC-10-30.

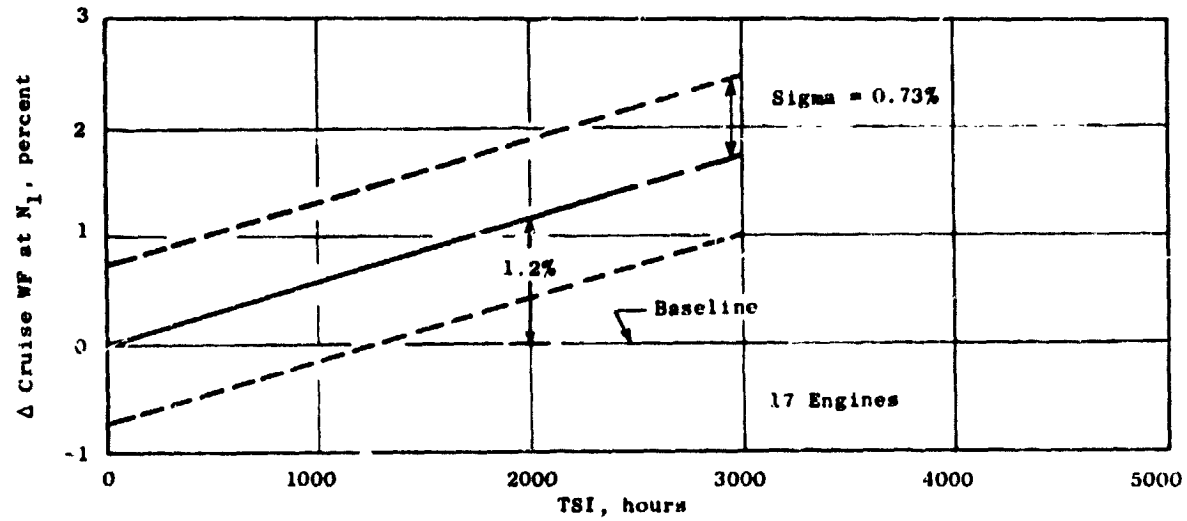

Figure 4-4. Fuel Flow Deterioration - Initial Installation A300B.

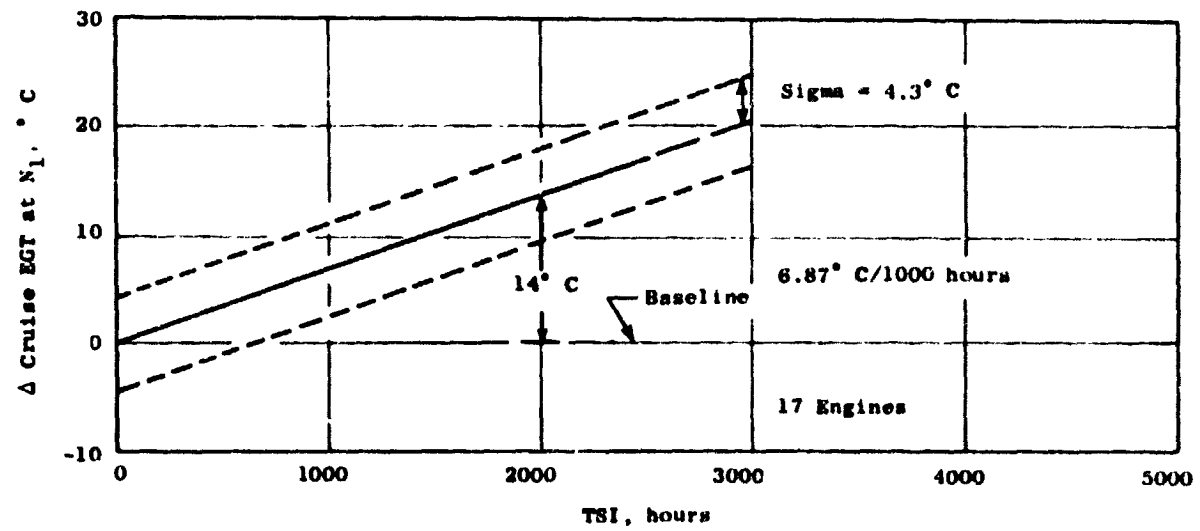

Figure 4-5. EGT Deterioration - Initial Installation A300B.

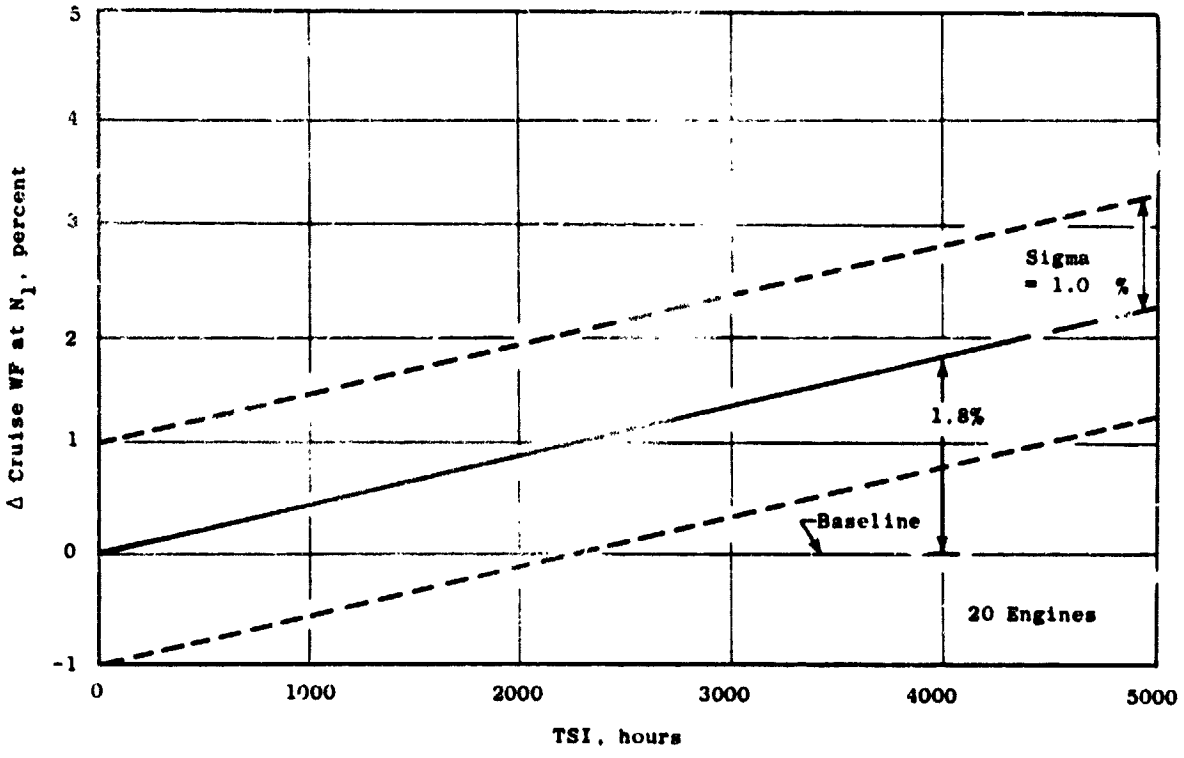

Figure 4-6. Fuel Flow Deterioration - Initial Installation B747.

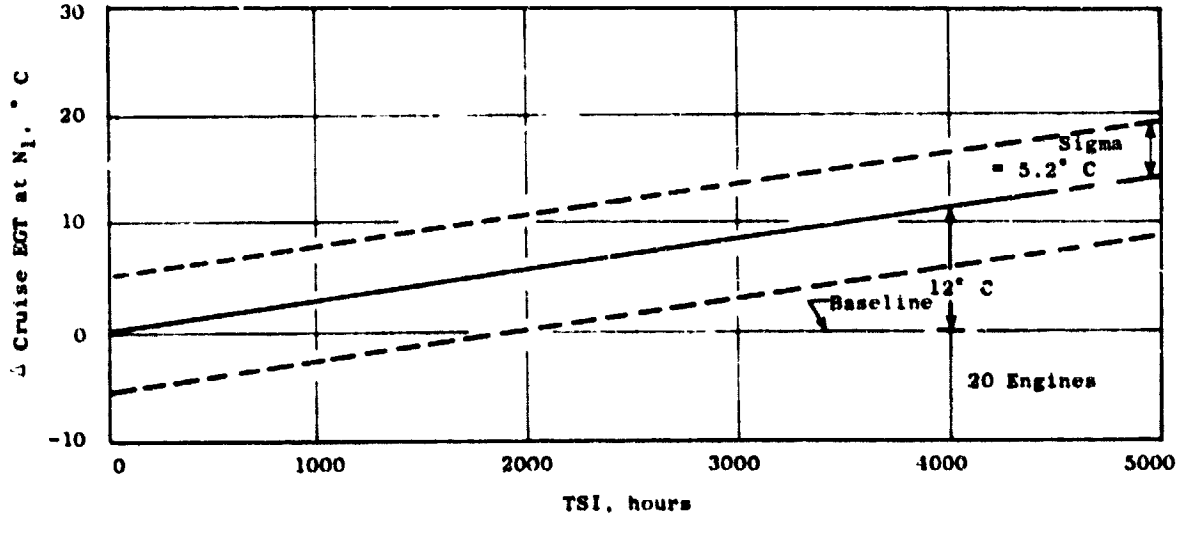

Figure 4-7. EGT Deterioration - Initial Installation B747.

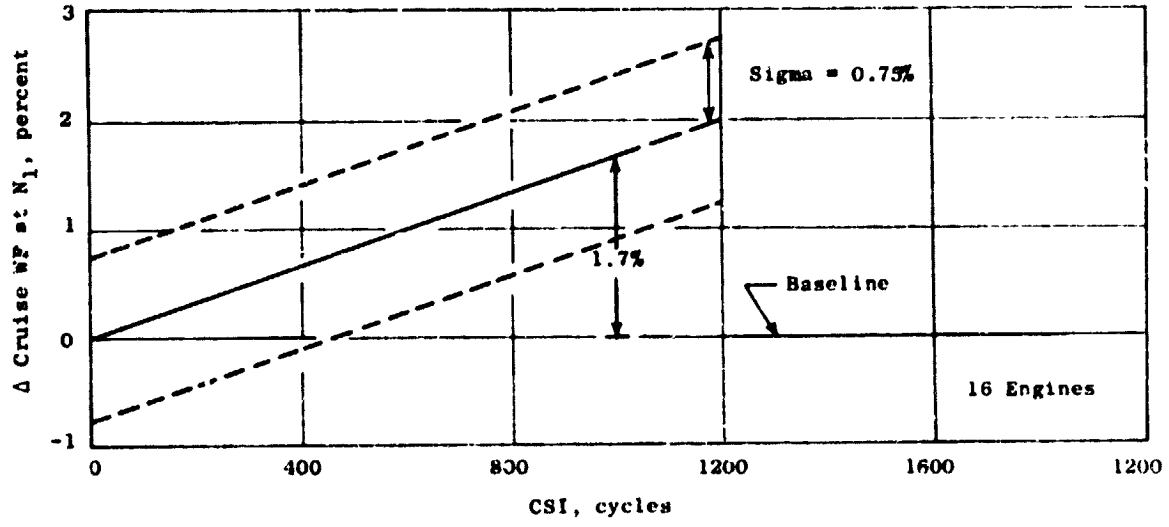

Figure 4-8. Fuel Flow Deterioration - Initial Installation DC-10-30.

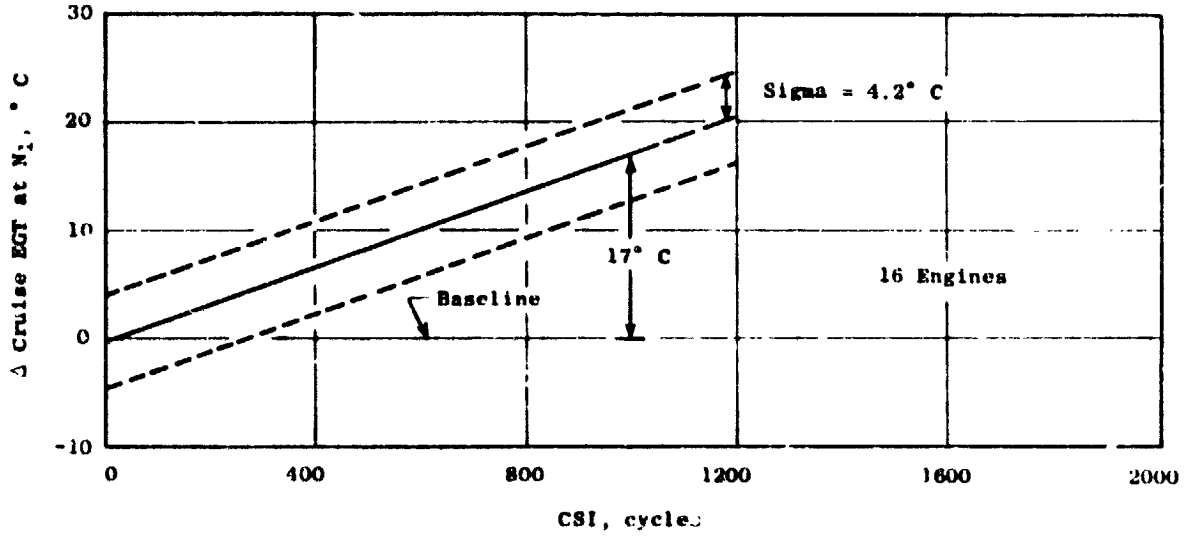

Figure 4-9. EGT Deterioration - Initial Installation DC-10-30.

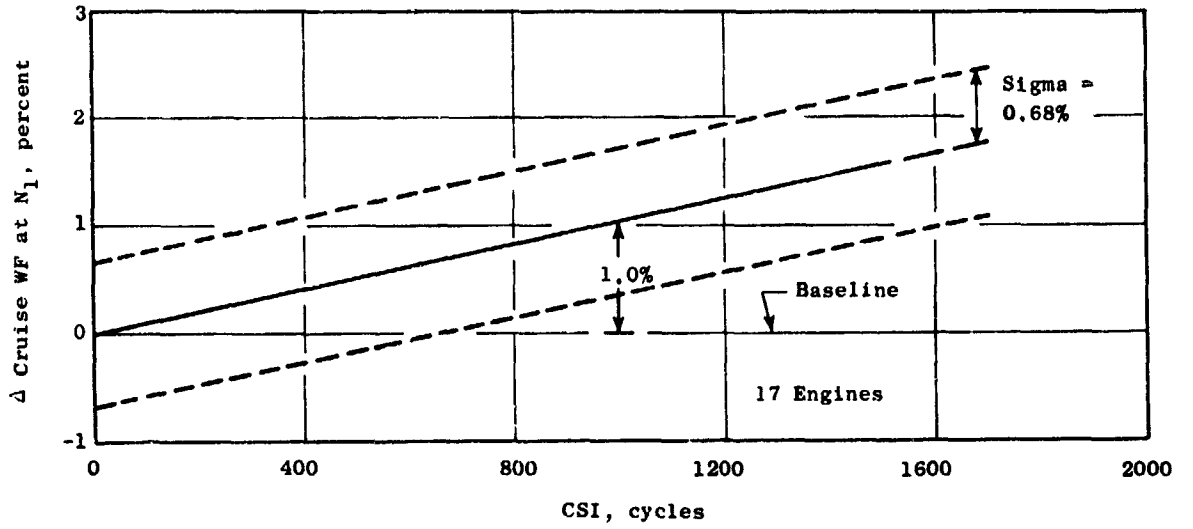

Figure 4-10. Fuel Flow Deterioration - Initial Installation A300-B.

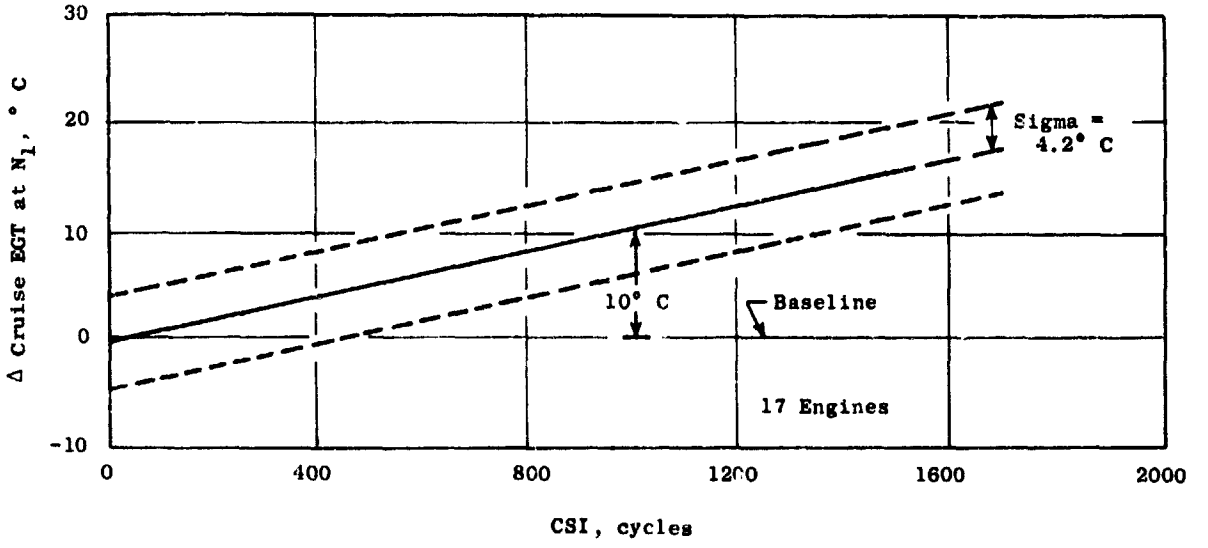

Figure 4-11. EGT Deterioration - Initial Installation A300-B.

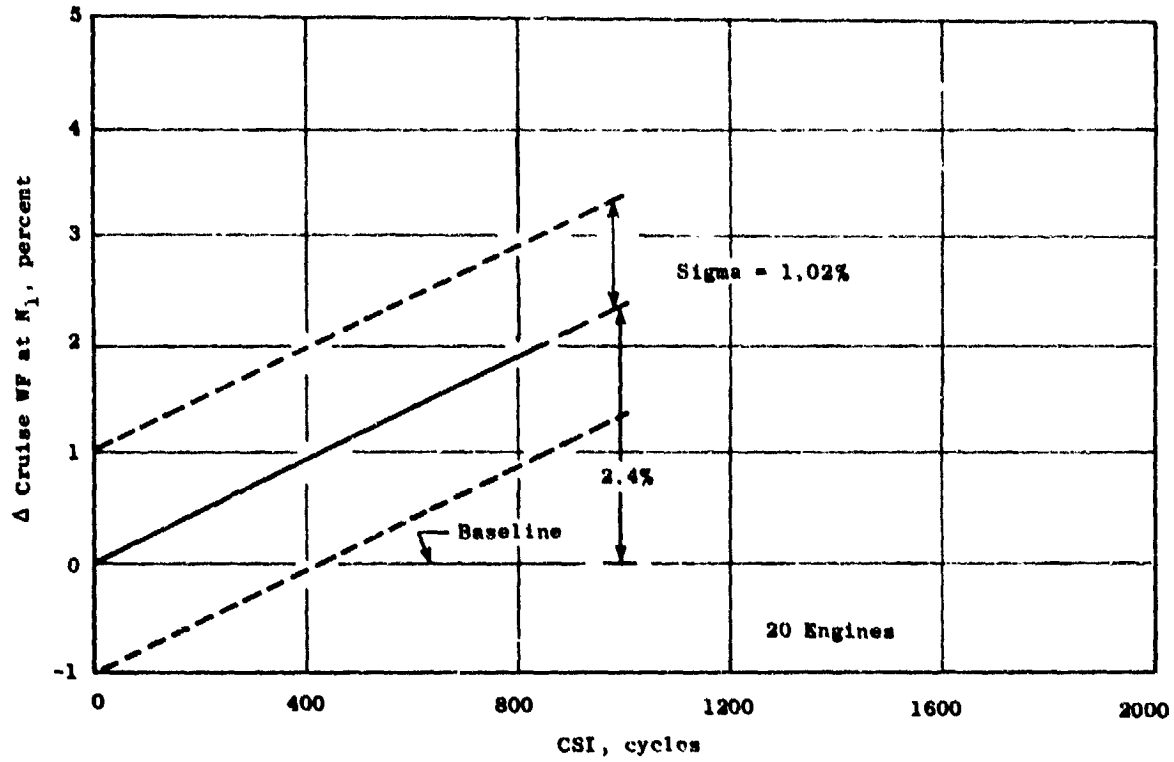

Figure 4-12. Fuel Flow Deterioration - Initial Installation B747.

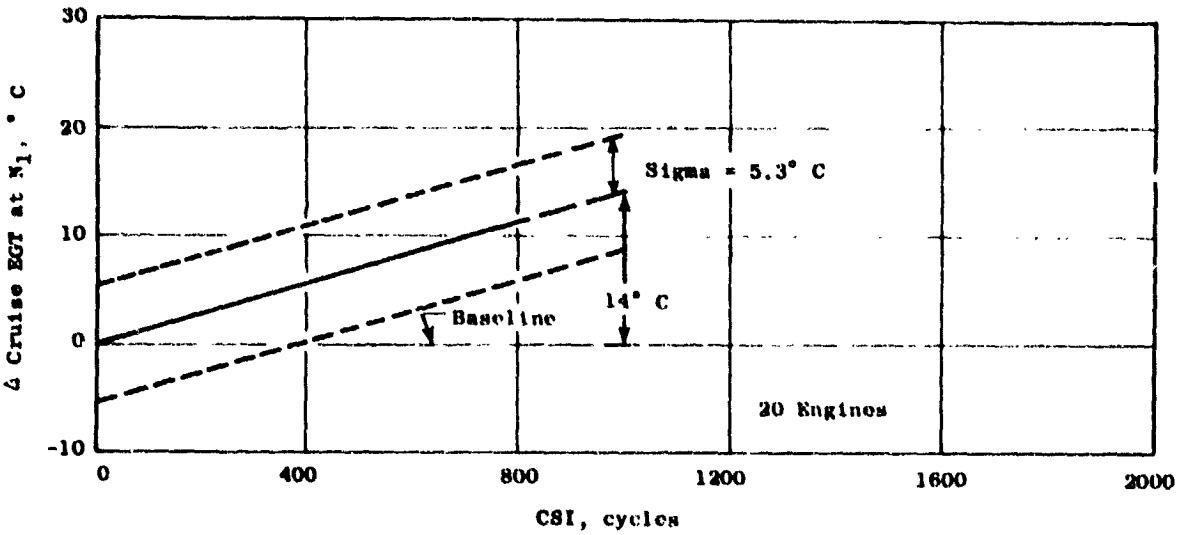

Figure 4-13. EGT Deterioration - Initial Installation B747.

Comparative deterioration rates for the CF6-50 engine installed on the three different aircraft types was established using the data presented in Figures 4-2 through 4-13. The losses in takeoff EGT margin and cruise sfc as a rate per 1,000 hours and per 1,000 cycles are presented in Table 4-VI.

Table 4-VI. Initial Installation Deterioracion Rates.

Aircraft Type	Hour/Cycle Ratio	Per 1000 Hours		Per 1000 Cycles	
		Δ EGT (° C)	Δ sfc (%)	Δ EGT (° C)	Δ sfc (%)
A300-B	1.50	7	0.55	10	1.0
DC-10-30	3.42	5	0.5	17	1.7
B747	5.18	3	0.4	14	2.4

These data indicate that the shorter flight length (Hour/Cycle) produced a higher deterioration rate for a given number of hours. On the other hand, the shorter flight length generally produces less deterioration for a given number of cycles. This is understandable, since the shorter flight length for a given number of cycles accumulates fewer hours; i.e., 1,000 A300-B cycles will accumulate 1,500 hours while the same number of cycles on the B747 aircraft will produce 5,180 hours. It is known and supported by these data that both hours and cycles have an effect on deterioration rate and, in the practical sense, the contribution from the individual sources cannot be properly isolated.

While the data presented in Table 4-VI generally support the aforementioned logic, some inconsistencies in the rates at "1,000 cycles" are evident. The sfc level recorded for the B747 aircraft appears higher than expected based on the EGT loss. This difference has been somewhat influenced by the data quality since its standard deviation is 1.02 percent compared with 0.68 and 0.75 percent for the other two samples. The EGT and sfc levels recorded for the DC-10-30 aircraft both appear high based on the comparative results presented at "1,000 hours." This same condition was observed for the multiple-build engines, and a detailed explanation including the most likely cause is presented in the discussion of multiple-build engines presented later in this report.

Performance at First Removal:

The second source of available performance data to describe the long-term deterioration characteristics for the initial installation engine was from a limited number of inbound tests of deteriorated engines prior to refurbishment. Test cell calibration runs of a deteriorated engine can be used to correlate the observed cruise losses with measured sea level losses at the time of removal. A direct measurement of sfc loss is available from the sea level inbound test cell run, which permits correlation with the cruise sfc loss (actual

fuel burn) calculated from cruise fuel flow trends. This is required since sfc is not directly measured during cruise operation because thrust measurements are not available. Test cell calibration data from inbound deteriorated engines are also used for the hardware studies to verify module performance assessments based on hardware inspection results.

Inbound test cell performance data obtained prior to engine refurbishment were available for three deteriorated engines. Each engine (two DC-10-30 and one B747) had accumulated over 4,000 hours of revenue service, and the average time at removal was 4,660 hours and 902 cycles. The significant test cell data for these deteriorated engines is presented in Table 4-VII.

Table 4-VII. Inbound Test Cell Performance Data.

Aircraft Type	Hours/Cycles	Δ EGT (° C)	Δ sfc Cruise (%)	Δ EGT/Δ sfc katio
DC-10-30	4,754/1,039	38	3.0	12.7
DC-10-30	4,758/917	34	1.0	34.0
B747	4,467/750	39	2.6	15.0

As shown, the Δ EGT increases for the three individual engines are consistent, but Δ sfc's show a large variance for the three individual engines. This large variance for individual engines is also typical for cruise performance data; this being the reason why a large data sample size is required to produce meaningful results. While the average loss of 2.2 percent in cruise fuel burn for the three engines compares well with an estimated 2.1 percent for the fleet (presented and discussed in the following paragraph), the data is only of limited use due to the small sample size.

The cruise sfc (fuel burn) deterioration established for the initial installation of a production new CF6-50 engine based on the foregoing studies is presented in Table 4-VIII.

Since the hours selected for the data presented in Table 4-VIII are compatible with fleet removal data, these results are considered representative for the fleet and are the best representation of the deterioration characteristics for the initial installation of the CF6-50 model engine.

Unrestored Performance Losses - A second major element of engine deterioration is unrestored loss, i.e., the performance loss remaining after a typical refurbishment by the airline as compared with the production new baseline.

Table 4-VIII. Initial Installation - Long-Term Deterioration.

Aircraft Type	Short Term (%)	Long Term (%)	Total at Removal* (%)	Hours at Removal
DC-10-30	0.7	1.5	2.2	3,000
A300-B	0.7	1.1	1.8	2,000
B747	0.7	1.6	2.3	4,000
* Short Term plus Long Term				

After an engine is rebuilt, its performance is measured in a test cell to assure the engine meets operational and performance requirements. This calibration test not only establishes the performance level for the refurbished engine, but also serves as the baseline for future on-wing deterioration determinations.

The policy for most of the 54 airlines who utilize the CF6-50 engine is to join a consortium where refurbishment of the various aircraft and engines is performed by one of the member airlines, generally termed the central agent. For purposes of this study, data from one of these central agents (one who provides the major overhaul/refurbishment for approximately 30 percent of the total fleet) was used for assessment of unrestored losses.

This specific airline was chosen as representative for a number of reasons. First, this shop routinely refurbishes 15 to 20 engines a month which is about four times greater than the next largest of the seven other central agents. Second, this shop, except for routine line maintenance repairs, performs all maintenance and repairs for all members of its consortium, whereas other consortiums permit extensive module replacement and some repair by its member airlines. The policy of permitting only minimum repairs by airlines other than the central agent not only contributes to a larger total of engines being refurbished each month by the central agent, but also yields more consistency in the individual modules since they are all processed by the same source. In addition, the test cell recalibrations are conducted with a fixed conical nozzle (slave test cell equipment), whereas other central agents utilize the turbine reverser exhaust system assigned for revenue service. The former practice produces more consistent test data and a better understanding of engine deterioration by eliminating any variation in exhaust nozzle area due to normal tolerances and/or deterioration of the turbine reverser.

The test cell performance results are generally available from a time-sharing computer network established between this airline and General Electric in Evendale, Ohio. Overall performance level trends can be derived from these data and compared with new engine levels as shipped from production. Sufficient instrumentation is not available to properly isolate the performance effects for the major components (high pressure compressor, high pressure

turbine, low pressure turbine, and fan), but a reasonable estimate can be generated to isolate the contribution from the core and low pressure systems.

All airline cells are correlated with the General Electric production test cell at Evendale and a cell factor has been derived for thrust adjustment. This is a Regulatory requirement, since secondary airflow for a given cell (cell pumping) does produce a significant effect on thrust and is dependent of the test cell size, inlet and discharge areas, and other considerations. These test cell considerations can also result in differences in other airline performance data with respect to that obtained in the production cell. While adjustment factors for parameters other than thrust are not required for airline trending purposes, accurate factors are required for comparison with the production new baseline. These factors were derived during a recent cell correlation for the representative airline, and the necessary adjustments have been included in all analyses.

A total of 224 tests of refurbished engines conducted during 1979 were analyzed to determine the representative performance levels. The average test cell performance level for CF6-50 refurbished engines which had been subjected to from one to twelve refurbishments, show no increasing or decreasing trends. Individual plots of sfc and EGT margin representing the averages of at least 20 individual engines are shown plotted against the averages of all engines in Figures 4-14 and 4-15. The data are plotted for both accumulated engine hours and accumulated engine cycles. These findings are in agreement with the results obtained for the CF6-6 engines in that the unrestored performance levels are essentially the same after refurbishment irrespective of how many shop visits to which the engine has been subjected, once it has seen at least two shop visits. (There were not enough data to be confident concerning the first shop visit.) This means the average amount of restored performance was coincidentally equivalent to the average loss during the previous installation. It must be recognized, however, that these results were based on averaging a large number of engines in the fleet which indicated considerable variance for the individual engines in both the amount unrestored during a shop visit and that lost during service operation.

When engines are returned to the shop for repair, they are normally separated into the component modules which are then dispersed to separate repair stations. The modules lose their engine identity; rarely are the same modules reassembled into the same engine after repair. The use of the individual modules is random, thus eliminating the tendency for the shorter time engines with fewer rebuilds and less accumulated time to be significantly different than the longer time engines. The engine modules are also not separated by "aircraft installation" during repairs since all engine parts, except for several controls and accessories items, are identical among the model designations used on the three different aircraft.

Since no trend was evident based on accumulated engine time, the average unrestored overall performance level is best represented by determining the mean levels from the available data. The average overall unrestored levels, relative to average performance of new engines as included in Figures 4-14 and 4-15, are tabulated in Table 4-IX.

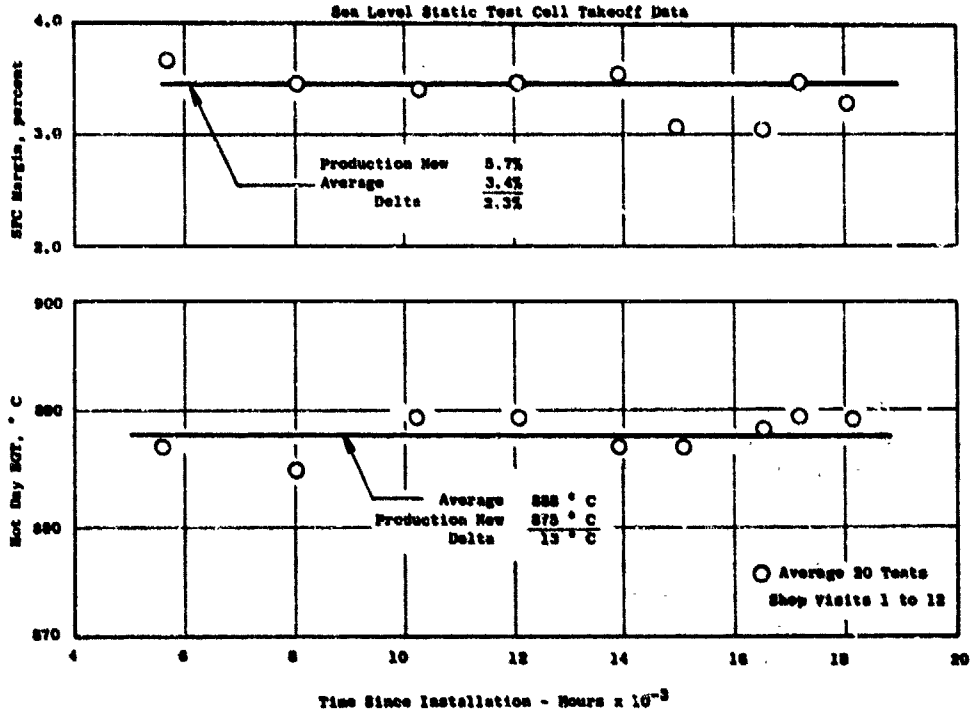

Figure 4-14. Test Cell Data - Typical Engines - (Hours)

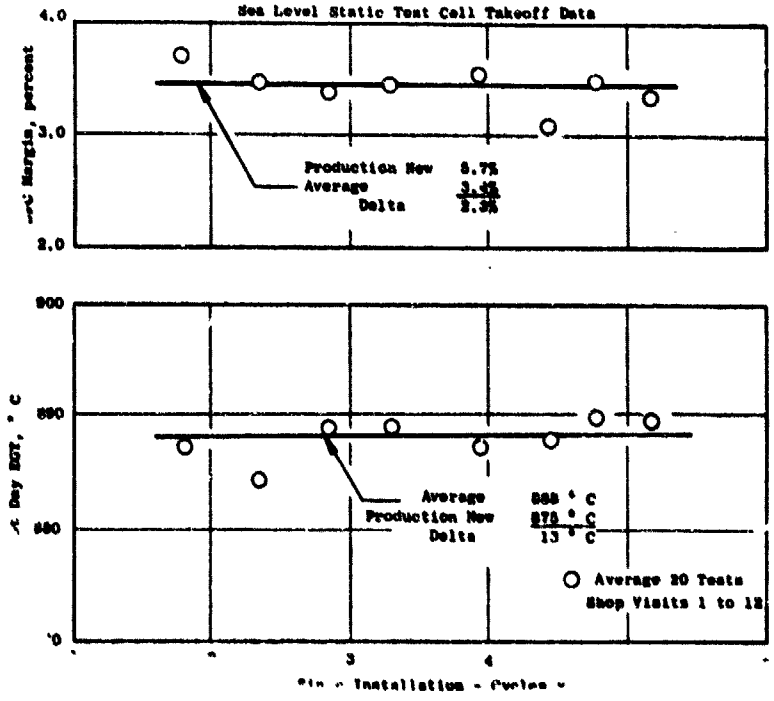

Figure 4-15. Test Cell Data - Typical Engines - (Cycles).

Table 4-IX. Unrestored Performance Loss.

	SLS Takeoff	Cruise Equivalent
Δ sfc (%)	2.3	1.8
Δ EGT (° C)	13.0	---

The cruise equivalent sfc was derived using the thermodynamic cycles and other factors previously discussed. Since the engine hardware is not separated by engine type (aircraft installation) and the engine modules are completely intermixed among engines during repairs, these data are considered representative of the unrestored losses for the CF6-50 model engine.

The outbound performance levels for the CF6-50 engines refurbished by five other repair sources were also examined as part of these studies. Analysis of that data, which included one engine that had completed 11 shop visits, also indicated that an increasing or decreasing trend with accumulated time was not evident. These data are shown in Figures 4-16 and 4-17 and are plotted for both accumulated hours (Time Since New) and cycles (Cycles Since New). Each data point presented in Figures 4-16 and 4-17 represents a single engine while each data point in Figures 4-14 and 4-15 represents the average of at least 20 engines - this being the reason for the indicated differences in the spread for the data points.

While this limited data did agree with the previous finding that unrestored losses are relatively constant for each shop visit, the mean levels for these data do not agree well with the levels determined for the representative central overhaul agent. Compared with the average levels from Figures 4-14 through 4-17, the average for these limited engines was 0.4 percent poorer in sfc and was 12° C worse in EGT margin. Additional analysis of the data which spanned a 3-year time period indicated the majority of the data was from airlines who were not central agents, i.e., those that performed only limited replacement/repair of engine modules during a shop visit. Therefore, these engines are not representative of the typical refurbished engine, and the limited repairs during the shop visits are the probable cause for the poorer performance margins.

Multiple Installation (Multiple-Build) Engines - Cruise performance trend data were collected and examined for CF6-50 engines installed on the three different aircraft types to determine the deterioration characteristics for the multiple-build engine classification. The long-term deterioration characteristics were quantified separately for each aircraft type, and comparisons were conducted in an effort to better understand the contributions from the many variables.

The incremental cruise performance losses in EGT and fuel burn were derived from aircraft cockpit trend data relative to the earliest available measured cruise performance data point (explained more fully in Appendix A). Cruise

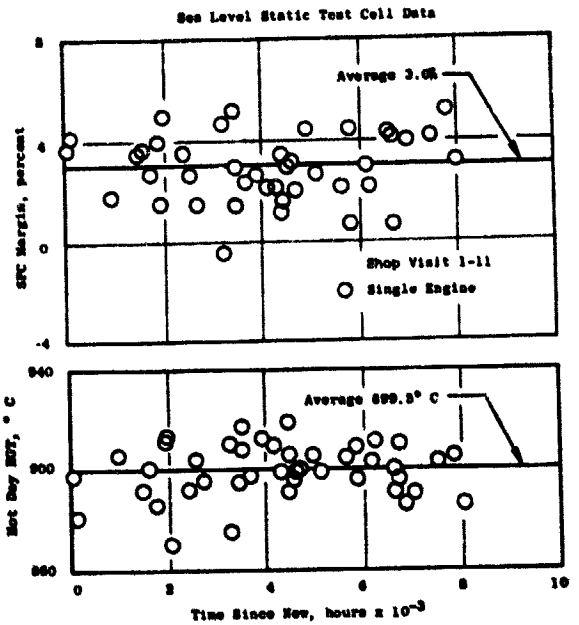

Figure 4-16. Test Cell Data - Nontypical Refurbished Engines (Hours).

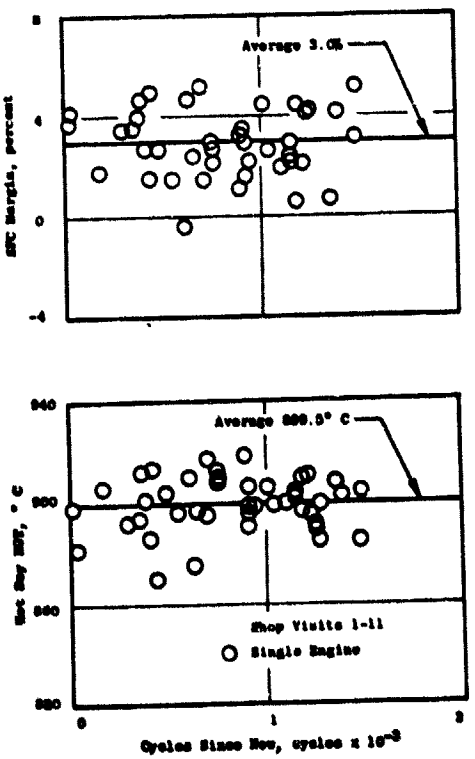

Figure 4-17. Test Cell Data - Nontypical Refurbished Engines (Cycles).

trend data in sufficient quantity and quality were available from five operators of DC-10-30 aircraft, and two operators each of the A300-B and B747 types. Data for several aircraft types were available from the same airline, and usable data from one operator were available for all three aircraft types.

During the investigation for performance deterioration of the CF6-6D model engine, it was decided to "screen" all available data. The basic question was whether to use all data regardless of time-on-wing, which includes infant mortality failures as well as better than average engines; or restrict the data base to some specific time-on-wing criteria. It was determined for those studies (Reference 1) that while the average of all engines provides the best statistical fleet average for costs or other airline considerations, the best method for this program was to restrict the data to eliminate those engines with nontypical time at removal (both better and worse). This is believed to represent the best approach for describing the long-term deterioration characteristics for the average engine; and the CF6-50 engine data base was restricted to produce a time-on-wing band as small as possible consistent with yielding an adequate sample size.

Examination of available records from DC-10-30 aircraft installations showed a range of engine time-on-wing up to 5,000 hours with most of the data in the 2,000- to 4,000-hour range. The mean time-on-wing for the fleet during this time period was 3,030 hours. The distribution of the installation duration for the performance data obtained as part of the long-term deterioration study is shown in the schematic in Figure 4-18. Engines outside the 2,000- to 4,000-hour category were considered not typical of long-term deterioration characteristics and were not used in the study.

Sufficient quantities of cruise trend data were available from only two airlines utilizing B747 aircraft. Removal records indicate the average time-on-wing for a multiple-build engine installed on a B747 aircraft was 3,850 hours. Figure 4-18 also shows the distribution of these data, and engines outside the 2,500- to 4,000-hour range were excluded from this study.

Similarly, sufficient data was available from two operators of A300-B aircraft for this study. The nominal on-wing time is 2,000 hours for multiple-build engines installed on this type aircraft. The distribution shown in the schematic presented in Figure 4-18 was the basis for excluding engines outside the 1,300- to 2,500-hour range.

Actual plots of all cruise trend data available for multiple build engines installed on the three aircraft are presented in Appendix B. The actual cruise trend plots for the engines selected for this program are presented in a separate section of Appendix B. Average values of cruise fuel flow (WFM) and EGT at constant speed (N_1) are presented as a function of time and cycles since overhaul (TSO and CSO).

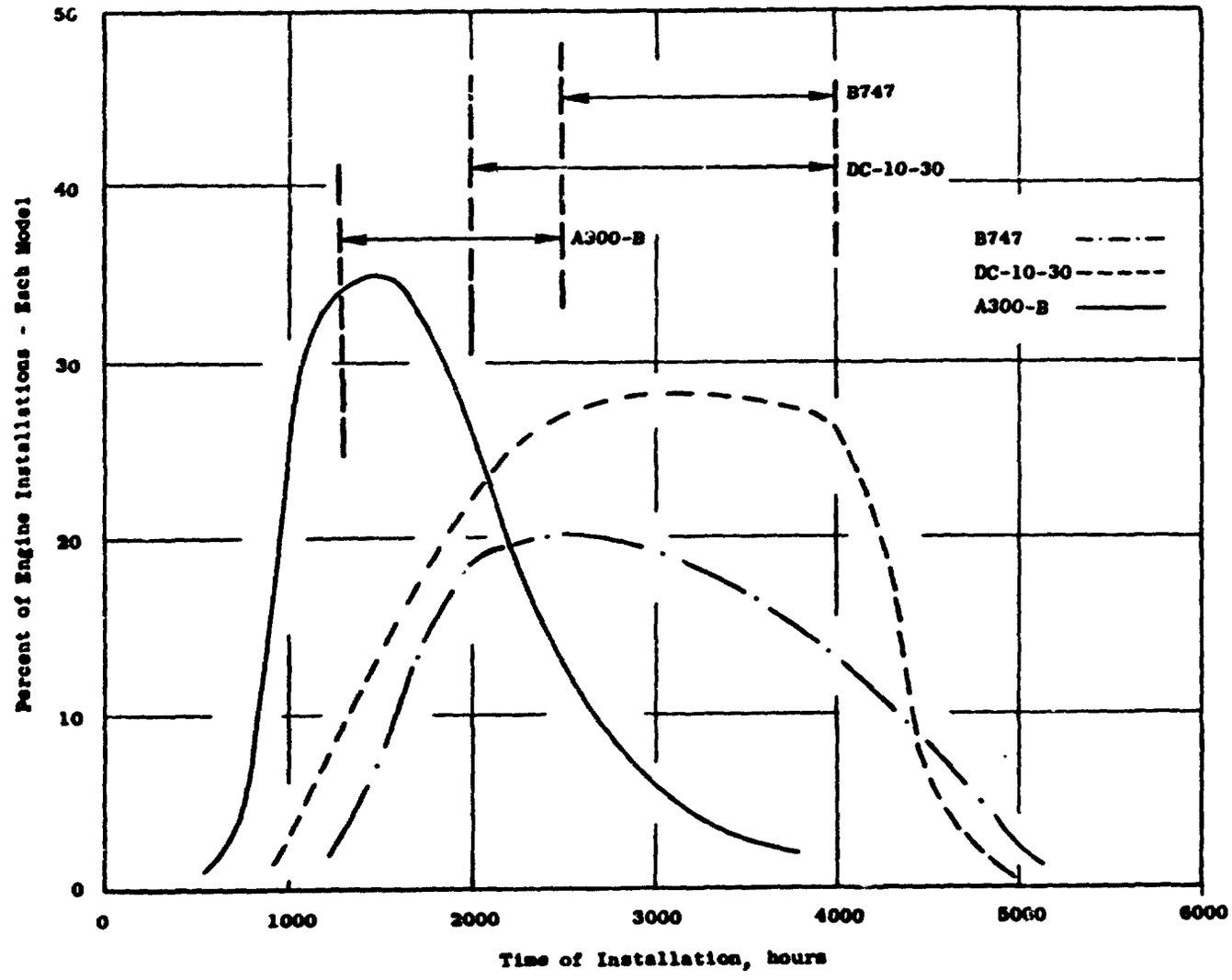

Figure 4-18. Distribution for Multiple-Build Engines.

Statistical curve fits of these data were generated using the least-square polynomial curve fit techniques for polynomials to the third degree of the form:

$$Y = A_0 + A_1X + A_2X^2 + A_3X^3$$

The cruise data had been obtained for individual engine installations and were normalized relative to the first data point for each installation. Stepwise regression techniques were used to identify "best fit" curves for the normalized data from multiple build installations. The resulting composite fits of multiple-build cruise trend data for all three aircraft types were linear with both TSO and CSO. The standard errors of estimate (SEE) (approximately equal to the standard deviation) are shown on each curve. Although there is a wide spread in the individual data points, the confidence levels associated with the average or composite trends are over 99 percent. Examination of alternate curve fits showed some higher order polynomials yielded nearly equal quantitative results. However, the shape of these curves does not appear to be characteristic of the shape of the individual engine deterioration curves and is believed to be caused by dilution of the sample by a higher proportion of lower time engines. Therefore, the linear curve fit was used for data unless otherwise specified.

Figures 4-19 and 4-20 present the cruise fuel burn deterioration trends for the CF6-50 engine as a function of hours and cycles for each aircraft type. The data base and data fit procedure previously described were used to produce a single curve and sigma variation (dashed lines) for each configuration. Note that the cruise fuel burn deterioration curves were generated from cruise fuel flow trend plots at constant fan speed by applying the proper adjustment factor to obtain equivalent cruise sfc. These data are considered most representative to describe the magnitude and trends of performance deterioration for the CF6-50 engines.

As presented in Figures 4-19 and 4-20, the total delta performance loss was generally the same for each aircraft type at nominal removal times (0.8 percent, 0.8 percent and 0.95 percent), but the actual deterioration rate (loss per unit time) was significantly different. Deterioration rates for each aircraft type with respect to accumulated hours and cycles are compared in Figure 4-21 and Table 4-X. Table 4-X shows the wide variance in deterioration rates at three selected intervals: nominal time-to-removal, 2,000 hours since refurbishment, and 700 cycles since refurbishment. The possible reasons for the observed differences are discussed in the following sections of this report.

Operational Variables - Cruise trend data were further examined to evaluate the influence of operational variables on engine deterioration rate. Variables that were expected to have an effect on the different deterioration rates noted for the three aircraft types include: user airline, average flight length, typical power derate at takeoff, aircraft type, installed position on aircraft, and airline maintenance (shop). In actual practice, these variables are combined to make it difficult to isolate the individual effects. Aircraft type and average flight length tend to be associated, as

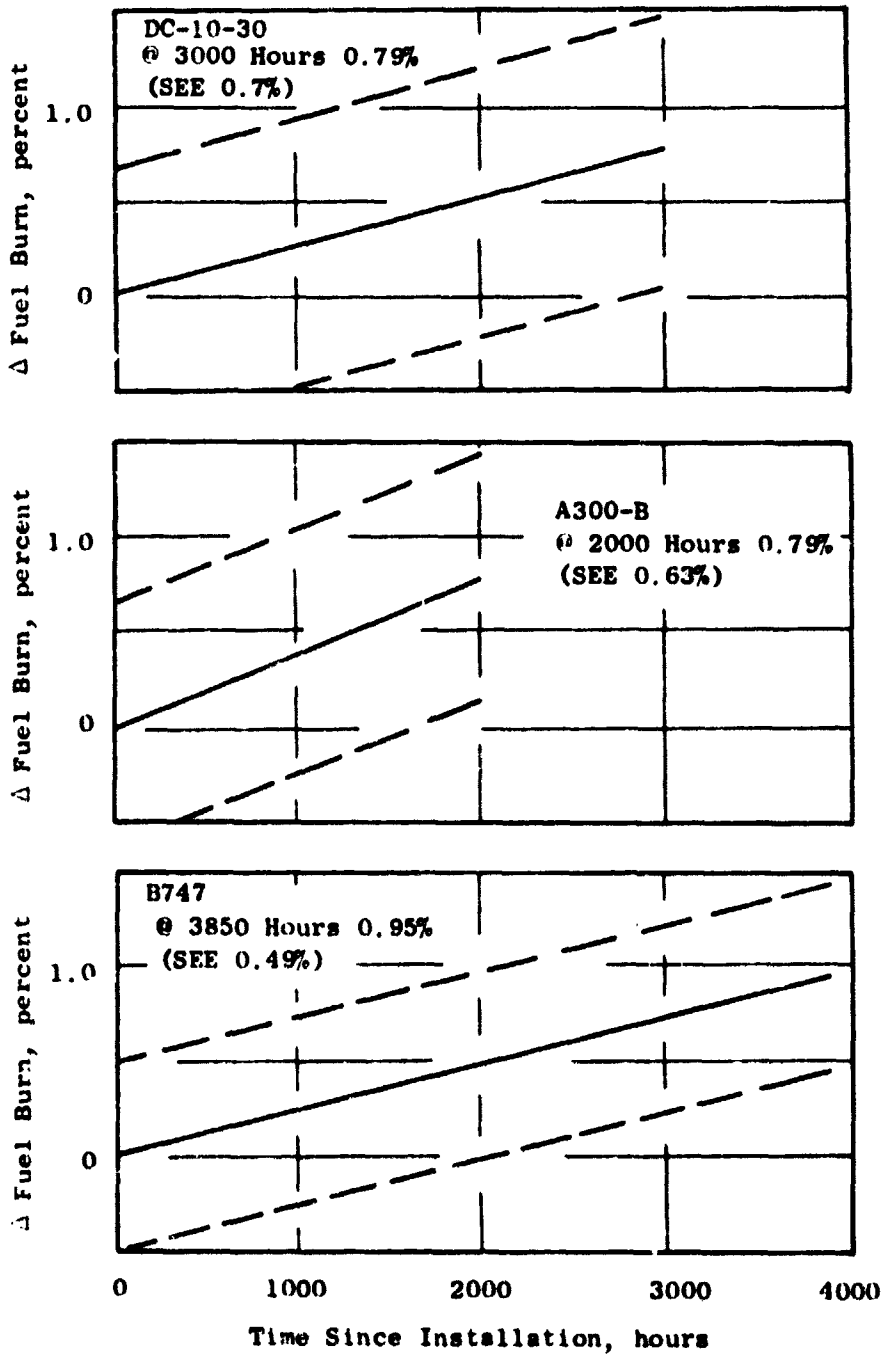

Figure 4-19. Multiple-Build Engine Deterioration - Hours.

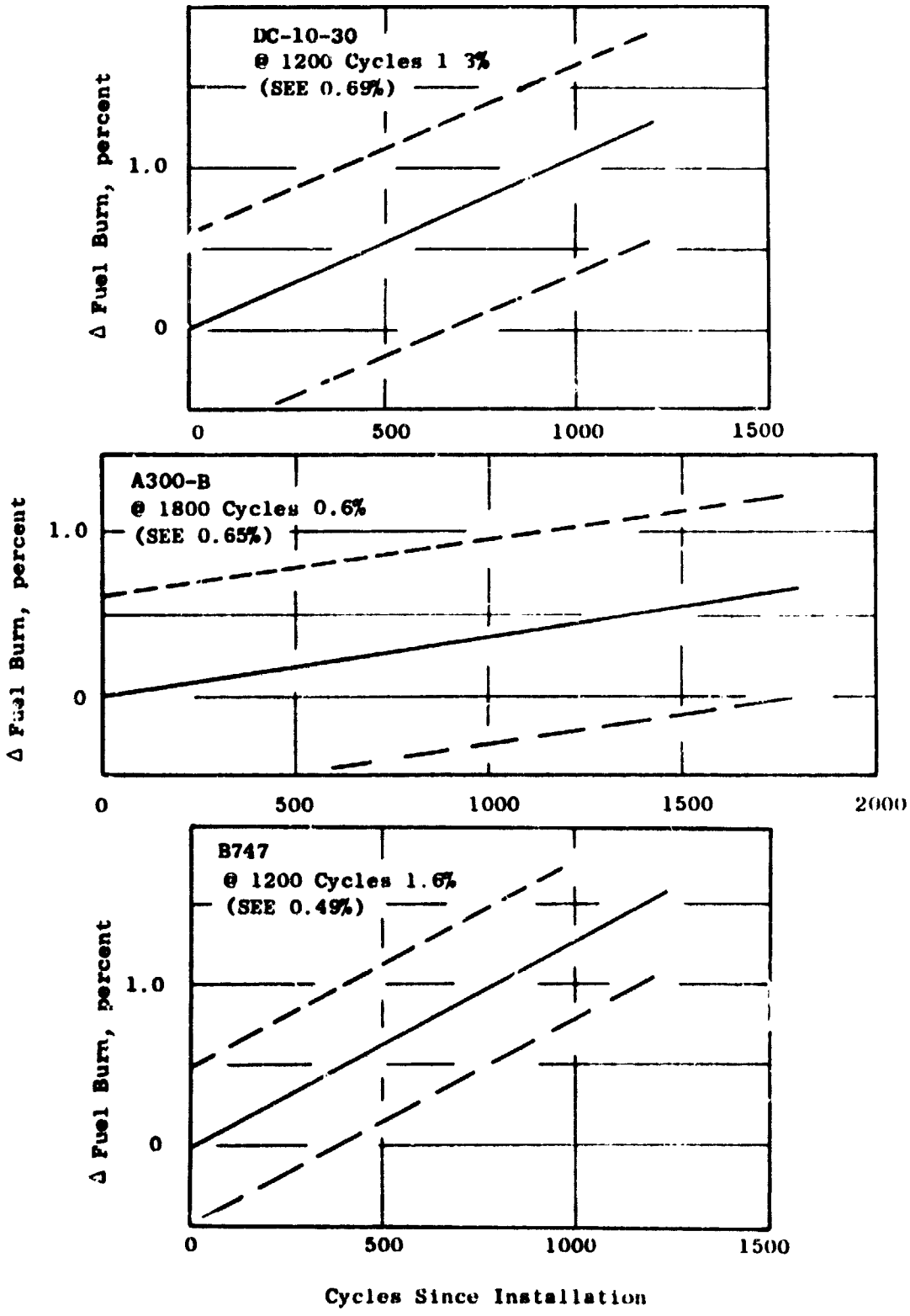

Figure 4-20. Multiple-Build Engine Deterioration - Cycles.

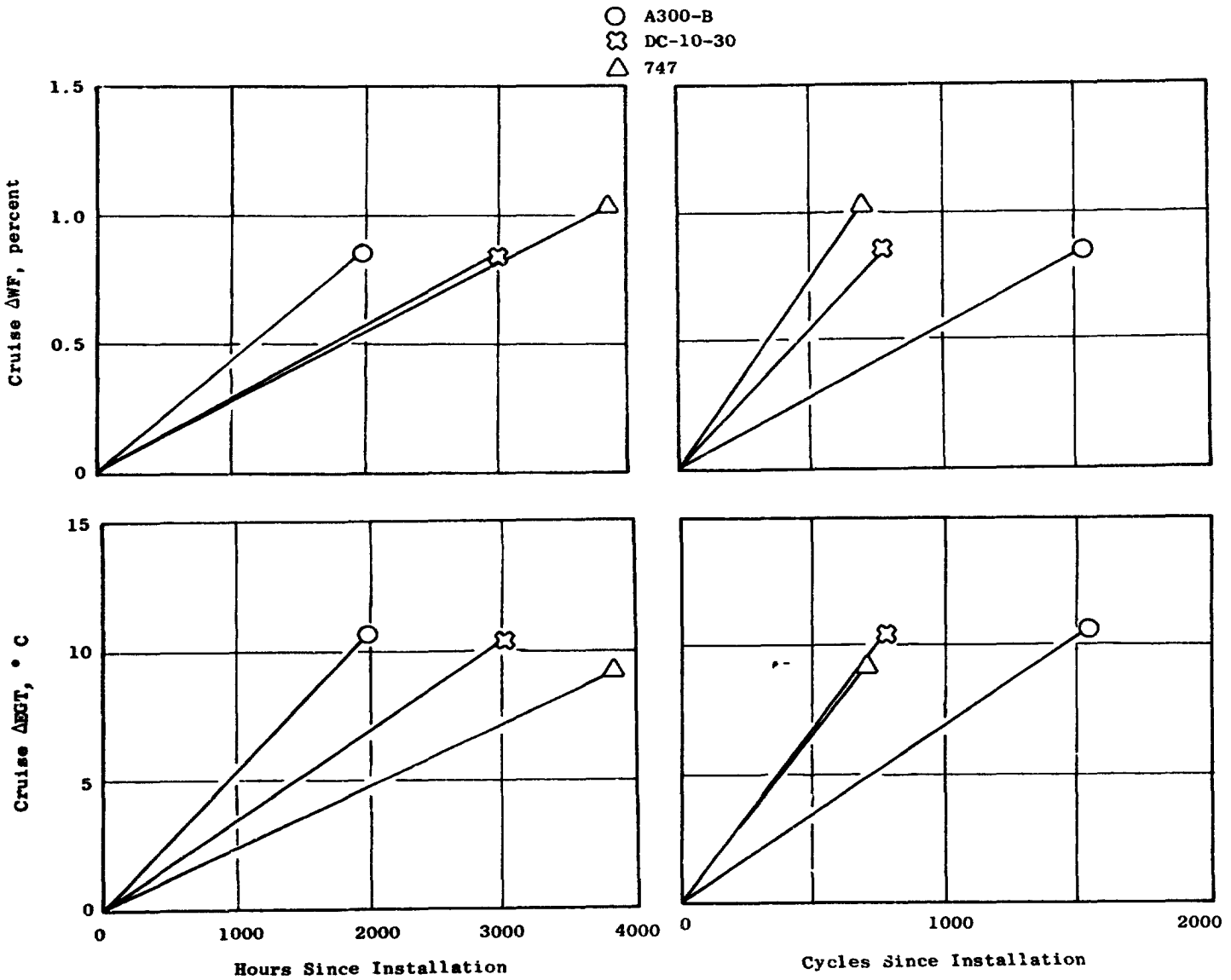

Figure 4-21. Composite/Multiple-Build Deterioration Characteristics Vs. Time and Cycles.

Table 4-X. Composite CF6-50 Deterioration Rates.

Hour/Cycle Ratio	Nominal Time-to-Removal				
	Aircraft Type	Nominal TSI (Hours)	ΔEGT (° C)	ΔWFM (%)	ΔEGT/ΔWFM (° C/%)
5.5	B747	(3,850)	9.3	1.04	8.9
3.9	DC-10-30	(3,030)	10.6	0.87	12.2
1.3	A300-B	(?,000)	10.8	0.87	12.4
		At 2,000 Hours			
5.5	B747		4.8	0.54	8.9
3.9	DC-10-30		7.0	0.57	12.3
1.3	A300-B		10.8	0.87	12.4
		At 700 Cycles			
5.5	B747		8.7	1.02	8.5
3.9	DC-10-30		10.0	0.81	12.3
1.3	A300-B		3.1	0.26	11.9

does user airline, with flight lengths and typical takeoff derate. In addition, data samples suitable for isolating the individual effects tended to be too small to be statistically significant.

Comparisons that were found to have the most significant effect on deterioration rate proved to be average flight length and derate at takeoff power. It will be shown that these two effects, which are a function of the aircraft type and user airline can account for the different deterioration rates noted for the three aircraft types. Some of the other potential contributors proved more difficult to isolate or were of insignificant magnitude, but the cumulative effects for all other variables appeared to have only minor significance.

The major results from the studies conducted to determine the major causes for the differences in deterioration rates noted for the three aircraft types are discussed in the following paragraphs.

User Airline:

Data from five operators of DC-10-30 aircraft with CF6-50 multiple build engines installed were analyzed to determine whether different airlines tended to produce significant differences in the performance deterioration rate.

Nine installations of DC-10-30 aircraft in the nominal 3,000-hour category were selected for each airline. The available data sample for the B747 and A300-B aircraft were limited to two airlines for each configuration and, as such, only limited comparisons could be conducted for those aircraft types.

Best curve fits using the regression techniques discussed earlier were established for all data. Some curve fits were best described by the second order term in the polynomial, while others required a linear fit. The analyses were conducted for both hours and cycles, but the data quality for the A300-B based on cycles, as indicated by the curve fit, was unacceptable and that comparison was not included.

Cruise trend plots of both fuel flow and EGT at constant fan speed are presented for accumulated hours in Figures 4-22 through 4-24, and for accumulated cycles in Figures 4-25 and 4-26. A tabular comparison of these results is presented in Table 4-XI. Each airline is arbitrarily listed by a letter designation (which has no significance to the airline), and the maintenance shop or central agent that performs the major refurbishment for the listed airlines is also shown.

The data as presented in Table 4-XI indicate no significant differences in the deterioration rates for four of the five operators of the DC-10-30 aircraft. The engines being utilized by the other operator (Airline C) deteriorate at a much slower rate for both accumulated hours and cycles. This operator utilizes the DC-10-30 aircraft for a significantly longer flight length (5.17 hours compared with a 3.6-hour average), and also refurbishes his own engines. The longer flight length (less cycles at constant hours) is known to be responsible for lower deterioration rates; but if all other variables are equal, the longer flight length should produce more deterioration at constant cycles. The generally higher deterioration rate experienced at constant cycles results from the higher number of accumulated hours, i.e., in the case of Airline C, at 800 cycles the accumulated hours would be 4,136 (800 x 5.17) compared with only 2,880 (800 x 3.6) hours for the average for the DC-10-30 aircraft. These data suggest that some other variable in addition to flight length is contributing to the observed differences in deterioration rates.

The comparison for the two operators of B747 aircraft indicated only slight differences as shown in Table 4-XI. The deterioration in both EGT and fuel flow were similar as were the flight length and refurbishment source. The data indicate a slight inconsistency in that the deterioration for Airline E was slightly higher than that for Airline F at constant hours even though the flight length was greater. These differences could suggest an influence from another variable; however, these differences are considered within measurement accuracies based on the data sample size.

Comparison of A300-B data from the two operators indicates a significant difference in deterioration at constant hours as shown in Table 4-XI. The refurbishment source can be eliminated since it is common, and the one obvious variable is the flight length. Note, again the longer flight length (50 percent higher) correlates with the lower deterioration rate.

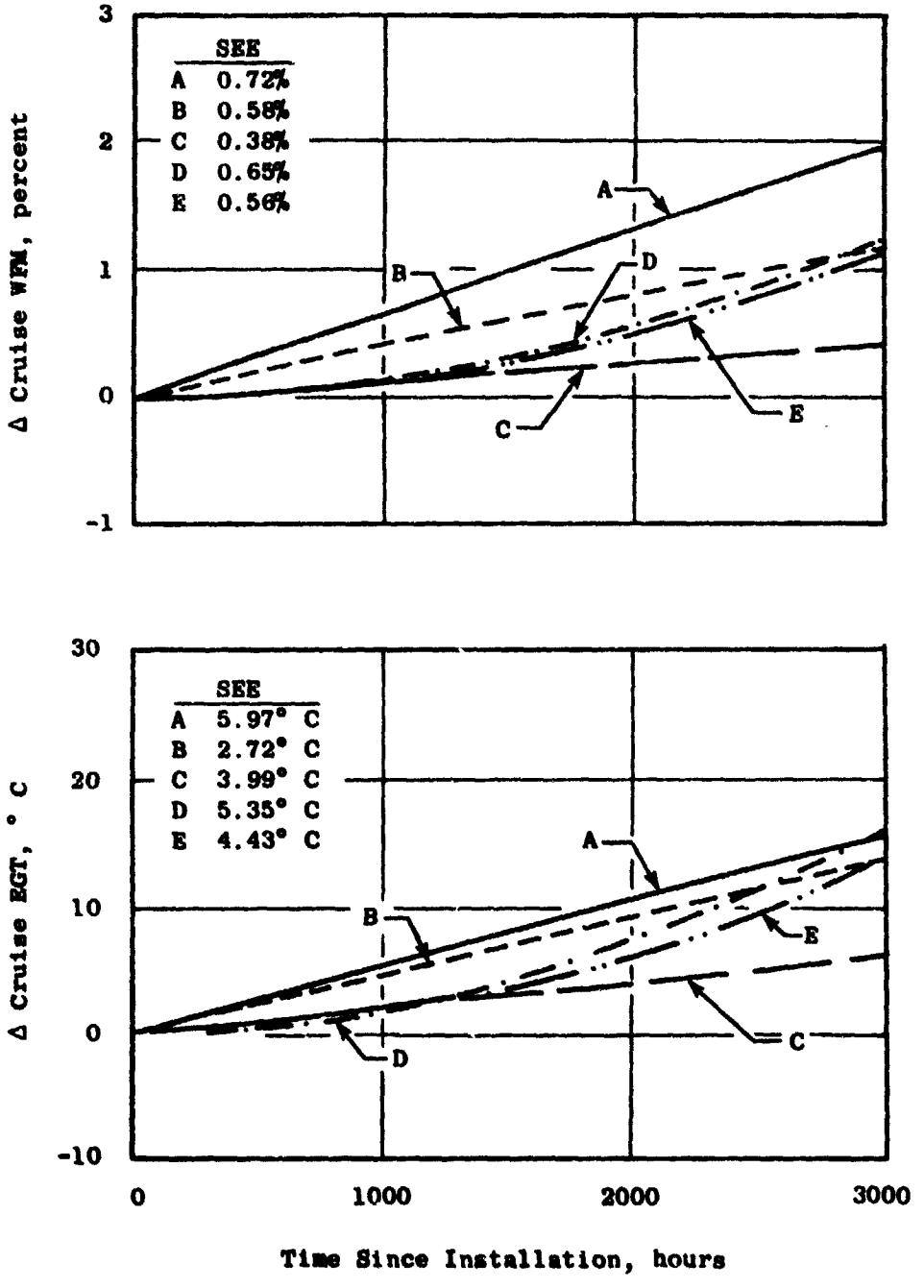

Figure 4-22. Comparison of Multiple-Build Engine Deterioration Rates (DC-10-30) - Hours.

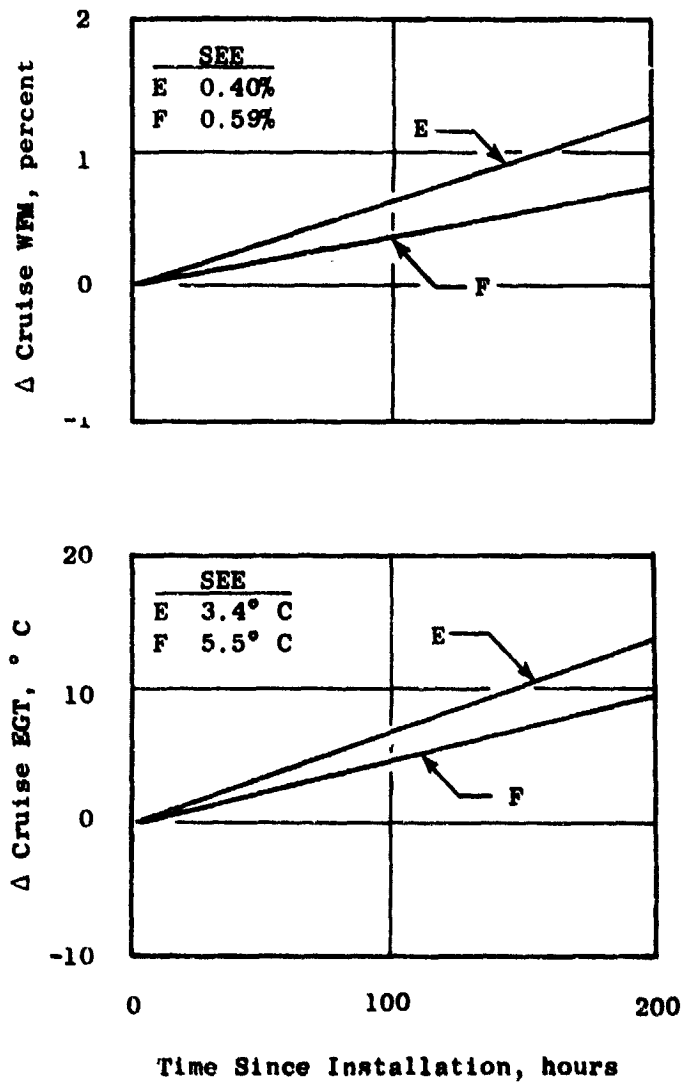

Figure 4-23. Comparison of Multiple-Build Engine Deterioration Rates (A300-B) - Hours.

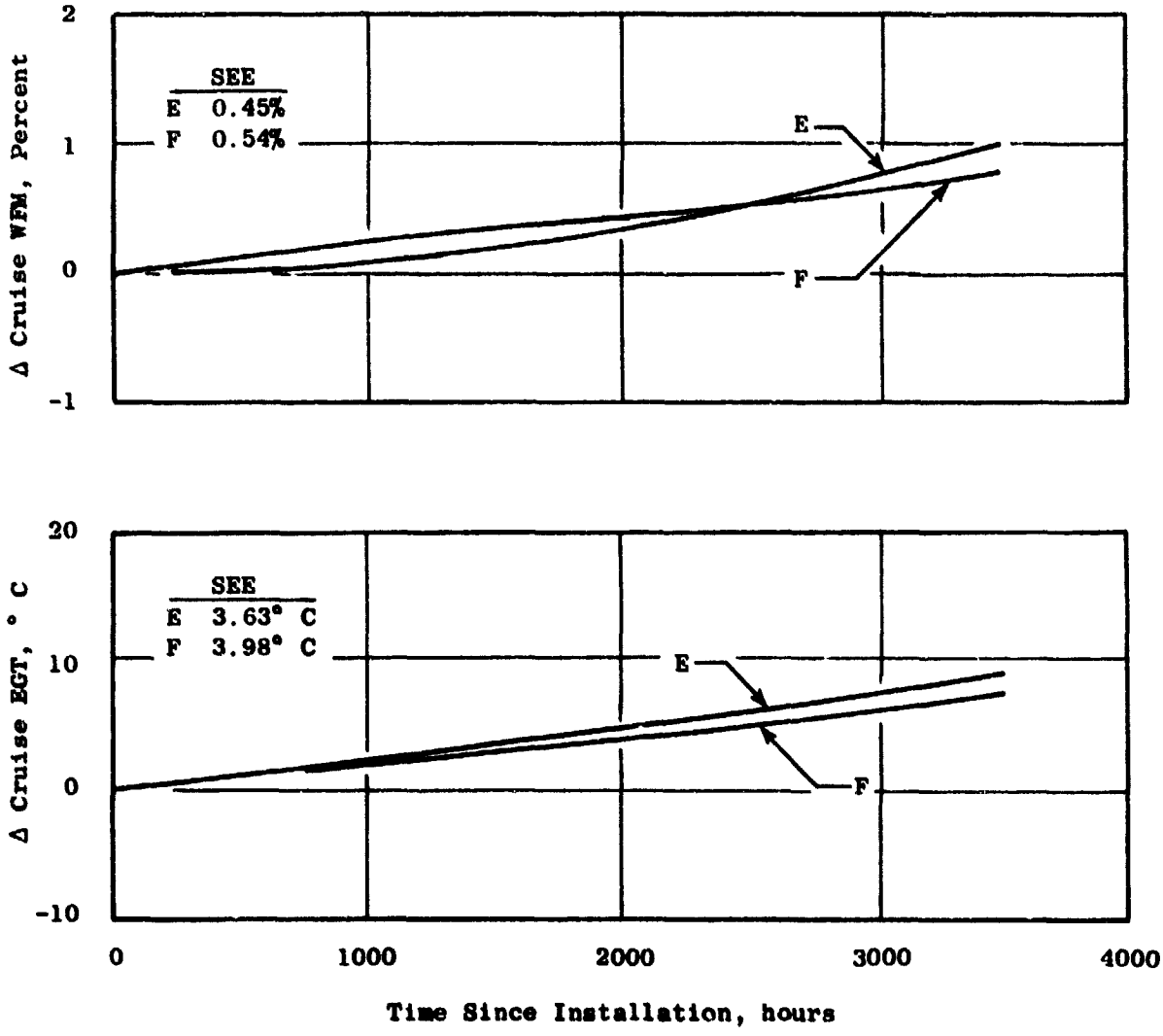

Figure 4-24. Comparison of Multiple-Build Engine Deterioration Rates (B747) - Hours.

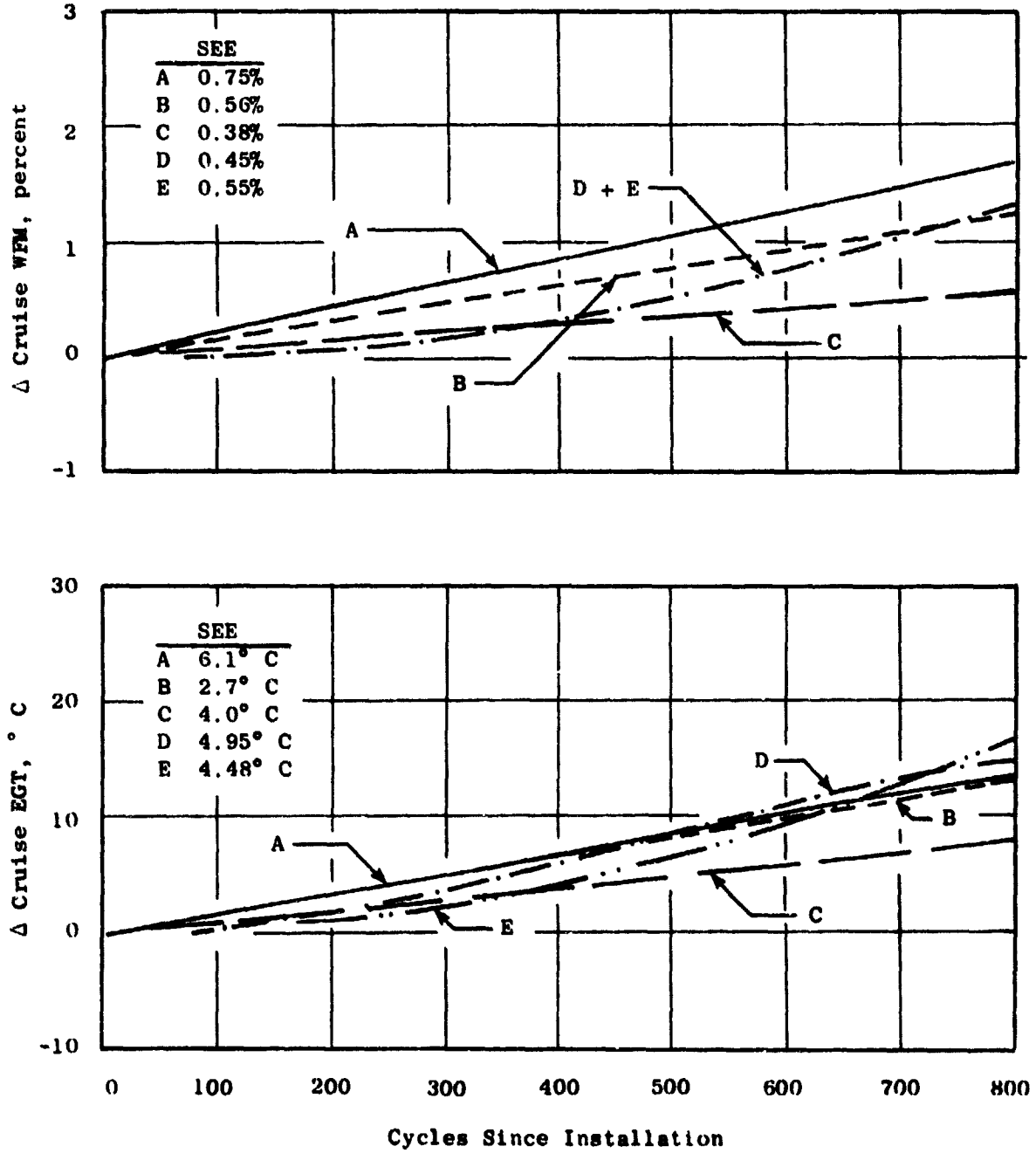

Figure 4-25. Comparison of Multiple-Build Engine Deterioration Rates (DC-10-30) - Cycles.

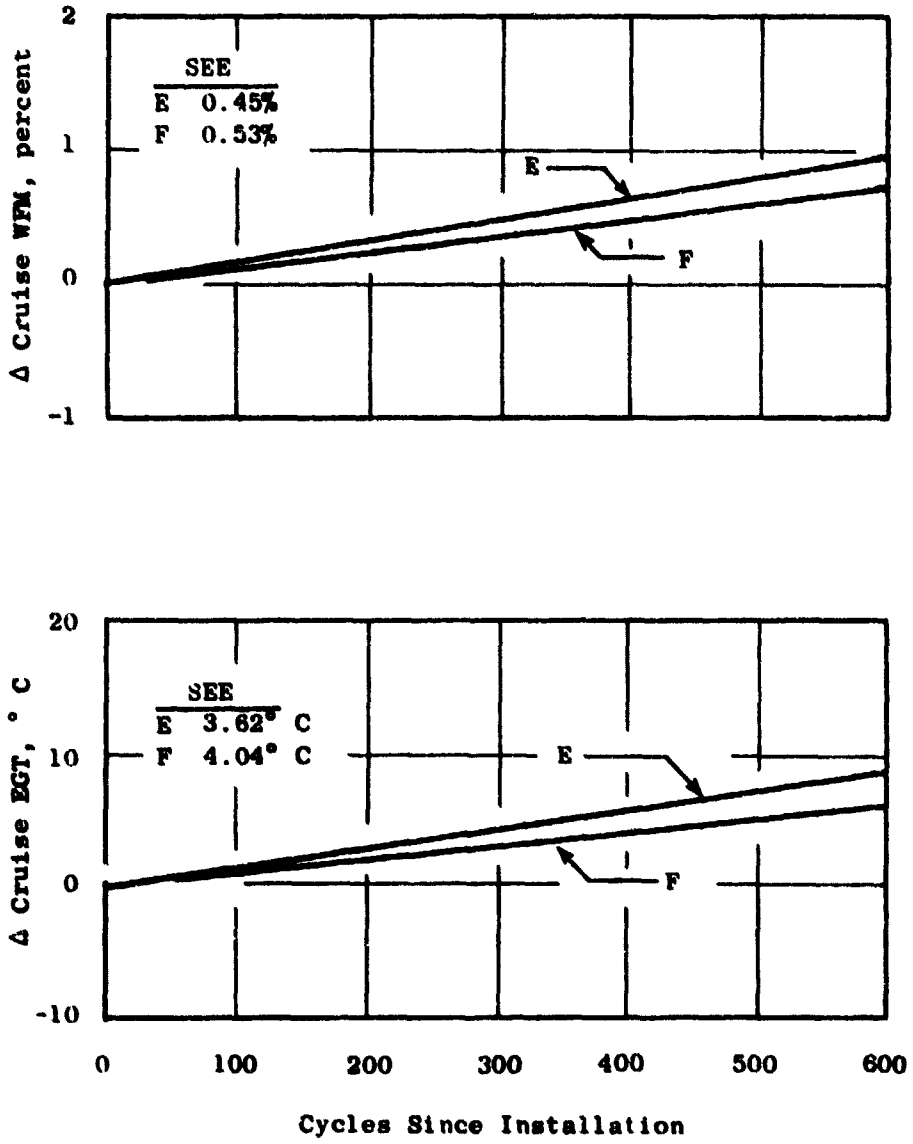

Figure 4-26. Comparison of Multiple-Build Engine Deterioration Rates (B747) - Cycles.

Table 4-XI. Comparison of Deterioration Rates by Airlines.

Airline	Repair Source*	Hour/Cycle Ratio	3000 Hours ΔEGT °F	3000 Hours ΔWFM %	3000 Hours ΔEGT/ΔWFM °C/%	800 Cycles ΔEGT °C	800 Cycles ΔWFM %	800 Cycles ΔEGT/ΔWFM °C/%
DC-10-30 Aircraft								
A	2	3.48	15.3	1.58	9.7	13.6	1.21	11.2
B	1	3.65	13.5	1.17	11.5	13.1	1.25	10.5
C	3	5.17	5.8	0.39	14.8	7.9	0.56	14.1
D	1	3.32	15.9	1.23	12.9	15.1	1.34	11.3
E	1	4.10	13.5	1.11	12.2	16.6	1.33	12.5
B747 Aircraft			3500 Hours			600 Cycles		
E	1	5.62	8.9	1.01	8.8	8.5	0.93	9.1
F	1	5.30	7.5	0.79	9.5	6.0	0.70	8.6
A300-B Aircraft			2000 Hours					
E	1	1.07	12.6	1.03	12.2			
F	1	1.55	9.7	0.72	13.5			

*1 = Major Refurbishment Source (Consortium Selected for This Program)
2 = Another Major Refurbishment Source
3 = Independent Airline (Own Maintenance)

The comparisons shown in Table 4-XI tend to indicate at face value that engine deterioration rate can be correlated with the user airline; however, detailed analysis indicated that flight length produced a better correlation. These studies also indicated that another variable(s) must be isolated to achieve an acceptable correlation.

Aircraft Type:

While the previous discussions compared the results for the same aircraft operated by different airlines, the data sample size was also sufficient to compare the deterioration rates for the different aircraft type when operated by the same airline. Data were available from one airline (designated E in previous discussions) who operates all three aircraft types with CF6-50 engines installed. The results from the comparisons at a constant 2,000 hours are presented in Table 4-XII.

Table 4-XII. Performance Deterioration at 2,000 Hours - (Airline E).

Aircraft	Hour/Cycle Ratio	ΔEGT (° C)	ΔWFM (%)	ΔEGT/ΔWFM (° C/%)
B747	5.62	5.0	0.34	14.7
DC-10-30	4.10	6.1	0.50	12.2
A300-B	1.07	12.6	1.03	12.3

These data again indicate a good correlation for the rate of performance deterioration with flight length at constant hours. As shown, the shorter flight length of 1.07 hour for the A300-B produced a significantly higher deterioration rate than experienced on either the DC-10-30 or B747 aircraft.

An interesting observation from these data - not directly associated with the studies to determine the reason for the differences in deterioration rates for the three aircraft types - is the ratio of ΔEGT/ΔWFM. This ratio is a good indicator to isolate the influence of the core engine from the low pressure components. Deterioration of core engine components (high pressure turbine or compressor) produces a large increase in both EGT and fuel flow while deterioration of low pressure components (fan or low pressure turbine) results in a large increase in fuel flow but only a small change in EGT. Hence, deterioration of the low pressure components produces a much lower ratio for ΔEGT/ΔWFM than does deterioration of the high pressure components. It is interesting to note that the ratio of ΔEGT/ΔWFM for all three aircraft types are similar, indicating that while deterioration is more rapid for the A300-B, the hardware deterioration sources may be similar.

Another comparison of aircraft types operated by the same airline was available from another airline. This airline operates both A300-B and B747 aircraft and the data base was sufficient to obtain comparative data at 2,000 hours as presented in Table 4-XIII.

Table 4-XIII. Performance Deterioration by Aircraft Types (Airline F).

Aircraft	Hour/Cycle Ratio	ΔEGT (° C)	ΔWFM (%)	ΔEGT/ΔWFM (° C/%)
B747	5.30	4.3	0.45	9.5
A300-B	1.55	9.7	0.72	13.5

As shown, these data reinforce the previous findings which indicated a correlation between flight length (hours/cycles) and deterioration rate at constant hours.

These studies have indicated that the user airline per se, does not correlate with deterioration rate. This means that each airline may not obtain similar deterioration rates for each aircraft type since other variables that affect deterioration rate, such as flight length, could be different for each airline. The studies also indicated a good correlation between flight length and deterioration rate, but did not completely eliminate the aircraft type as a significant contributor.

Takeoff Derate:

The search for a variable that would interrelate with flight length to possibly produce a good explanation for the different deterioration rates noted for the various airlines and aircraft types, quickly led to average derate at takeoff power. Factory testing and airline experience has indicated that the maximum temperature level achieved during each flight produces a significant effect on engine performance deterioration. Experience has also indicated that the route structures flown by the various airlines and the type of aircraft being utilized were generally the factors which indicated the amount of derate (reduced thrust) that was utilized for individual takeoffs. Since the derate policy and route structure are different for each airline, these items produced a wide variance in the average takeoff derate utilized by the individual airlines.

Cruise performance trend data, engine removal times and other statistics were reviewed to determine the influence of average takeoff derate on deterioration. The previous comparisons were all conducted at constant hours and indicated a wide difference in the deterioration rates for the three aircraft

types. However, comparison of data for the individual aircraft types indicated very little difference in the magnitude of deterioration at typical engine removal times. The average deterioration for both fuel flow and EGT are presented in Figure 4-27. Note, these are averages by aircraft types for the entire fleets, and the average flight lengths are slightly different than that presented during previous discussions. Even though the average removal times vary from 2,000 to 3,850 hours, the similarity of the magnitudes of deterioration suggests that the engine stays on wing until a certain level of deterioration has occurred. This is in agreement with the previous finding which indicated that the sources of deterioration (high or low pressure components) do not appear to change drastically with increased or decreased deterioration rates.

Figure 4-28 shows there is a marked relation between the average flight length and the number of hours or cycles until removal. As shown, the short flight length of the A300-B produces approximately twice as many cycles and half as many hours before removal as the longer flight lengths of the DC-10-30 and B747 aircraft. This substartiates the data previously presented in that both hours and cycles have a significant effect on deterioration and the individual contributions cannot be separated. Indeed, as a first-order approximation, the simple product of hours to removal times cycles at removal is fairly constant over these flight cycle lengths as shown in Figure 4-29.

The average derate in takeoff power is likely to be significantly different for each aircraft type when utilized on the same route structures due to aircraft design considerations. Twin-engined aircraft are, by nature, relatively more overpowered at takeoff than three-engined or four-engined aircraft due to engine-out considerations. Average flight length is also likely to have an effect on takeoff derate for each specific aircraft type due to the takeoff gross weight differences based on required fuel loads.

Typical levels of takeoff power derate utilized for some individual airlines were available, and used in conjunction with the deterioration data presented at typical removal times to investigate the effects of takeoff power derate. Figures 4-30 and 4-31 show EGT and fuel flow deterioration for nine individual airlines using the three different aircraft types, as well as the composite or average value for each aircraft type based on the data presented in Figure 4-29. The data are plotted in Figures 4-30 and 4-31 as a function of flight length versus delta deterioration (EGT and WFM) at removal, and the average takeoff derate employed by the individual airlines is shown in parentheses. The individual airline data show somewhat more spread than the composite data, with a significant tendency for the utilization of more derate to indicate less deterioration. This is based upon examination of the individual data points clustered around either the 1.5, 3.5, or 5.5 average hours/cycle values, which generally indicate that more derate correlates with less total deterioration at removal.

The real impact of takeoff power derate is apparent upon the examination of the rate at which performance deterioration takes place. Figures 4-32 and 4-33 show deterioration rates for cruise fuel flow and EGT for individual airlines and the fleet composite as a function of flight length. Note that the

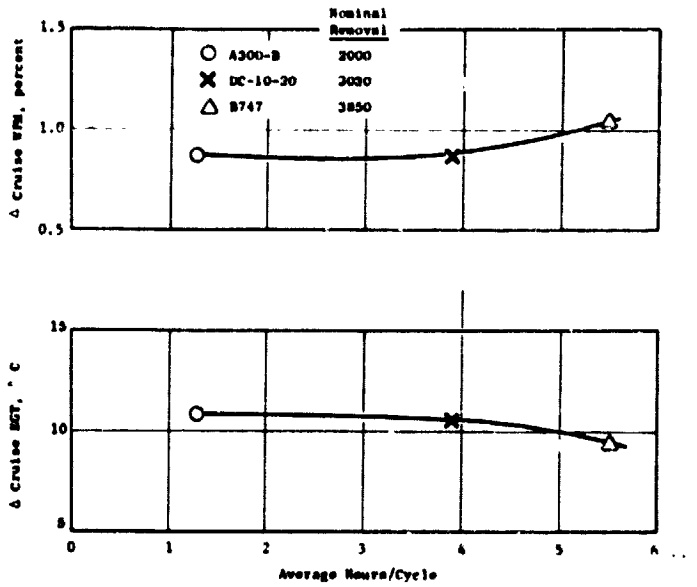

Figure 4-27. Effect of Flight Length on Deterioration at Removal.

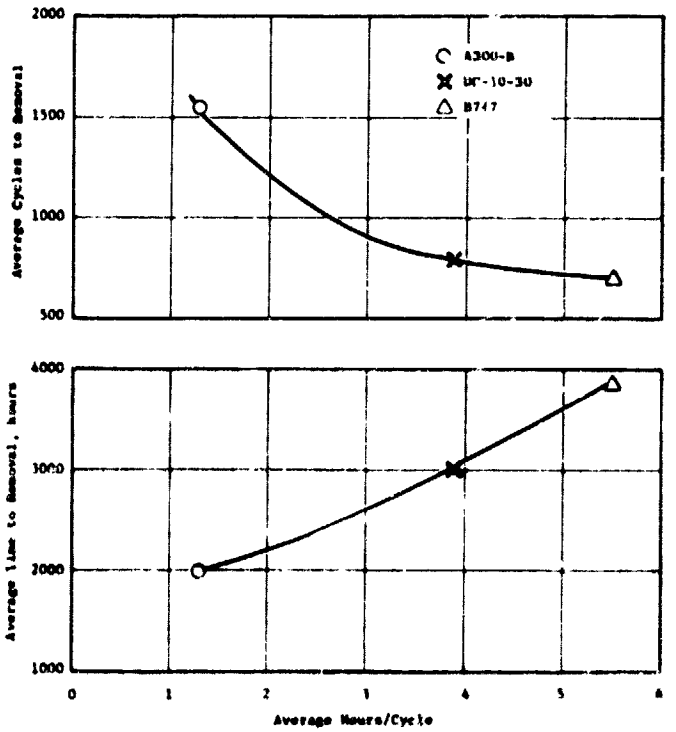

Figure 4-28. Effect of Flight Length on Time to Removal.

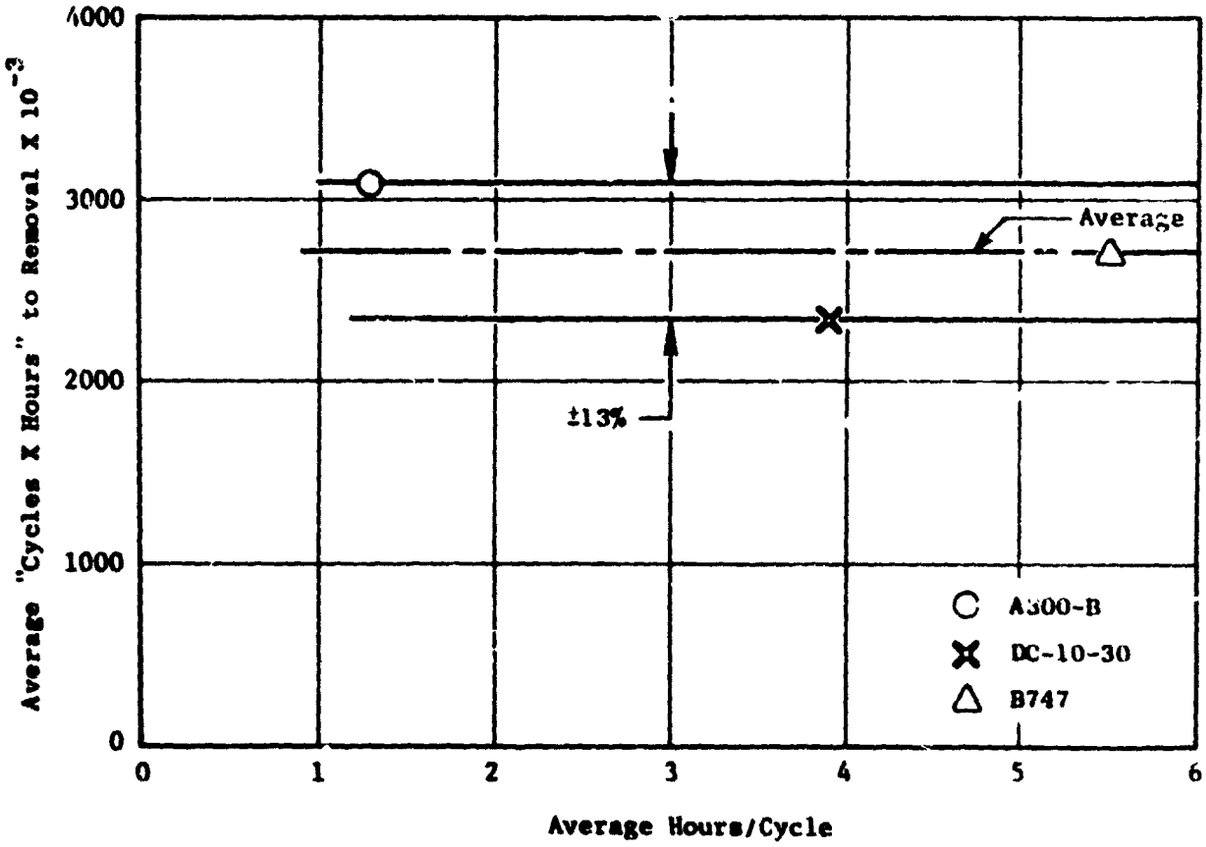

Figure 4-29. Flight Length Vs. "Cycle Times Hours" at Removal.

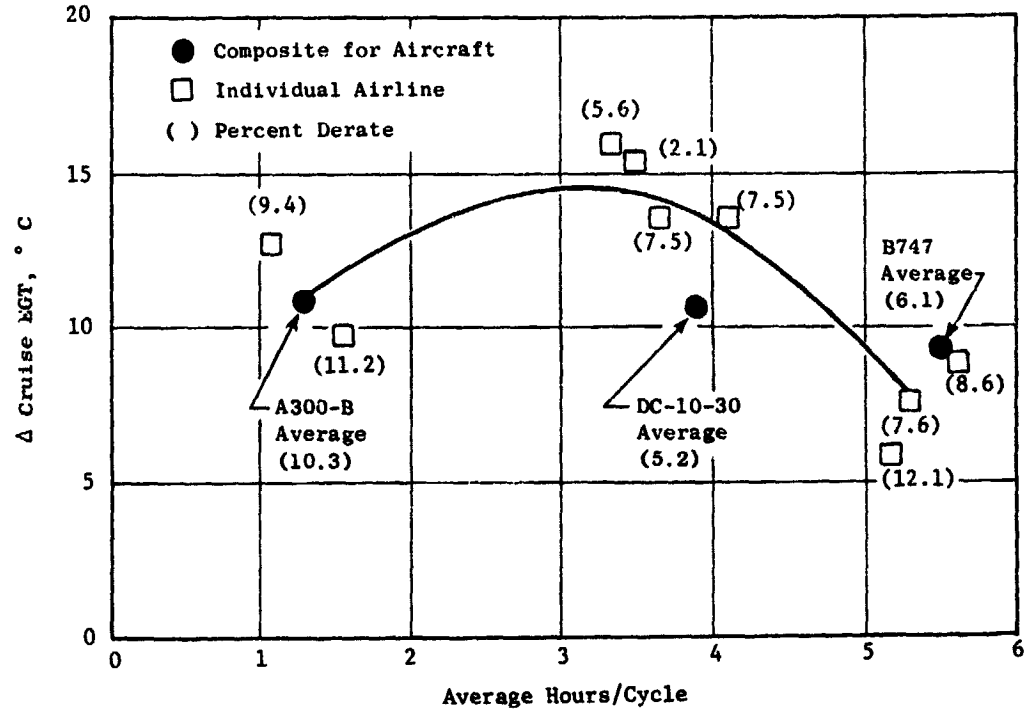

Figure 4-30. EGT Deterioration for Flight Length/Derate.

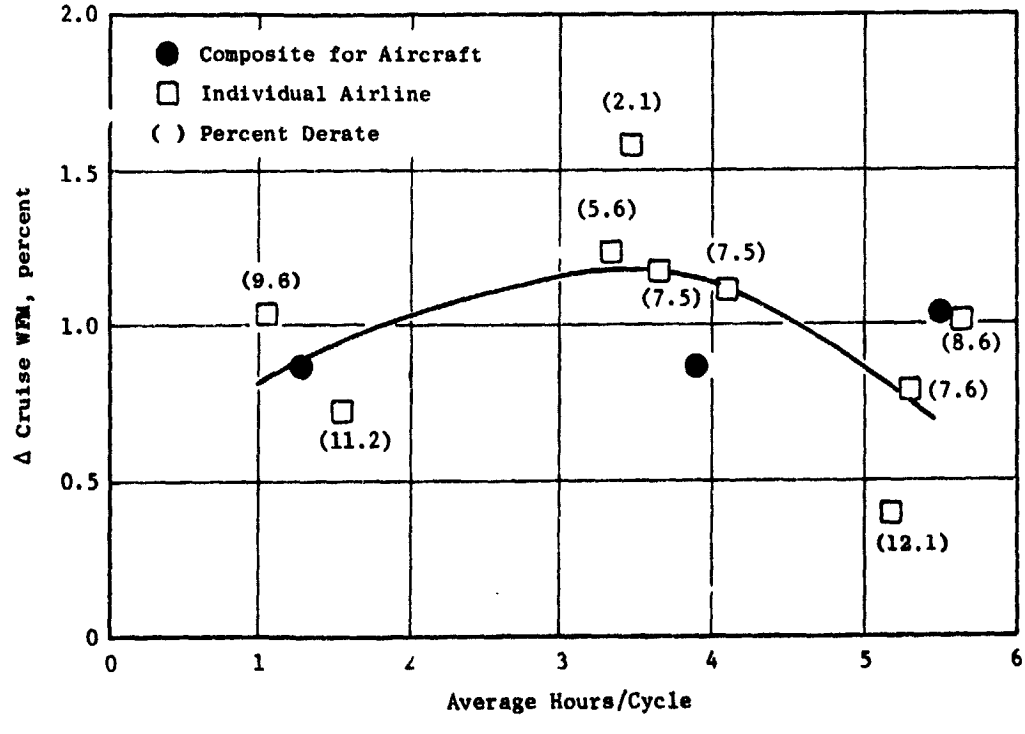

Figure 4-31. Fuel Flow Deterioration for Flight Length/Derate

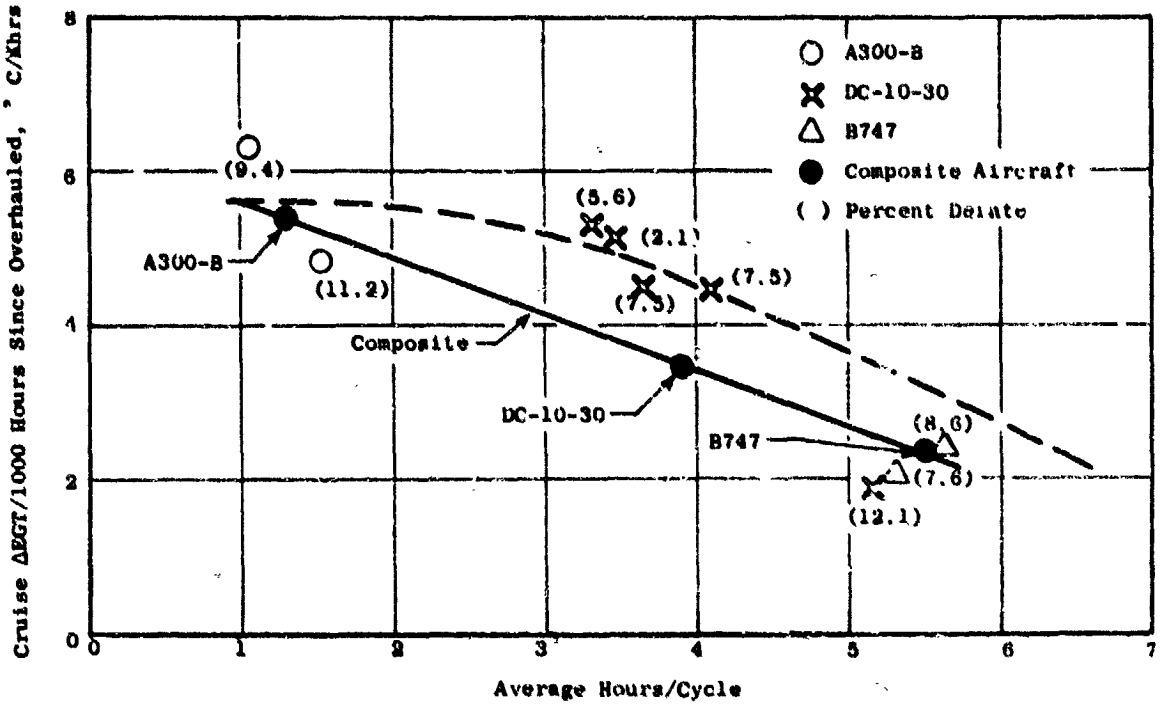

Figure 4-32. EGT Deterioration for Flight Length and Derate.

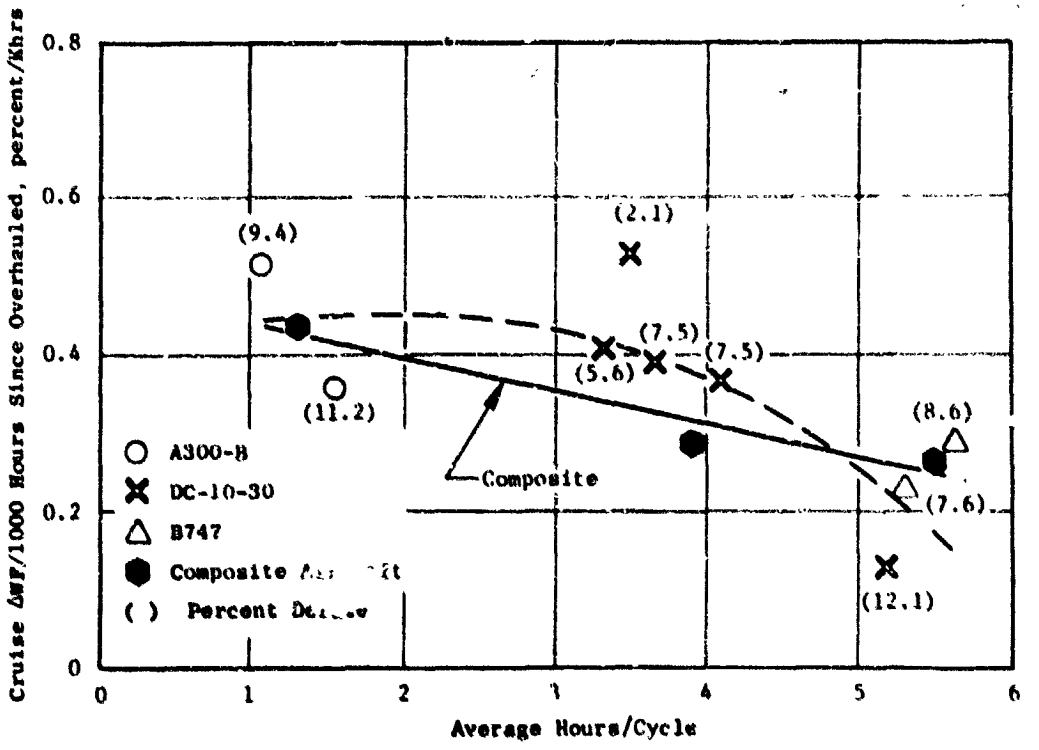

Figure 4-33. Fuel Flow Deterioration for Flight Length and Derate.

rate of deterioration is substantially lower for airlines with long flight lengths and large amounts of derate at constant hours which now explains several apparent inconsistencies noted in previous discussions.

As shown in Figures 4-30 and 4-31, the shorter A300-B flight cycle resulted in less deterioration at removal than did the engines installed for the longer DC-10-30 flight lengths. A re-evaluation of that data in light of the derate effects indicates that the cause can be attributed to takeoff derate since the average for the A300-B was 10.3 percent as compared with 5.6 percent for the DC-10-30 operators.

In the previous discussion concerning performance deterioration for five airlines which operated DC-10-30 aircraft, the operator termed Airline C sustained considerably less deterioration than the other four individual operators, a fact that could not be explained only by flight length. Interestingly, this operator utilized the DC-10-30 aircraft on a flight length comparable to the longer flight length of typical B747 users, and with the highest level of derate for any airline with this approximate flight length. This airline exhibited the lowest deterioration rate for all the individual airlines as shown in Figures 4-32 and 4-33. (DC-10-30 aircraft plot at 5.2 hours/cycle and 12.1 percent derate). The data clearly show that the missing link was average takeoff derate, and the combination of the longer flight length and more derate produced the lower deterioration rate for that airline.

The variances in engine deterioration rates noted for the three aircraft types were not due to inherent design differences, but were directly the result of flight length and average takeoff derate. The deterioration rates tend at face value to correlate with aircraft type only because each type aircraft is generally utilized by the individual airlines for similar flight lengths and with similar levels of takeoff derate. When the utilization of a specific aircraft type fell outside the normal flight length/derate range for that aircraft type, the deterioration rate continued to correlate with the flight length and derate parameters and not by aircraft type.

Summary of Performance Studies

These studies indicated that the average short-term loss for the CF6-50 model engine was equivalent to 0.7 percent in cruise sfc. While slight differences were observed in the short-term loss for the three different aircraft types, the analyses indicated sufficient similarity, and that the 0.7 percent increase in cruise sfc would best describe the loss for all three aircraft types.

The average unrestored loss remaining after refurbishment of the CF6-50 engine is equivalent to a 1.8 percent increase in cruise sfc. Engine hardware is not segregated by aircraft model during engine refurbishment; thus the average unrestored loss is representative of the CF6-50 fleet regardless of aircraft installation.

The long-term performance deterioration characteristics for the CF6-50 engine cannot be described by a single summary chart or curve that represents the entire fleet. It has been shown that differences in flight lengths and average takeoff derate, which tend to correlate with aircraft types, produce significant differences in the rate and magnitude of performance deterioration. Therefore, the long-term performance deterioration characteristics must be described by utilizing separate charts for each aircraft type.

Figures 4-34 through 4-36 present the deterioration characteristics that best describe the average loss for the CF6-50 engine while utilized on the three aircraft types. Since the unrestored losses were independent of shop visit number (i.e., no indication of increasing or decreasing trend) the data presented in Figures 4-34 through 4-36 are considered representative for the current fleets.

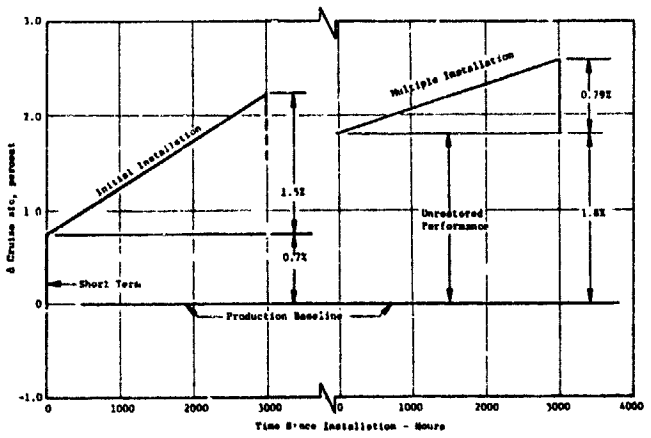

Figure 4-34. Typical Deterioration for DC-10-30 Installation.

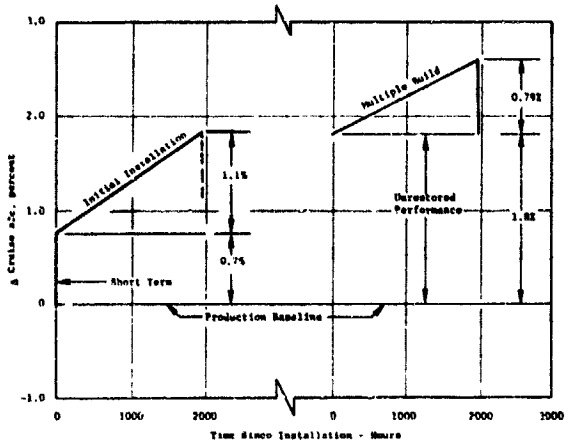

Figure 4-35. Typical Deterioration for A300B Installation.

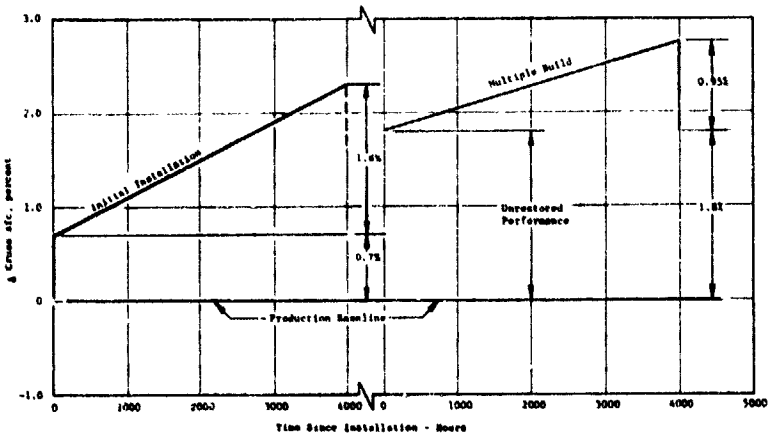

Figure 4-36. Typical Deterioration for B747 Installation.

HARDWARE INSPECTION RESULTS

In order to obtain a representative sample of deteriorated hardware data, a multifaceted program was established to collect, document, and analyze used parts data from a number of different airline and General Electric facilities. Historical data were obtained as available from airline and contractor files and independent overhaul sources. It was readily apparent based on initial reviews that available historical data were generally not the correct type nor of sufficient detail to satisfy the objectives of this program.

Accordingly, a program was established with two specific airlines to obtain the required data in sufficient detail to satisfy the program objectives. The selected airlines were the central overhaul agents for the two largest airline consortiums which operate over 50% of all CF6-50 engines. Teams of General Electric personnel visted these central agents for periodic hardware reviews. A team was established for each of the four major engine sections (fan, high pressure compressor, high pressure turbine, and low pressure turbine). Each team consisted of a mechanical designer, aerodynamicist, airline service hardware engineer, performance engineer, and a performance restoration specialist. These teams were totally responsible for their assigned hardware; and evaluated in addition to hardware conditions, shop procedures, quality of repairs, current workscopes, and adequacy of field inspections.

In addition, a General Electric-funded program was established which made available an engine for selective refurbishment. This engine was disassembled to expose a selected module, and the teams then documented detailed hardware conditions and prepared a refurbishment plan. The selective refurbishment of each module was followed by a test cell run to measure the effectiveness of the modifications. This permitted the correlation of the measured performance gains with that expected based on analytical studies. While the results from the 12 refurbishment/test cycles are not discussed as a separate item, they have provided additional insight into the deterioration characteristics of the CF6-50 model engine.

The design team analysis consisted of a detailed summary of the salient inspection measurements where deterioration modes were categorized as either a clearance change, airfoil quality degradation, or an internal/external leakage. Influence coefficients were used by the aero designers to analytical convert changes in hardware conditions to losses in component efficiencies and flows. These, in turn, were stated in terms of cruise sfc deterioration by the use of engine computer cycle model derivatives. These model assessments were then refined using the back-to-back engine test data to finalize the deterioration characteristics for each module. In addition, the teams conducted analyses to determine potential causes for the deterioration, and participated in cost effectiveness studies which are discussed later in this report.

As noted previously, the long-term studies were conducted to determine performance deterioration characteristics for the initial installation (new) and multiple-build (repaired) engines, and to isolate the unrestored losses for the multiple-build engines. The characteristics for the initial installation engines are most representative of the engine model, since all parts are considered new even though they have experienced the short-term losses prior to revenue service. The multiple-build engines include a mixture of used, new, and repaired parts and are most representative of the current airline fleet.

Very little hardware data were available specifically for use in empirically determining deterioration characteristics for the initial installation engine. The majority of the hardware data samples were in-service in excess of 2,000 hours; therefore, while the magnitude of deterioration could be established for a fixed time in excess of 2,000 hours, the deterioration curve shape could not be empirically derived for each module. The procedure used to "average" the results and to estimate the deterioration curve shape was as follows:

- A representative time-to-repair was selected as the "anchor point" for each module based on hardware data analysis and engine removal statistics. The selected number of hours was that best judged to represent the nominal time-to-repair for each module.

- The hardware team used the empirical hardware data to determine the expected loss for the anchor point for each module.

- The teams then estimated the shape of the deterioration curve for each module using common sense and engineering logic in conjunction with the available hardware data.

The shape of the deterioration curve based on hardware inspection results is considered reasonable, but not necessarily reliable due to the small amount of empirical data and large application of common sense and logic. However, the curve shape is best described by cruise performance data since a sufficient data sample size was available for all areas of the curve. The curve shape for the individual damage mechanisms based on hardware inspection data is considered of minor importance, and is used only for cost effectiveness studies where inaccuracies do not have a major effect.

Hardware inspection data describing the deterioration modes and inspection findings are presented in the following paragraphs. First, a discussion of deterioration sources and magnitudes observed for parts prior to repair (multiple-build deteriorated engine) are documented for each of the four major sections of the engine. This is followed by presentation of data obtained during reviews of hardware after refurbishment, which would be typical of engines re-entering revenue service. As noted previously, a discussion of the results for the Initial Installation Engine will not be included due to the lack of sufficient hardware inspection data.

Deteriorated Engine

Hardware inspection data describing the deterioration modes and inspection findings are presented for the fan, high pressure compressor, high pressure turbine, and low pressure turbine sections in the following paragraphs.

Fan Section - Deterioration of the fan section is generally time-dependent (rather than event-oriented) and can be categorized into two broad classifications: (1) flowpath deterioration and (2) airfoil quality degradation. Each of these two classifications will be discussed separately. The results are based on inspecting airline modules that have accumulated 10,000 to 12,000 hours since new, and which have logged 3,000 to 5,000 hours since the last shop visit. A cross section of the basic fan module is presented in Figure 4-37, which notes the pertinent areas of performance deterioration.

The sources of flowpath deterioration (Figure 4-37) include shroud erosion, outlet guide vane (OGV) spacer cracking, splitter erosion, and protrusion of inlet guide vane (IGV) inner bushings.

Fan Blade Clearance:

A shroud is provided as part of the fan casing to control the clearance between the tip of the fan blade and the static structure. Two types of shroud material are used for CF6-50 engines; epoxy microballoon and open cell honeycomb. Most of the engines in the fleet utilize the epoxy microballoon material which is rugged and easy to replace. A particular advantage of this type shroud is that additional microballoon material can be added if needed to obtain desired tip clearances. The open cell honeycomb material can only be replaced at the manufacturer's facility, and there is no way of adding material to reduce (or control) tip clearance. The initial blade-to-shroud cold clearances are set such that blade tip rubs are not experienced during normal engine operation, but instead occur only in the event of a large rotor unbalance. The epoxy microballoon shrouds also include circumferential grooves designed to reduce force loads during rubs with large rotor unbalance.

Clearances between the fan blade tip and shroud are set to achieve a minimum of 0.175 inch with a maximum allowable average of 0.201 inch. The minimum clearance is designed to prevent blade tip rubs while the average clearance, which considers blade tip and shroud runouts, is designated for fan performance reasons. Measurements from engines removed from revenue service indicated that the average clearance was 0.213 inch which compares with the production new engine average of 0.193 inch. Part of this clearance increase is attributed to the airline shop maintenance practice of controlling only the minimum clearance since clearance measurements are required only when replacing the fan rotor or fan casing. Any underminimum clearances observed during engine buildup are opened by local grinding of the shroud which results in an increased average clearance. The method of measuring clearances is to use a dial gage with two pins that locate the correct axial plane for the measurements. Because pins are used, the tendency is to measure the high point on

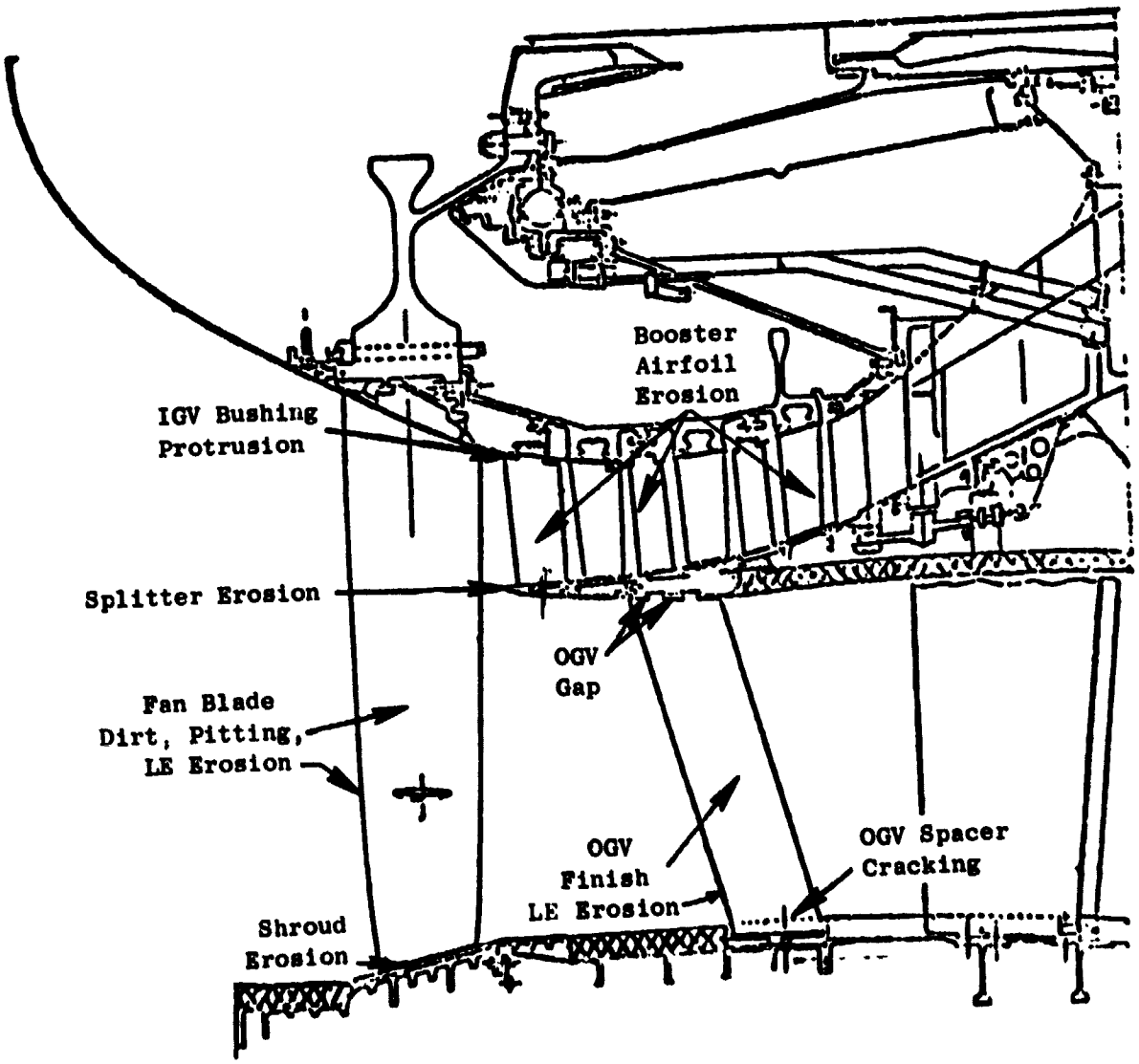

Figure 4-37. CF6-50 Deterioration Modes - Fan Section.

the shroud rather than the low points or valleys which produced a clearance value which is tighter than actual. A picture of a dial gage and how it is used is shown in Figure 4-38.

Blade tip rubs were not observed on any shroud, but it was noted that erosion of the shroud material occurs with increasing time. This condition, as shown in Figure 4-39, also contributes to increased fan blade-to-shroud clearance. The amount of erosion is a function of the operational environment (sandy runways, heavily treated runways for ice control, etc.) and the position on the aircraft (wing engines showing somewhat more erosion than tail engines on the DC-10). It is very difficult to isolate the effect of shroud erosion from other potential contributors to increased fan blade clearances since shroud material removal is a function of both erosion and shop rework. However, it was estimated by visual observations that material loss due to erosion was approximately 2 to 3 mils for each 1,000 hours of engine operation. Large differences in apparent erosion for individual shrouds were also noted and most likely attributable to differences in operational characteristics which were previously noted.

Another condition that contributed to shroud deterioration was the poor quality of microballon replacement as shown in Figure 4-40. It appears that when the microballon material was installed in the metal mesh structure in the casing, the material was not completely filled in the lower portion of the mesh structure. These gaps (or holes) are exposed during subsequent machining operations required to produce the correct tip clearances and to incorporate the circumferential grooves.

The combined effect of the shop maintenance practices and erosion for an engine after 6,000 hours of operation results in a fan tip running clearance increase of 0.020 inch. This is equivalent to a 0.77 percent loss in fan efficiency and a 0.38 percent increase in cruise fuel burn.

Booster Shroud Erosion:

As shown in Figure 4-37, the booster consists of three stages of blades and vanes and outlet guide vanes. Open cell aluminum honeycomb shrouds are incorporated to provide correct blade tip clearances. Booster modules are infrequently disassembled during routine shop visits, but experience indicates that they are only a very minor contribution to engine performance deterioration. Some erosion of the honeycomb material shrouds was observed, particularly in local areas which were in direct alignment with the preceding stator airfoil. These effects were estimated to be approximately 10 mils after 6,000 hours of operation, which is eqivalent to a booster efficiency loss of 0.24 points and 0.03 percent in cruise fuel burn.

OGV Spacer Cracking:

Nylon spacers are used between the bypass outlet guide vanes along the outer flowpath. These plastic spacers fit snugly against the concave side of one vane and the convex side of the adjacent vane. With time, the edge of the

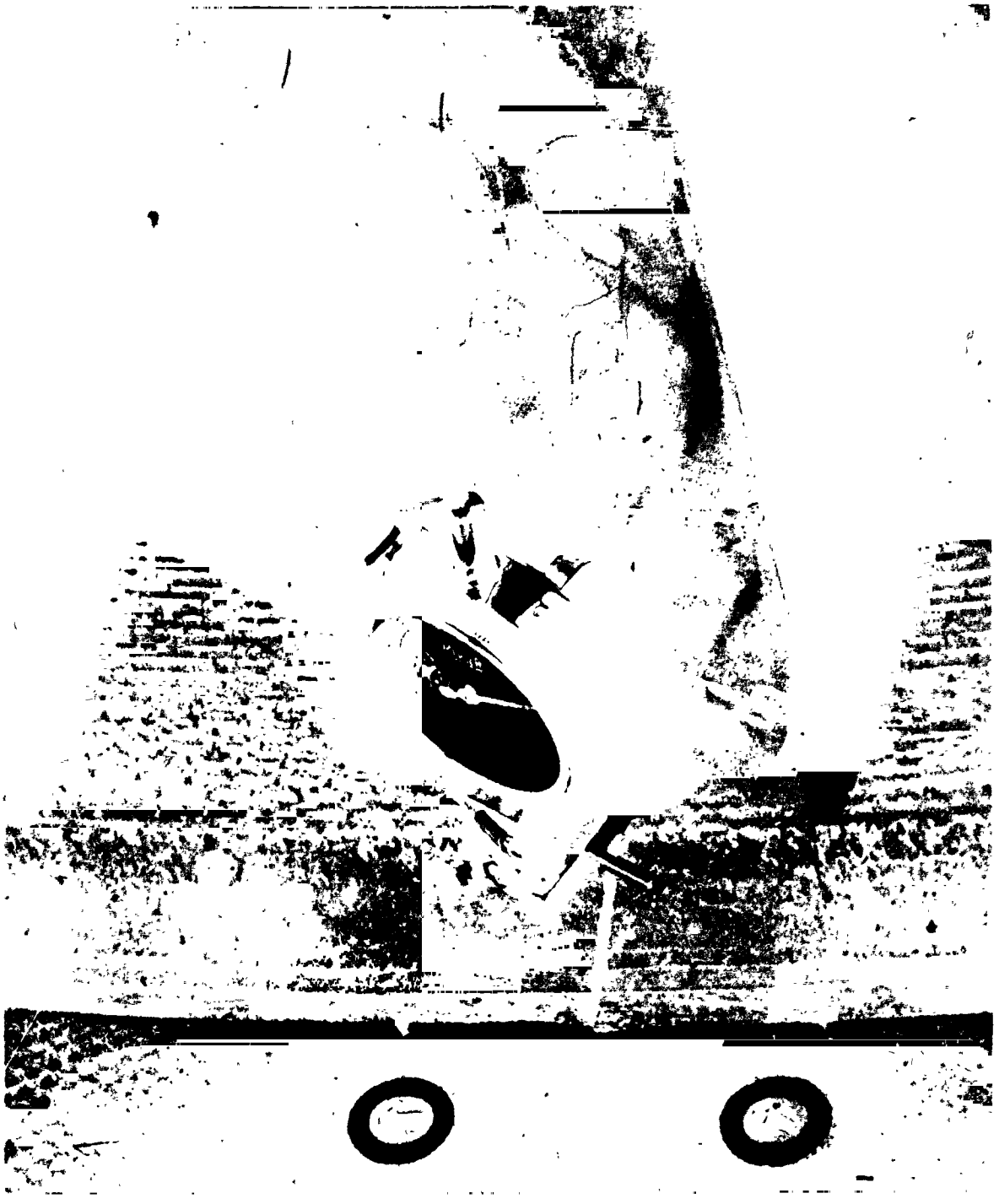

Figure 4-38. Dial Gage Shown Measuring Fan Blade Tip Clearance Near Leading Edge of the Blade.

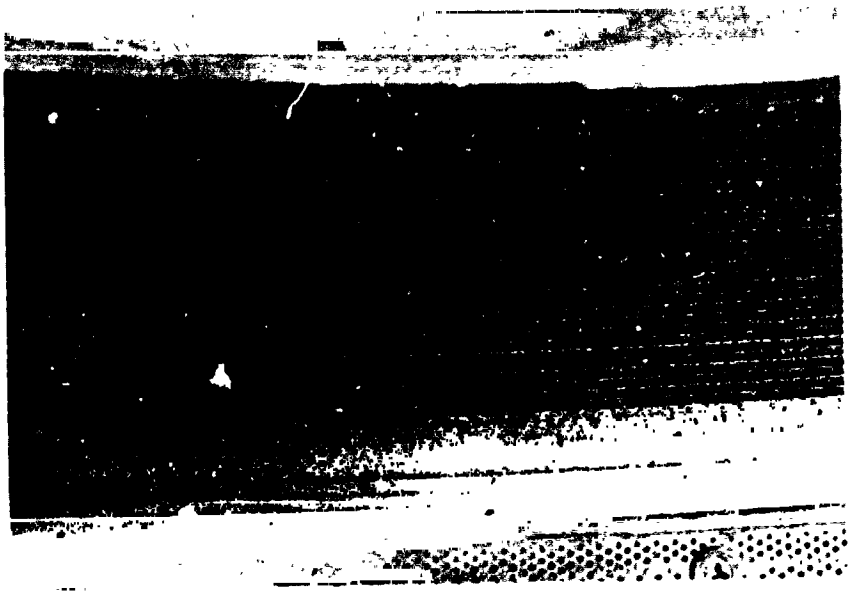

Figure 4-39. Epoxy Microballoon Fan Shroud Material Showing Typical Erosion Effects After Revenue Service.

Figure 4-10. Epoxy Microballoon Fan Shroud Material with Open Cells After Repair.

spacer adjacent to the vane airfoil may crack, causing a piece to eventually break away from the spacer. This results in a leakage path as well as allowing flow recirculation. The accepted repair for this condition is to replace the spacer or to fill in the gap with a material such as a room-temperature vulcanizing (RTV) compound, which provides an excellent flowpath filler. Most of the repairs observed, however, had very poor filler radii and poor smoothing of the RTV, so that a blockage was formed. Figure 4-41 compares examples of both good and poor installation. Since the quality of this repair is variable and the performance impact small, it is difficult to estimate an efficiency loss. An improvement in performance, however, can be realized by replacing the poor quality RTV repair with a new nylon spacer or replacing the RTV.

Splitter Leading Edge Erosion:

A flow splitter aft of the fan blade is provided which also forms the bypass ID flowpath and booster stage OD. The leading edge was blunt and heavily eroded on all modules. The erosion appears to have occurred during the initial 4,000 to 6,000 hours with little additional bluntness beyond the 6,000-hour mark. The "as new" leading edge shape is similar to a 65 series airfoil leading edge on a circular arc meanline. The erosion produces a blunt nose of about 0.15-inch thick, and the leading edge drag coefficient was estimated to have increased by a unit of 1.0 based on thickness frontal area. This results in a net bypass efficiency loss of 0.12 points which is equivalent to 0.07 percent increase in cruise fuel burn.

Inner IGV Bushings:

The inner end of the booster IGV utilizes a nylon bushing that conforms to and provides part of the inner flowpath, and also stabilizes the inner section of the vane. This nylon bushing tends to work itself out into the flowpath by as much as 0.10 inch, causing a flow blockage. This condition can be remedied by using an adhesive like RTV, which has proved to be successful in keeping the nylon bushing flush with the flowpath surface. Since this condition varies from engine to engine and within an engine, a loss in performance will not be presented for the average engine, but controlling with an adhesive will result in a small performance improvement.

Airfoil quality degradation is the second of two general classifications of fan section deterioration and includes the fan blade leading edge quality, airfoil quality of fan and booster blades and vanes, and condition of bypass OGV's.

Fan Blade Leading Edge:

The shape of the fan blade leading edge is extremely important for optimum performance. Erosion of the leading edge in 6,000 to 8,000 hours of engine operation has been observed to be a significant deterioration mode (Figure 4-42). While it is difficult to analytically assess the performance effects

Figure 4-41. Fan Outlet Guide Vanes with Repaired Nylon Spacers.

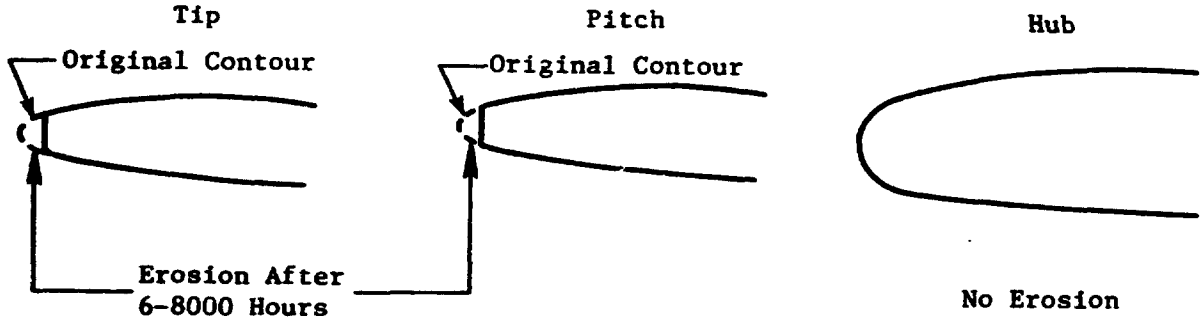

Figure 4-42. Erosion Pattern on Stage 1 Fan Blade.

from changes to the fan blade leading edge shape, factory and field testing have permitted a reasonable assessment. This experience consists of back-to-back factory engine tests to measure engine performance with only the fan blade leading edges deliberately blunted between runs. In addition, back-to-back engine performance tests were also conducted utilizing typical revenue service fan blades with eroded leading edges reworked between runs using the tool supplied for this purpose.

Based on this background and visual observations, the average performance degradation due to fan blade leading edge bluntness after 6,000 hours of engine operation was estimated at 0.9 percent fan efficiency, which is equivalent to 0.44 percent cruise fuel burn. It is noted that the leading edge condition varied significantly between parts. This is as expected since erosion/impact conditions are dependent on geographical area, ground time, etc.

Fan Blade Airfoil Quality:

Small pock marks approximately 0.004-inch to 0.006-inch deep were observed in the concave surface of the fan blade airfoil in the first 2 to 3 inches above the hub. There was a large difference in the number of indentations observed in blades from different engines, suggesting they may be a function of engine position and environment as well as time. During a shop visit, the indentations can not be removed since complete removal would result in excessive removal of blade material, resulting in thinning of the airfoil. Dirt buildup on both the concave and convex side of the fan blade was present, and reviews indicate that the dirt accumulates during the first few hundred hours of operation and does not seem to worsen with additional time. This dirt is typically of the "cosmetic" variety and can be removed simply by washing the blades with a commercial solvent. Both the surface finish and dirt accumulation effects relating to efficiency are subjective evaluations.

The pitting observed on the fan blade pressure side of the airfoil degrades the new blade surface finish from a required 55μ in./in. AA to an estimated 120μ in./in. AA in about 6,000 hours. This roughness increase occurs primarily over the first 3 inches of the airfoil chord and over the entire span. This results in a loss of 0.06 percent fan efficiency, or 0.03 percent cruise fuel burn based on analytical calculations.

Dirt deposition on airfoils is a surface roughness condition; but direct measurements cannot be obtained since the measurement stylus cuts away the dirt surface. Again, back-to-back testing between as-received and cleaned blades has been completed in both factory and field test cells. Based on this experience, it was estimated that the loss due to dirt accumulation after 6,000 engine hours was 0.24 percent in fan efficiency or 0.12 percent in cruise fuel burn.

Fan Outlet Guide Vane Degradation:

Significant erosion and impact deterioration have been observed on the fan (bypass) OGV's, as these parts are typically not repaired during a shop visit. The polyurethene protective coating has been lost and the leading edge blunted due to erosion. The surface finish has increased from 20μ in./in. AA to approximately 160μ in./in. AA on the suction side and to 180μ in./in. AA on the pressure side due to the loss of the protective coating.

The increased surface finish drag results in a fan efficiency loss of 0.36 percent, and the blunt leading edge is estimated to sustain an additional 0.12 percent loss in fan efficiency. This is equivalent to 0.18 percent and 0.06 percent loss in cruise fuel burn, respectively. It is estimated that this level of deterioration occurs by 4,000 to 6,000 hours of service and then remains relatively constant.

Booster Airfoils:

As noted previously, booster modules are only infrequently disassembled during routine shop visits. Visual observations indicated minor erosion of the rotor blades and stator vanes with some blunting of the leading edge. Surface finish measurements generally indicated roughness in the order of 45 to 55μ in./in. AA as compared with 24μ in./in. AA for new parts. This degradation is equivalent to a booster efficiency loss of 0.06 percent and a 0.01 percent increase in cruise fuel burn.

A summary of the fan section performance deterioration is presented in Table 4-XIV. The data have been presented as the estimated average loss for 6,000 hours of operation, although some parts of the module might accumulate 15,000 hours with little or no repairs. The total loss assessed for the fan section after 6,000 hours of engine operation is 1.32 percent in cruise fuel burn which is equivalent to a 0.88 percent increase in fuel burn in 4,000 hours. Airfoil quality degradation represents 64 percent of the loss; the remaining 36 percent is attributed to flowpath deterioration.

An estimate of the fan section deterioration characteristics with time is depicted in Figure 4-43. This curve presents the best estimate for the deterioration rate for each damage mechanism based on extrapolation of available data. The rate was assumed to be linear for each damage mechanism where empirical data were not sufficient to make a realistic estimate.

Table 4-XIV. Estimated Deterioration in Fan Section After 6000 Hours.

	Δ SFC at Cruise, percent
Fan Blade	
Tip Clearance	0.38
Leading Edge Contour	0.44
Surface Roughness	0.03
Dirt Accumulation	0.12
Splitter Leading Edge	0.07
Bypass OGV	
Leading Edge	0.06
Roughness	0.18
Booster	
Tip Clearance	0.03
Surface Roughness	0.01
Net	1.32%

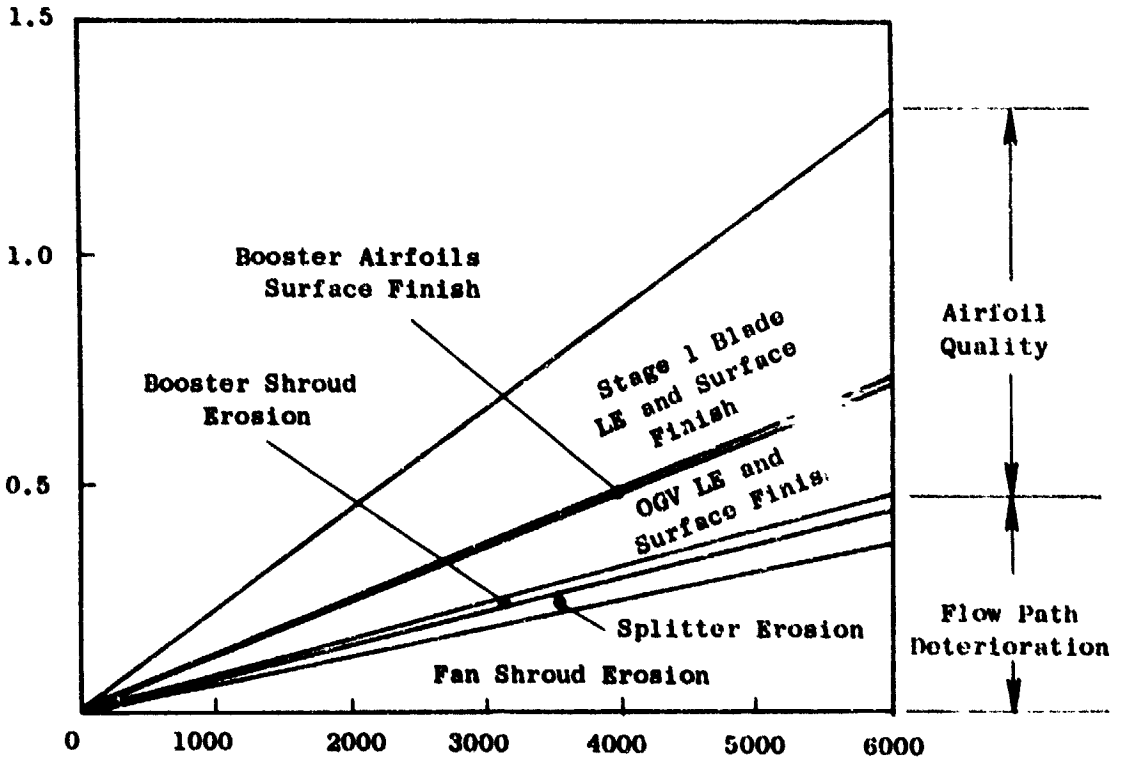

Figure 4-43. Fan Section - Estimated Deterioration Characteristics at 6000 Hours.

High Pressure Compressor Section - Performance deterioration of the high pressure compressor (HPC) can result from a number of factors. These factors can be generally classified as either airfoil tip clearance changes, airfoil quality degradation, or leakage. A cross section of the HPC module showing the deterioration modes is presented in Figure 4-44.

Airfoil Tip Clearance:

Increases in blade-to-casing or vane-to-rotor spool clearances can result from coating losses or rubs, and from blades and vanes which may have been shortened in prior rubs or as a result of inadequate shop procedures.

Flowpath Coatings used in the HPC are intended to provide protection from abrasion of the casing and rotor structure, to provide an abradable material which allows for small local rubs without causing a major change in blade or vane height, and to minimize or prevent HPC mechanical damage. The abrasive material used is Metco 450 plasma spray, which affords protection for the casing and rotor structural members. This material also provides a bonding surface for an abradable aluminum spray coating used in the forward stages as shown in Figure 4-45. Revenue service experience indicated, however, that the aft stages of aluminum coating suffered degradation due to spalling. This condition occurs as a result of thermal cycling which causes the aluminum/Metco 450 bond coat interface to fail due to the differences in thermal expansion between the aluminum and structural surface. Figure 4-46 illustrates a typical example of spalled coatings.

Figure 4-47 shows the percentage of coating spalled for the aft stages of the compressor after 4,000 and 8,000 hours. Evidence of spalled coatings on the rotor forward of Stage 7, and on the casing forward of Stage 8 was nonexistent. The average losses in the aluminum coating result in a clearance increase of approximately 0.015 inch, and small additional sfc losses due to increases in flowpath surface roughness.

Airfoil Tip Rubs produce increased radial tip clearances, increased roughness of the rubcoat, and roughness of the airfoil surface finish due to the deposited aluminum debris liberated as a result of the rub. Tip rubs are most likely to occur during takeoff at aircraft rotation, or during a hot rotor reburst at low altitudes. Rotor blade rubs were observed on the aluminum coating of the upper casing in Stages 3 through 9 over an arc of abou 120 degrees and to a maximum depth of about 0.010 inch. The performance effects from these rubs are small, since (unlike in the HP turbine) the rubs locally remove the coating material with only a negligible change in blade length. Vane tip-to-spool rubs were not observed, as expected, since these clearances are set to specifically avoid any rubs during engine operation.

Blade and Vane Tip Clearances changes as a result of changes in roundness of the HPC casing were observed, but these clearance changes did not occur during in-service operation. The compressor stator casing consists of a titanium forward casing and an Inco 718 steel rear casing which are rabbeted and bolted

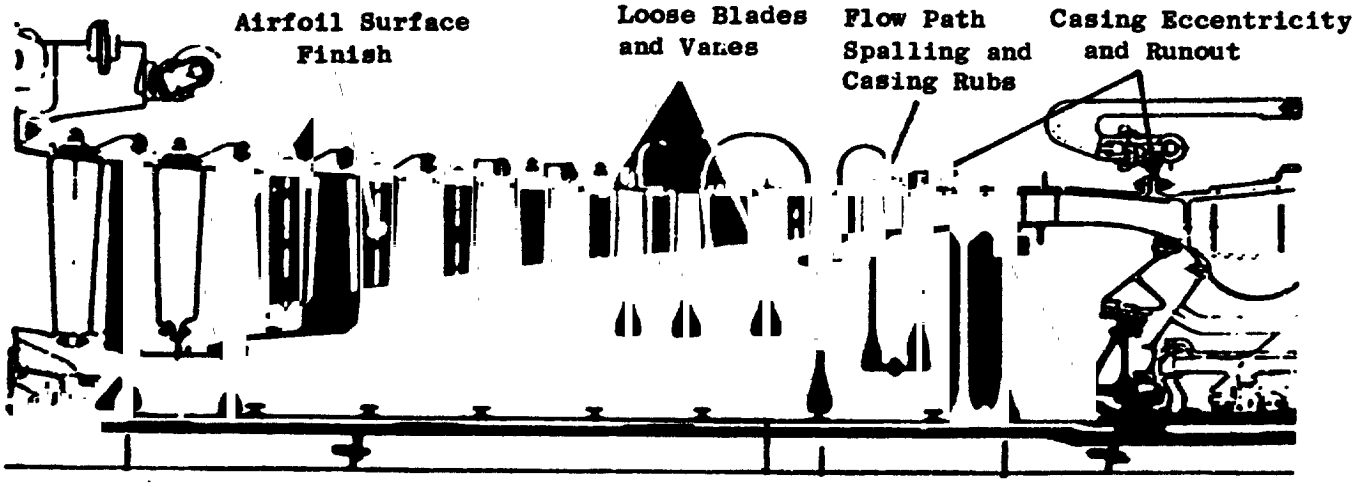

Figure 4-44. CF6-50 Deterioration Modes - HP Compressor Section.

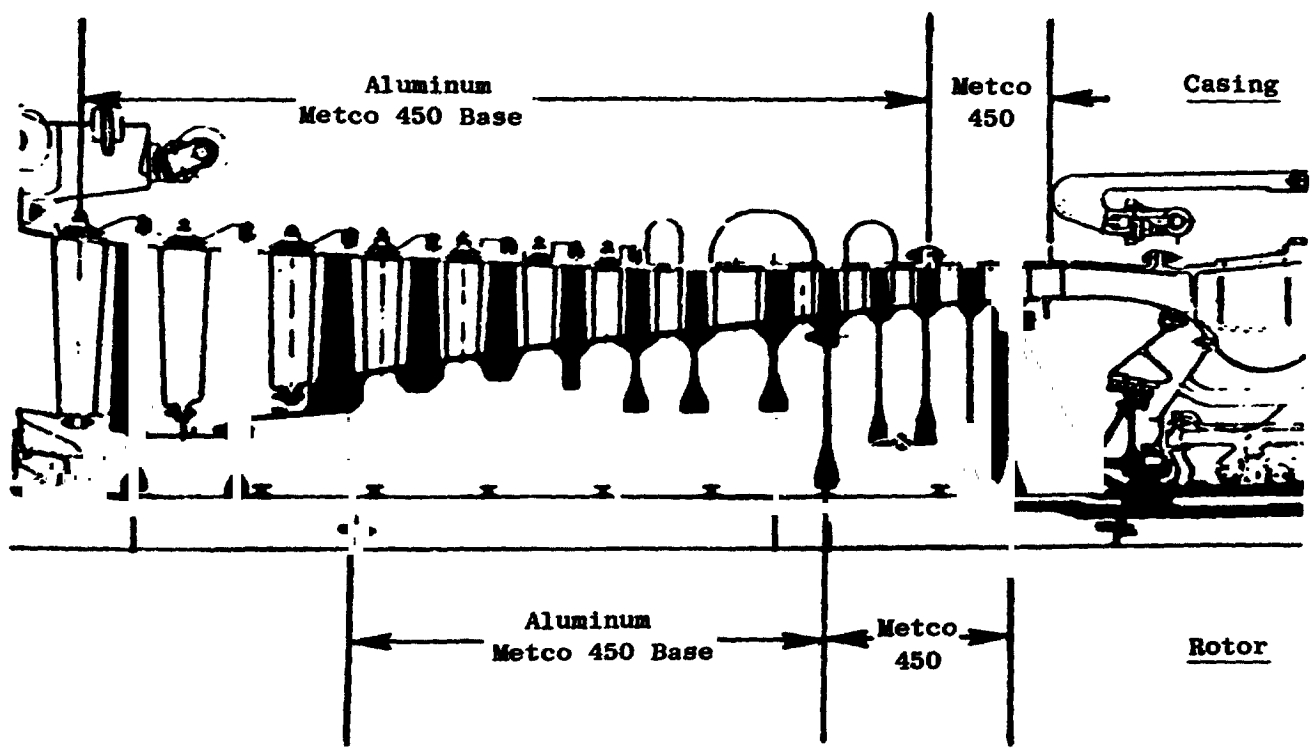

Figure 4-45. CF6-50 Flowpath Coatings - HP Compressor Section.

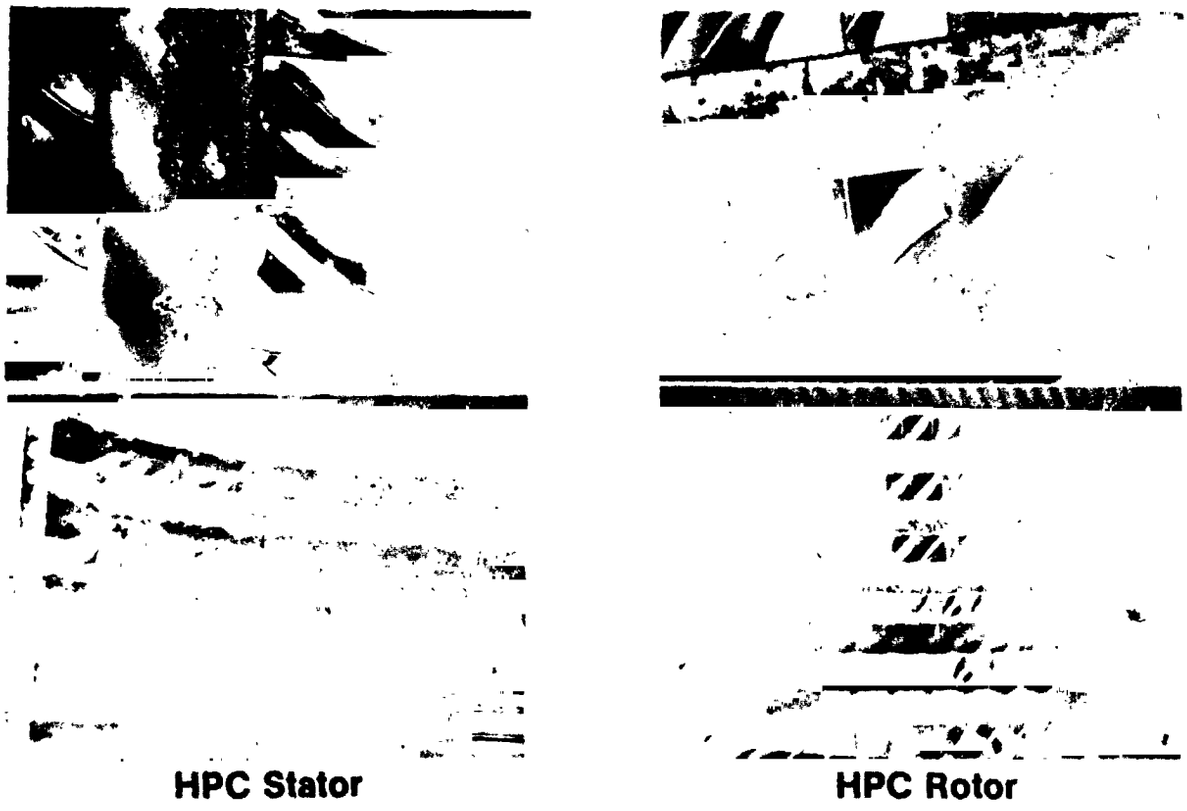

Figure 4-46. Examples of Spalled Coatings in HPC.

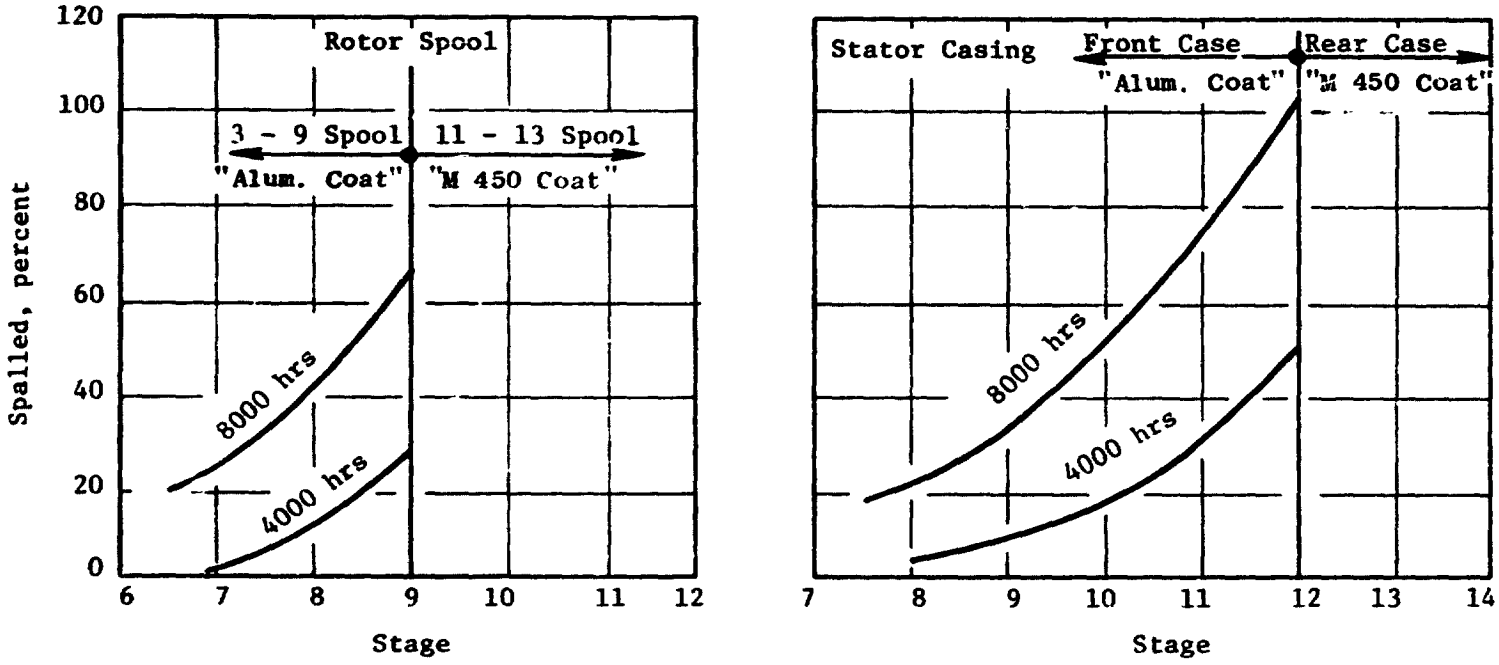

Figure 4-47. Abradable Rub Coating Deterioration.

together using clearance bolts. At operating conditions, relatively high stresses are induced in the titanium flange because the thermal coefficient of expansion of the front casing is much lower than that of the rear casing. These stresses cause the titanium flange to creep, permanently increasing the rabbet diameter. As the permanent deformation of the flange increases, the thermal stresses diminish by creep relaxation and eventually the flange growth stops. As long as the joint is not split, the two casings are held concentric by the bolt clamp load. However, during repair, if the casings are split and then reassembled, they may become eccentric because of the loose rabbet (Figure 4-48). Furthermore, the thermal stresses in the titanium flange will be large again because the clamp load is sufficient to hold the two flanges together by friction. Consequently, the flange growth and the accompanying stress relaxation will resume during subsequent engine operation.

Rabbet growth versus service time is plotted in Figure 4-48 which includes data from both the factory test and the field engines. The data show considerable spread because the rabbet growth depends on the service use, and on the number of times the casings have been split and reassembled.

During an engine rebuild, the blades and vanes are assembled into the spool and casing and subjected to a machining operation to produce a calculated blade-to-casing and vane-to-rotor spool minimum clearance. Casing distortions (Figure 4-49) necessitate additional machining to correct local areas of underminimum clearances, which produce larger average clearances and a loss in performance. All blade tips must be machined by the additional amount equal to the casing eccentricity, while the vane tips are machined locally consistent with the casing eccentricity. Therefore, the average clearance increase for the vanes is less than that produced for the blade tips.

Casing out-of-roundness also produces an effect on average clearance similar to that presented for casing eccentricity and is illustrated in Figure 4-49. As shown in Sketch A in this figure, all blade tips must be machined shorter by the magnitude of the casing out-of-roundness to produce the correct minimum clearances. The vanes, as shown in Figure 4-49 (Sketch B), only need to be shortened in the area of the casing which is inwardly displaced.

Stator casing out-of-roundness was investigated for both production new and airline service parts. The airline service parts were inspected both during the repair with the rub coat material stripped and after refurbishment. The sample size and inspection results are presented in Table 4-XV. These data show a significant out-of-roundness condition for both nonrepaired and refurbished casings compared with data obtained from factory new parts. The average of these data and maximum out-of-roundness values obtained are presented by stage in Figure 4-50.

To determine the average clearance increase from casing distortion, 36 refurbished casing subassemblies were measured for vane tip radii. The results are summarized in Figure 4-51 showing the average maximum deviation for the vane tip radii. For blades, it was assumed that the average clearance was

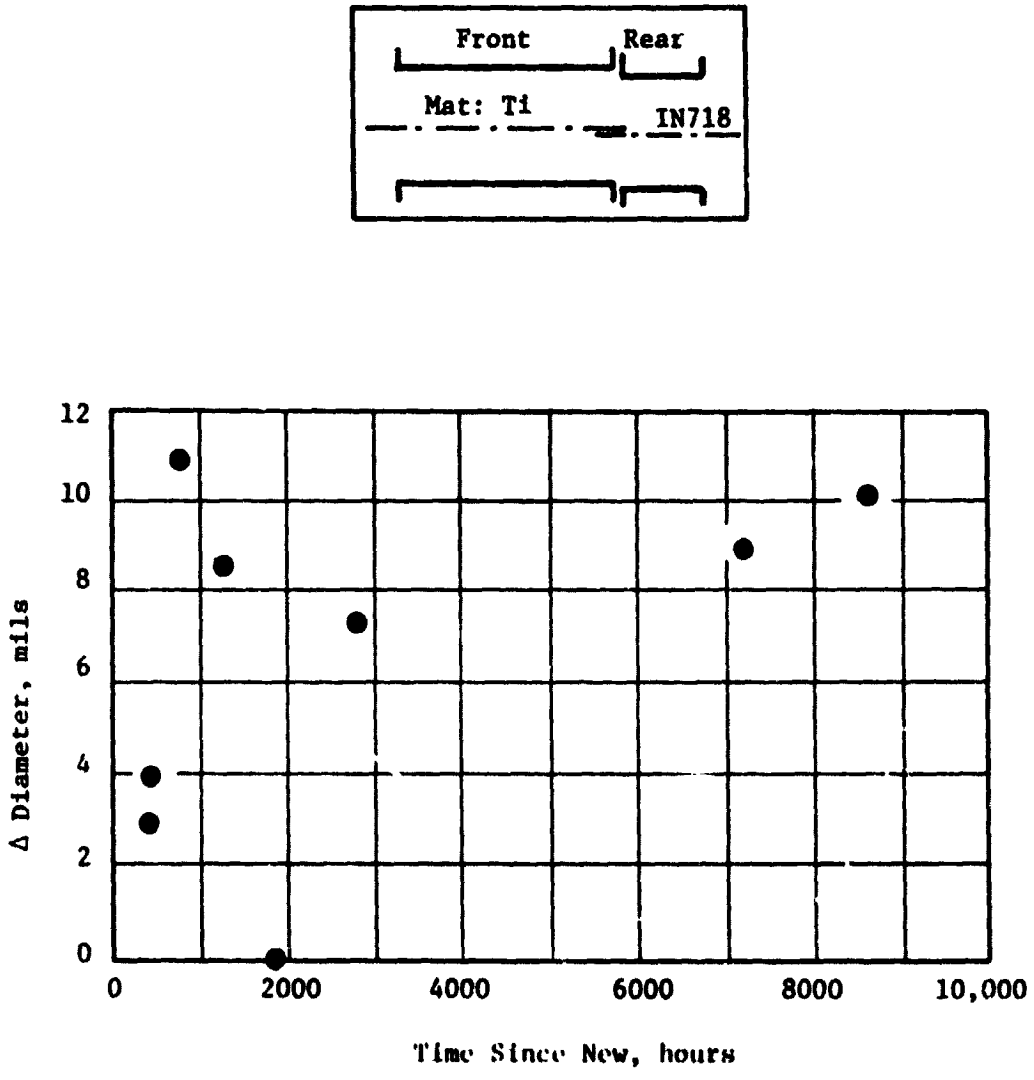

Figure 4-48. Flange Growth/Casing Eccentricity.

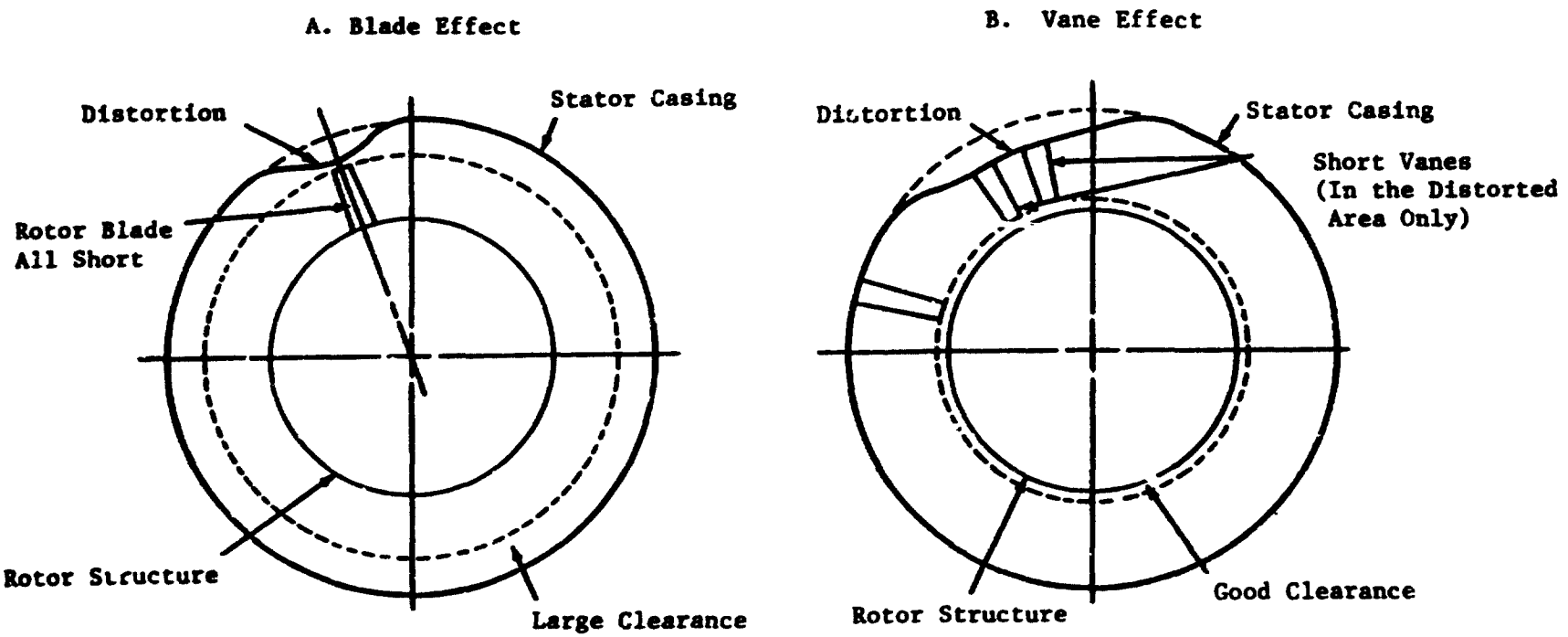

Figure 4-49. Effect of Casing Distortion.

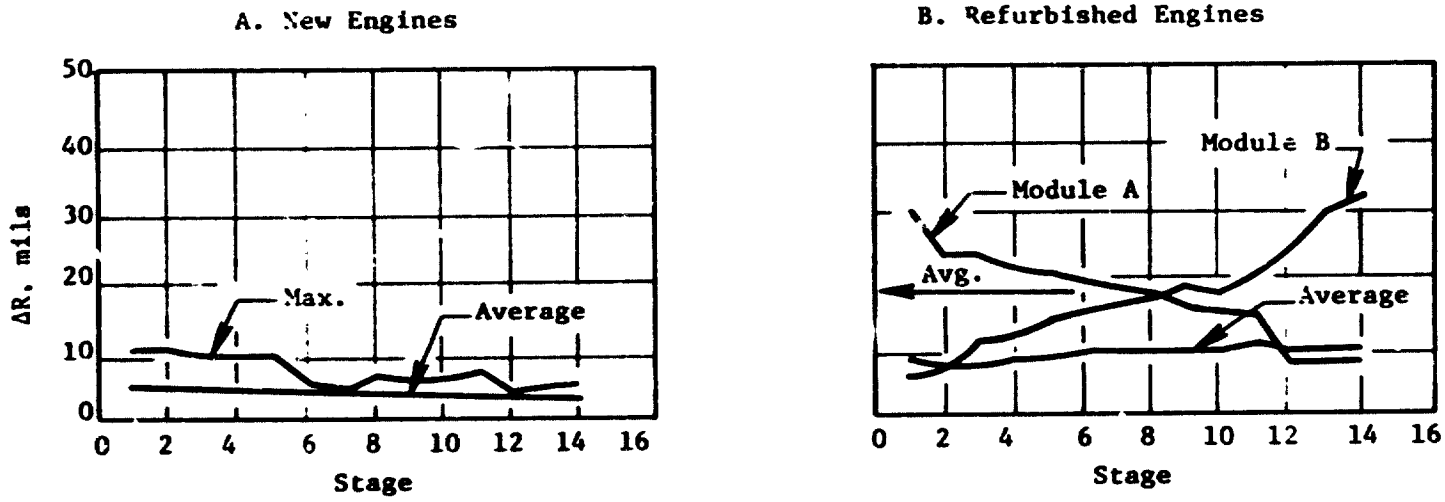

Figure 4-50. Casing Out of Roundness.

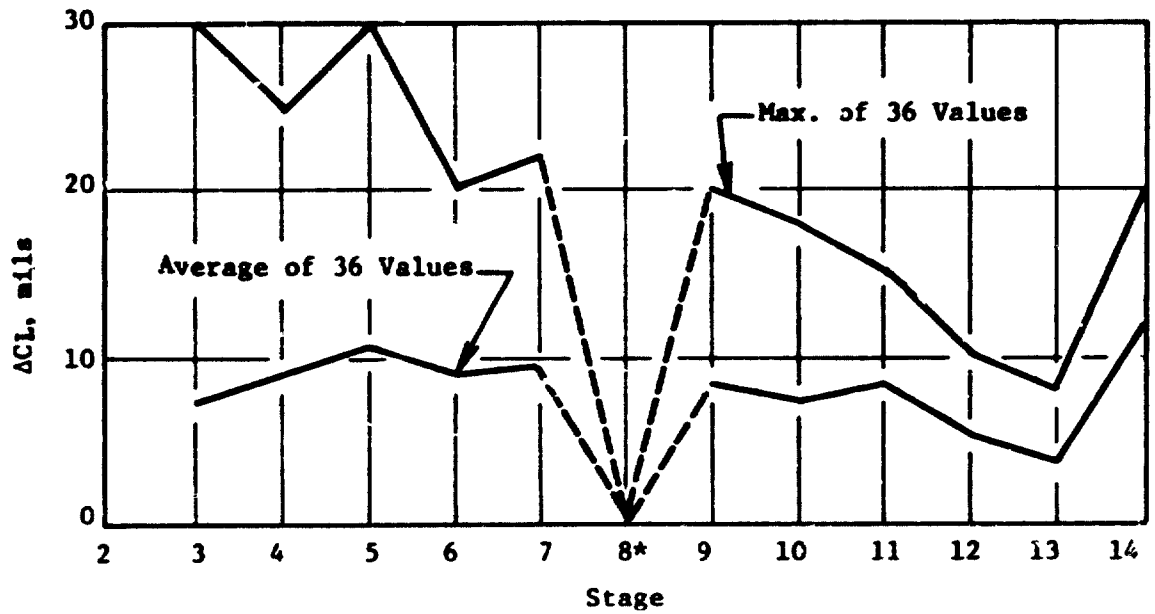

* Stage 8 Vanes are not Reworked.

Figure 4-51. Clearance Difference from Nominal Versus Stage - Short Vanes Result of Assembly Rework.

Table 4-XV. Casing Out of Roundness.

	Max. Rad - Min. Rad. (Mils)		Sample Size
	Avg.	Max.	
New Casings	5.0	11	23
Field Casings Stripped	13.2	64	26
Field Casings Refurbished	8.5	32	26

equal to the casing out-of-roundness. This assumption was found to significantly underestimate the blade effect as will be discussed in the next paragraphs.

While the individual compressor rotor and casing subassemblies are machined as individual modules to meet a calculated minimum clearance, actual verification of the clearance is required during engine buildup. This is accomplished by applying "wax strips" of known thicknesses on the casing and rotor spool lands, and then installing the casing halves (top and bottom) around the rotor. The rotor is rotated through 360 degrees; the casings are removed, and the wax strips are examined and measured. If rubs are noted on the wax strips, then hand grinding of the blades and vanes is performed to produce the desired minimum clearance.

A specific engine that failed to meet minimum performance standards after having been refurbished was disassembled and inspected. Inspection of the HP compressor which had been refurbished prior to the test cell run, indicated a large out-of-roundness condition of the casing as shown in Figure 4-52. An inspection of the rotor blade tips revealed a generally rounded condition rather than the expected square shape; a sketch showing this condition is included in Figure 4-52. This shape resulted from hand grinding during engine buildup to achieve the required minimum clearance. As noted in Figure 4-52, casing out-of-roundness was less than 0.020 inch in Stage 13, but the blades were up to 0.040 inch shorter at the leading and trailing edges. This was typical for this engine, and is a good example of how the average clearance effects from eccentric and/or out-of-round casing can be magnified. Hand grinding cannot be as closely controlled as machine grinding, and sometimes requires several "trial and error" rework cycles to produce the required minimum clearances. The procedure is also time consuming to recheck clearances and to reapply the wax strips, and the rework man tends to remove "more than enough" material the first time to avoid repeat cycles. A procedural change has been specified to require remachining rather than hand grinding if the required rework exceeds a specified level.

The total average increase in clearances per stage for a typical 4,000-hour compressor is presented in Figure 4-53. The individual increases due to rub coat spalling, blade tip rub, eccentricity, and out-of-roundness are shown.

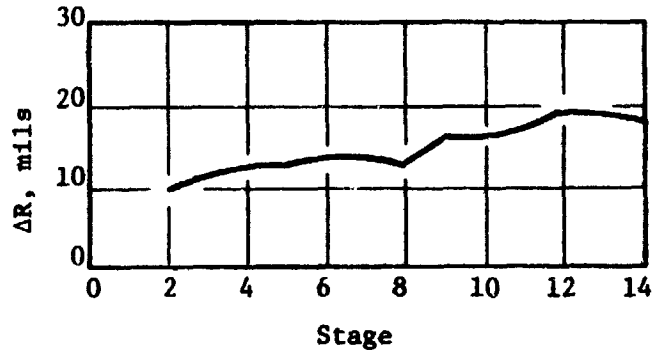

Casing Out of Roundness Versus Stage

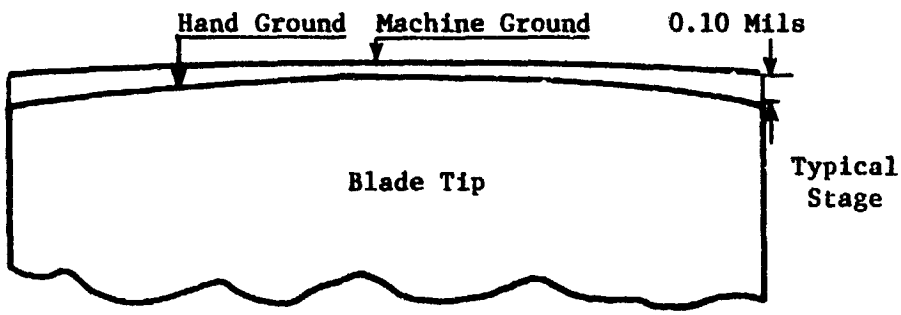

Hand Grinding of Blade Tips at Assembly

Figure 4-52. Types of Deterioration Modes: Casing Out of Roundness and Hand Grinding of Blade Tips.

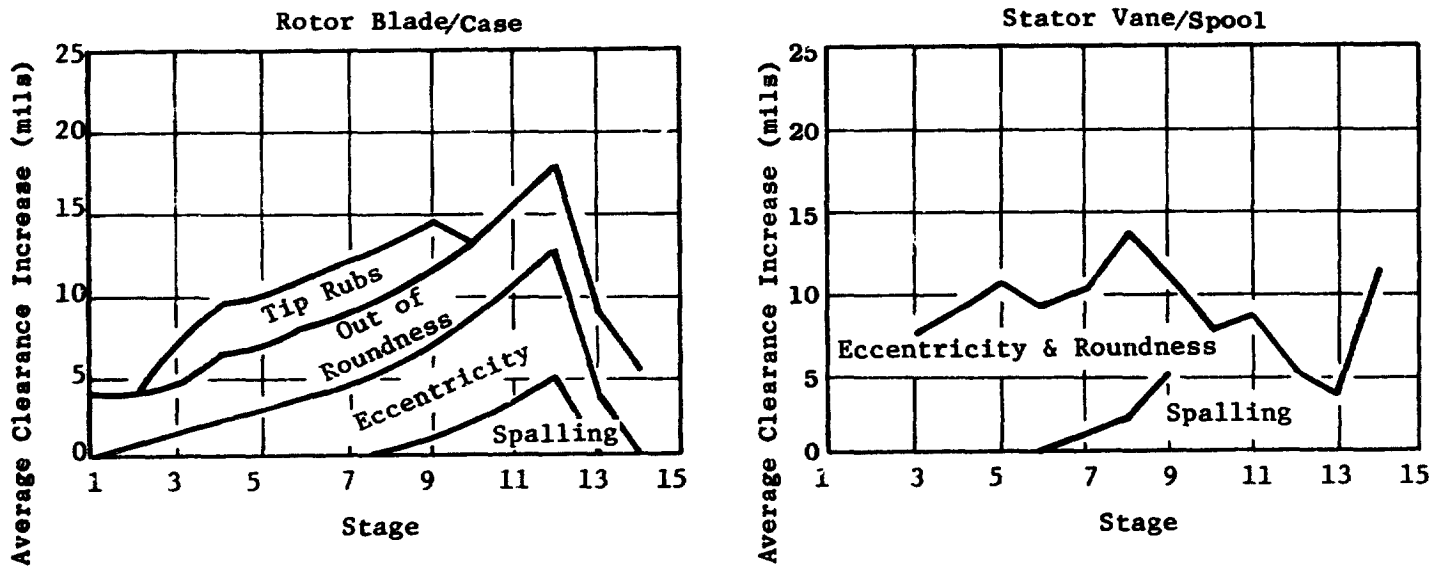

Figure 4-53. HP Compressor Tip Clearance Increase After (4000 Hours).

Airfoil Quality:

Performance deterioration resulting from airfoil contour changes, erosion of the airfoil tips, increased airfoil surface roughness, and leading edge bluntness have also been evaluated for the CF6-50 HP compressor.

Changes in Airfoil Contour may occur due to mechanical damage which is caused either by tip rubs or by ingested objects. The rub induced damage, under normal operating conditions, is minor. It occurs only in the cases of the most severe rubs and is manifested as blade leading and trailing edge tip curls. The ingested object damage involves a few blades and does not produce a measureable performance degradation in an average engine.

Airfoil Tip Erosion (Figure 4-54) is a form of deterioration which is not considered to be a fleet-wide problem since it appears to be event oriented and related to flight route structure. Tip erosion has been observed to occur in some engines either taking off from, or landing at, airports with a sandy environment or which have runways that are treated with sand or salt during the winter months.

Surface Finish measurements of some blades and vanes are made for varying service times, and the data obtained are summarized in Figure 4-55 and 4-56. The results are plotted versus service time and also versus stages, and no definitive trend was indicated. It is evident that the finish deteriorates in service, but there is no clear indication as to which stages are affected the most, or how long it takes to stabilize. Surface finish may be affected by the enviroment which also produces blade erosion, and this may explain the rather wide spread in the data.

The average airfoil surface finish was 45μ in./in. AA relative to a 24μ in./in. AA average for new airfoils. This results in a loss of 0.27 percent HP compressor efficiency equivalent to a 0.11 percent cruise fuel burn. Similarly, the surface roughness increase for the spalled casing and spool surface (described in the HP Compressor Clearance Section) resulted in a loss of 0.015 percent HP compressor efficiency or 0.01 percent cruise fuel burn.

Leading Edge Bluntness was also determined to be a source of airfoil quality degradation. Although difficult to assess, it was estimated that the airfoil leading edge was eroded to a flat surface about 5-mils wide. This would result in an HP compressor efficiency loss of 0.28 percent or 0.11 percent in cruise fuel burn.

Leakages:

Another potential factor in HP compressor degradation is the level of internal and external airflow leakages which are illustrated in Figure 4-57.

Loose Blades resulting from wear of the protective coatings provided on the blade and disk dovetail interfaces which, in turn, increase blade platform-to-disk clearances in Stages 3 and aft, produce excessive airfoil hub flow recirculation. In Stages 1 and 2, this wear increases clearances between

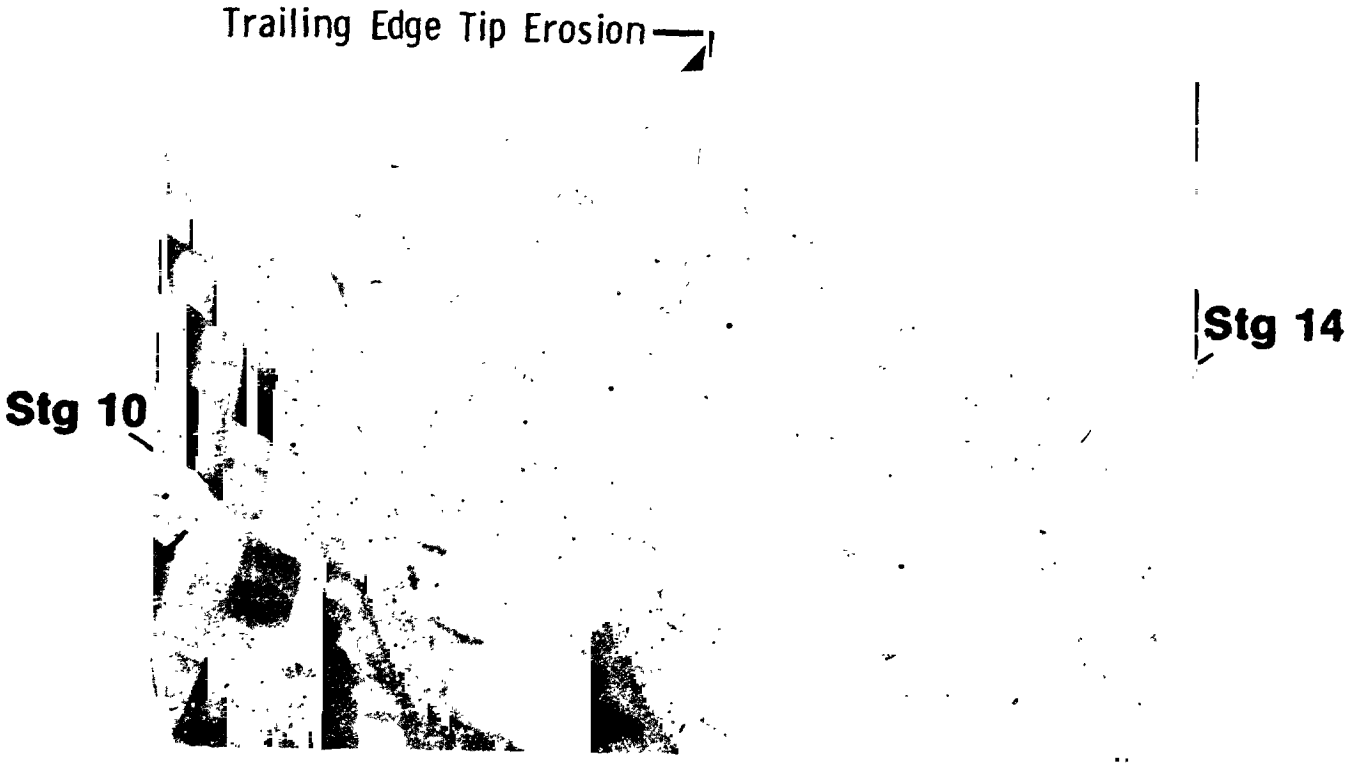

Figure 1-54. Example of Airfoil Tip Erosion.

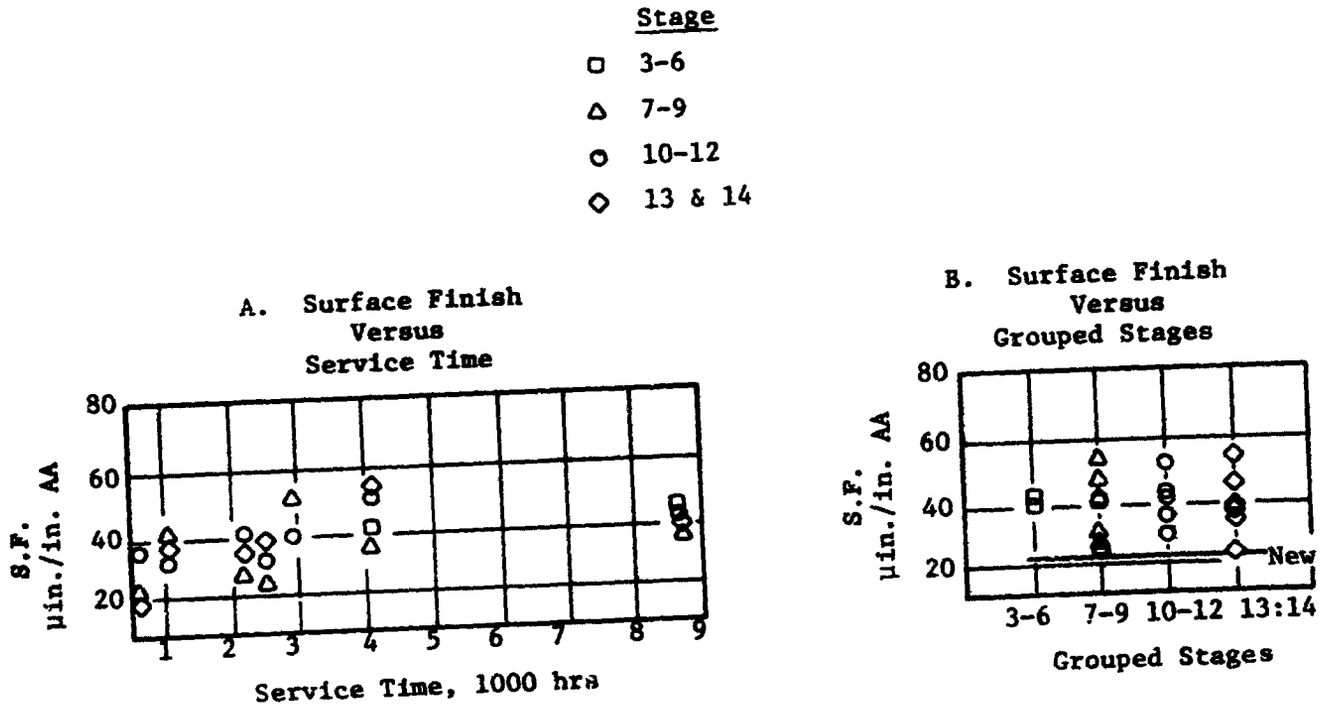

Figure 4-55. Degradation of Rotor Blade Surface Finish.

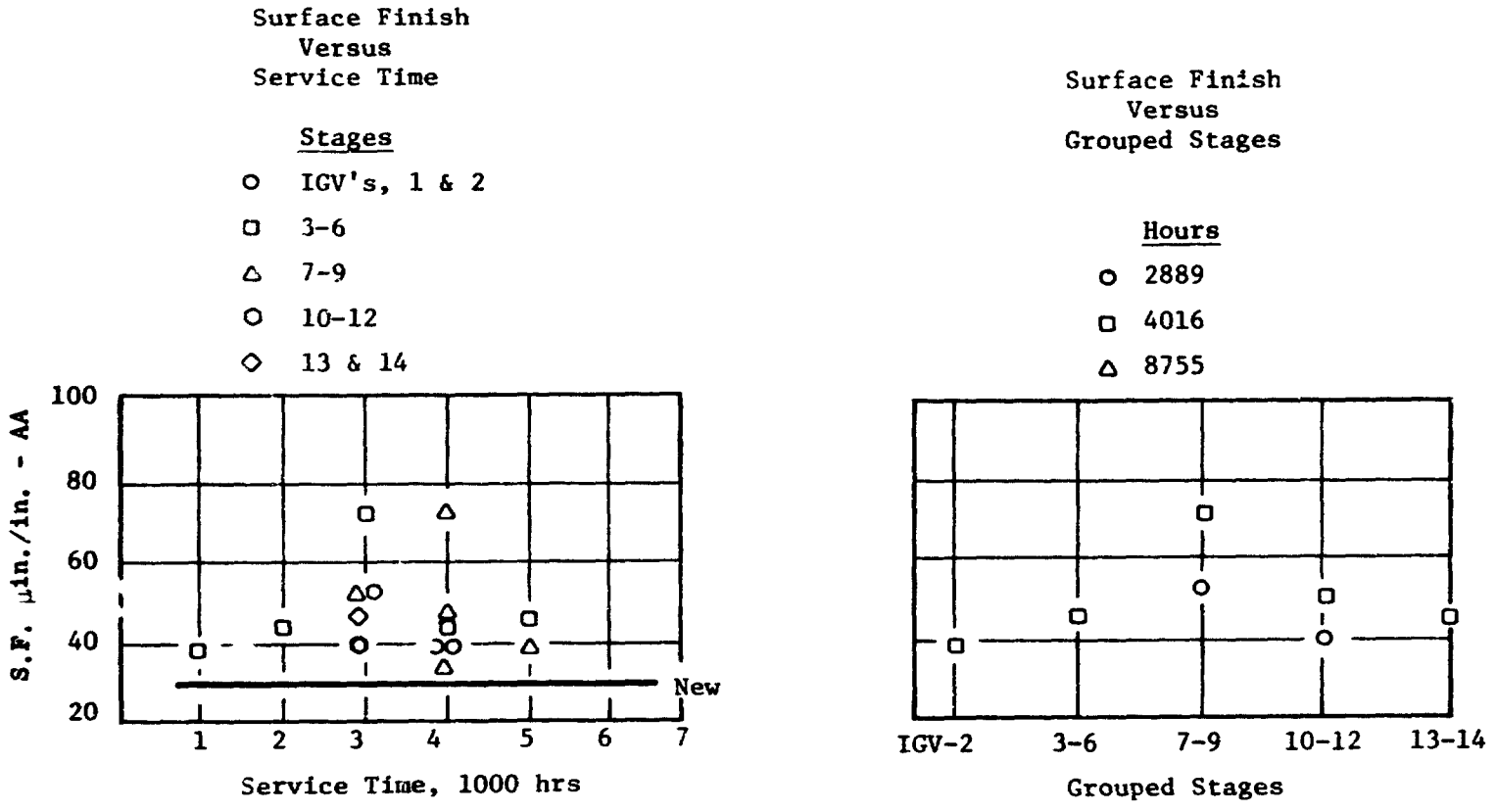

Figure 4-56. Degradation of Stator Vane Surface Finish.

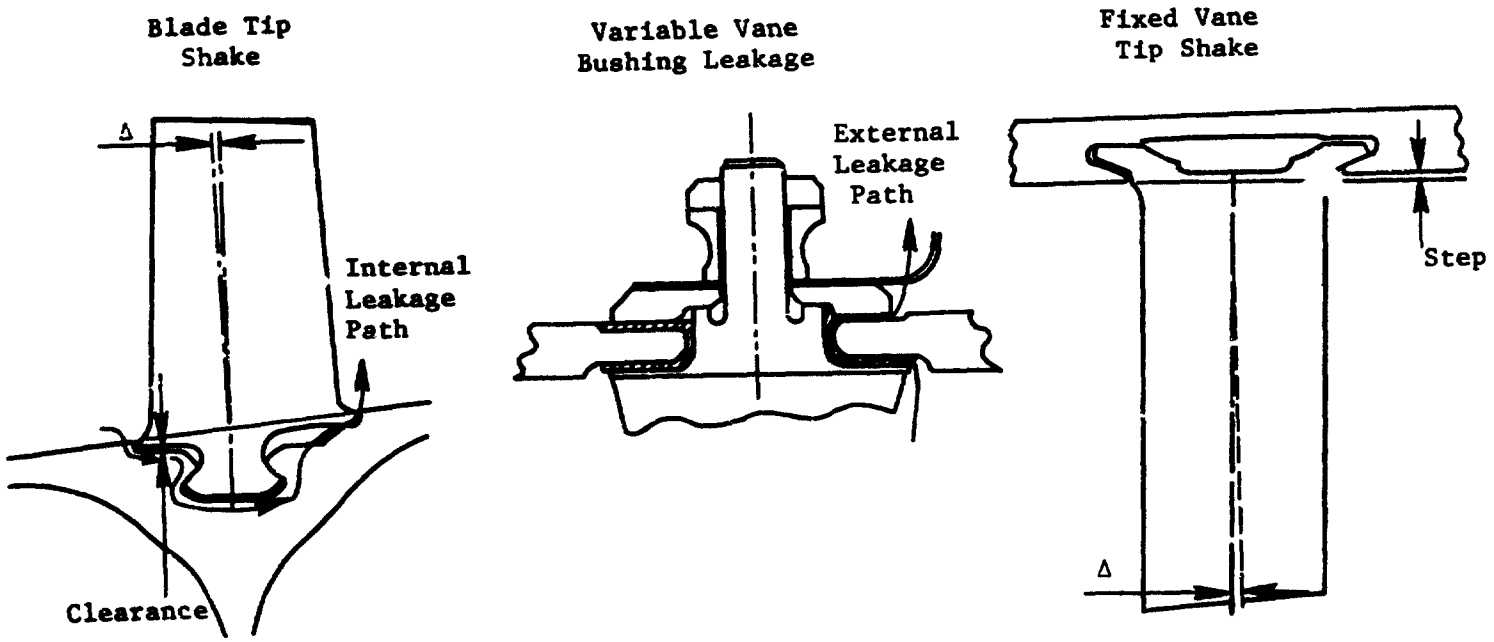

Figure 4-57. Loose Blades and Vanes.

the blade dovetail base and the disk dovetail slot bottom. Tip shake data, a good indicator for dovetail clearances, are plotted versus stages in Figure 4-58.

Loose Vanes caused by wear of the washers and bushing of the vane-to-casing bearing surfaces, result in external air leakage (Reference Figure 4-57). The wear is most pronounced in Stage 5 because of the highest unit bearing loads and the operating temperature. Furthermore, for a given clearance, the losses are greatest in Stage 5 because of the greatest pressure drop across the leakage path. The average life of bushings and washers for Stage 5 is shown in Figure 4-59.

In the fixed stator vanes, Stage 6 and aft, dovetail wear is more pronounced on the aft side, thereby producing aft-facing steps (flow disturbances) and, hence, a loss in performance. Depth of the steps is related to the vane tip shake in the axial direction as shown in Figure 4-57. Vane tip shakes measured in compressor stator casing assemblies are plotted in Figure 4-58.

Overall Leakage Losses are summarized in Table 4-XV. The losses are assessed to be 0.11 percent HP compressor efficiency and 0.041 percent cruise fuel burn for the loose blade and stationary vanes, and an additional 0.15 percent fuel burn loss for the variable vane leakage.

A summary of the sources of performance deterioration for the CF6-50 high pressure compressor is presented in Table 4-XVI. As shown, the major loss is due to increased tip clearances for the blade and vane airfoils which represents 44 percent of the total assessed loss.

The estimated rate of deterioration for each damage mechanism isolated during this study is presented in Figure 4-60. The short airfoil effect is shown as a constant loss since the deterioration occurs during engine refurbishment and not during revenue service.

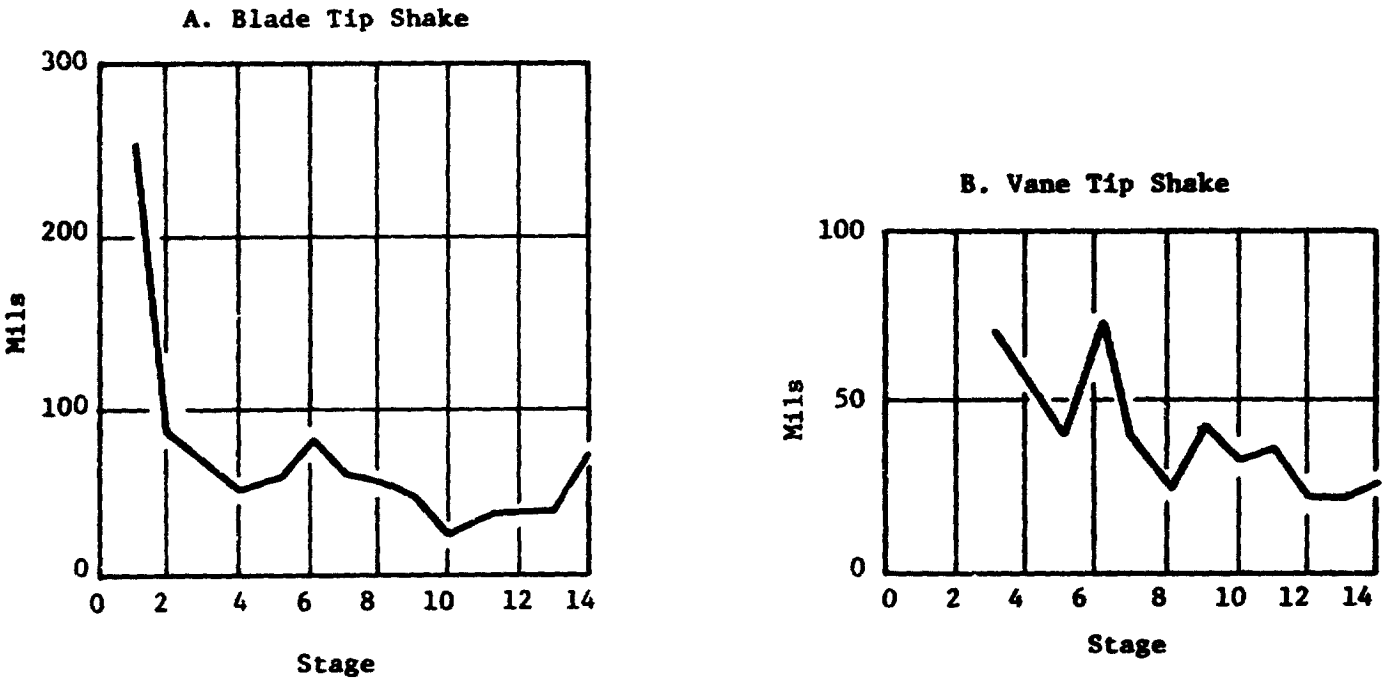

Figure 4-58. Blade and Vane Dovetail Looseness (4000 Hours).

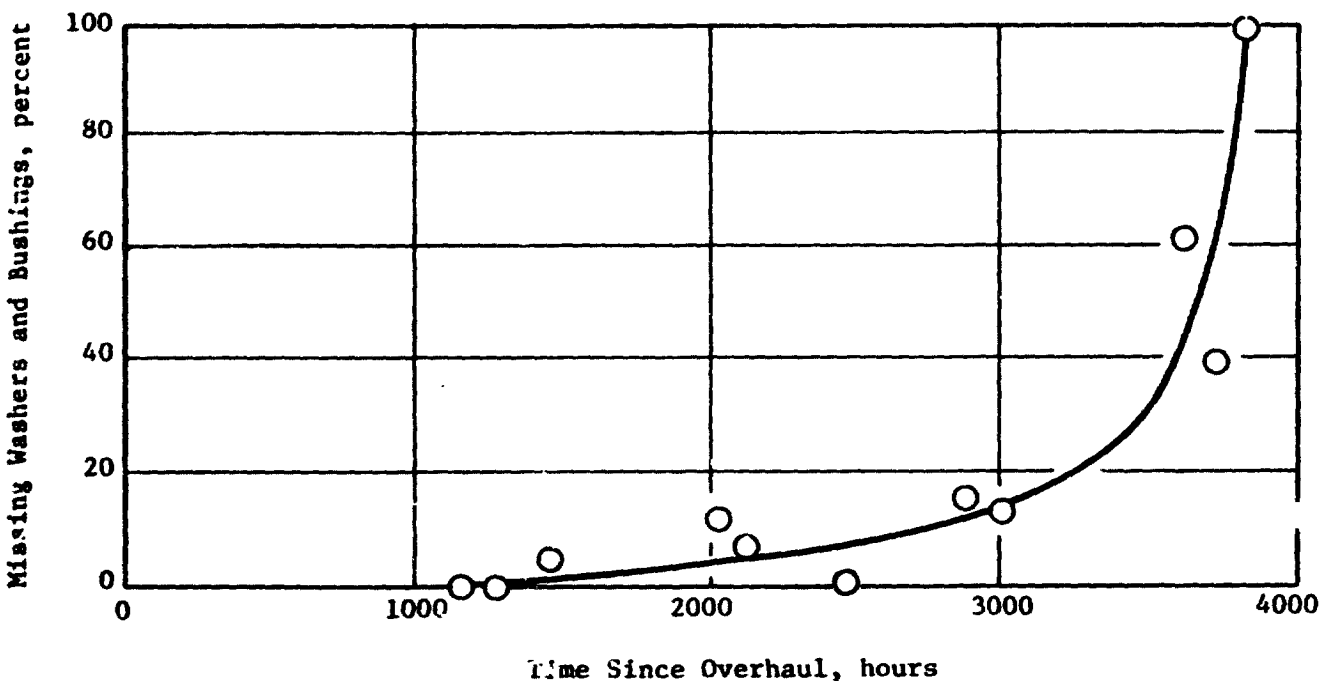

Figure 4-59. Stage 5 VSV Bushing Life.

Table 4-XVI. HP Compressor Section - Estimated Deterioration at 4000 Hours.

	Δ SFC at Cruise (percent)
Increase in Airfoil Tip Clearances	0.33
Airfoil Leading Edge Bluntness	0.11
Airfoil Finish Degradation	0.11
Casing and Spool Coating Degradation	0.01
Variable Vane Leakage	0.15
Loose Blade and Vane Losses	0.04
Net	0.75

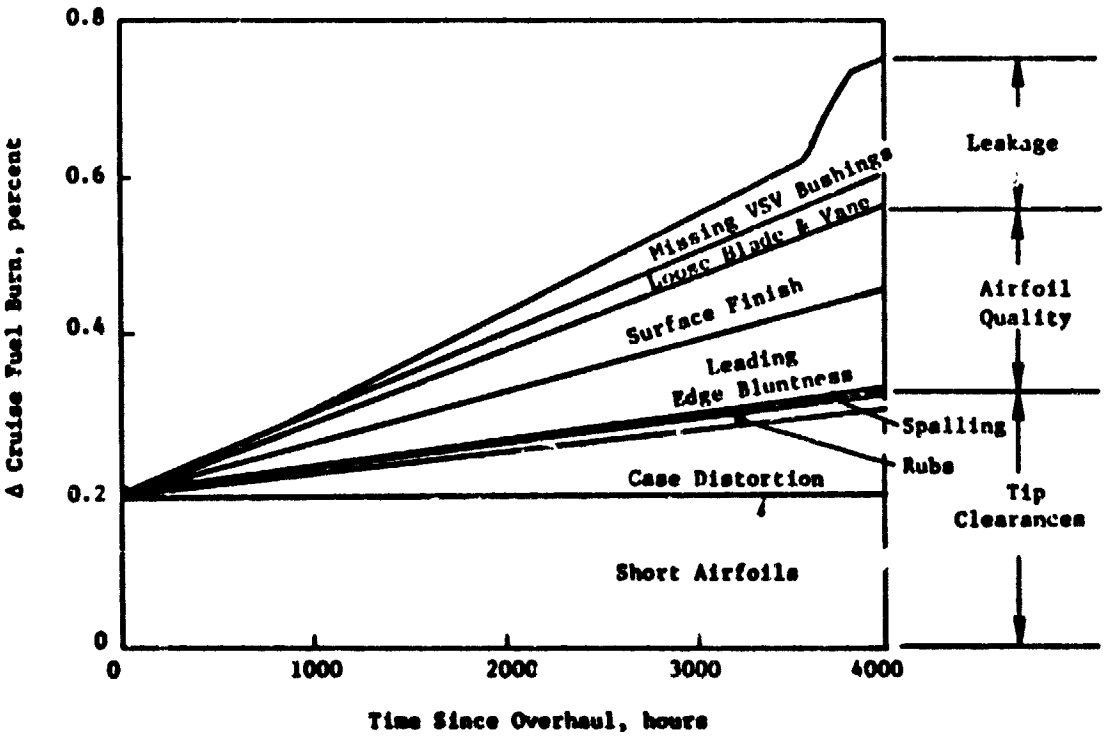

Figure 4-60. HP Compressor Section - Estimated Deterioration Characteristics at 4000 Hours.

High Pressure Turbine Section - The primary causes of high pressure turbine (HPT) deterioration are changes in blade tip-to-shroud clearance, airfoil surface finish, and internal leakage (parasitics). Figure 4-61 is a schematic indicating areas of interest.

Blade Tip Clearances:

Experience from the CF6-6D engine indicated that the major cause for increased blade tip-to-shroud clearance was rubs. These rubs are very local; but since the shroud is not abradable, the blade tips are all shortened during a rub resulting in a significant increase in average clearance. This has led to the development of a procedure for monitoring blade tip rubs without engine disassembly. Notches of varying depths are incorporated in the tips of several HPT blades during rotor assembly. The HPT blades are readily inspected with the engine installed through borescope ports incorporated for condition monitoring, and the remaining notches are "counted" during routine inspection. Since the notches are successively deeper (Figure 4-62) blade length change can be determined, thus affording a general assessment of the rotor blade tip-to-shroud clearance change. This approach was also used to evaluate tip rubs for CF6-50 high pressure turbine blades.

A more accurate assessment of blade tip-to-shroud clearance change is obtained from in-shop measurements of blade and shroud radii prior to repair of deteriorated components. This requires measurement of each blade tip near both the leading and trailing edge with the rotor assembly in a lathe bed, and each shroud at the corresponding axial location. The radius is obtained for each individual shroud in three separate locations (each end and middle) with the assembly restrained on a special fixture. These measurements are very difficult to obtain from the airlines since the checks are not standard, are time consuming, and utilize the same fixtures as used to build up modules for spare engines.

The data from both measurement systems (i.e., visual inspection of blade tip notches and in-shop dimensional inspections) are shown in Figures 4-63 and 4-64. As shown, there is no clear correlation of blade tip wear with accumulated time. However, averaging the data for approximate 500-hour intervals and plotting against a common "zero" point did indicate a trend as shown in Figures 4-65 and 4-66. Figure 4-65 indicates that the majority of the loss due to Stage 1 clearance increase occurs during the initial 1,500 hours of operation and remains relatively constant. The data sample size for the points beyond 2,000 hours is small, and the dotted line represents our best estimate for 4,000 hours of operation. Similarly, the majority of the increased clearance for Stage 2 occurs early (at approximately 1,000 hours), and then remains relatively constant. The dotted line (Figure 4-66) also represents the best esimtate for 4,000 hours of operation.

While the primary cause for clearance increase is blade tip rubs, the erosion and oxidation of blade tips and shrouds also produce a minor affect. While not directly discernible from the empirical data, the estimated losses shown in Figures 4-65 and 4-66 after 4,000 hours include calculated effects for these secondary sources.

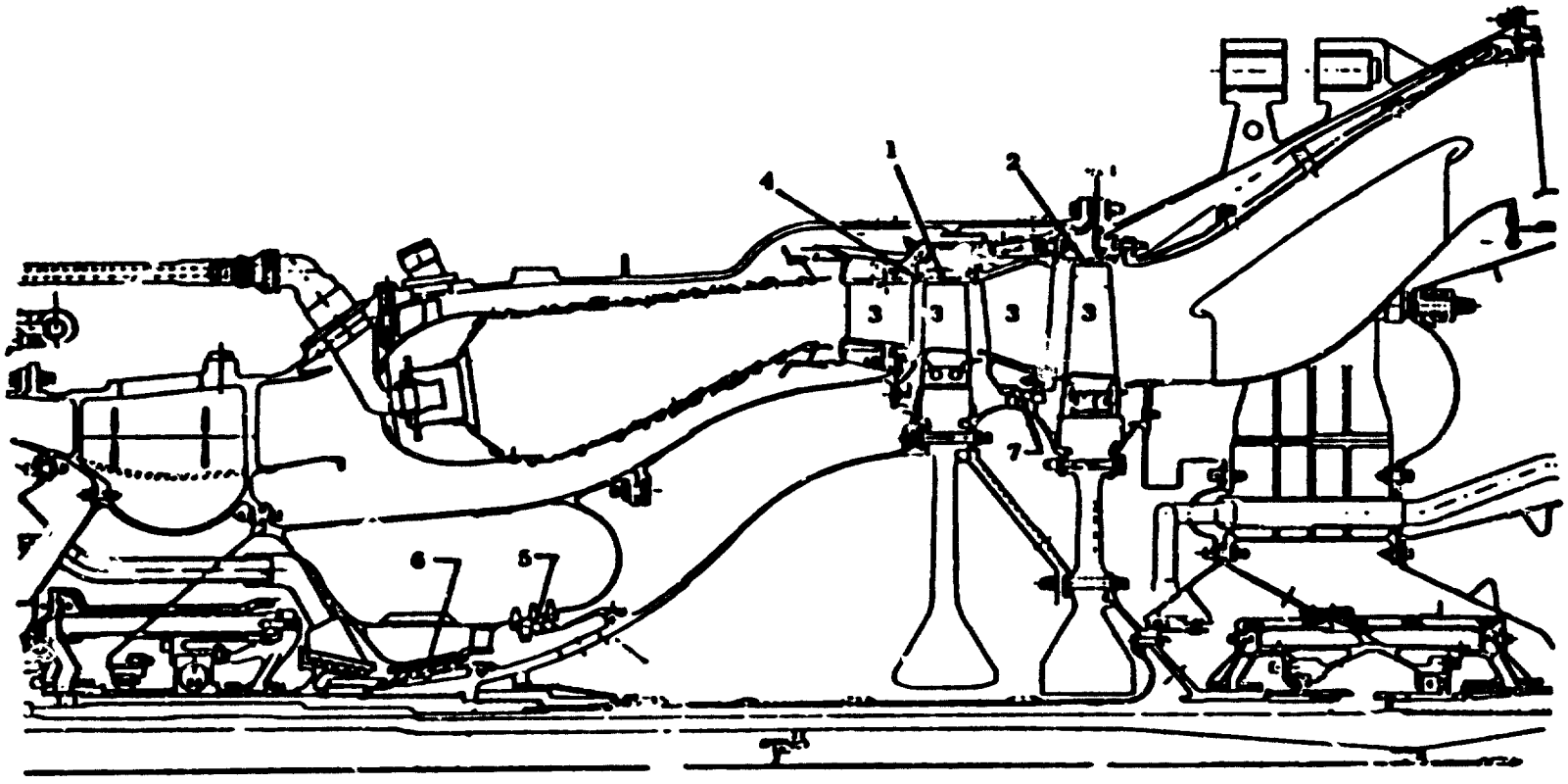

1 Stage 1 Blade Tip Clearance Increase
2 Stage 2 Blade Tip Clearance Increase
3 Airfoil Surface Finish Degradation
4 Stage 1 Nozzle Outer Band Leakage
5 Balance Piston Seal Leakage
6 CDP Seal Leakage
7 Interstage Airseal Leakage

Figure 4-61. CF6-50 Deterioration Modes - HP Turbine Section.

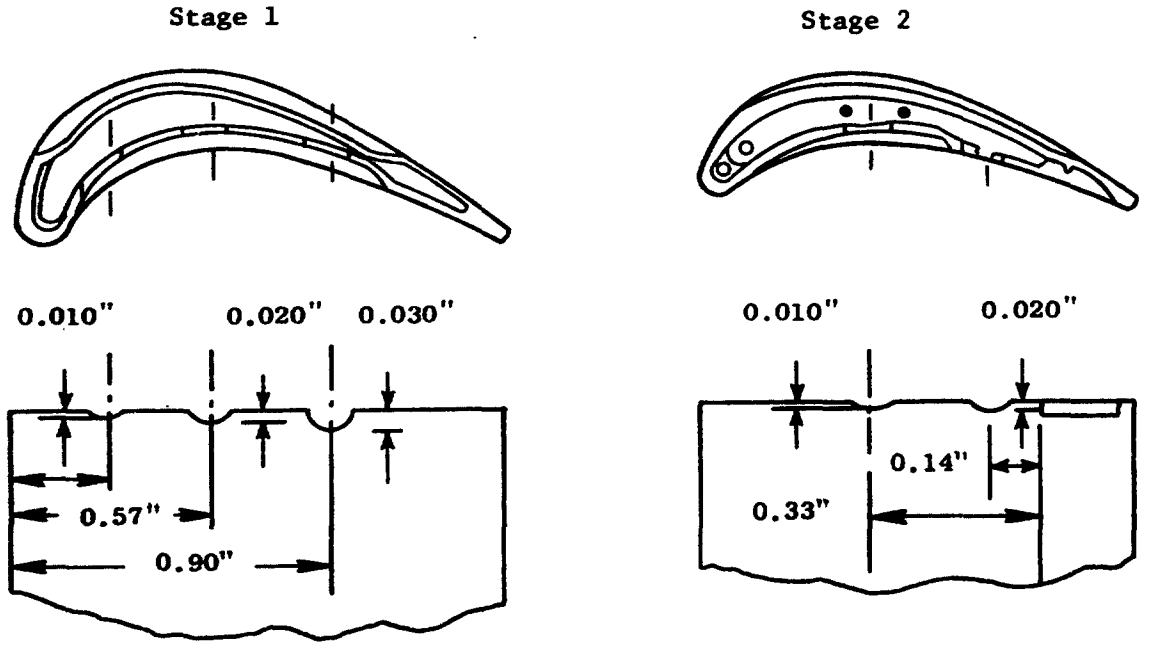

Figure 4-62. HP Turbine Blade Tip Notches (Concave Side Only).

C-2

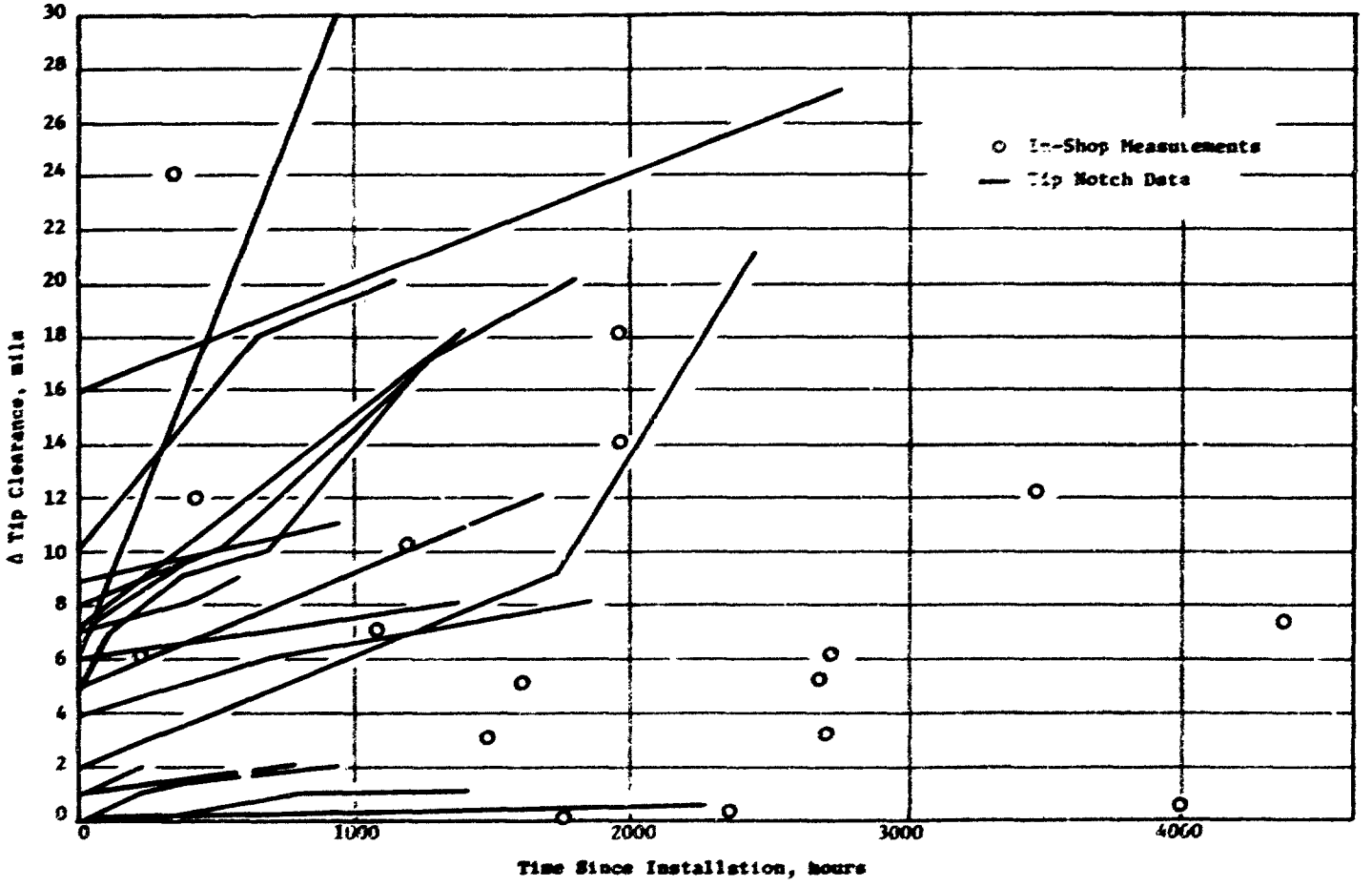

Figure 4-63. Stage 1 Blade Δ Tip Clearance Versus Time.

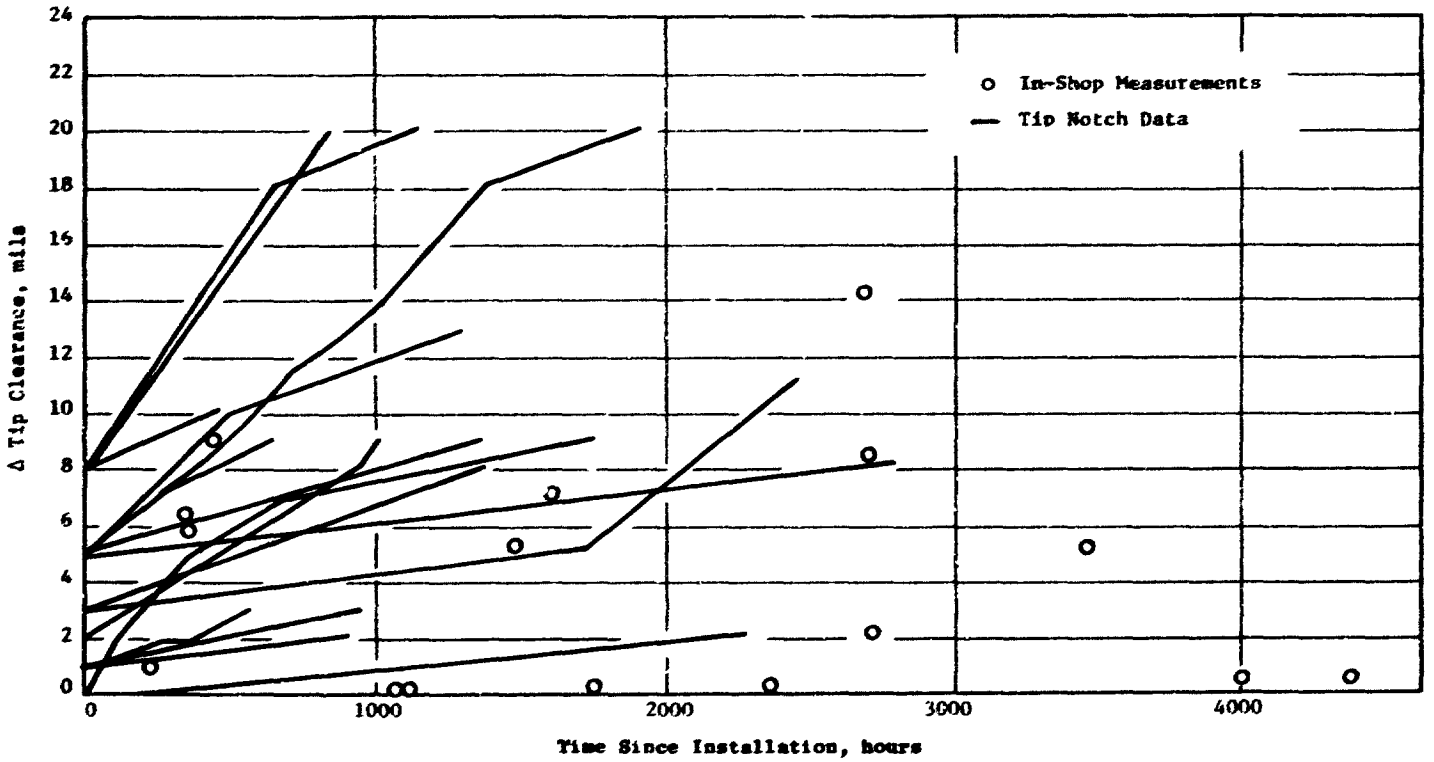

Figure 4-64. Stage 2 Blade Δ Tip Clearance Versus Time.

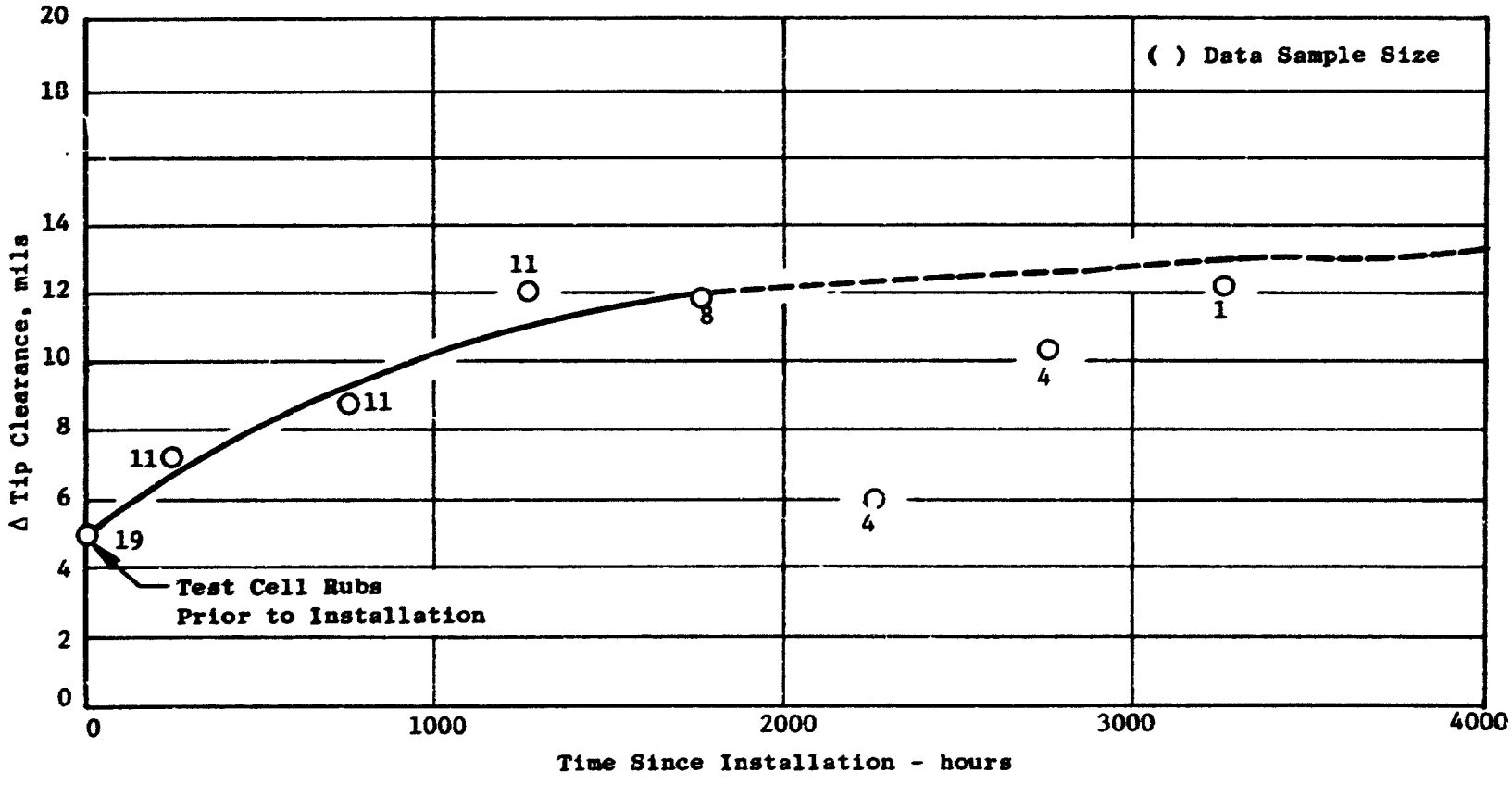

Figure 4-65. Trend of Stage 1 HP Turbine Blade Tip Clearance.

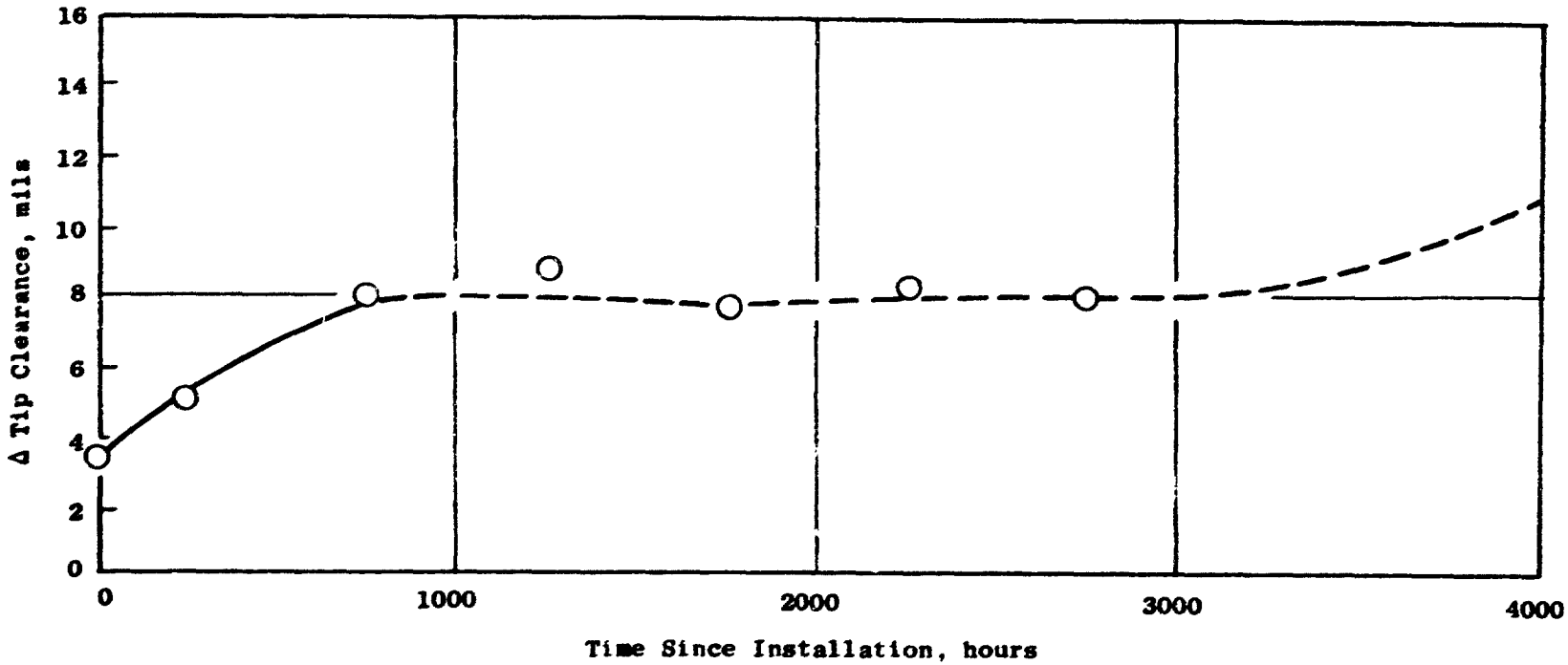

Figure 4-66. Trend in Change of Stage 2 HP Turbine Tip Clearance.

The combined performance effects from the 13-mils increase in Stage 1 clearance and 11 mils in Stage 2 after 4,000 hours is 0.81 percent in HP turbine efficiency, which is equivalent to a 0.55 percent increase in cruise fuel burn.

Blade tip-to-shroud rubs are caused by many factors; the primary effects being shroud support distortion, shroud swelling and bowing, shrinkage of the shroud supports, and thermal mismatch between rotating and static structures during engine transients.

Analytical predictions of Stage 1 and 2 shroud distortions at takeoff and cruise power are illustrated in Figures 4-67 through 4-71. Three takeoff transients (10, 80, and 120 seconds), stabilized takeoffs, and cruise settings are presented. These out-of-roundness distortions are considered to be repeatable, and the arrows indicate the locations where rubs would most frequently occur. Each curve (Figures 4-67 through 4-71) also indicates the calculated round engine clearance. The difference between the round engine clearance and the out-of-roundness shown represents the unrepeatable (randomly varying in magnitude and location) out-of-roundness which can occur before rubs are incurred. Unrepeatable out-of-roundness causes are related to such things as individual part and assembly tolerances, side "g" loads, combustor pattern factor, and nacelle air leaks. Figures 4-72 and 4-73 are polar histograms of the field experience from 58 engines which present the number of rub occurrences versus circumferential location. Comparison of the out-of-roundness predictions (Figures 4-67 through 4-71) with field experience (Figures 4-72 and 4-73) reveal reasonably good agreement.

Another variable that influences shroud rubs is the change in the radial dimensions of the Stage 1 shroud support. Measurements of the shroud support reveal that the support (and shrouds) creep radially inward, and the rate of creep becomes less with accumulated time. The average radial inward shrink is 0.006 inch after 4,000 hours.

Although not normal during revenue service, it is possible that a sequence of operational events could result in turbine blade rubs and therefore increased blade-to-shroud clearances during subsequent operation. This sequence of events could lead to what is referred to as a "warm" or "hot" rotor reburst condition. This can occur when an engine, after operating at high power conditions, is decelerated to idle or low power for a short period of time (less than 5 minutes) and then is rapidly accelerated to a high power condition. During the short period of time at idle speed, the HPT components do not reach a thermal equilibrium before the engine is re-accelerated. The static structure tends to cool more rapidly than the rotor during this short interval at idle speed producing tighter-than-normal clearances. Then the subsequent rapid acceleration can produce rubs due to decreased clearances at idle coupled with the clearance closure which results from blade loading. This sequence of events for thermal growth of the static structure and rotor is depicted in Figure 4-74. For this example, the engine is re-accelerated about 150 seconds after the chop-to-idle-speed operation was initiated.

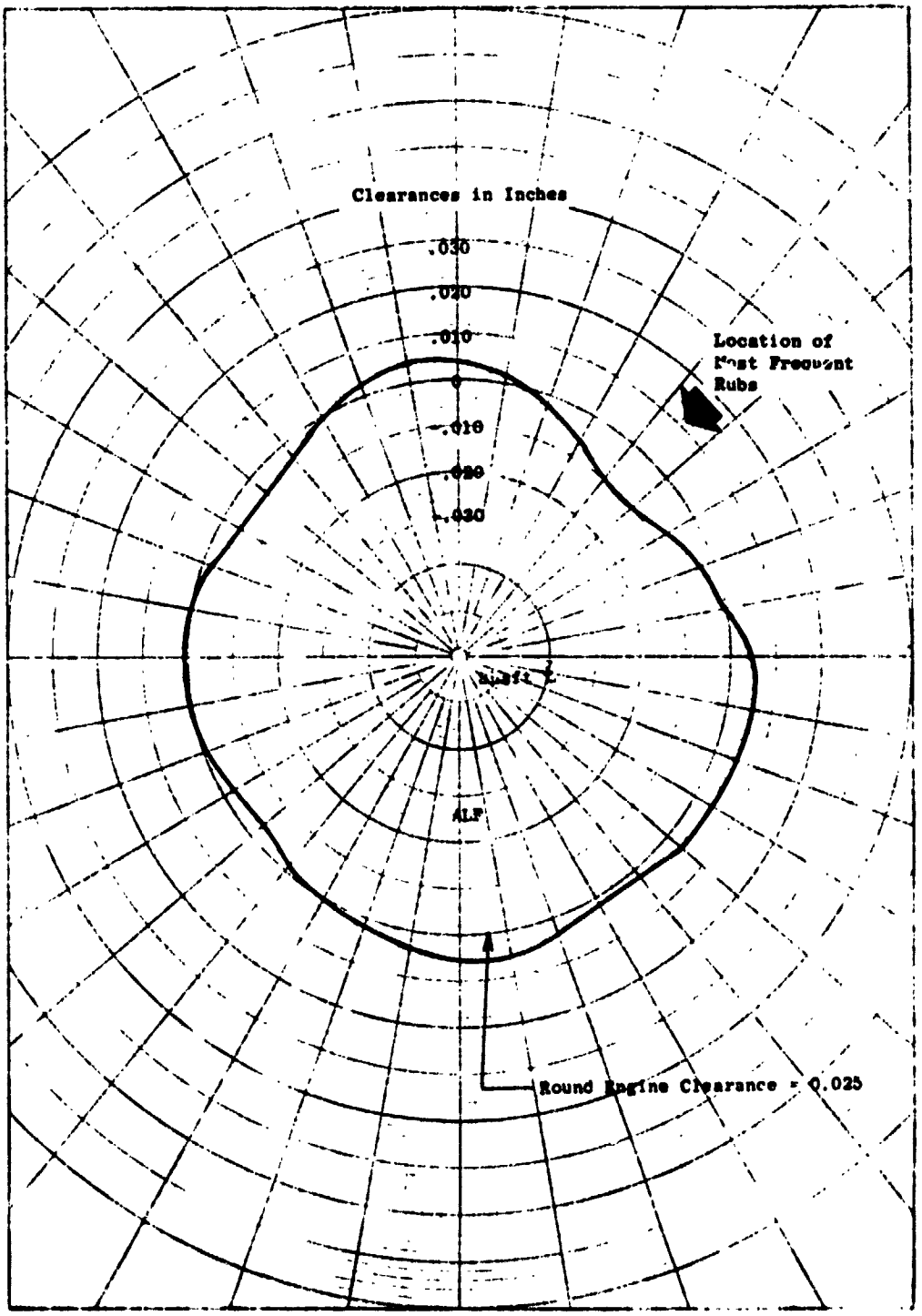

Figure 4-67. CF6-50C HPT Stage 1 Shroud Distortion at 10 Seconds into a Takeoff Transient.

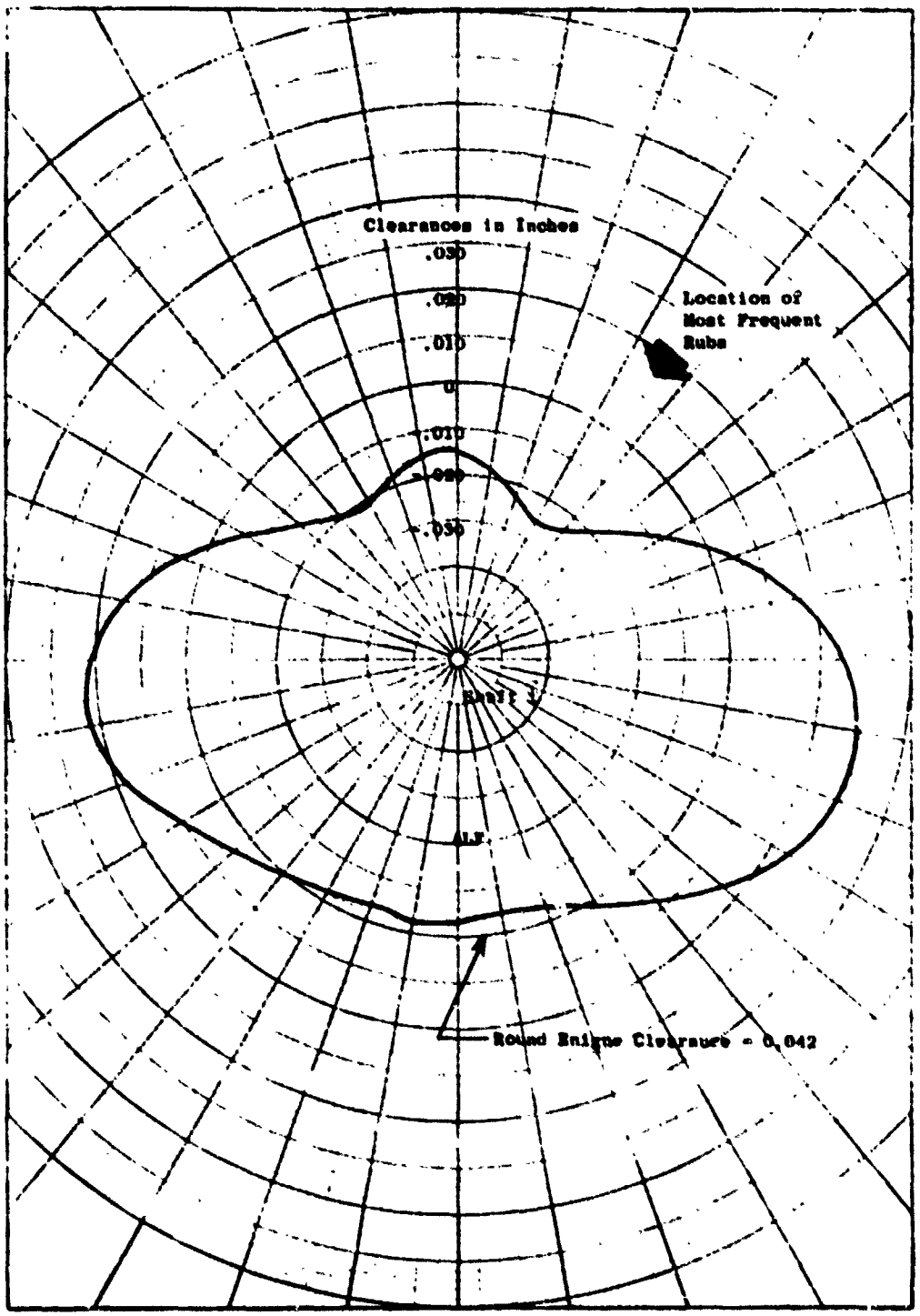

Figure 4-68. CF6-50C HPT Stage 1 Shroud Distortion at 80 Seconds into a Takeoff Transient.

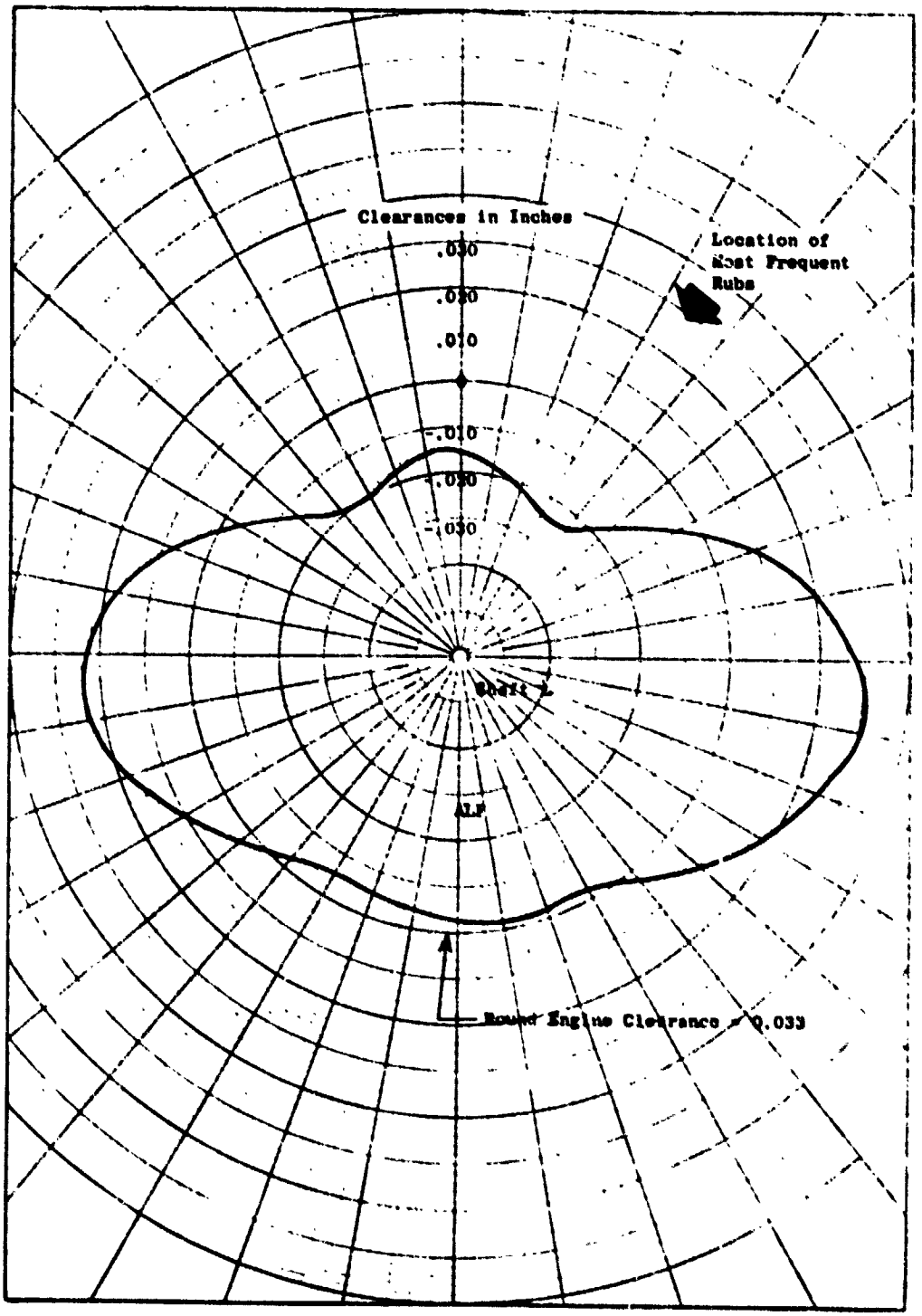

Figure 4-69. CF6-50C HPT Stage 1 Shroud Distortion at 120 Seconds into a Takeoff Transient.

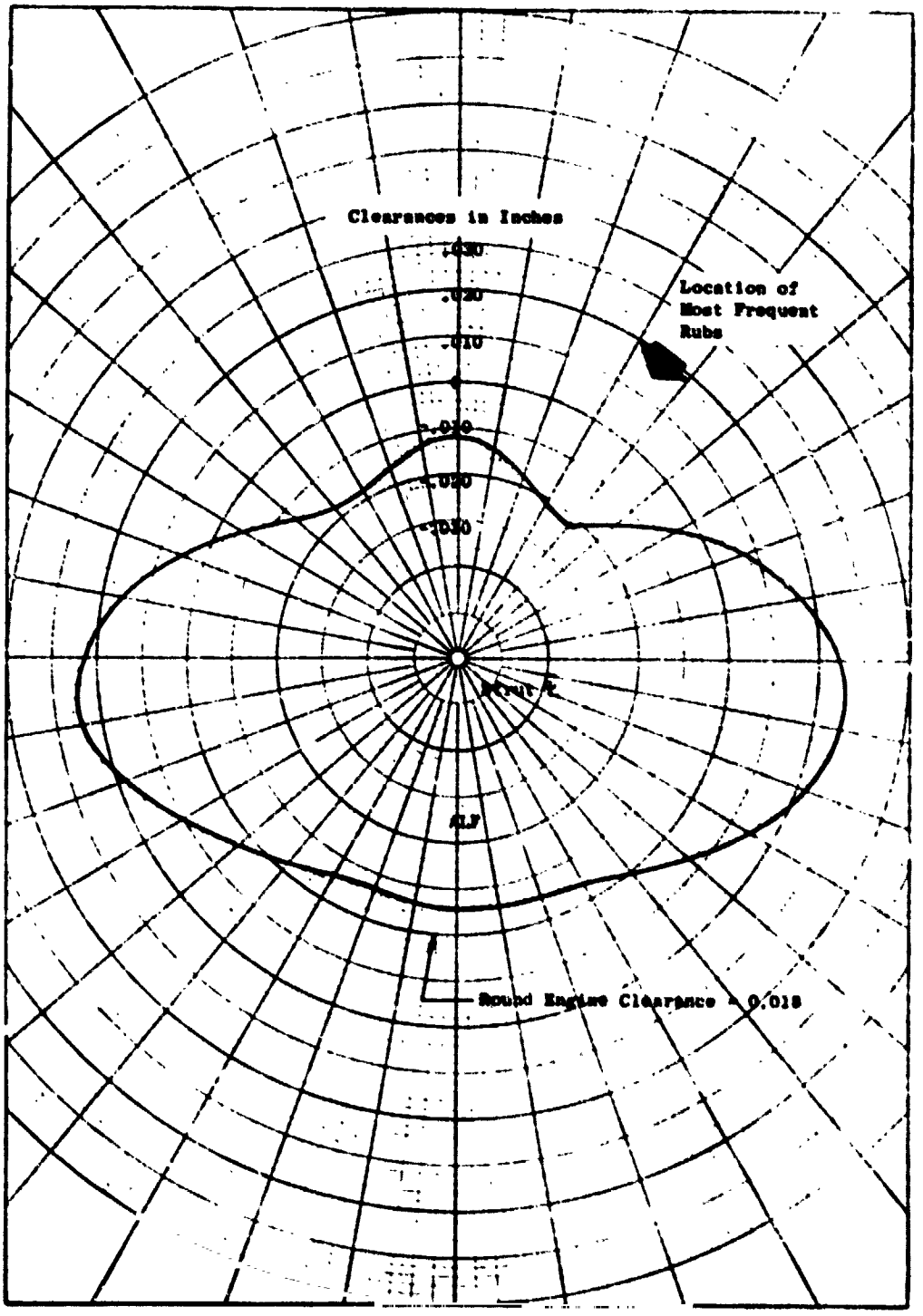

Figure 4-70. CF6-50C HPT Stage 1 Shroud Distortion at Steady-State Takeoff.

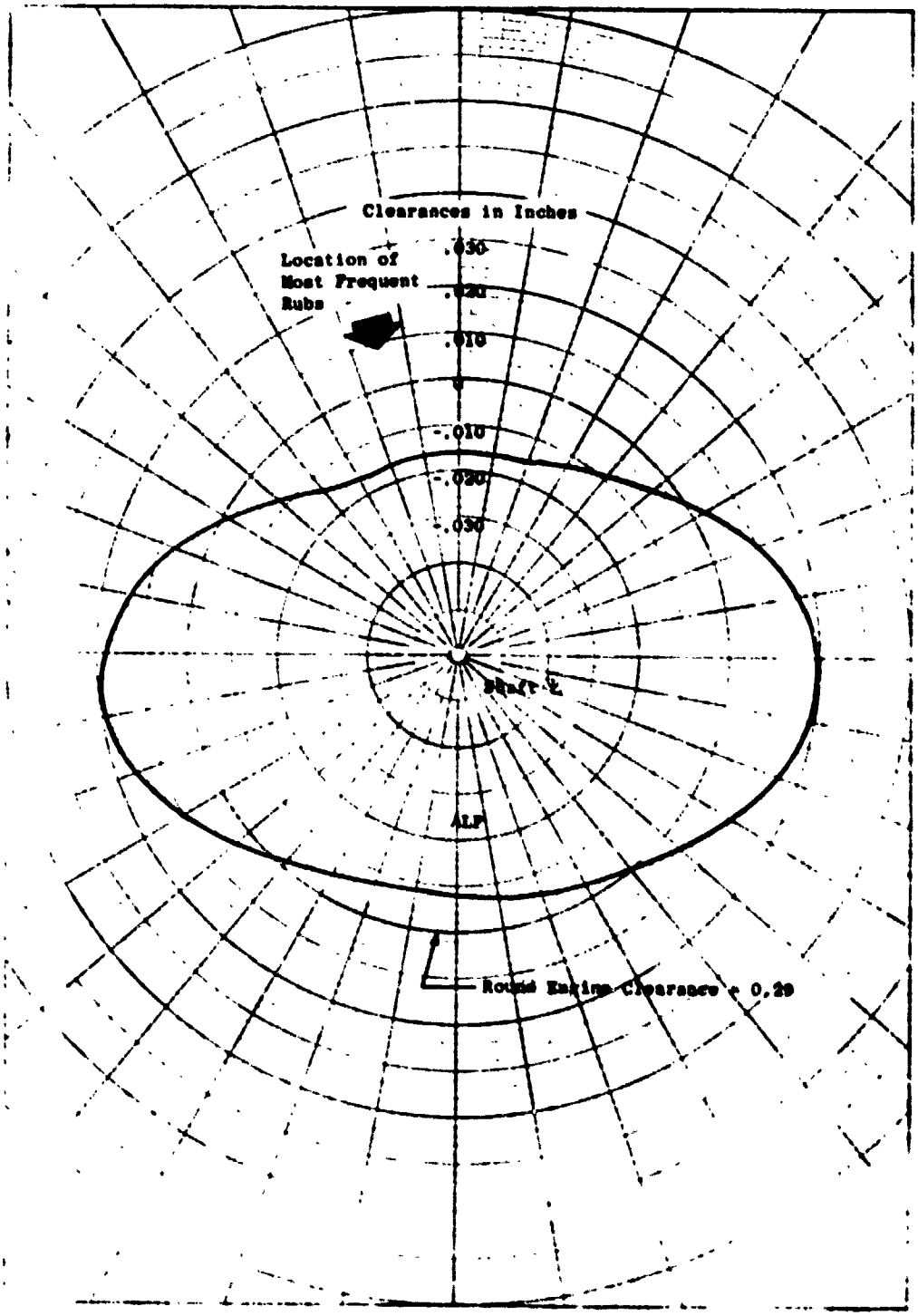

Figure 4-71. CF6-50C HPT Shroud Distortion at Steady-State Cruise.

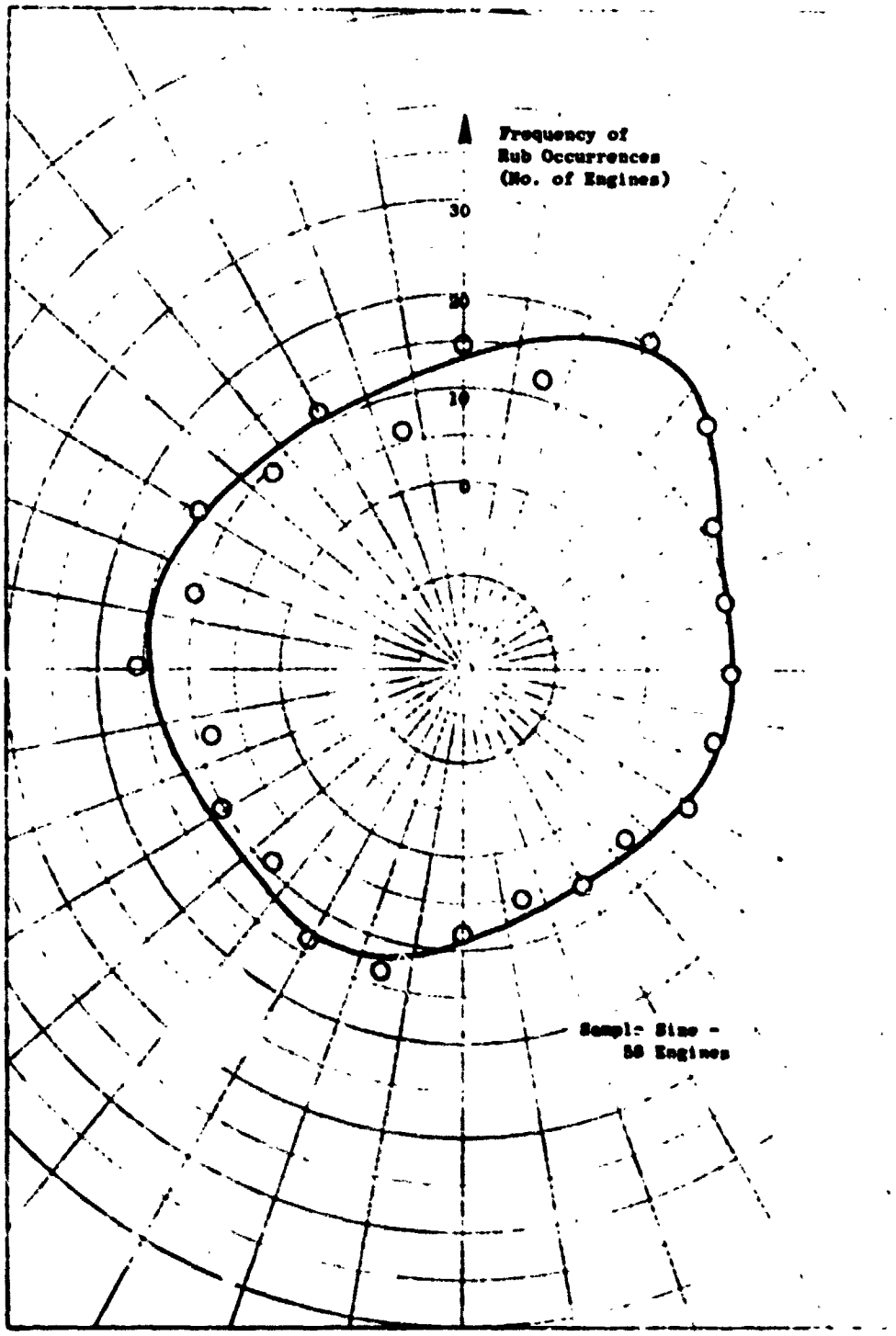

Figure 4-72. CF6-50C HPT Stage 1 Shroud Rub Histogram.

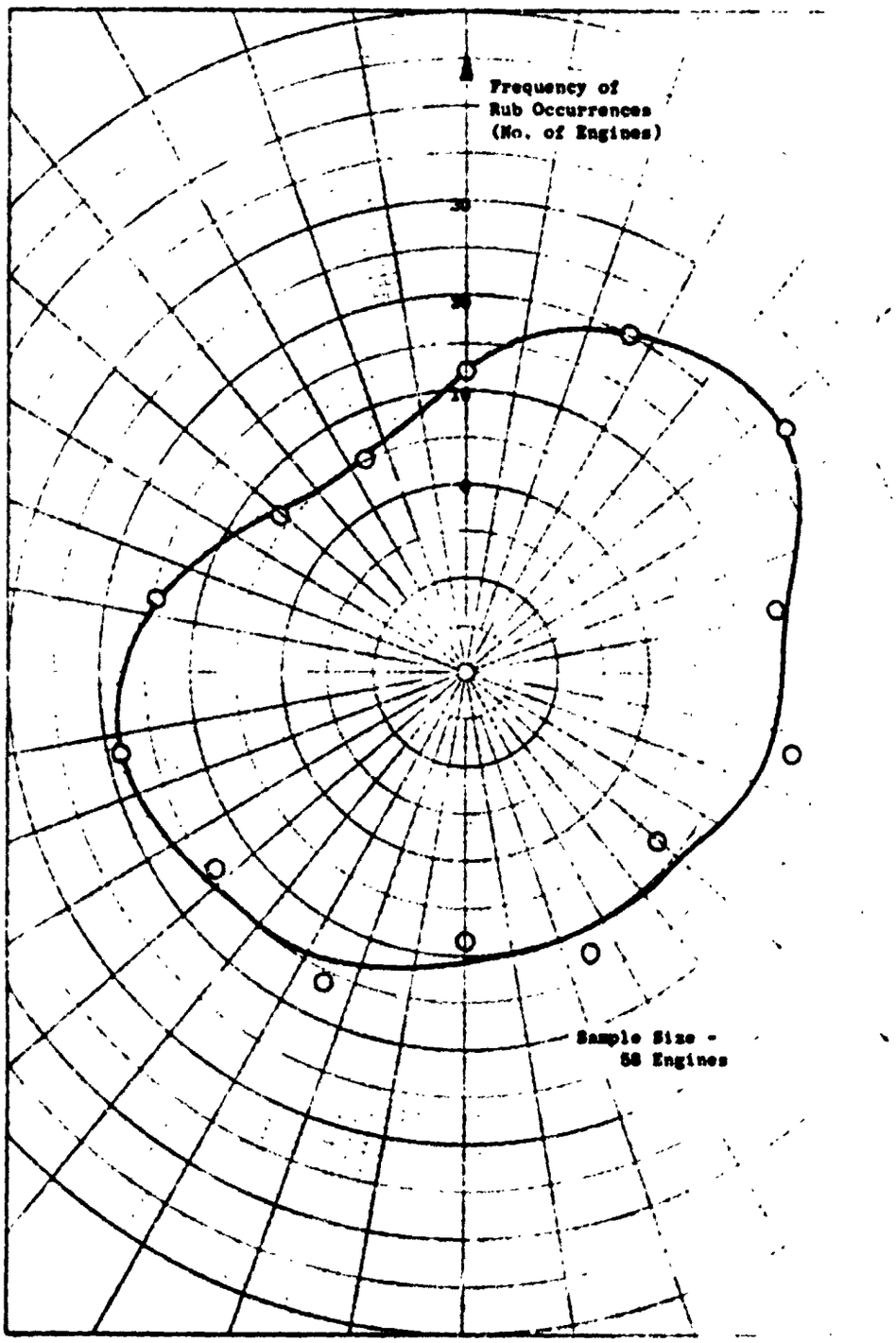

Figure 4-73. CF6-50C HPT Stage 2 Shroud Rub Histogram.

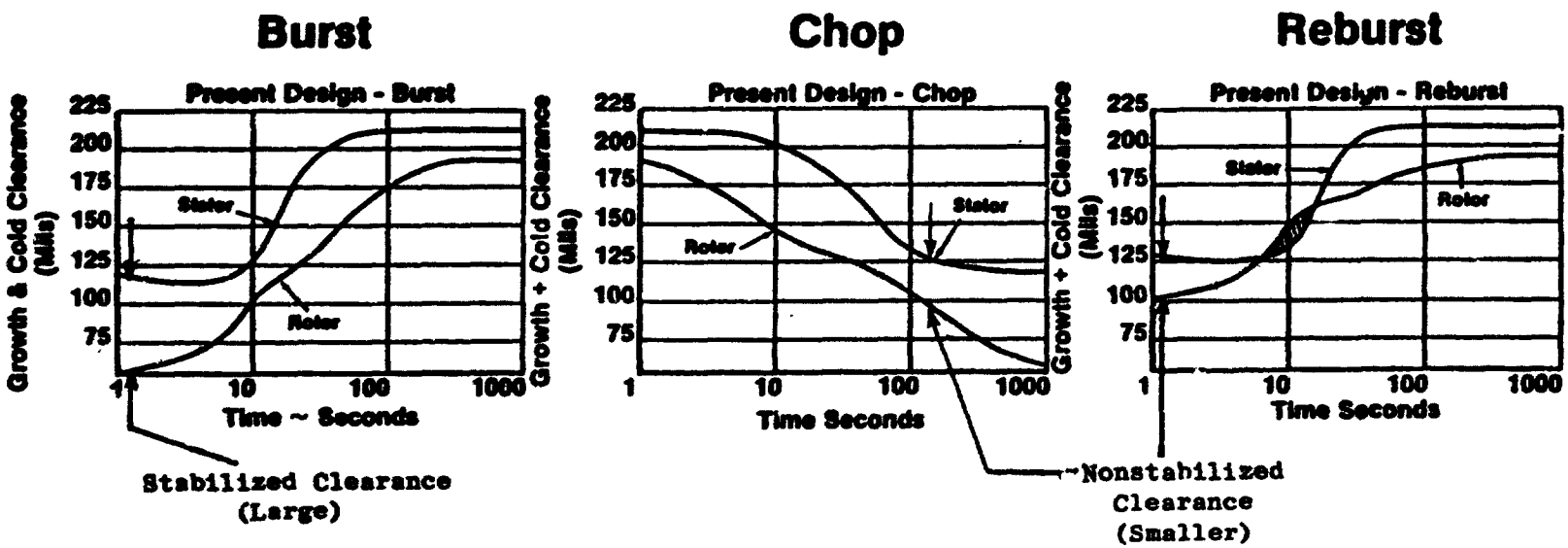

Figure 4-74. HPT Stage 1 Blade Tip Clearauce During Transient Operation.

Analysis indicates that a completely round engine would not sustain rubs during this maneuver; however, the out-of-round conditions previously discussed can produce significant shroud rubs. Severe hot rotor reburst, while not prohibited, are not considered typical of revenue service. It is probable, however, that such operational maneuvers do occur during revenue service and are a significant contributor to tip rubs. Based on these data and calculations, it is believed that tip rubs are not necessarily time-dependent, but are more event-oriented (i.e., rubs occur during a single or several hot rotor reburst transients). This is supported by short-term studies conducted on the CF6-6D engine where significant losses were attributed to thermal mismatch between rotating and stationary structures (Reference 2).

Airfoil Surface Finish:

Another possible source of HPT performance degradation is airfoil surface finish. Measurements were obtained on both the convex and concave surfaces of the blades and vanes of both stages. Three measurements (located near the tip, pitch, and root) were obtained and averaged for each component and each airfoil surface.

Surface finish measurements were obtained on parts with approximately 4,000 to 12,000 hours of accumulated service time. These data produced a considerable range in the surface roughness levels as shown in Figure 4-75. There was no correlation or trend of the data for surface finish with accumulated service time. The concave surface was consistently rougher; its performance effect, however, was minimal when compared with the convex surface since the same change in surface roughness produces only one-fifth the effect for the concave surface as it does for the convex (suction) side.

These data are similar to those observed for the CF6-6D engine parts, and a reason for the poor correlation with accumulated service time has not been isolated. Variables, such as gas flow environment (erosive quality of air), combustor efficiency, quality of fuel, and route structure can all contribute to surface finish degradation. Surface finish degradation may occur relatively early in the life cycle (i.e., initial 1,500 to 2,000 hours), and the data obtained for the same parts with additional service time would not reveal any differences. Additional efforts to more fully understand this trend were not possible since the necessary hardware inspection data for shorter time parts were not available or obtainable.

A comparison of available data with new part specifications resulted in the following estimated changes for the convex surfaces after 6,000 hours of revenue service:

Stage 1		Stage 2	
Vane	Blade	Vane	Blade
8μ in./in. AA	13μ in./in. AA	28μ in./in. AA	Zero

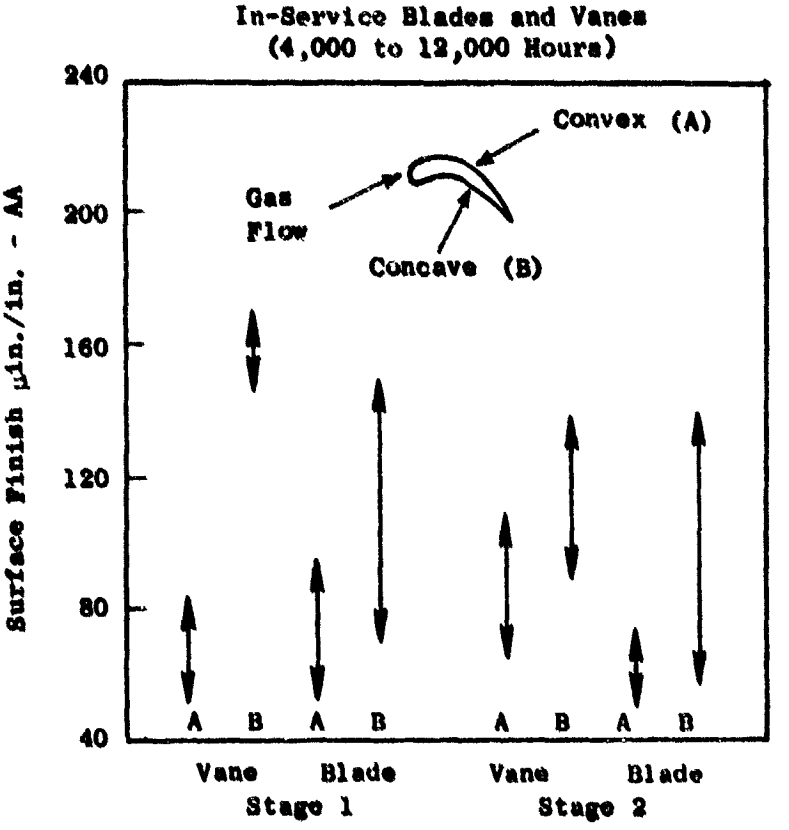

The Concave Surface is Consistently Rougher than the Convex Surface but has Less Effect on Turbine Efficiency.

Figure 4-75. CF6-50 HPT Airfoil Surface Finish Range.

The total effect of increased airfoil roughness is 0.15 percent loss in HPT efficiency, as shown in Figures 4-76 and 4-77, which is equivalent to 0.10 percent increase in cruise fuel burn.

Internal Leakage (Parasitics):

Hot section components, in particular HPT parts, utilize compressor air for cooling and other durability considerations. After serving its purpose, this air is ducted back into the gas stream which exits through the core exhaust nozzle. Since it bypasses part of the HPT rotor energy extraction process, this still produces a performance loss. Increases in these flows due either to changes in seal clearances incorporated to control these flows or part distortions which produce additional leakage paths, are termed parasitics (losses). Areas in the HPT which may be a source for a parasitic loss include a distorted Stage 1 nozzle outer band and the pressure balance, interstage or aft CDP seals.

Distortion of the HPT nozzle outer band produces a leakage path for compressor air to enter the gas stream just forward of the Stage 1 HPT blade creating a mixing loss. The nozzle aft band mates axially against the Stage 2 nozzle support, but distortion of the circumferential outer band in an axial direction produces the leakage area. A sketch of an individual nozzle showing the axial leakage area (X) is presented in Figure 4-78. The average change (X) for 50 long-time parts was 0.008 inch, with an average time of 6,000 hours. This average flange distortion produces a leakage area of 0.207 $in.^2$ for all vanes and is equivalent to 0.15 percent increased cruise fuel flow after 6,000 hours or 0.1 percent after 4,000 hours of operation.

Examination of the pressure balance seal and aft CDP seal for 14 engines revealed a small increase in clearance. The average rubs were 0.009 inch and 0.008 inch, respectively, which were very near the average for production engines after acceptance tests. A loss was not assigned to this mechanism.

The average interstage seal clearance was not found to increase within measurement accuracies from a nominal 0.110 inch noted for new engines. This does not represent an in-service deterioration loss; but does represent an area for potential product improvement.

The deterioration assessment for the high pressure turbine listing the individual damage mechanisms is presented in Table 4-XVII. The increase in Stage 1 and 2 blade tip clearances results in the dominant loss which represents over 73 percent of the assessed loss. Rubs which occur as a result of thermal mismatch between the rotating and stationary structures were the primary cause for the increased clearances.

The best estimate for the deterioration rate for each damage mechanism is presented in Figure 4-79. A dotted line is shown for the tip clearance effect after approximately 1,000 hours. This is intended to represent an "unknown" condition; but as previously discussed, is expected to occur during one or two rub events rather than being time-dependent.

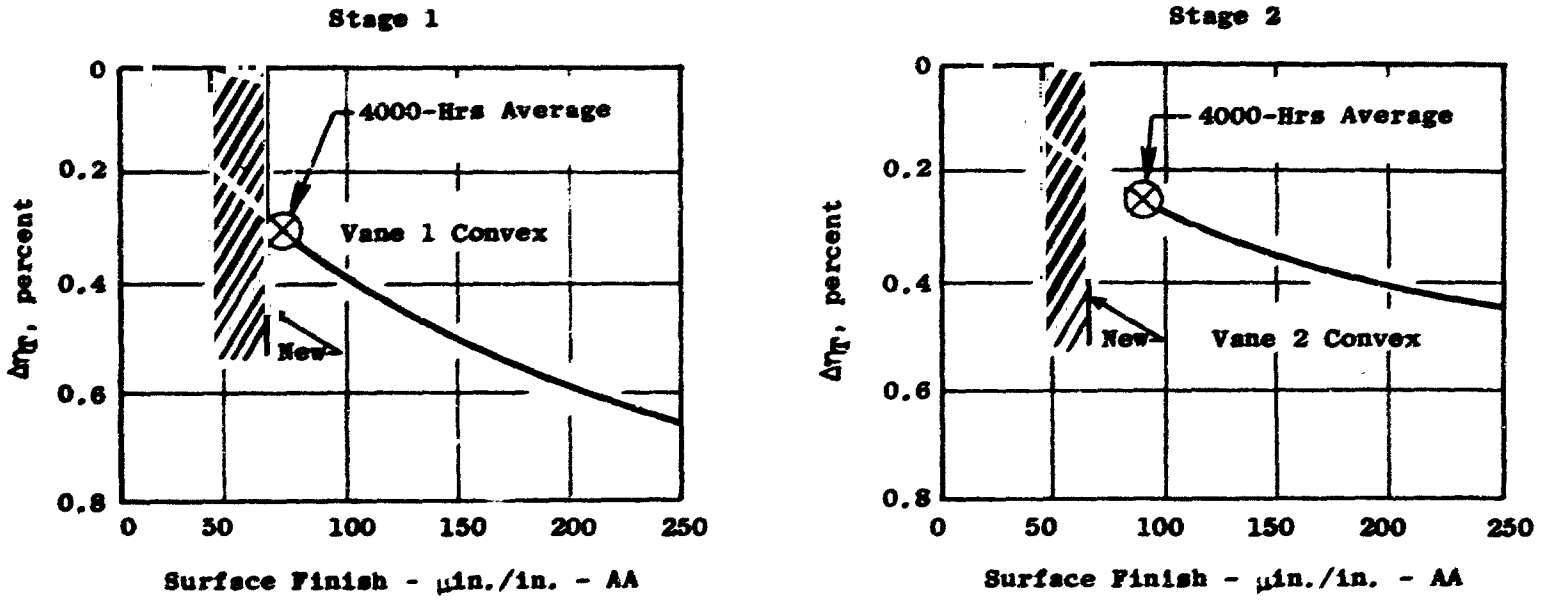

Figure 4-76. HPT Vane Surface Roughness Average.

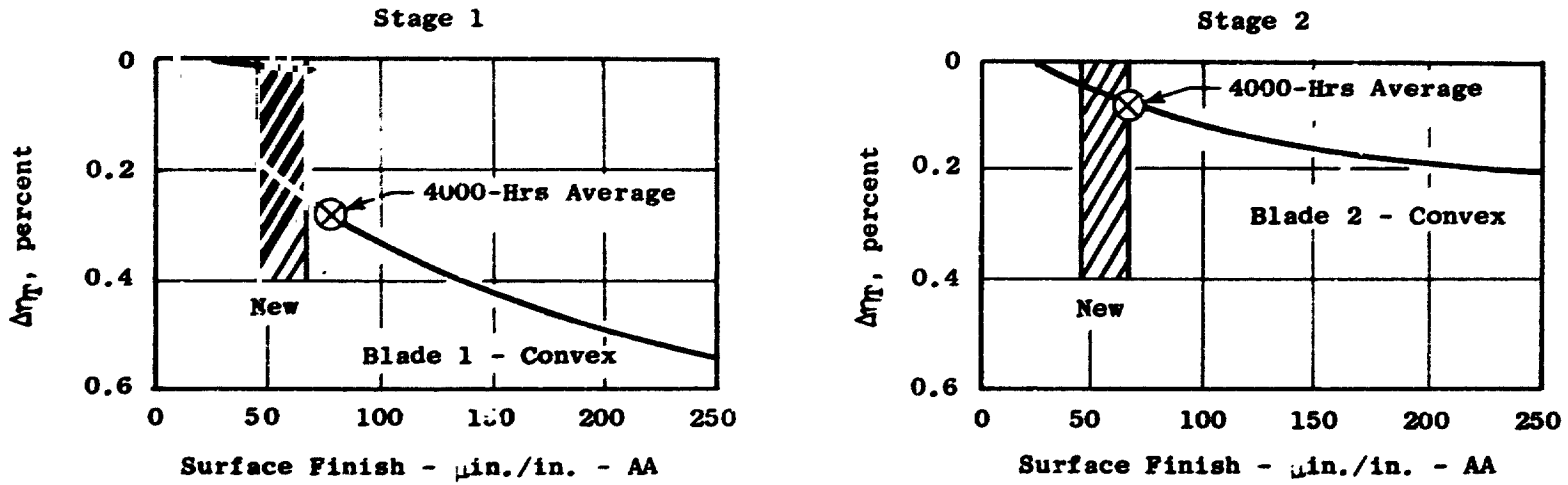

Figure 4-77. HPT Blade Surface Roughness Average.

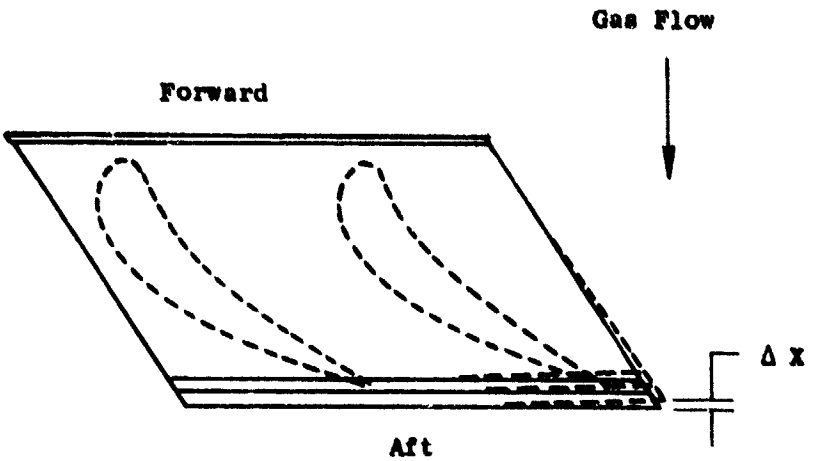

Figure 4-78. Stage 1 HPT Nozzle Distortion - HPT Internal Leakage.

Table 4-XVII. HP Turbine Section - Estimated Deterioration at 4,000 Hours.

		Δ SFC at Cruise, %
Increase in Blade Tip Clearances -	Stage 1	0.42
	Stage 2	0.13
Stage 1 Nozzle Band Leakage		0.10
Surface Finish Degradation		0.10
	Net	0.75

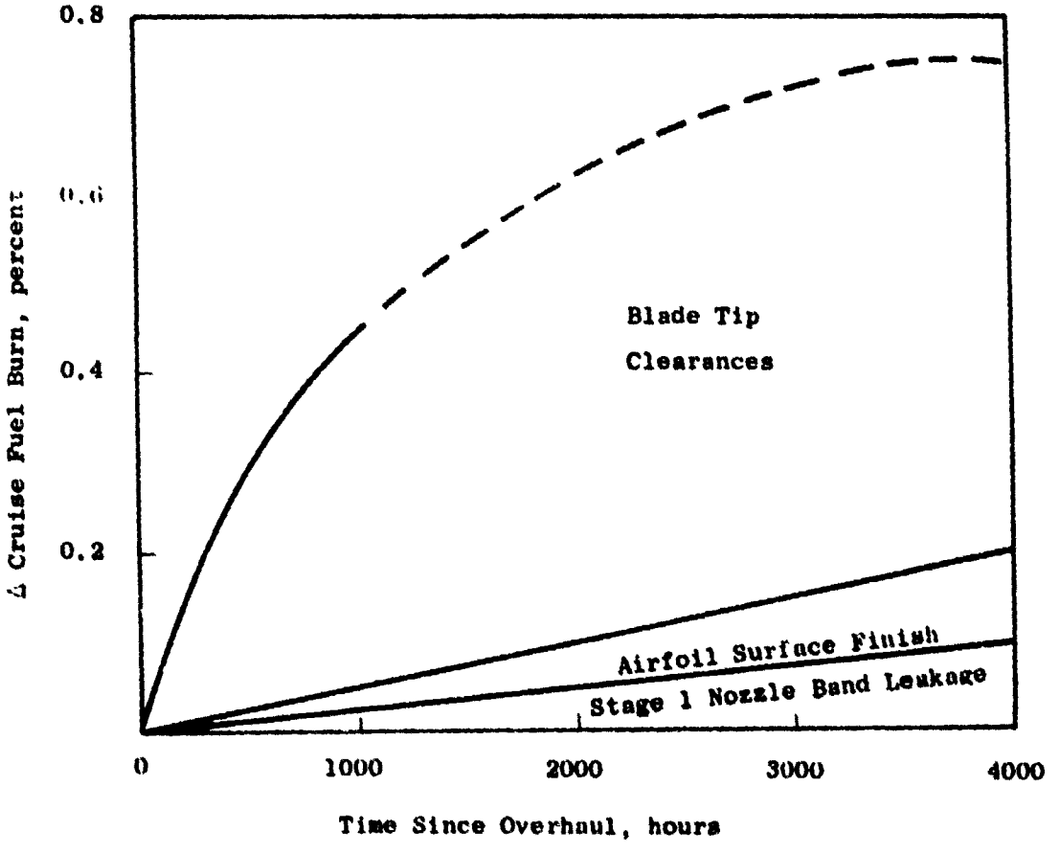

Figure 4-79. HP Turbine Section - Estimated Deterioration Characteristics.

Low Pressure Turbine Section - Deterioration of low pressure turbine (LPT) components occurs primarily as a result of increased blade tip-to-shroud and interstage seal clearances, and increased airfoil surface roughness. A cross section of the LPT section is presented in Figure 4-80 showing deterioration modes.

Clearances:

Increases in running clearances occur with time, as repeated rubs between blade tip seals and stationary shrouds lead to wearing away of the honeycomb shroud material and, to a lesser extent, the blade seal teeth. Transient operations such as hot rotor reburst and windmilling air starts result in relatively more radial rotor-to-stator closure which, in extreme cases, can also lead to increased running clearances.

The contribution of rotor components toward increased clearances was examined. Measurements of CF6-6D type low pressure turbine rotors, particularly those reported in Reference 1 which deals with back-to-back LPT module tests, have indicated that significant seal tip wear was occurring. However, radii checks on several inbound CF6-50 LPT rotors showed that blade seal teeth had not been significantly shortened as a result of rubs. This latter finding is more consistent with examinations of individual blades in the repair/refurbishment cycle, which revealed that most blades do not require repair to meet seal teeth radial dimensions. It has been concluded from these observations that wear of rotating components (blade seal teeth or rotating interstage seal teeth) was not a significant contributor to increased clearances.

Observations of the stationary honeycomb shrouds and interstage seals produced different results. The rotating low pressure turbine components experience axial mismatch with their static components, as much as 0.3 inch during engine operation. While this condition produces wider wear grooves in seals than experienced in other sections of the engine, analysis indicates that the minimum clearance is still controlled by the depth of the wear groove. Measurements of those grooves using soft plastic or castone impressions did not yield an acceptable reproducible record. Scale measurements at eight equally spaced circumferential locations indicated the average wear depth was 0.065 inch. This represents an average of 35 mils increase in the steady state cruise clearance when compared with similar data obtained from production new engines after their acceptance runs. Similarly, average wear depths in the stationary interstage seal were 0.070 inch which is a 40-mil increase in steady state cruise clearance over the production acceptance level.

The calculated performance effects from these rubs are shown in Figures 4-81 and 4-82. The estimated increase of 0.035 inch in blade tip/shroud clearance is equivalent to a 0.43 percent loss in LPT efficiency while the 0.040-inch increase in interstage seal clearance is equivalent to a 0.32 percent loss in LPT efficiency for the typical parts with 5,000 hours. This 0.75 percent loss in LPT efficiency results in a 0.52 percent increase in cruise fuel burn which is equivalent to 0.41 percent after 4,000 hours.

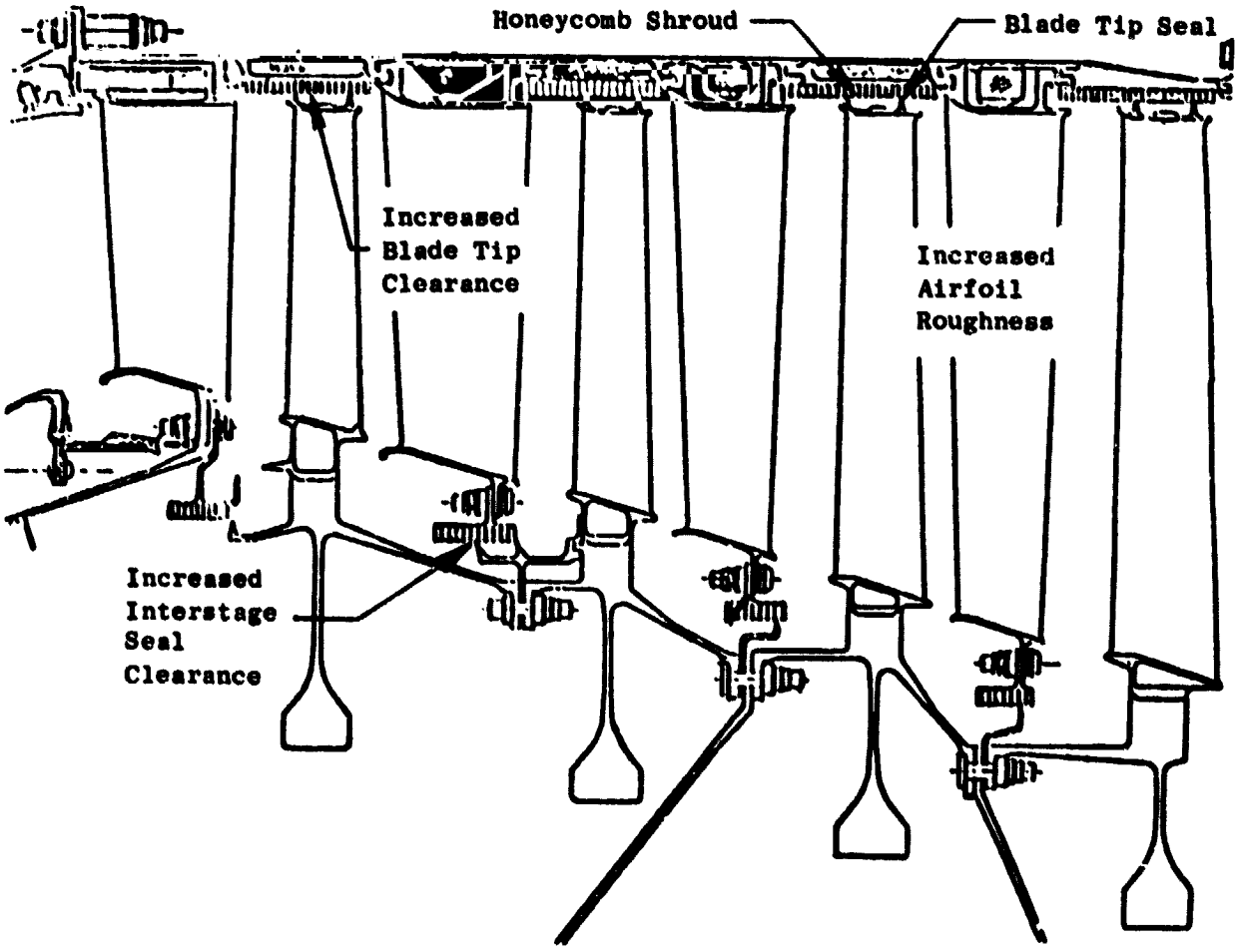

Figure 4-80. CF6-50 LP Turbine Section Deterioration Modes.

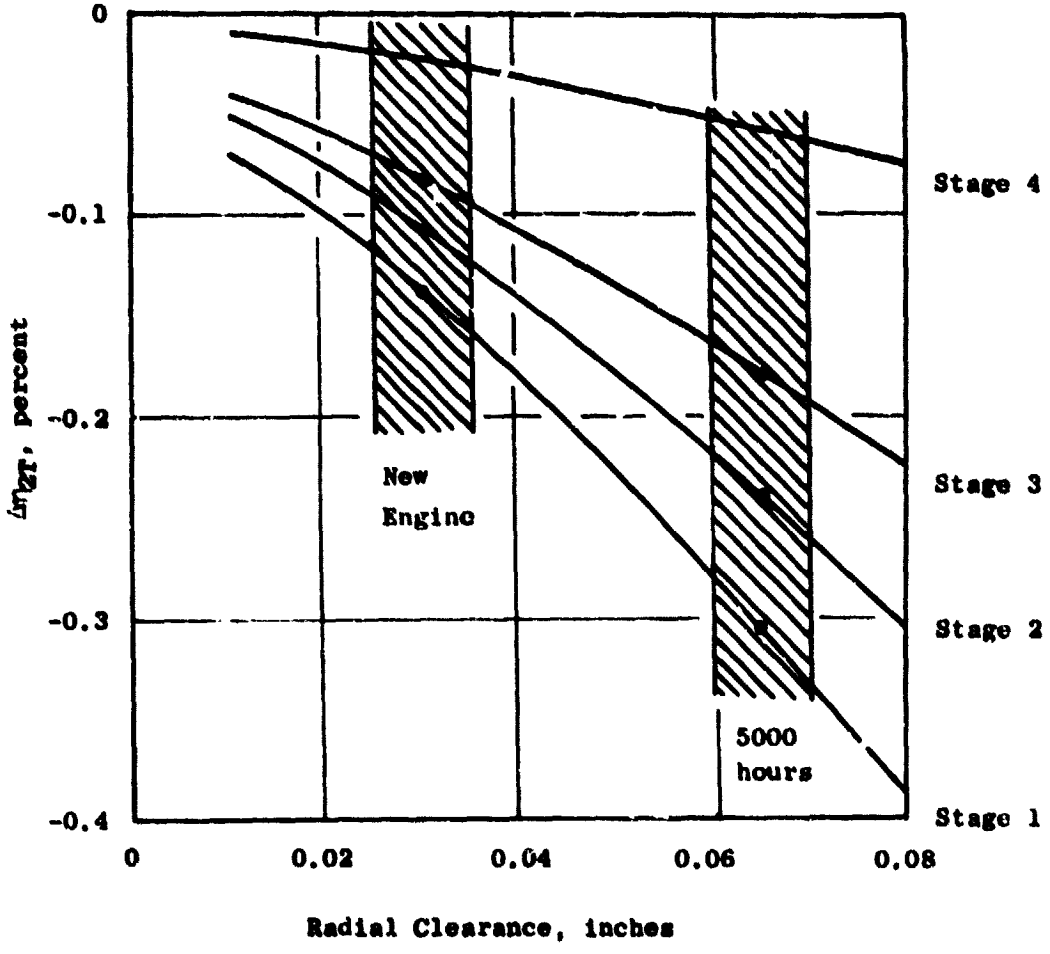

Figure 4-81. Effects of LPT Blade Tip/Shroud Clearance on Efficiency at Cruise.

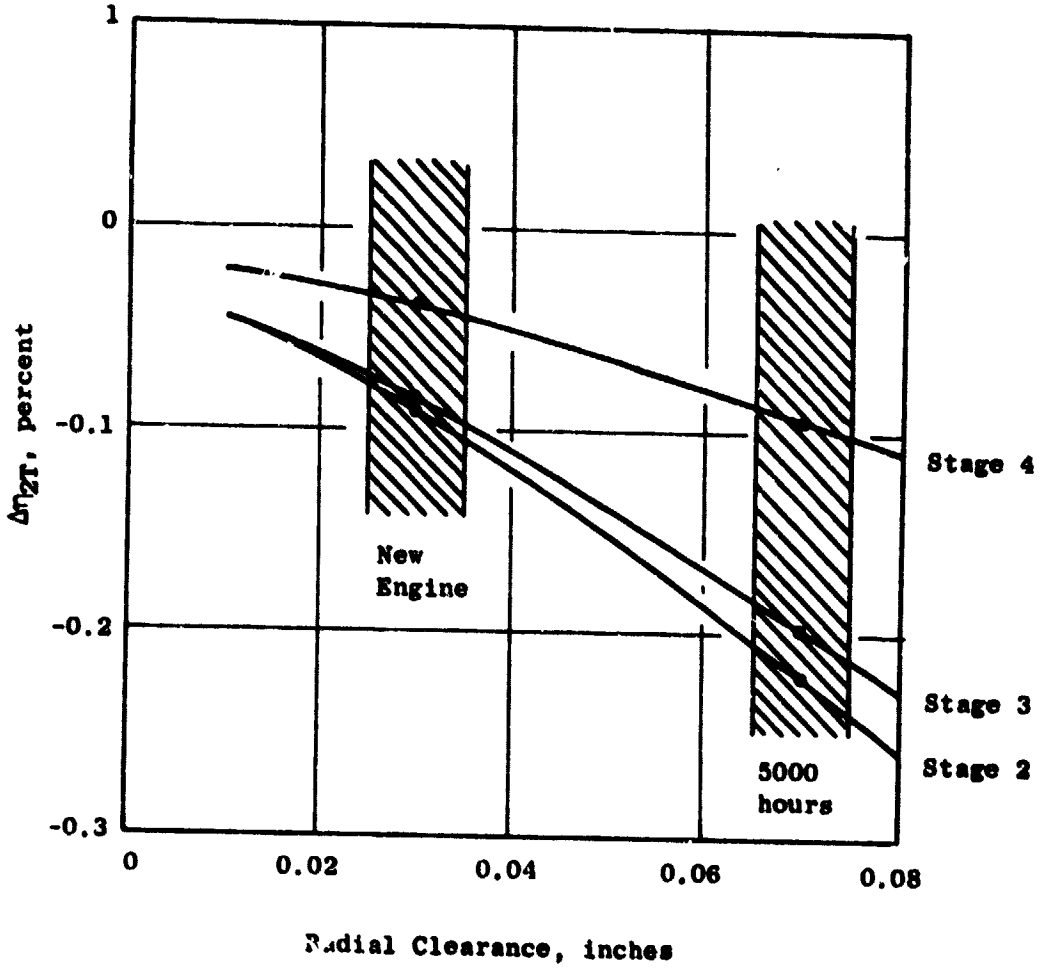

Figure 4-82. Effects of LPT Interstage Seal Clearance on Efficiency at Cruise.

Airfoil Surface Finish:

The other significant deterioration mode was increased airfoil surface roughness. Summaries of blade and vane surface finish measurements versus time for a sample of airfoils are presented in Figures 4-83 and 4-84. Increased surface roughness results from airborne and engine-induced particulates which result in surface buildup, oxidation, and hot corrosion. There are various corrosion mechanisms which occur in the temperature ranges in which LPT airfoils operate.

Surface finish data collected for the CF6-50 engine parts appear to consist of two populations: one in which significant metal attack had occurred and the other group where little or no metal attack was observed. Efforts to date have isolated two levels of accelerated oxidation (commonly called sulfidation) in which the operating temperature level is the primary difference. For low temperature corrosion, the surface finish is degraded by the presence of deposits consisting primarily of layers of airborne carbon contaminants and iron oxide. These deposits tend to provide some measure of metal protection; hence, the metal attack from corrosion is somewhat self-arresting. Removal of these deposits utilizing normal cleaning procedures generally restores the surface to a nearly as-new condition.

Deposits which degrade the surface finish were also noted for the higher temperature corrosion, but an additional and more lasting effect is also experienced. These deposits contain much larger amounts of sulfates which, while molten, remove the normal protective oxide scales formed on the surface of the metal thus destroying the metal's normal resistance to oxidation. The protective oxide scales do not reform as long as the sulfates' deposits remain on the surface. The loss of the protective oxide scales produces accelerated oxidation of the parent metal which also degrades the surface finish. These deposits can be removed using normal cleaning procedures, but the surface condition when there is parent metal attack is not restored by cleaning alone. The higher temperature corrosion is more likely to be experienced in the Stage 1 and 2 parts, since their metal temperatures are in the optimum range to produce this condition. However, experience to date indicates both types of conditions tend to overlap, and the distinction by stage in the LPT is less obvious. Most airfoil surfaces reviewed as part of this program have conformed to the lower rate of surface roughness increase as shown in Figures 4-83 and 4-84. Many of those have revealed corrosion in the sense of metallurgical attack, but this condition has not yet led to dramatic increases in surface roughness. In general, surface roughness effects are small, and the dashed lines shown in Figures 4-83 and 4-84 are the best estimates for average conditions. It also appears from these data that surface roughness continues to increase to 6,000 to 7,000 hours, and then remains relatively constant. Using the performance derivatives presented in Figures 4-85 and 4-86, average surface roughness changes of 32μ in./in. AA for the vanes and 50μ in./in. AA for the blades after 5,000 hours result in an approximate 0.07 percent decrease in LPT efficiency and a 0.03 percent increase in cruise sfc after 4,000 hours.

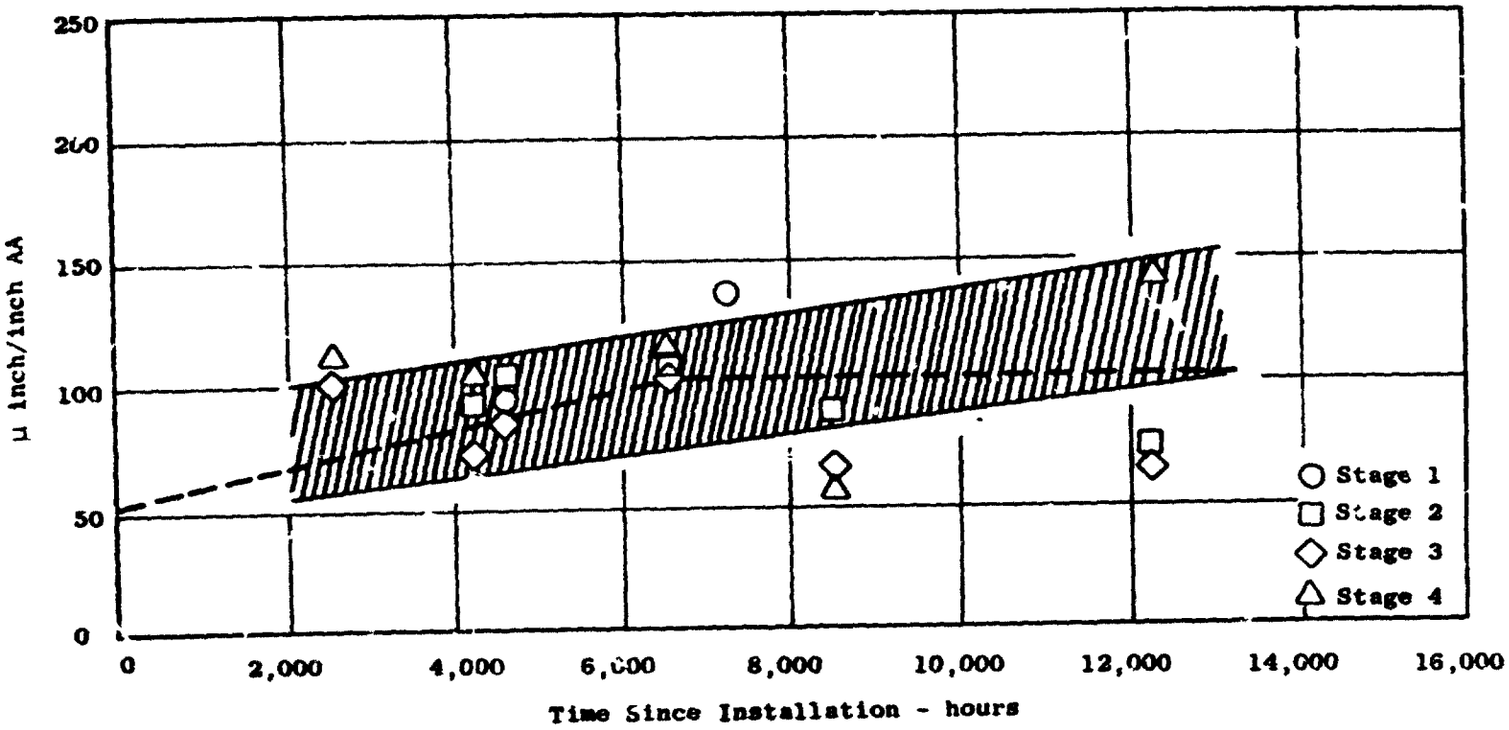

Figure 4-83. Degradation of LP Turbine Vane Surface Finish (Convex Side).

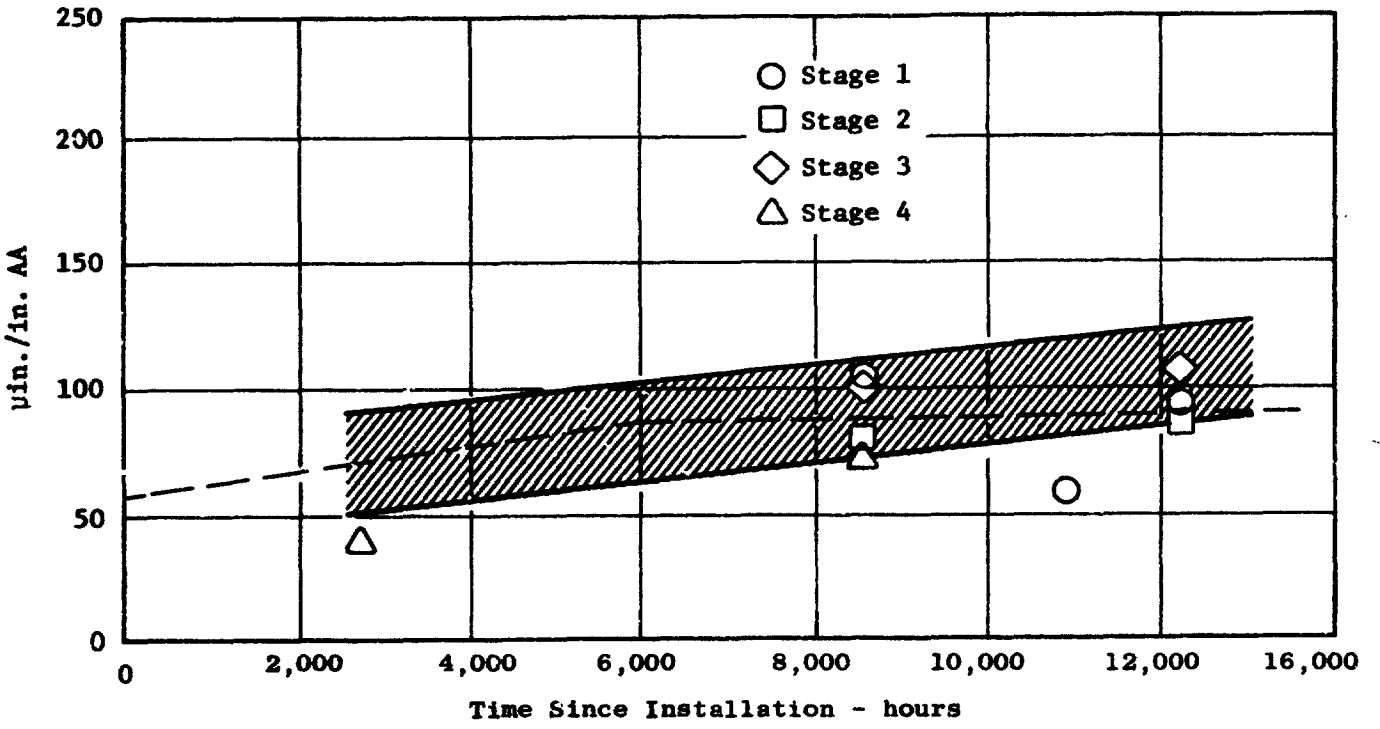

Figure 4-84. Degradation of LP Turbine Blade Surface Finish (Convex Side).

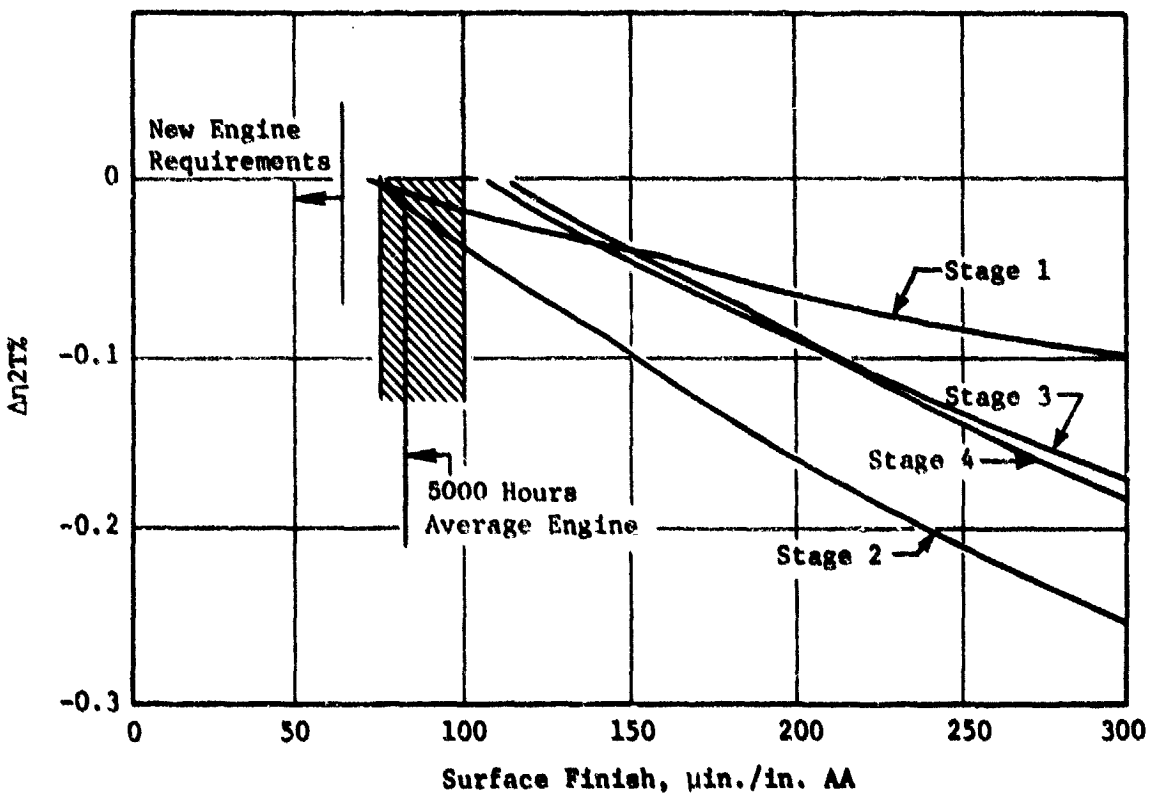

Figure 4-85. LPT Vane Surface Finish - Efficiency Effects at Cruise.

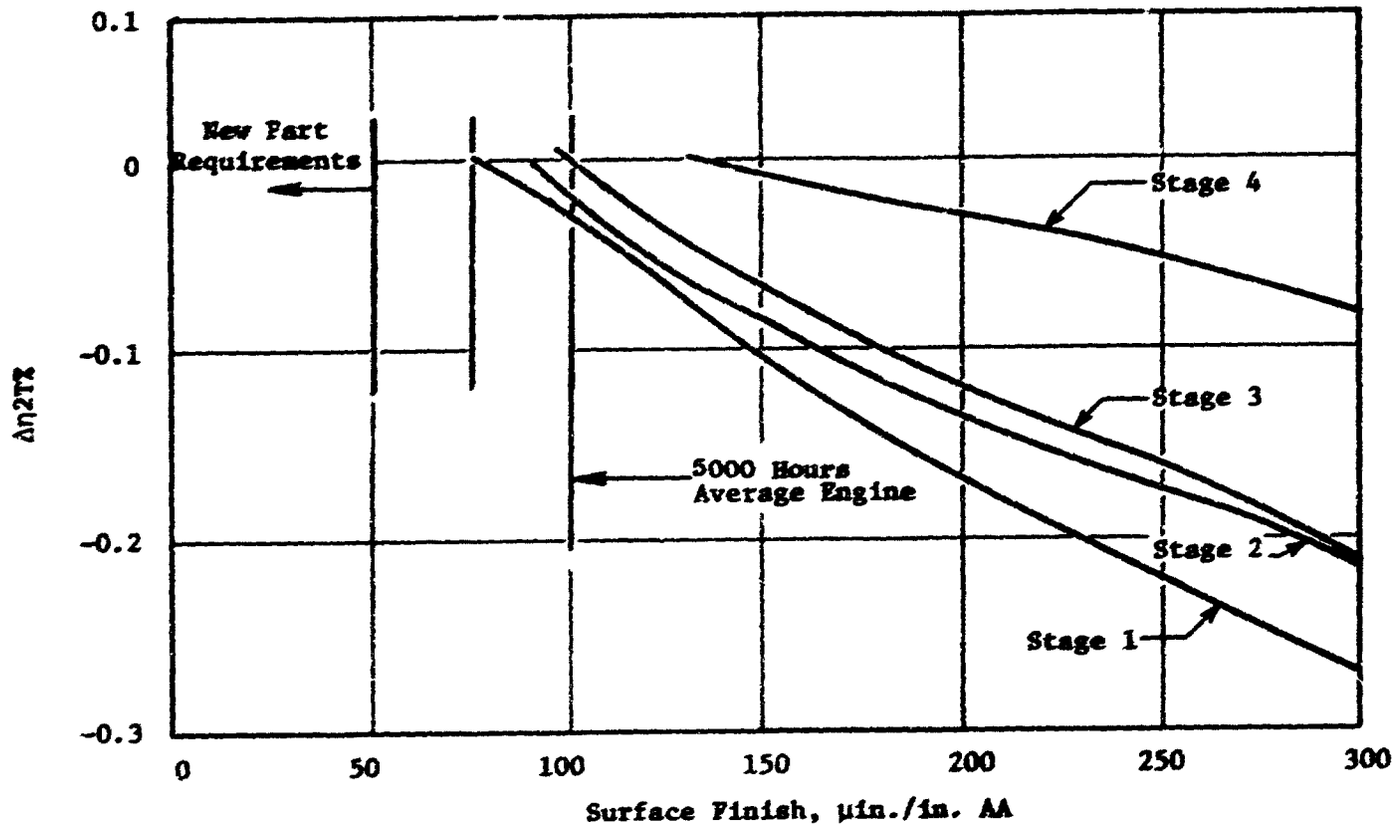

Figure 4-86. LPT Blade Surface Finish - Efficiency Effects at Cruise.

The deterioration modes and magnitude of loss assessed from inspection of low pressure turbine parts is presented in Table 4-XVIII. The dominant deterioration mode is increased clearances between the blade tips and tip static shrouds and between the rotating and stationary interstage seals. It was shown that, unlike the high pressure turbine rubs which result in shorter airfoils, these rubs produce large grooves in the stationary shrouds and seals which produce the increases in running clearances.

The best estimate for the rate of loss for each damage mechanism which contributes to low pressure turbine deterioration is presented in Figure 4-87. It was estimated that blade tip and interstage seal rubs occur by 5,000 hours and that airfoil surface finish continues to degrade through 6,000 total hours.

Table XVIII. LP Turbine Section - Estimated Deterioration at 4,000 Hours.

	Δ SFC ° Cruise, %
Increase in Blade Tip Clearances	0.24
Increase in Interstage Seal Clearances	0.17
Surface Finish Degradation	0.03
Net	0.44

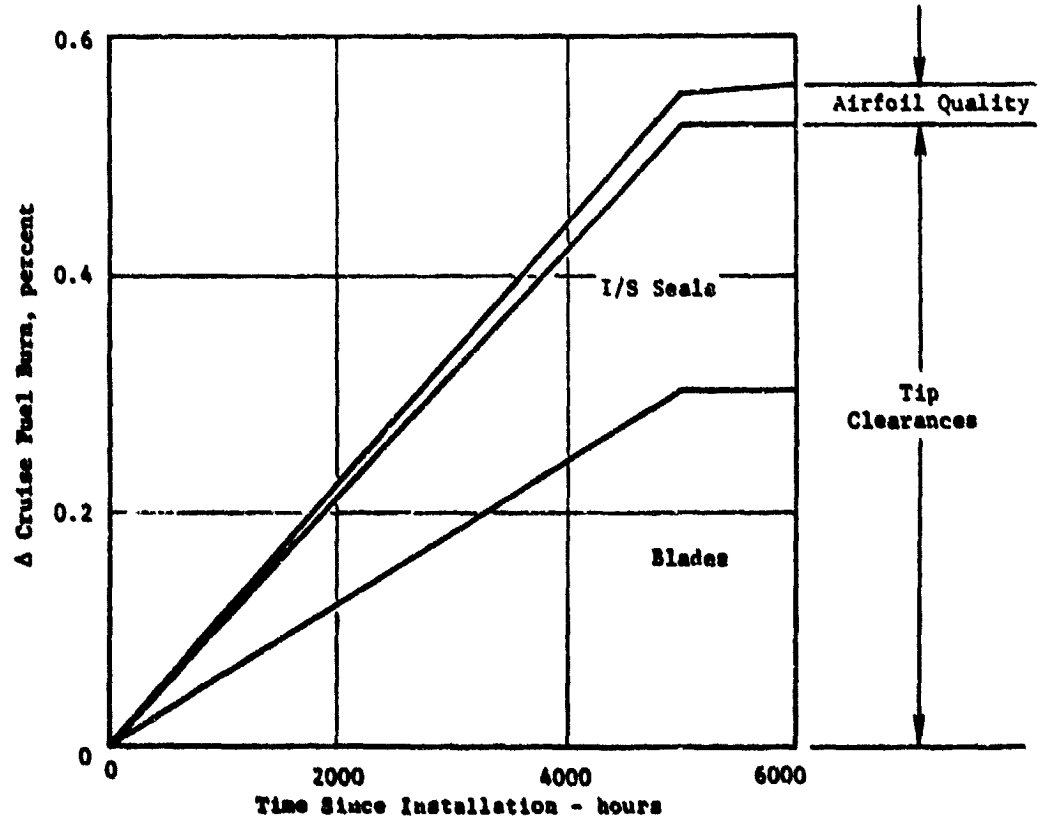

Figure 4-87. LPT Section - Estimated Deterioration Characteristics at 6000 Hours.

Refurbished Engine

Hardware inspection data and a general discussion of the observations and findings concerning refurbished engine modules are presented in the following paragraphs. The data are presented in the same format as that used to document the deteriorated engine, i.e., for the four major sections of the engine: fan, high pressure compressor, high pressure turbine, and low pressure turbine. The data were generated by the hardware inspection teams during their on-site reviews, and supplemented with data obtained during the normal day-to-day relationships between the airlines and General Electric on-site and in-house engineering personnel.

For the reasons noted in Section 4.0 of this report, one airline which provides overhaul for all CF6-50 engines within a major consortium was selected to provide hardware data which best described the unrestored losses. These hardware data are the best representation of an average engine produced by this same refurbishment source. While the performance data were simply the average of the individual data, the average hardware results must be obtained by estimating the percentage of modules that are refurbished for each specific item, and then average weighing all items.

Fan Section - Although the fan section represents the largest amount of fuel burn deterioration, very little restoration is currently being accomplished on this module. Fan section deterioration is generally superficial damage which does not require repair to restore mechanical integrity. Since the fan section has good mechanical integrity and is not frequently disassembled for repairs, the opportunity to restore performance deterioration items is seldom available. This is the primary reason for the small amount of refurbishment currently being performed on fan section components.

Fan Blade Clearances:

Fan blade clearances are not being restored to the new production average values. In fact, as presented in the section describing the deteriorated engine, the average fan blade tip clearance actually increases during refurbishment as a result of local shroud rework to meet the specified minimum clearance. The average tip clearance increase of 0.020 inch shown for a 6,000-hour deteriorated engine is assumed for the average refurbished engine. This is equivalent to an increase fuel burn of 0.38 percent.

Blade Surface Quality:

The fan blade leading edge is recontoured during most of the shop visits. While the quality of the rework is good, the average edge shape is not quite as good as that produced for the production new engine. The combination of edge shape quality and total parts repaired (75 percent) produced an unrestored loss for the average engine of 0.12 percent in cruise fuel burn. The fan blades are properly cleaned during each shop visit which eliminates the 0.12 percent in-service cruise fuel burn loss from that source. It was also estimated

that the average surface roughness for the fan blade was improved during the cleaning and leading edge rework processes, reducing the in-service loss but leaving a residual condition equivalent to 0.01 percent cruise fuel burn loss.

Booster and Bypass OGV:

The booster is rarely disassembled due to excellent mechanical capabilities; therefore, the performance deterioration items are not restored. This is also true for the fan bypass OGV's which are seldom removed from the fan casing and, therefore, not repaired.

Since repairs are not made to these parts, the increased fuel burn for the booster and bypass OGV for the refurbished engine is assumed equivalent to that presented for the 6,000-hour deteriorated engine. These values are 0.24 percent increase in cruise fuel burn for changes in roughness and leading edge shape for the bypass OGV's and 0.04 percent increase in cruise fuel burn for the increased airfoil roughness and tip clearances in the booster. An additional loss equivalent to 0.07 percent in increased cruise fuel burn is attributed to the leading edge of the splitter which is also not normally reworked during a shop visit.

A summary of the unrestored losses remaining after typical refurbishment of the fan and booster module is presented in Table 4-XIX. As shown, the average unrestored loss is 0.86 percent in cruise fuel burn which represents 65 percent of the total noted for a deteriorated module with an average of 6,000 accumulated hours.

Table 4-XIX. Average Refurbished Fan Module.

	Δ Cruise Fuel Burn, %
Fan Blade	
Tip Clearance	0.38
Leading Edge Contour	0.12
Surface Roughness	0.01
Bypass OGV	
Leading Edge	0.06
Roughness	0.18
Booster	
Tip Clearance	0.03
Surface Roughness	0.01
Splitter Leading Edge	0.07
Total	0.86

High Pressure Compressor Section - The major source of HP compressor deterioration was increased tip clearance between the blades and casing, and vanes and rotor spool. These increased clearances were largely the result of casing distortion and eccentricity which required rework of the blade and vane tips to meet minimum clearance requirements. Rework of the blades and vanes produced larger-than-desired average clearances, since the shortened blades and vanes were reused from build to build (Section 4.0).

This rework procedure was noted during the early stages of this program and corrective action incorporated by most airlines. Not only have some of the blades and vanes, shortened as a result of the unacceptable procedure, been replaced, but controls have been incorporated to prevent a recurrence of this problem. In addition, more attention is being paid to resolving casing distortion and eccentricity during shop visits. As a result of the incorporation of these controls, the estimated loss resulting from increased clearances for the refurbished engine used in this study is estimated as 0.16 percent in cruise fuel burn. This is slightly less than half of the 0.33 percent noted based on inspections of deteriorated hardware.

In addition to the improvement in clearances, blade and vane replacement and cleaning have reduced the loss in cruise fuel burn of 0.22 percent for leading edge bluntness and surface finish to 0.08 percent. The loss attributed to variable stator bushing leakage is recovered during each shop visit, as is the loss attributed to loose blades and vanes. The compressor casings are not reworked to repair the wear coating during each shop visit, and the deterioration loss of 0.01 percent attributed to this condition is included for the unrestored engine.

The unrestored losses for the high pressure compressor are summarized in Table 4-XX. The 0.25 percent increase in cruise fuel burn for the typical refurbished high pressure compressor represents only 33 percent of the total losses documented for a deteriorated compressor after 6,000 hours.

Table 4-XX. Average Refurbished HP Compressor Module.

	Δ Cruise Fuel Burn, %
Blade and Vane Tip Clearance	0.16
Airfoil Leading Edge Bluntness	0.05
Airfoil Surface Finish	0.03
Casing/Spool Surface Finish	0.01
Total	0.25

HP Turbine Section - The high pressure turbine is refurbished every shop visit because of durability limitations. As a result of the refurbishment process, most of the performance loss is also restored, since the mechanical distress contributes to the performance losses.

The reasons for performance loss remaining after restoration of the high pressure turbine module are limited to distortion of the Stage 1 nozzle guide vanes and airfoil surface roughness. The distortion of the Stage 1 nozzle vanes, which produces a parasitic leakage path, is automatically corrected when new or repaired vanes are incorporated. It is estimated that 50 percent of the vanes are replaced during each shop visit which reduces the 0.10 percent increase in cruise fuel burn loss assessed for the deteriorated parts to 0.05 percent for the refurbished module. The convex surfaces on the blades and vanes are not materially improved during a typical shop visit, so the unrestored losses assessed for this condition are equivalent to the 0.10 percent loss presented for the deteriorated hardware.

The unrestored losses in a refurbished high pressure turbine module are summarized in Table 4-XXI. The 0.15 percent loss in cruise fuel burn represents only 20 percent of that assessed for the deteriorated components.

Table 4-XXI. Average Refurbished HPT Module.

	Δ Cruise Fuel Burn, %
Stage 1 Nozzle Distortion	0.16
Airfoil Surface Finish	0.10
Total	0.15

Low Pressure Turbine Section - The low pressure turbine module typically accumulated over 10,000 hours with little or no repair. This assembly has excellent durability, and disassembly to restore mechanical integrity is infrequently required. Since the module is only infrequently disassembled, the unrestored losses for the average module are equivalent to those of the deteriorated module.

The estimated losses for the average "refurbished" low pressure turbine module are presented in Table 4-XXII.

Table 4-XXII. Average Refurbished LPT Module.

	Δ Cruise Fuel Burn, %
Blade Tip Clearance	0.30
Interstage Seal Clearance	0.22
Airfoil Surface Finish	0.04
Total	0.56

Average Refurbished Engine - A model which depicts the unrestored losses for an average refurbished engine is merely the sum of the losses for the individual modules. The unrestored losses for the individual modules are presented in Table 4-XXIII. As shown, the average refurbished engine based on hardware inspection results has an increased fuel burn of 1.82 percent when reinstalled for additional revenue service.

Table 4-XXIII. Average Refurbished Engine Model.

	Δ Cruise Fuel Burn, %	
Fan Section		
Fan Blade Tip Clearance	0.38	
Fan Blade Leading Edge Contour	0.12	
Fan Blade Surface Finish	0.01	
Splitter Leading Edge	0.07	
Bypass OGV - Leading Edge	0.06	
Bypass OGV - Surface Finish	0.18	
Booster Tip Clearance	0.03	
Booster Airfoil Roughness	0.01	
Fan Total		0.86
HP Compressor		
Blade and Vane Tip Clearance	0.16	
Airfoil Leading Edge Bluntness	0.05	
Airfoil Surface Finish	0.03	
Casing/Spool Surface Finish	0.01	
HP Compressor Total		0.25
HP Turbine		
Stage 1 Nozzle Distortion	0.05	
Airfoil Surface Finish	0.10	
HP Turbine Total		0.15
LP Turbine		
Blade Tip Clearance	0.30	
Interstage Seal Clearance	0.22	
Airfoil Surface Finish	0.04	
LP Turbine Total		0.56
Average Engine Total		1.82

SUMMARY

PERFORMANCE DETERIORATION MODELS

Independent assessments of performance deterioration characteristcs for the CF6-50 model engine were presented as based on both empirical performance data and hardware inspection results. The hardware inspection results were used to isolate the specific damage mechanisms or sources of the performance deterioration. An equivalent fuel burn loss was assigned for each damage mechanism using analytical tools, such as thermodynamic cycle decks and influence coefficients. This method produces an accurate assessment of the damage mechanisms or sources of performance deterioration by direct comparison of the condition of used hardware with as-new parts, but the accuracy of the performance loss assigned for each source is dependent primarily on the accuracy of the analytical tools. Some of the analytical tools have been previously verified (or verified during this program) by the use of special engine or component tests, but many of the factors and subjective evaluations are based only on assumptions and analysis. While experience has indicated that the analytical tools produce reasonable results, it was necessary to verify the performance levels assigned to the hardware conditions before the results could be considered realistic.

Performance data were available to describe the performance deterioration characteristics for the initial installation and multiple build engines from installation to removal, and to determine the level of performance for the refurbished engine as it re-enters revenue service. While the primary use for the performance data was to describe the magnitude and rate of deterioration with time, these data were also used to verify the deterioration levels assessed using the hardware inspection results.

Hardware inspection data were obtained almost exclusively from engines which were disassembled for refurbishment during a shop visit. These hardware results could be summarized for the three specific types of engines: i.e., initial installation engine at nominal removal times, multiple build engine at nominal removal times, and an engine after typical refurbishment but prior to re-entering revenue service. While the loss assigned to each hardware condition cannot be individually verified, the losses for the individual parts could be summarized to produce a "total engine value" for each of the three engine designations. These, in turn, could be directly compared with the levels determined for each engine designation based on performance data. A good agreement between the two independent assessments of performance deterioration would produce confidence that the results were reasonable.

A comparison between the fuel burn deterioration assessed from the hardware inspection results and performance data for each of the three major engine designations (initial-installation, multiple build, and unrestored loss) are discussed in the following paragraphs.

Initial Installation Engine

A comparison of the cruise performance and hardware inspection results for the initial installation engine is presented in Figure 4-88. As shown, the comparison produced good agreement.

The hardware data results as presented in Section 4.0 of this report require adjustments in order to isolate the deterioration which did not occur in service (i.e., items that occur as a result of refurbishment during the initial or a subsequent shop visit). Items disregarded include a portion of the increase in average clearance for the fan blade tip and for the high pressure compressor blade and vane tips. The portion of the clearance change disregarded was the amount attributed to either shroud or airfoil tip rework required during engine rebuild to meet the specified minimum clearance.

Cruise performance losses were derived from cockpit data beginning with the first recording available during revenue service and trended to removal. This is the most convenient way of determining delta cruise performance level for the initial installation portion of the life cycle. The short-term losses, those which occur during aircraft checkout prior to revenue service, were separately derived. The total deterioration for the average initial installation engine at removal is the sum of the short term losses plus that experienced during 4,000 hours of revenue service.

The 4,000-hour nominal value for the initial installation engine was selected based on examination of fleet removal statistics and hardware inspection data. The hardware inspection results were summarized for each engine module in Section 4.0 of this report to obtain the equivalent losses after either 4,000 or 6,000 hours of revenue service. A review of the fleet removal statistics for the DC-10-30 aircraft indicated the nominal time to removal was 4,000 hours when ignoring "infant mortality" failures not representative of long-term deterioration. Since the DC-10-30 engines comprise over 70 percent of the ertire fleets, and hardware inspection results to describe the losses after 4,000 hours were available for all modules, that value was chosen for the comparison point.

Examination of the performance deterioration characteristics for the DC-10-30, B747, and A300-B aircraft indicates a similar rate (0.53 percent, 0.45 percent, and 0.55 percent per 1,000 hours, respectively). Therefore, a rate of 0.5 percent per 1,000 hours was selected as most appropriate for this study. Based on this rate, total deterioration for the average initial installation engine at removal was 2.7 percent in cruise fuel burn which is comprised of 0.7 percent for the short term and the remainder during revenue service.

The comparative values of 2.42 percent in cruise fuel burn based on hardware inspection results, and 2.7 percent based on cruise performance results as shown in Figure 4-88 indicate these data are reasonable and, therefore, the hardware results were considered representative for the initial installation engine.

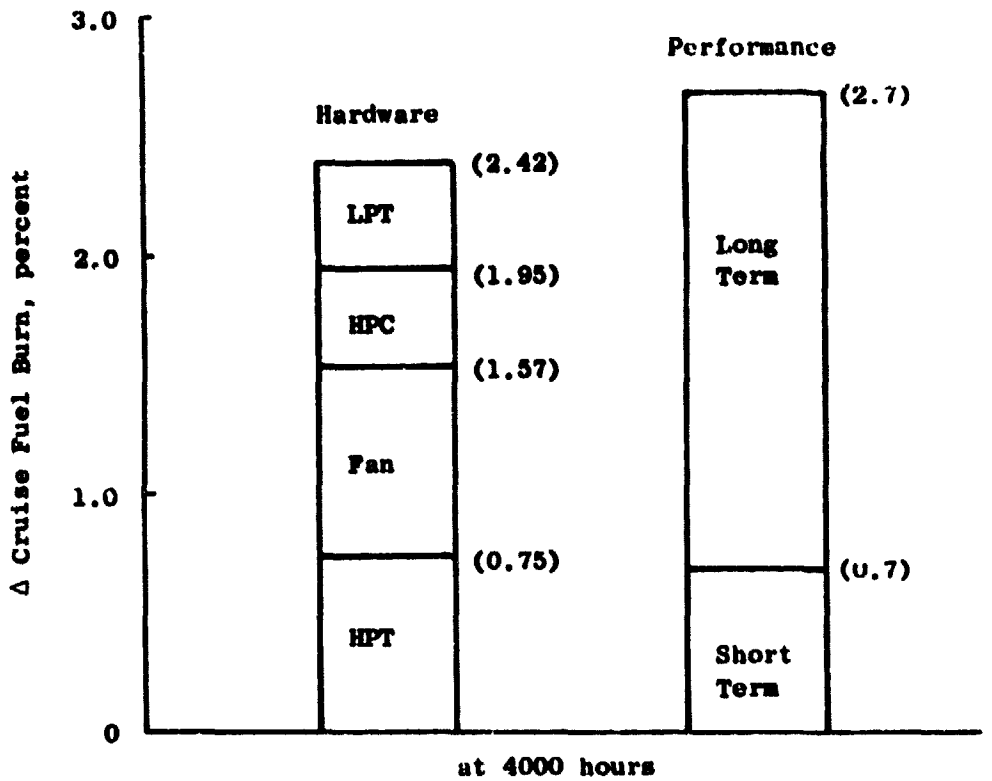

Figure 4-88. Initial Installation Engine at 4000 Hours.

Refurbished Engine

The performance losses documented for the refurbished engine based on hardware inspection results noted in Section 4.0 were compared with the average test cell calibration run for the refurbished engine. These data are presented in Figure 4-89.

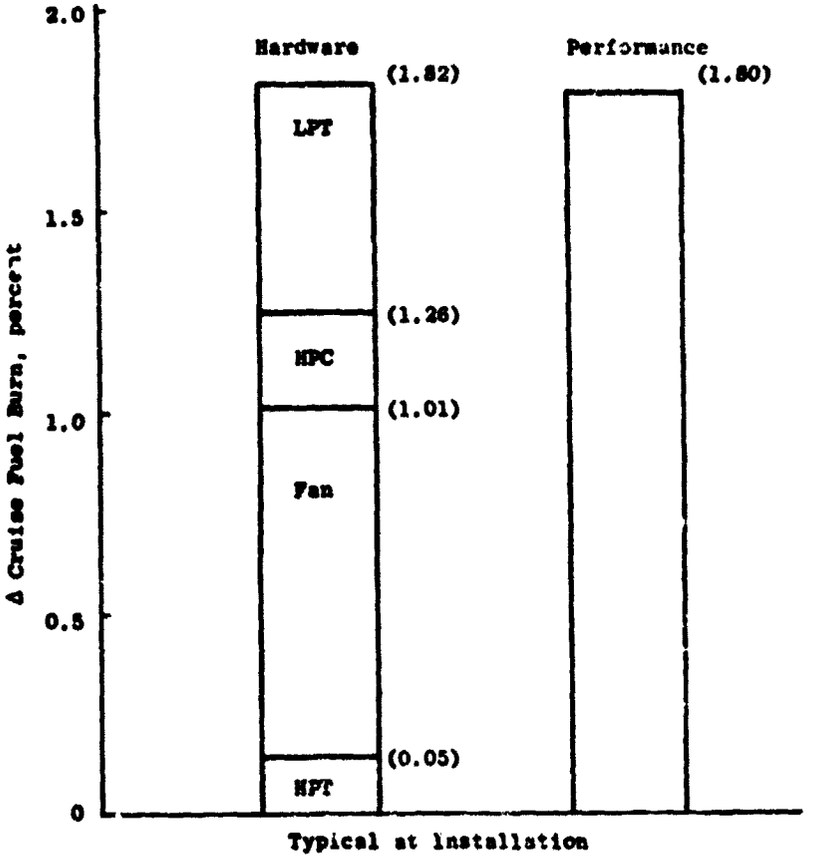

Figure 4-89. Unrestored Losses for Typical Engine.

Measured test cell performance data from one specific refurbishment source was obtained for all engines tested during 1979 and used to establish average performance characteristics (Rationale presented in Section 4.0). The equivalent performance loss ascertained from hardware inspection results required some adjustments to ensure that the hardware conditions were being documented for the same time period. This is explained in Section 4.0 of this report; and as presented, the most notable adjustment was for high pressure compressor clearances. Also, the decision not to include any refurbishment of the low pressure turbine module was predicated on investigations which indicated only a small percentage of these modules were refurbished during this period.

The good agreement between the fuel burn losses assessed from hardware inspection results for the refurbished engine and the corresponding performance levels measured during the engine recalibration in the test cell as shown in Figure 4-89 indicate that the hardware inspection data documenting the unrestored losses are realistic.

Multiple-Build Engine

The comparison of performance deterioration based on measured performance data with that assessed from the hardware inspection results for the multiple-build engine requires the use of data generated for the previous comparisons.

Cruise performance trends from installation to removal are used to document the on-wing deterioration characteristics for the multiple-build engine. These data are comprised of deltas or differences from the applicable aircraft flight manual; the initial trend data for each individual engine establishes the zero baseline. This is the simplest method for producing delta change for accumulated time, but disallows a direct comparison with the average production engine since the assumed zero reference has no relationship to the average production engine.

To provide the necessary link between production and field data, the projected delta established based on the average test cell calibration level for the refurbished engine was used. This value accurately describes the delta deterioration from the production new engine for the average multiple-build engine at installation. The simple addition of the cruise fuel burn deterioration equivalent to the measured test cell losses at installation plus the in-service delta loss measured from cockpit cruise recordings produces the total deterioration for the multiple build engines at removal.

The hardware inspection results were also adjusted using data from the previous comparisons to produce acceptable data representing the average engine at removal. (3,000 hours of revenue service was chosen since this value was near the nominal for multiple-build engines in the fleet.) Hardware inspection results which describe the unrestored losses remaining after refurbishment (Table 4-XXIII) were used as the baseline to describe each module at engine installation. The amount of deterioration that should be attributed to each hardware source during 3,000 hours of in-service operation was based on the estimated deterioration rates presented in the previous comparisons. The estimated in-service loss at 3,000 hours was then added to the unrestored loss isolated for each deterioration source to produce the total loss at removal. For example, the total loss attributed to the change in fan blade leading edge contour after 6,000 hours was 0.44 percent in cruise fuel burn. The average unrestored loss for this condition was 0.12 percent in cruise fuel burn. Therefore, one-half (3,000/6,000 hours) of the expected deterioration after 6,000 hours (0.44/2) was added to the 0.12 percent present at installation to arrive at the total of 0.34 percent in cruise fuel burn.

The comparison of the performance deterioration assessed from measured performance data with that assessed from the hardware inspection results for the average multiple-build engine after 3,000 hours of operation is presented in Figure 4-90. This good agreement indicates the assumptions were realistic, and the data presented for the multiple-build engines are reasonable representations for the fleet. These data also tend to verify that the other comparisons are valid, since the construction of the multiple-build model is heavily dependent on the results presented for those models.

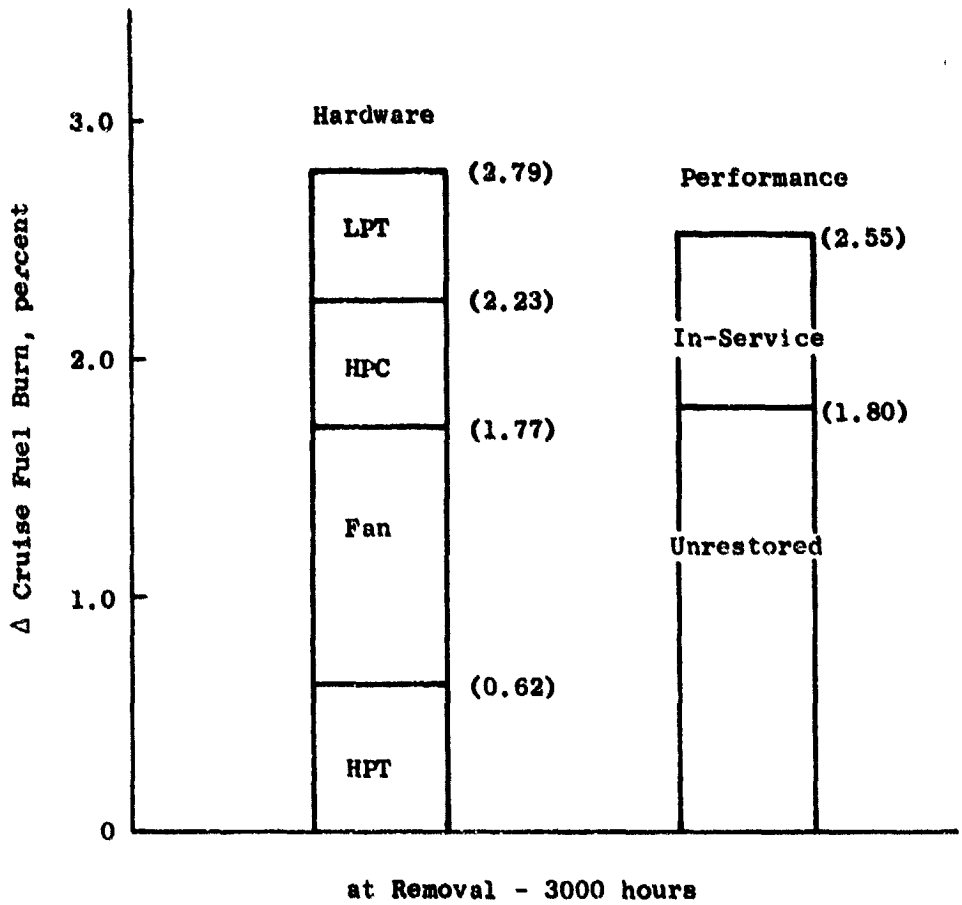

Figure 4-90. Multiple Build Engine at Removal.

5.0 RECOMMENDATIONS

The primary objective of this program was to identify performance deterioration characteristics which could be useful in reducing fuel burn, thus having a favorable impact on the national energy shortage. The most fruitful area for fuel conservation was shown to be in the unrestored performance area; that is, the in-service deterioration which is not corrected during subsequent shop visits. This represents over 71 percent of the total fuel burn deterioration calculated for the CF6-50 model engine at removal, and amounts to over 15 gallons of cruise fuel burn for every engine flight-hour. Immediate fuel burn reduction can be realized by more effective and/or additional restoration during each shop visit. While reducing energy consumption is important, the airlines require that any maintenance over and above that required to restore mechanical capabilities be cost-effective.

The General Electric hardware teams conducted cost-effectiveness feasibility studies for each of the deterioration items. These studies consisted simply of calculating the labor and material costs, with no attempt to incorporate other financial considerations. Note: the individual airlines have their own distinct ground rules on what is to be included in cost effectiveness studies, and generally include: labor and fuel costs, burden (overhead), investment and cost of money. The studies were not directed toward any specific airline(s), as the required input data are considered proprietary and, hence, direct airline input was not available. Reasonable assumptions were used by the teams based on normal airline relationships to determine the criteria to use for these studies. It is for these reasons that these studies are termed cost-effectiveness feasibility studies, and each airline has to adjust the results to its own specific criteria.

STUDY CRITERIA

Cost-effectiveness studies consist of two major items: additional costs for the modification, and expected reduction in operation costs, - the difference represents the potential savings. Additional costs were calculated using a labor rate of $36.00/hour (which includes an estimated overhead of 200 percent) and material costs based on the General Electric 1979 parts catalog. The teams estimated the labor needed to perform the modifications and included the man-hours required to disassemble/reinstall the individual parts into the specific modules. It was assumed that the individual modules were exposed as a result of normal mechanical repair. The "cost of money" was not included in the study, nor were any investment criteria ("bricks and mortar"). The determination of material costs assumed the vendor repair cost rather than new-part cost, where applicable.

The calculation of reduced operating costs required the establishment of the amount of performance to be restored, the "useful life" or hours until the gain is completely lost, and a "life factor" which represents the rate at

which the gain deteriorates. The useful life and life factor were derived for each condition by the hardware teams based on their observations, other General Electric studies or tests, analytical calculations and common sense. Figure 5-1 schematically describes the life factor and useful life items. Two different life factors are shown, and the area above the curve represents conditions where reduced fuel consumption is available. Experience indicated that the deterioration rate was generally linear with time and, therefore, a life factor of 0.5 was assigned unless otherwise determined. The amount to be gained for each condition was not assumed to be equivalent to its total assessed loss, but rather was estimated in terms of what percentage of the loss could be restored using current technology and tooling.

The fuel usage was calculated for a typical DC-10-30 mission (majority of flight hours), and was estimated at 850 gallons of fuel per engine flight hour at a cost of $1.00/gallon. The cost was based on the average amount which was charged a foreign consortium in late 1979, and was used because the CF6-50 powered aircraft are flown extensively by foreign airlines. These values produce a cost savings of $8.50/engine flight hour for each 1% in cruise fuel burn. The actual fuel consumption and cost will have to be determined by the individual airlines when they conduct their own cost effectiveness studies based on "then current" fuel costs and aircraft type.

An improvement in cruise fuel burn (sfc) will produce a corresponding improvement in EGT margin which will reduce hardware consumption because of lower operating temperatures, and possibly extend time on-wing between shop visits. While these are potentially significant cost reduction items, they are very difficult to generalize and are not included in these studies. Rather, this potential benefit, while not calculated, can be used to justify acceptance of marginally cost-effective items.

STUDIES

The data used to determine the cost effectiveness for the individual items are presented in Table 5-I. The items are arranged by the individual modules, and the column headings are those previously explained. The listing includes the major items isolated by these studies and is not presumed to include every single source. For the items where a materials cost is noted under the Modification column without a corresponding labor cost, the fixed vendor replacement repair cost is assumed. As shown in Table 5-I, the useful life for the repairs ranged from 4,000 to 12,000 hours, with most of the life factors assumed to be 0.5. This was necessitated by the lack of hardware inspection data below 2,000 hours; a condition which prevented an accurate assessment of the deterioration curve shape. Deterioration items which are restored during each shop visit, such as high pressure turbine blade-to-shroud clearance, are not included in the study.

These data (as shown in Table 5-I) were used to calculate the potential cost-effectiveness for each item using the labor and fuel costs previously presented. The pertinent data from the cost-effectiveness studies (without the

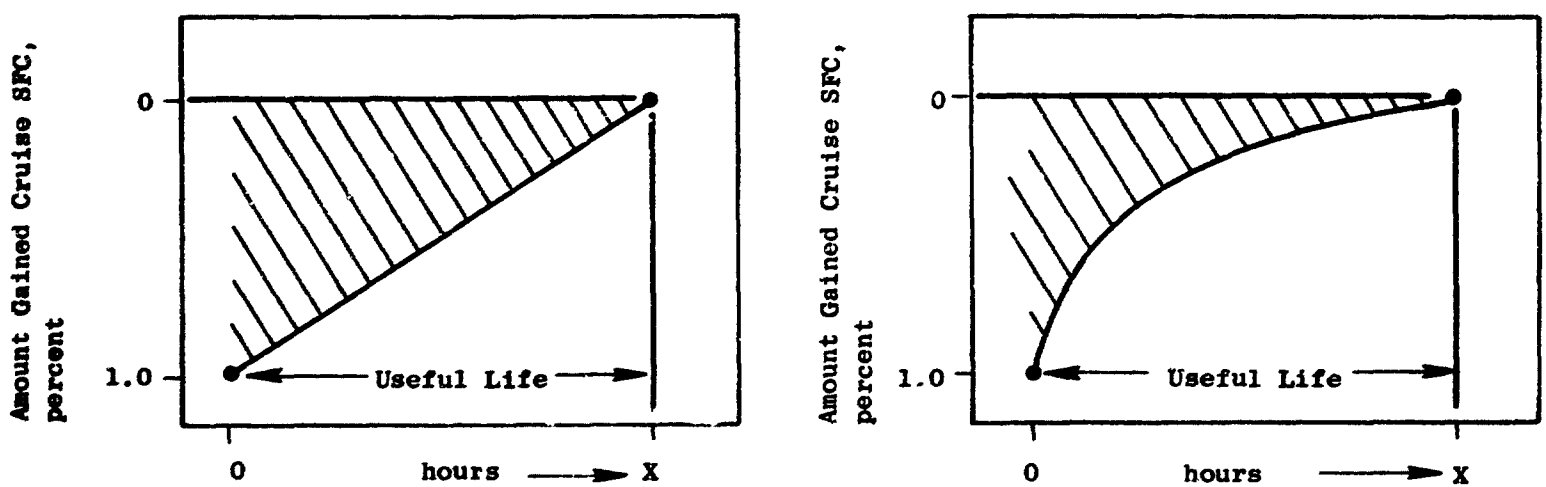

X - Hours when Gain is Completely Lost

Figure 5-1. Cost Effective Factors.

Table 5-I. Cost Reduction Studies.

	Reduction Costs			Additional Costs		
	sfc Gain (%)	Useful Gain (hrs)	Life Factor	Removal/ Install (hrs)	Modification Labor (hrs)	Modification Material ($)
Fan Section						
Fan Blade Tip Clear	0.38	12000	0.5	6	25	100
Fan Blade Leading Edge Contour	0.44	6000	0.5	1.5	9.5	---
Fan Blade Roughness	0.015	6000	0.5	1.5	6.5	
Splitter Leading Edge	0.07	9000	0.5	2.0	8.0	---
Bypass OGV - Finish	0.24	12000	0.5	7.0	---	1000
Booster Blade Tip Clear	0.03	6000	0.5	8.0	---	1000
Booster Airfoil Roughness	0.01	6000	0.5	8.0	8.0	---
Fan Blade Cleaning	Not Applicable - Restored					
High Pressure Compressor						
Blade/Vane Tip Clear	0.33	6000	1.0	54	---	11492
Blade Leading Edge Bluntness	0.11	6000	0.3	15	---	1518
Blade/Vane Roughness	0.11	6000	0.3	32	6	303
Casing/Spool Finish	0.01	6000	0.5	---	30	100
Variable Stator Bush Leak	Not Applicable - Restored					
High Pressure Turbine						
Stage 1 and 2 Tip Clear	Not Applicable - Restored					
Stage 1 Nozzle Leakage	0.10	4000	0.25	12	---	2875
Airfoil Surface Finish	0.10	4000	0.5	---	16	---
Low Pressure Turbine						
Blade Tip Clear	0.30	5000	0.5	16	---	7920
Interstage Seal Clear	0.22	5000	0.5	12	---	4402
Airfoil Surface Finish	0.04	6000	0.5	40	6	520

detailed calculations) are presented in Table 5-II. The savings are ultimately shown as a cost per engine flight hour to put all items on an "apples-to-apples" basis. These studies yielded potential savings ranging from a favorable $1.80/hour to a potential added expense of $0.42/hour. As noted earlier, any positive calculation, however marginal, is considered cost-effective based on the savings in part life expected from the corresponding reduction in EGT.

A review of the data presented in Table 5-II indicates that it is cost effective to restore items which would yield 1.7 percent in cruise fuel burn. Since the refurbished items deteriorate at different rates, the average potential fuel savings calculated was 8.4 gallons/engine flight hour.

However, this potential is somewhat misleading in that some of the listed items are currently being restored by some airlines on at least a part-time basis. There is a wide variance in the routine workscopes for the individual airlines and/or consortiums, and it is very difficult to arrive at the real potential for savings over-and-above what is being accomplished today. However, the total amount being restored for the entire fleet is considered small, and "best estimates" based on studies for the refurbished engine would indicate the level to be equivalent to 0.49 percent in cruise fuel burn. This is equal to approximately 29 percent of the items previously determined to be cost effective. The total engine flight hours projected for the CF6-50 model engines in 1980 for all three aircraft types is 3.1 million. If the estimated savings for the A300-B and B747 aircraft would be the same as for the DC-10-30 aircraft, then the cost effective items currently not being restored represent the potential to reduce fuel consumption by 26 million gallons while saving the airlines 16.6 million dollars during the next 12 months.

In summary, the majority of the unrestored losses for the CF6-50 model engine are cost-effective to restore. It is recommended that the airlines conduct their own cost-effectiveness studies and initiate action to more effectively restore fuel burn losses during each shop visit. This action, in conjunction with General Electric action to develop product improvement items to reduce the magnitude of deterioration, can make a notable impact on energy consumption in the 1980's.

Table 5-II. Cost Effective Study Results.

	Expected Gain		Costs		Savings/Hour	
	sfc (%)	Length (hrs)	Reduced ($)	Added ($)	Fuel (gals)	Dollars ($)
Fan Section						
Fan Blade Tip Clearance	0.38	12000	19380	1216	1.62	1.51
Fan Blade Leading Edge Contour	0.44	6000	11220	396	1.87	1.80
Fan Blade Roughness	0.015	6000	382	288	0.06	0.02
Splitter Leading Edge	0.07	9000	2677	360	0.30	0.26
Bypass OGV - Finish	0.24	12000	12240	1252	1.02	0.92
Booster Blade Tip Clearance	0.03	6000	765	1288	0.13	-0.09
Booster Airfoil Roughness	0.01	6000	255	576	0.04	-0.05
High Pressure Compressor						
Blade/Vane Tip Clearance	0.33	6000	16830	13436	2.81	0.57
Blade Leading Edge Bluntness	0.11	6000	1683	2058	0 28	-0.06
Blade/Vane Roughness	0.11	6000	1683	1671	0.28	---
Casing/Spool Finish	0.01	6000	255	1180	0.04	-0.15
High Pressure Turbine						
Stage 1 Nozzle Leakage	0.10	4000	850	3307	0.21	-0.61
Airfoil Surface Finish	0.10	4000	1700	576	0.43	0.28
Low Pressure Turbine						
Blade Tip Clearance	0.30	5000	6375	8496	1.28	-0.42
Interstage Seal Clearance	0.22	5000	4675	4834	0.94	-0.03
Airfoil Surface Finish	0.04	6000	1020	2176	0.17	-0.19

6.0 CONCLUDING REMARKS

The studies to determine the performance deterioration characteristics of the CF6-50 model engine specifically related to increased fuel burn revealed wide variances in the rates for individual engines. The current on-condition maintenance concept, as opposed to fixed-time-between-overhaul (TBO), together with the modular concept of the engine design, which permits selective refurbishment, contribute to this condition. In addition, cockpit recordings of performance parameters - in particular, fuel flow - were not as consistent as would be desired which also contributed to the wide variance for individual engines.

While the nature of this program was not such that explicit results could be formulated and verified to the "nth" degree by experiments, the salient results presented in this report are a reasonable and accurate representation of the deterioration characteristics for the CF6-50 model engines. This is based on the following key observations:

- Teams of General Electric technical personnel, experienced in all phases of engine/airline operation (mechanical design, aero design, performance restoration, performance analysis and airline service engineering), conducted the detailed data reviews, produced the results, and completed detailed analyses to ensure that their results agreed with the facts and/or engineering logic.

- Specific data obtained as part of this program or from special General Electric programs, including special hardware inspections, back-to-back testing to isolate specific deterioration modes, etc., in conjunction with the routine airline data, produced sufficiently large samples of data to adequately document deterioration characteristics at selected points in the engine life cycle. These points were at the time when the deteriorated engine was removed from the wing for the normal shop visit, and for the refurbished engine after repairs had been completed but prior to re-entry into revenue service. This permitted the most important program objectives to be determined using empirical performance and hardware inspection data. These same data were used to estimate other items, but the estimations were required only to achieve program objectives considered of minor importance.

- When engine performance levels assessed from hardware inspection data for the individual deterioration sources were compared with independently determined levels based exclusively on engine performance data, good agreement resulted for each major element of the engine life cycle.

- It was shown that the average flight length, hours-to-cycle ratio, and average reduced thrust during takeoff operation (derate) each have a significant effect on the performance deterioration characteristics. These effects are completely interrelated, and it was not possible to isolate the individual effects for hours, cycles, or takeoff derate.

- It was not possible to specify a common deterioration rate for the CF6-50 engine when utilized on the three different aircraft types (DC-10-30, A300-B, B747) due to the differences in operational variables (flight length and derate). Since these operational variables tended to correlate with aircraft type and not by airline or other differences, it was possible to establish the deterioration characteristics for the CF6-50 engine when tested on each aircraft type. The average performance characteristics were established as a function of hours (not cycles or derate) since this parameter is commonly used in the aviation industry for this purpose.

Therefore, based on these key observations, it is reasonable and prudent to believe the results obtained during these studies are a reasonable assessment of performance deterioration characteristics for the CF6-50 model engine. The more important results are presented in the following paragraphs:

- Short term losses equivalent to 0.7 percent in cruise fuel burn occurred during the initial checkout flight conducted by the aircraft manufacturer prior to delivery for revenue service. The magnitude of the short term loss was adjudged to be the same for each aircraft type. Hardware data were not available to ascertain the source(s) for this loss.

- The magnitude of deterioration for the average new engine during the initial installation for revenue service was determined for each aircraft type as follows:

Aircraft Type	Hours	Cruise Fuel Burn, %
DC-10-30	3,000	1.5
A300-B	2,000	1.1
B747	4,000	1.6

These are additive to the 0.7 percent short term loss.

- The unrestored loss for the typical airline refurbished engine was equivalent to a 1.8 percent in cruise fuel burn. This level was noted to be constant following the second shop visit, with no increasing or decreasing trend evident through at least 10 shop visits. The level is applicable for each aircraft type since hardware is not segregated by engine type during repair.

- The in-service deterioration for the typical multiple-build engine was established for each aircraft type as follows:

Aircraft Type	Hours	Cruise Fuel Burn, %
DC-10-30	3,030	0.77
A300-B	2,000	0.66
B747	3,850	0.97

- An instant loss (similar to short-term loss for production new engine) could not be isolated for the typical multiple-build refurbished engine entering revenue service.

- While product improvements are being developed in an effort to eliminate the major sources of performance deterioration, additional and/or more effective restoration during each shop visit is the most promising area for expeditious reduction in energy consumption.

- Cost effectiveness feasibility studies conducted as part of this effort indicated that more than 70 percent of the unrestored loss was cost-effective to restore Based on 3.1 million flight hours expected for CF6-50 engines during 1980, cost-effective items not currently being restored represent a potential for reducing fuel consumption by 26 million gallons with a net cost savings of $16.6 million at 1979 prices.

- The potential to make a notable impact on energy consumption in the 1980's has been demonstrated.

APPENDICES

Data are included in these appendices for the following items:

APPENDIX A - CRUISE TRENDING PROCEDURE

APPENDIX B - CRUISE PERFORMANCE DATA

APPENDIX C - LIST OF REFERENCES

APPENDIX D - SYMBOLS AND ACRONYMS

APPENDIX E - SPECIAL TERMINOLOGY

APPENDIX F - QUALITY ASSURANCE REPORT

APPENDIX A

CRUISE TRENDING PROCEDURE

Cruise performance data were obtained from airline revenue service cruise trends. Engine installed performance is recorded regularly for individual engines as a normal airline operational procedure. These cruise data consist of cockpit measurements for significant engine parameters, notably fuel flow (WFM), exhaust gas temperature (EGT), fan rotational speed (N1), and core rotational speed (N2), recorded during stabilized operation at altitude. This information is used by the CF6 operators to monitor the relative health of each engine, to anticipate normal maintenance requirements of the engines, and to assess the performance trends of their fleets.

For the CF6 family of engines, fuel flow and EGT measurements are compared to values from the "Flight Planning and Cruise Control Manual" (FP & CCM) for the same flight condition and N1. This manual is a tabulation of baseline reference curves for installed engine performance under various operating conditions. The baseline is representative of the installed performance of early CF6 production engines used in a flight test program to define reference engine performance.

The cruise performance data points were stored in computer files and utilized to develop statistical trends. Each data point represented an average level obtained from between four and twenty airplane flights. Airline trends in the Contractor's files had generally been normalized to the "FP & CCM" by the operator, and in the one case, smoothed for each engine by a running average of four out of the last six readings. In cases where only as-measured cockpit readings were available, these data were normalized by the Contractor. In all cases, sufficient readings were averaged to yield performance data points which were representative of the individual engines at that period of time.

APPENDIX B

CRUISE PERFORMANCE DATA

Performance data used in this report are presented in Figures B-1 to B-4 in terms of ΔWFM and ΔEGT performance at N1, relative to "FP & CCM." Cruise data points used to determine composite statistical curve fits are shown in Figures B-5 to B-28 for multple-build engines on DC-10-30, 747, and A300 aircraft. The remaining figures present individual engine deterioration characteristics for similar time-since-installation comparison among aircraft type, airline-to-airline, route structure, maintenance shop, and the effects of installed position. These curves are computer plotted, and the X-axis shows time since overhaul as the computer words for time since installation.

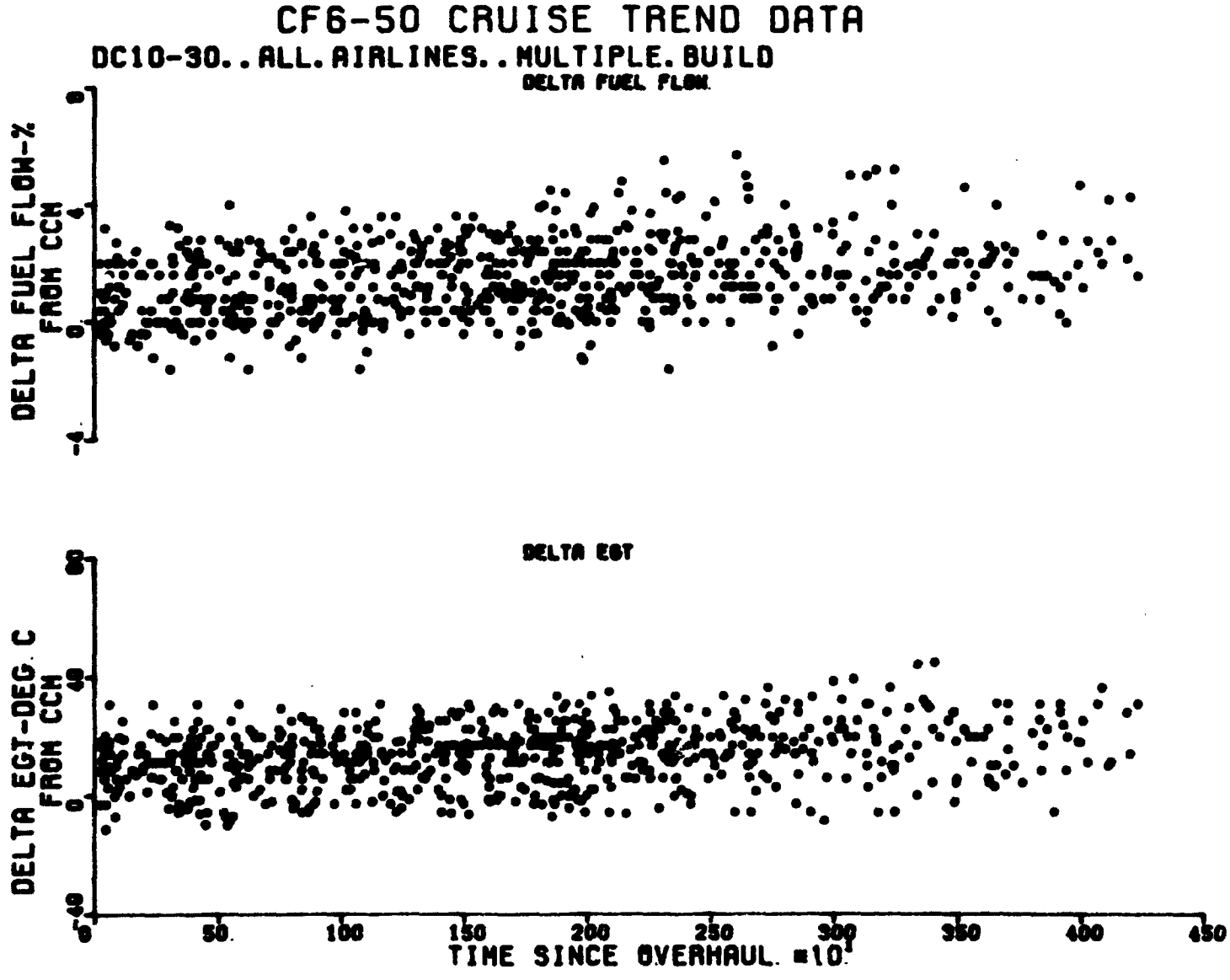

Figure B-1. CF6-50 Cruise Trend Data.

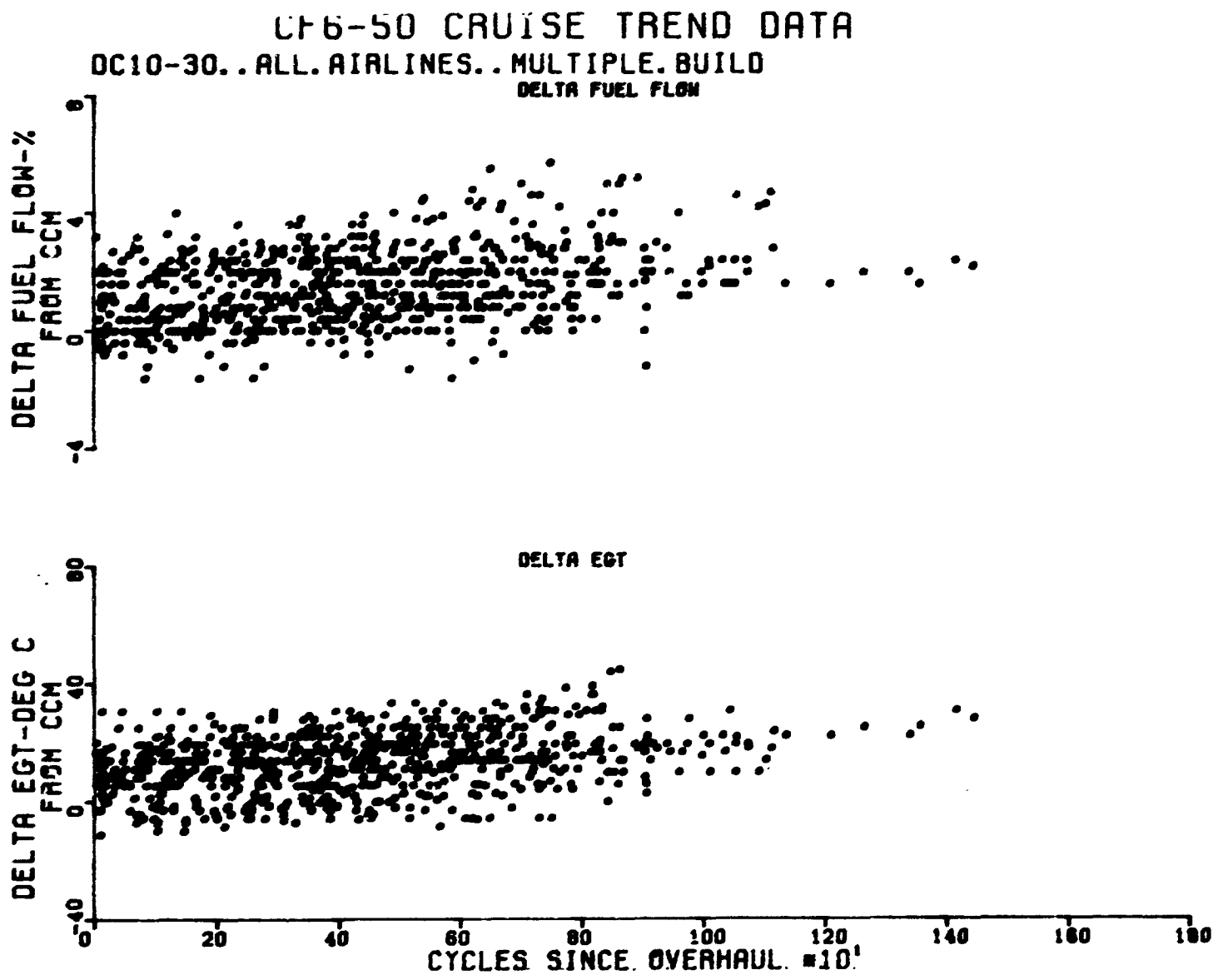

Figure B-2. CF6-50 Cruise Trend Data.

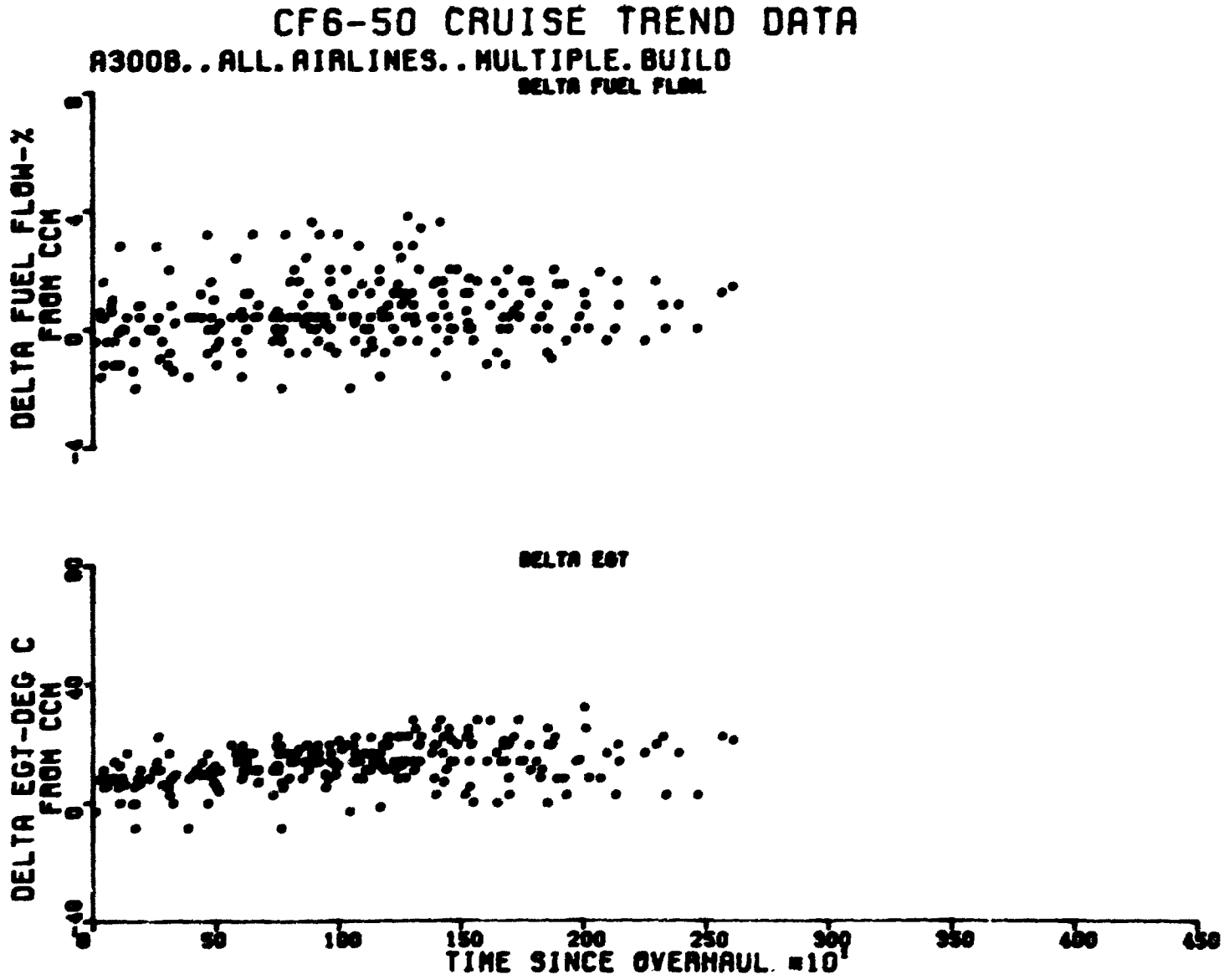

Figure B-3. CF6-50 Cruise Trend Data.

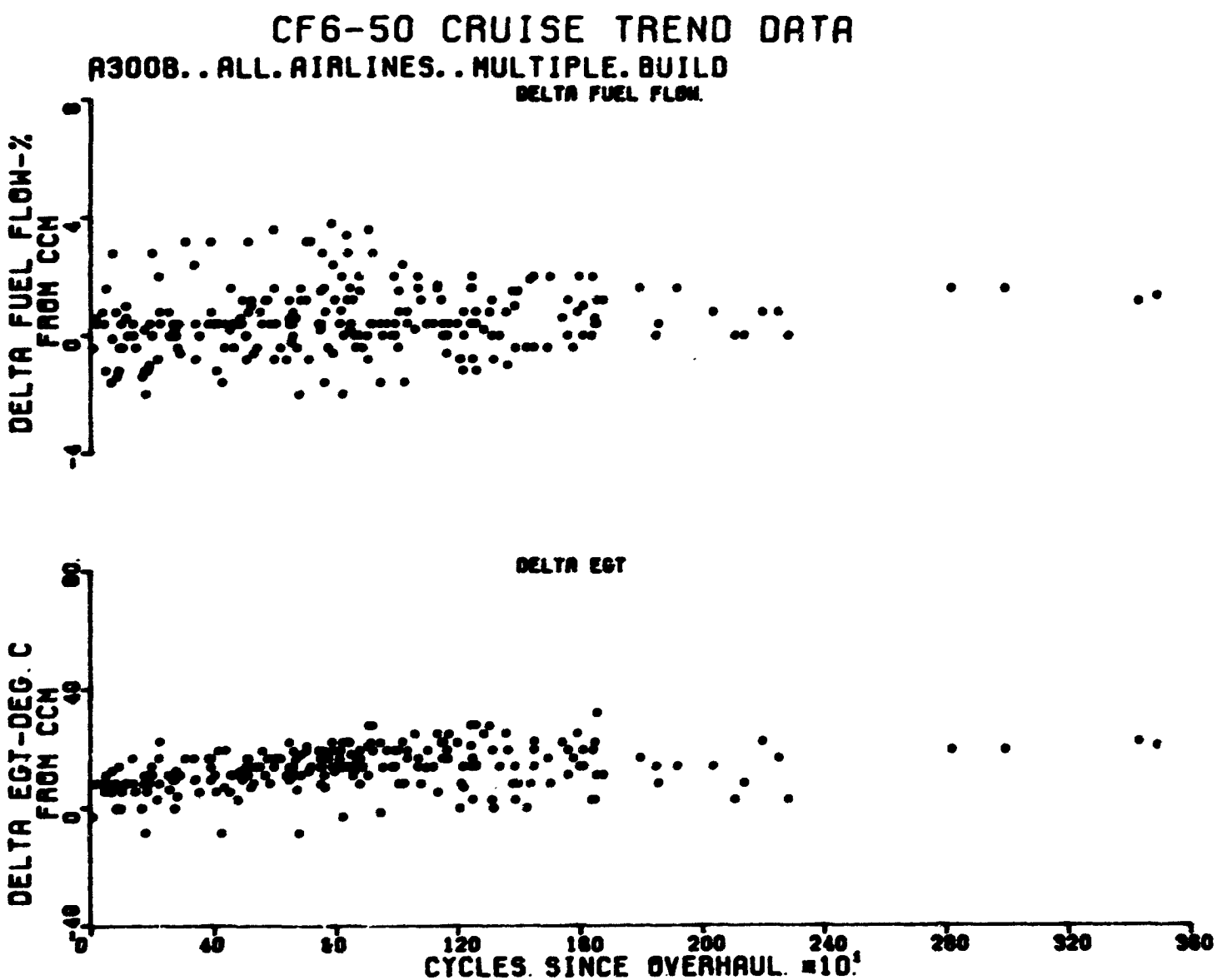

Figure B-4. CF6-50 Cruise Trend Data.

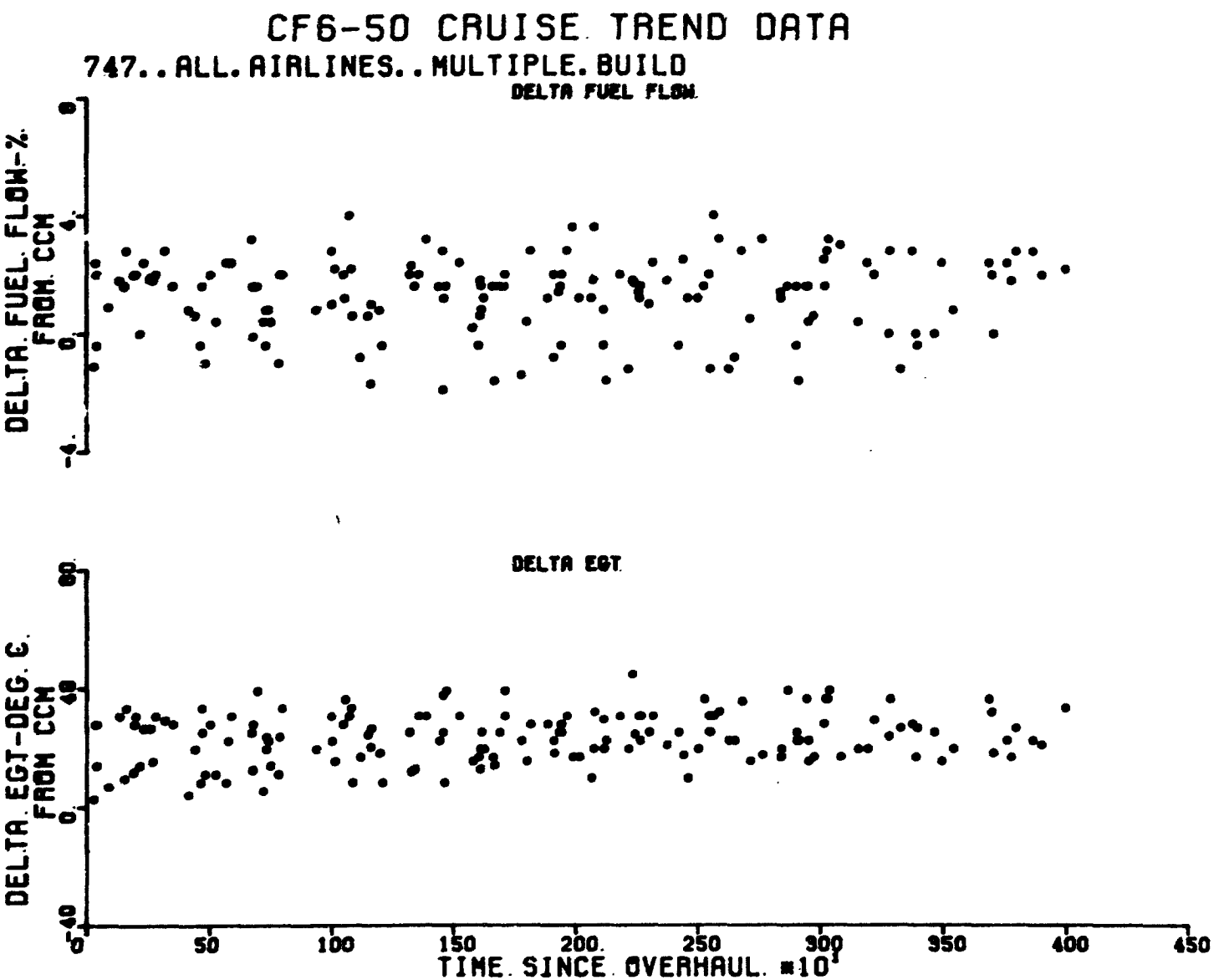

Figure B-5. CF6-50 Cruise Trend Data.

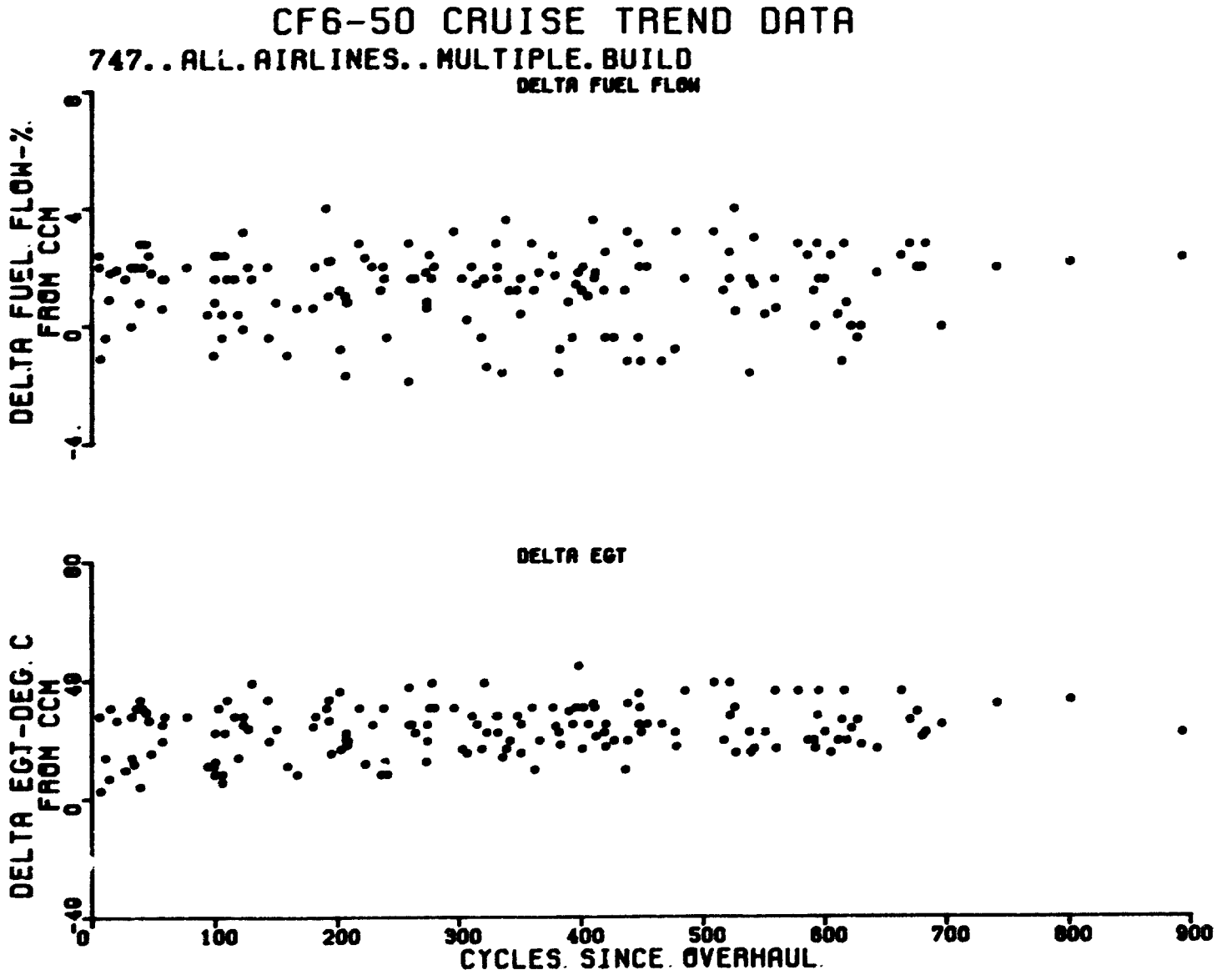

Figure B-6. CF6-50 Cruise Trend Data.

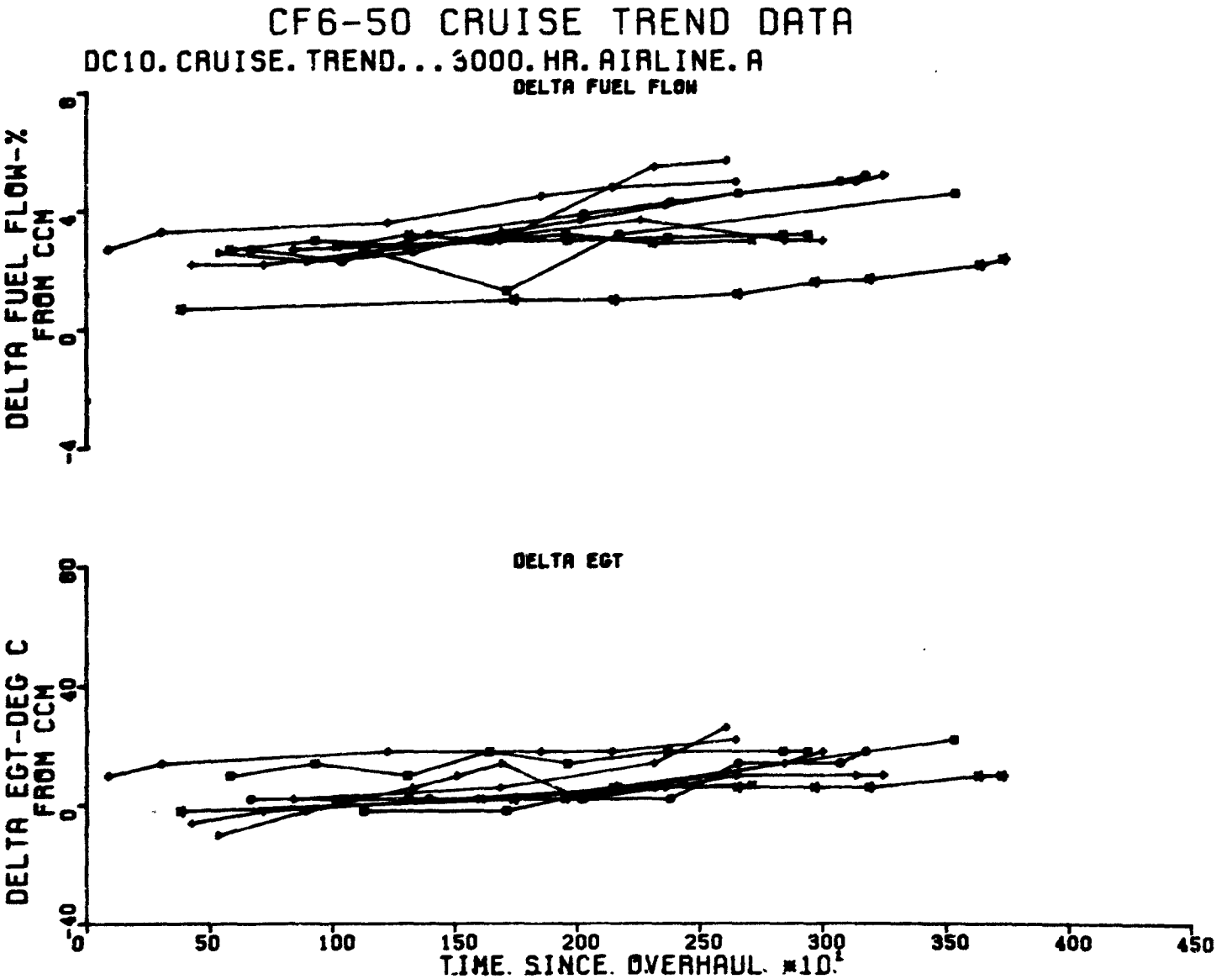

Figure B-7. CF6-50 Cruise Trend Data.

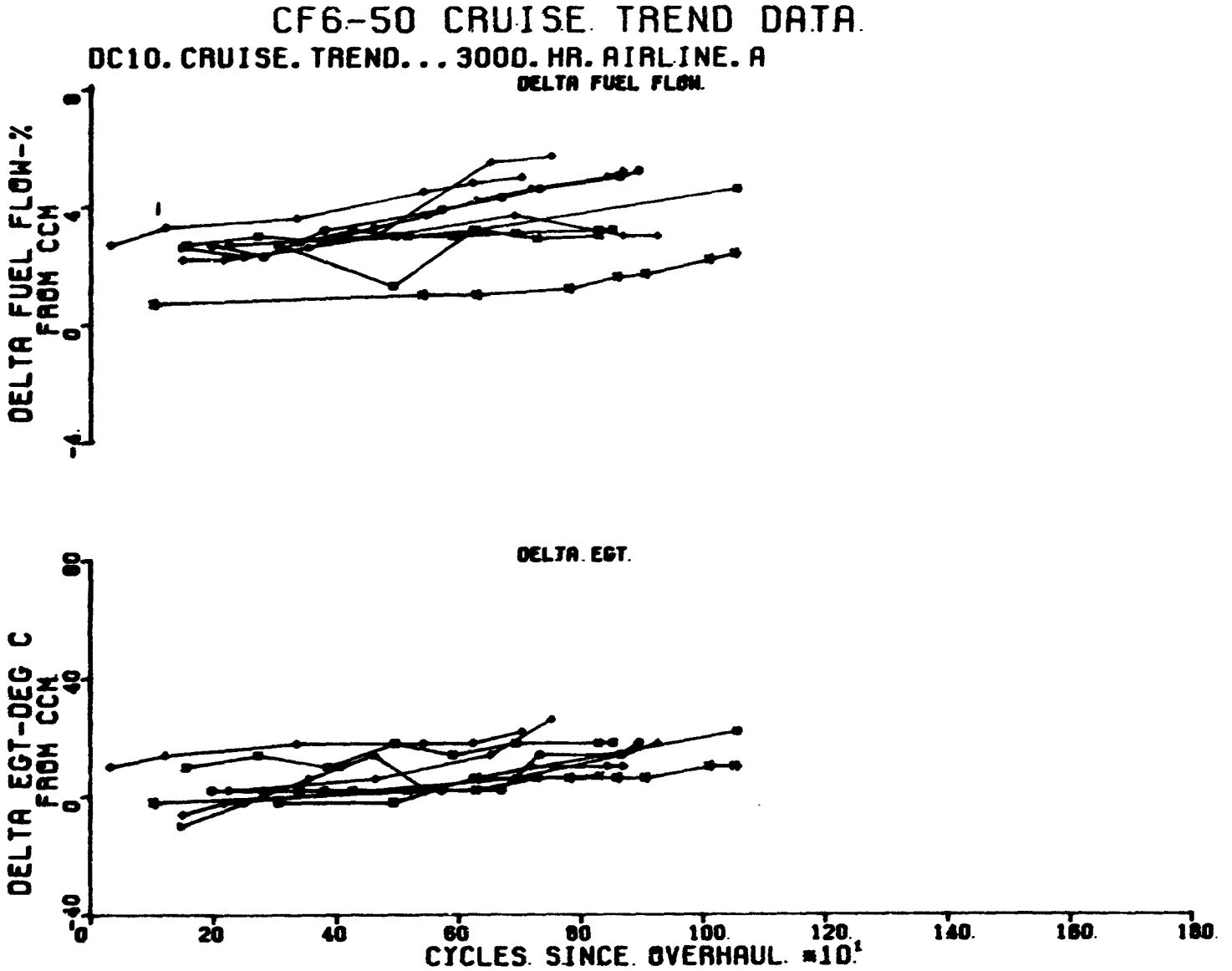

Figure B-8. CF6-50 Cruise Trend Data.

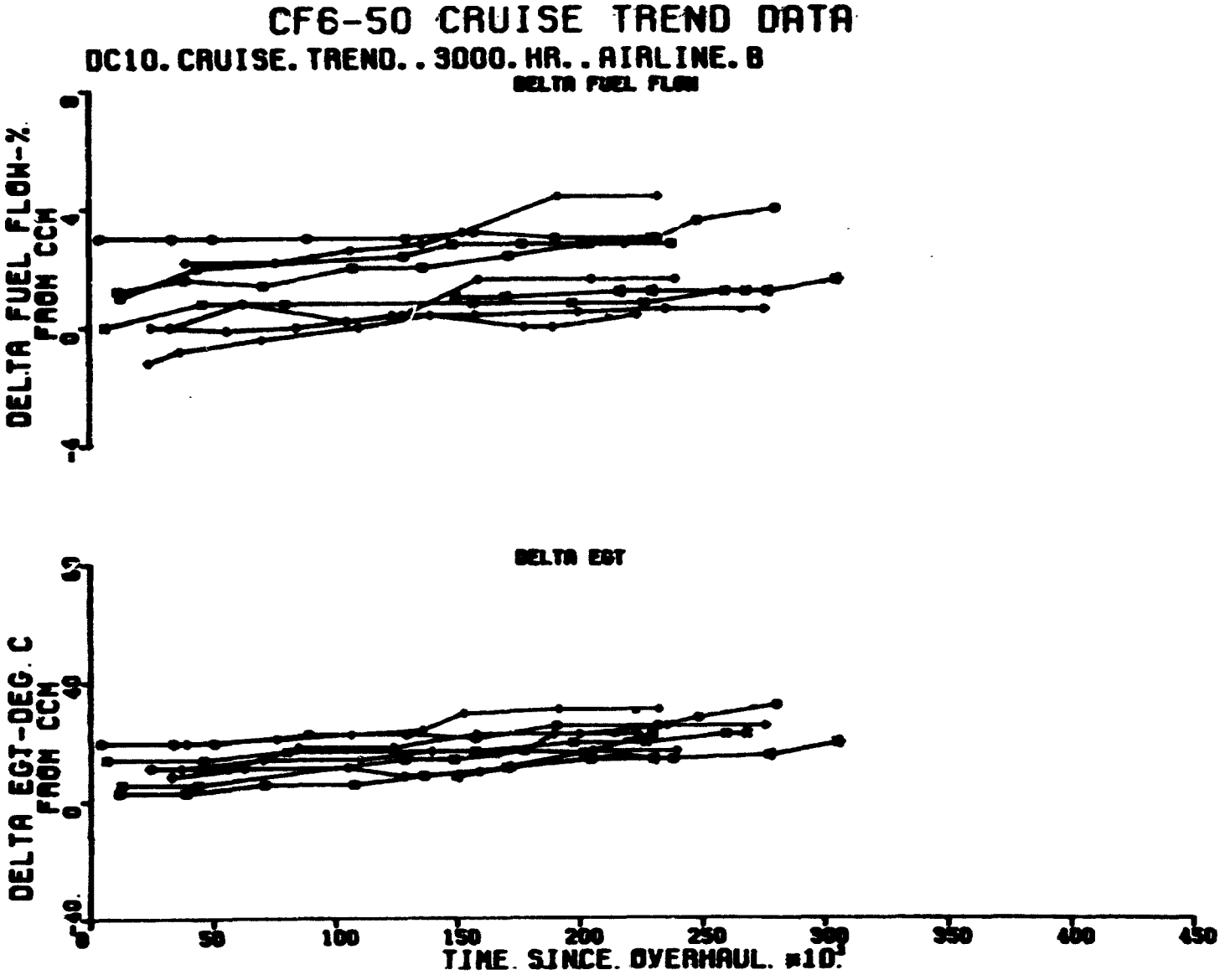

Figure B-9. CF6-50 Cruise Trend Data.

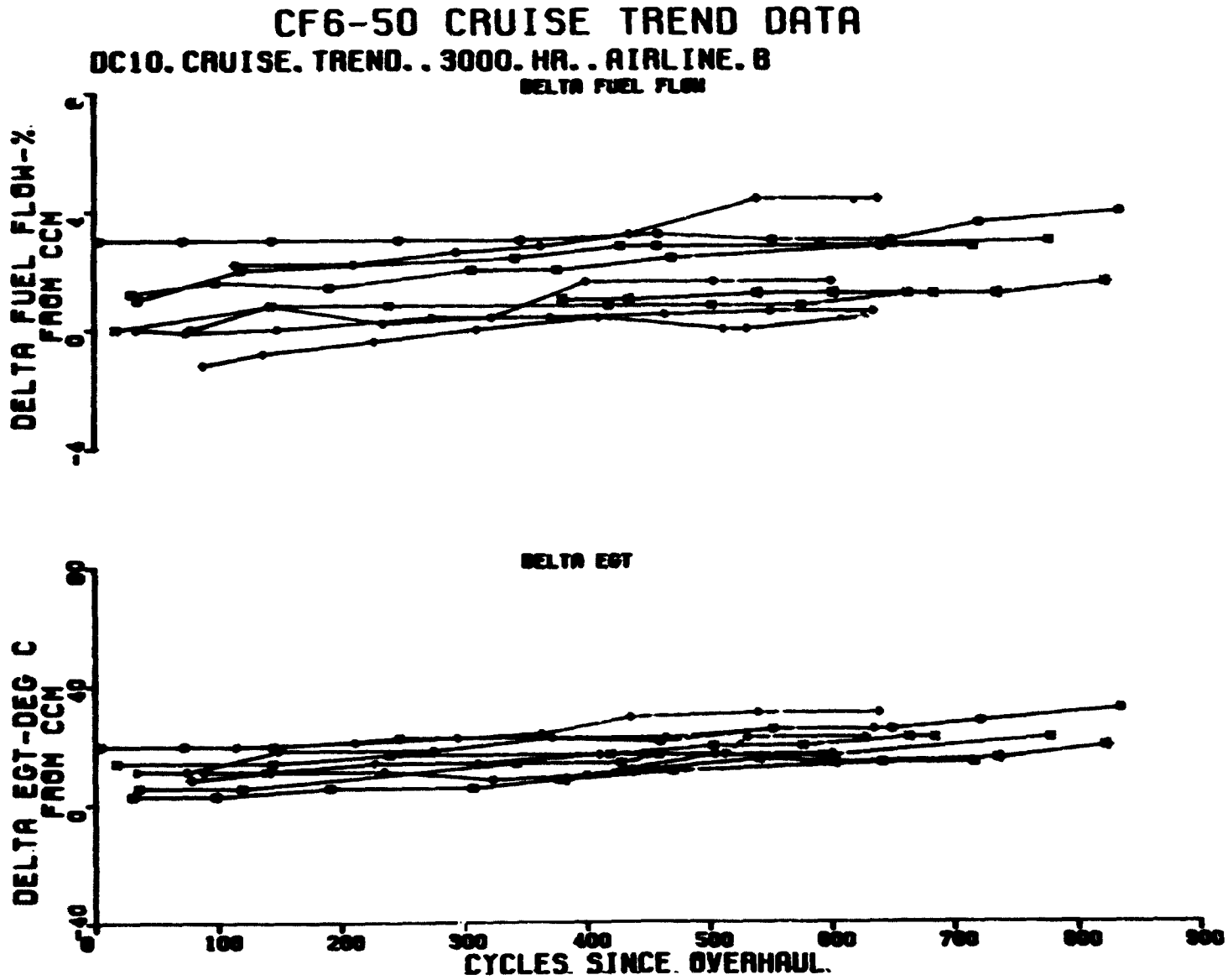

Figure B-10. CF6-50 Cruise Trend Data.

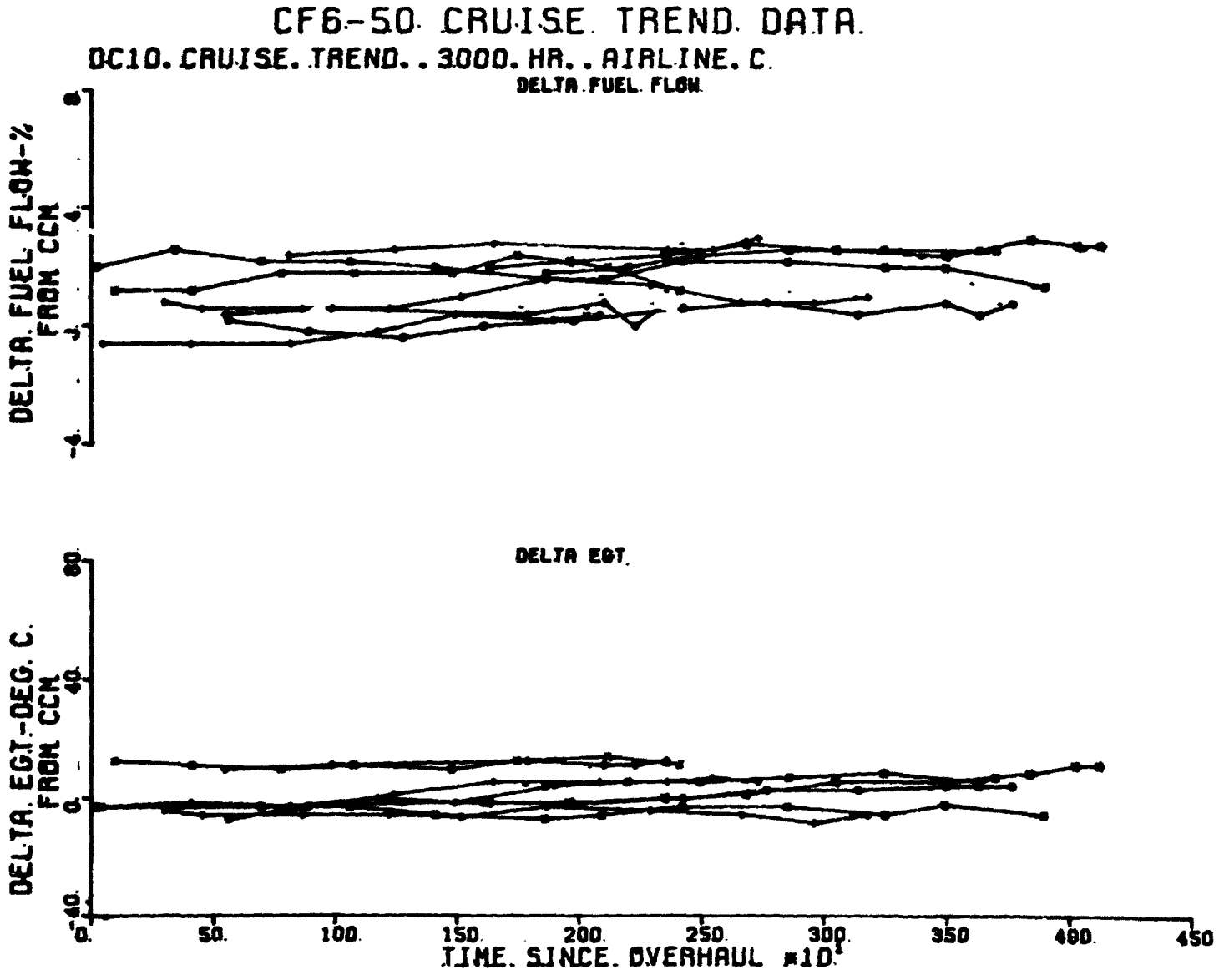

Figure B-11. CF6-50 Cruise Trend Data.

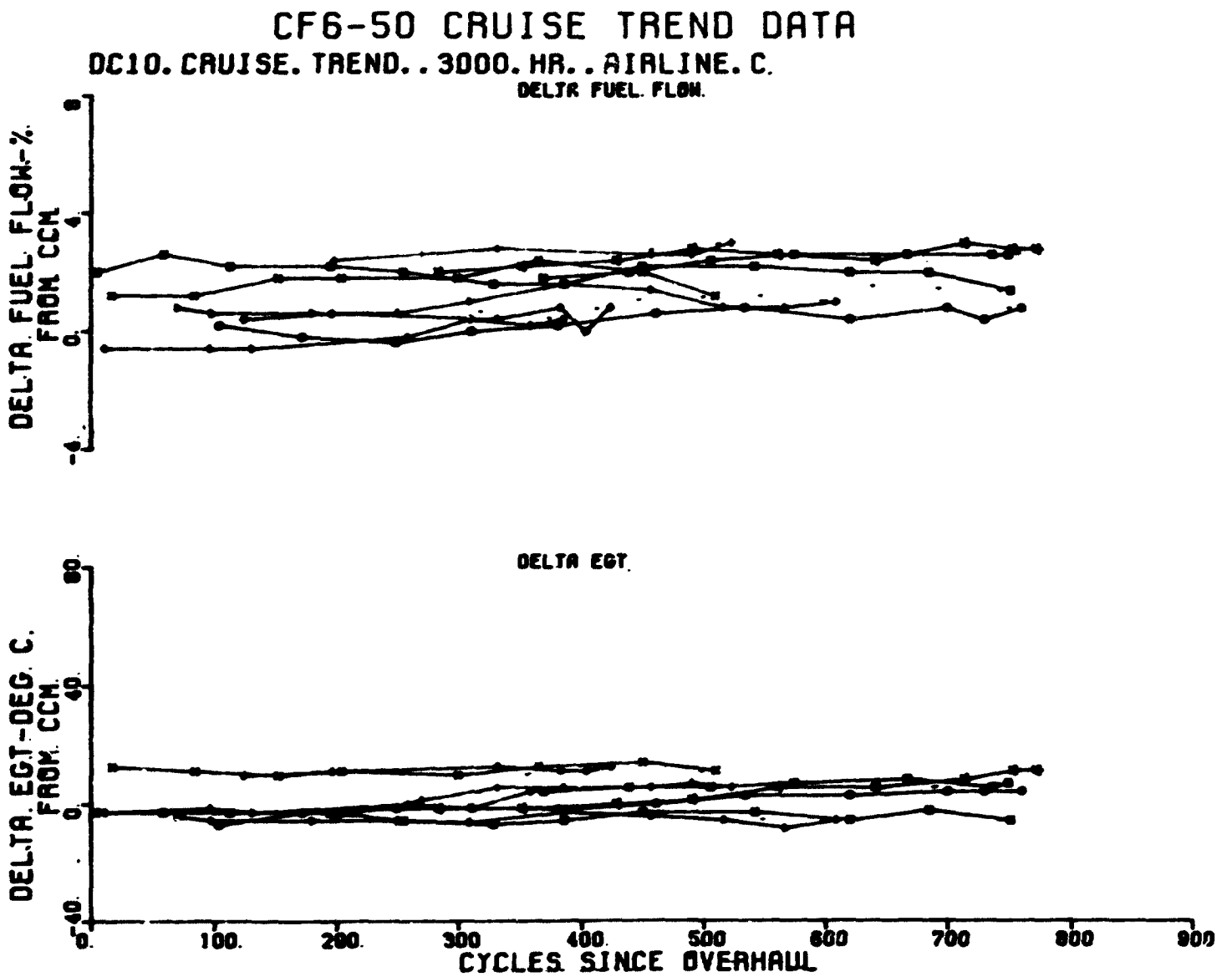

Figure B-12. CF6-50 Cruise Trend Data.

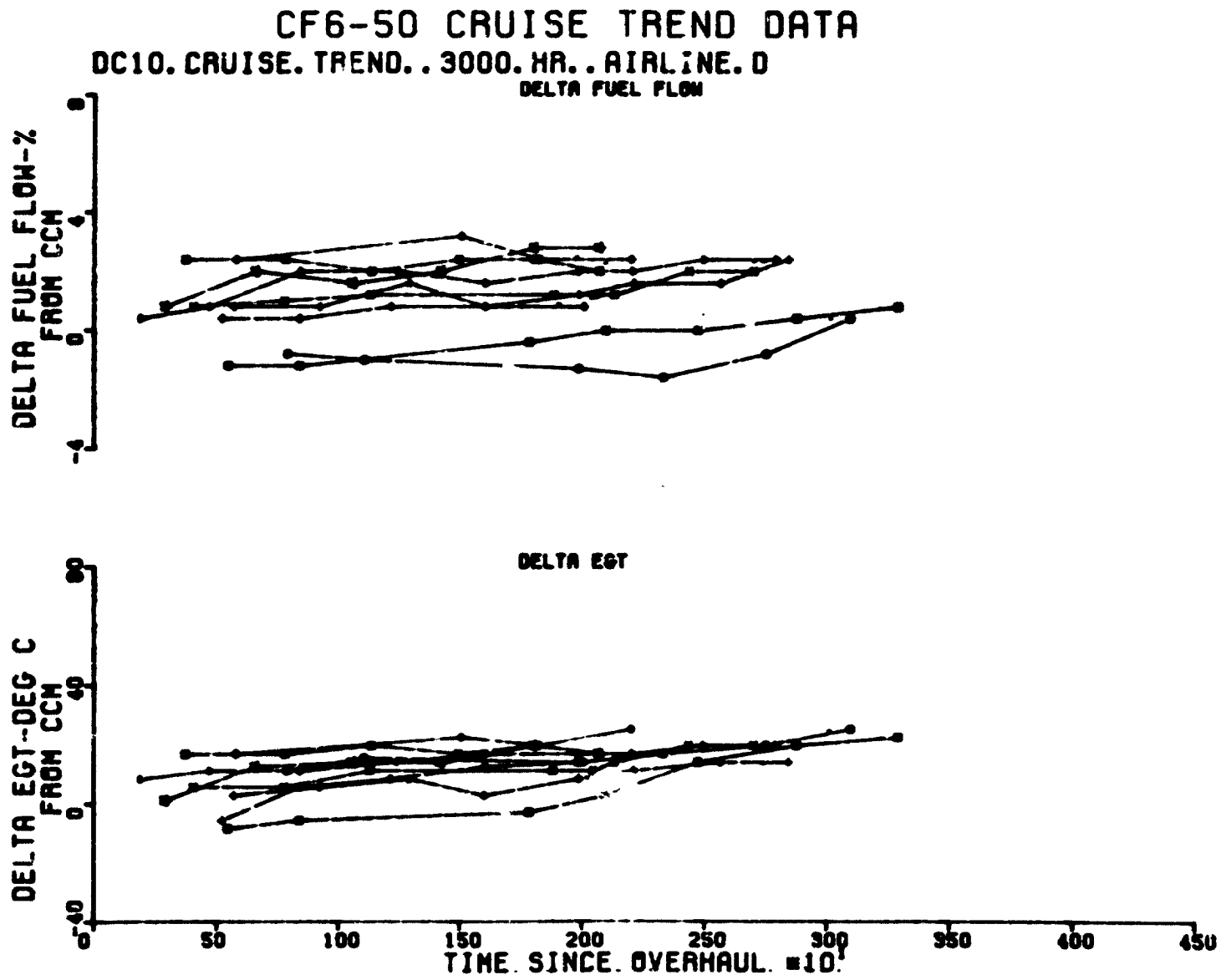

Figure B-13. CF6-50 Cruise Trend Data.

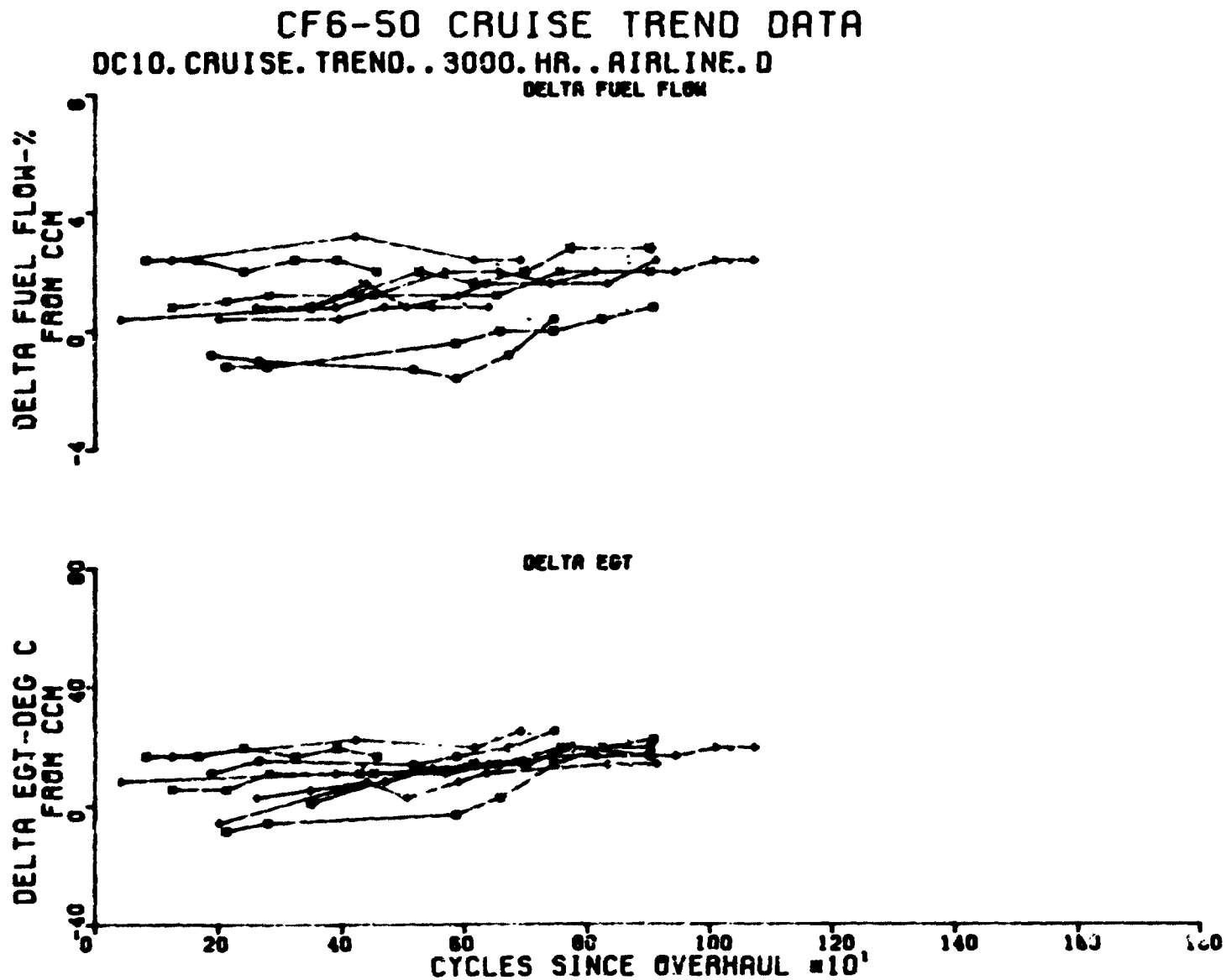

Figure B-14. CF6-50 Cruise Trend Data.

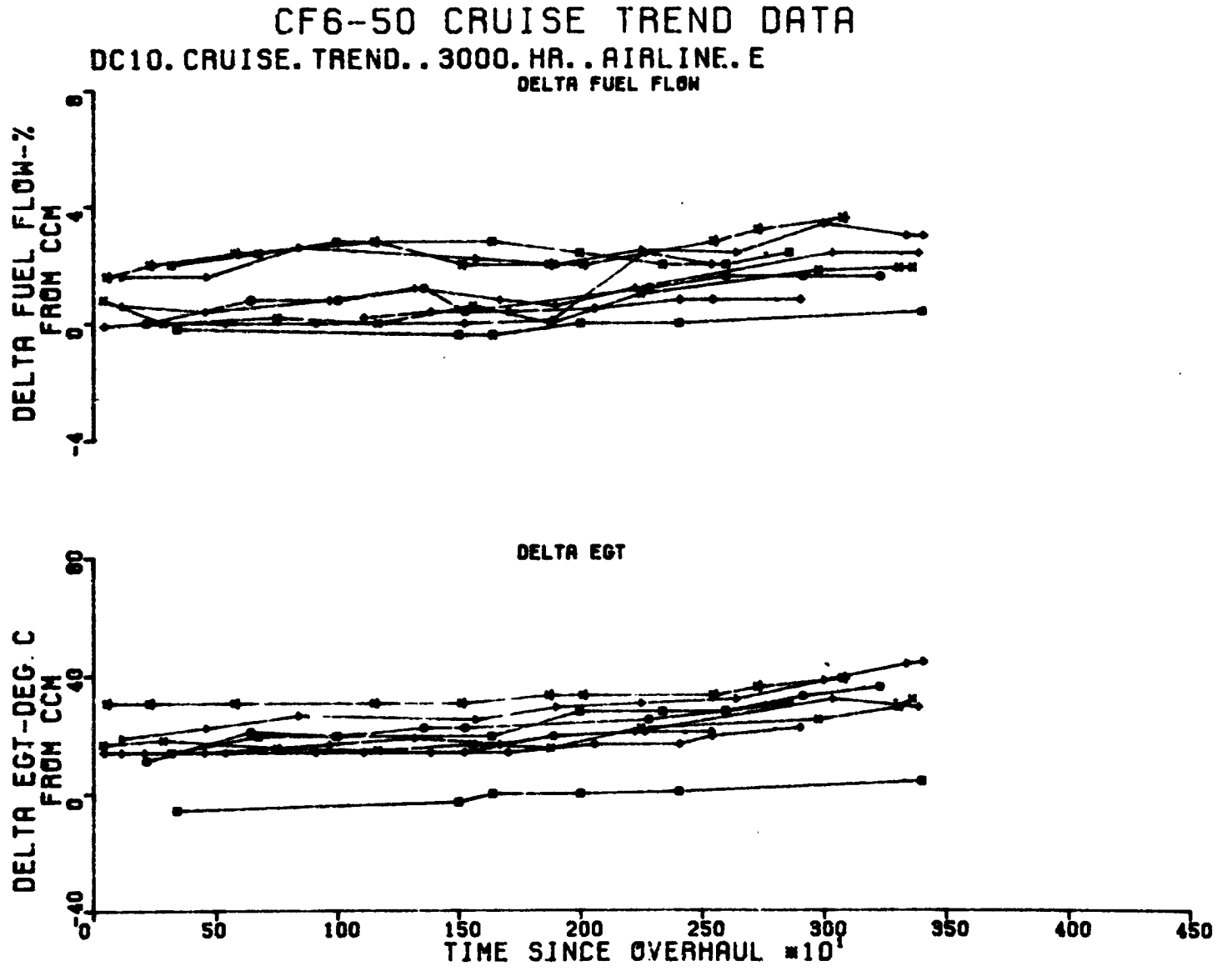

Figure B-15. CF6-50 Cruise Trend Data.

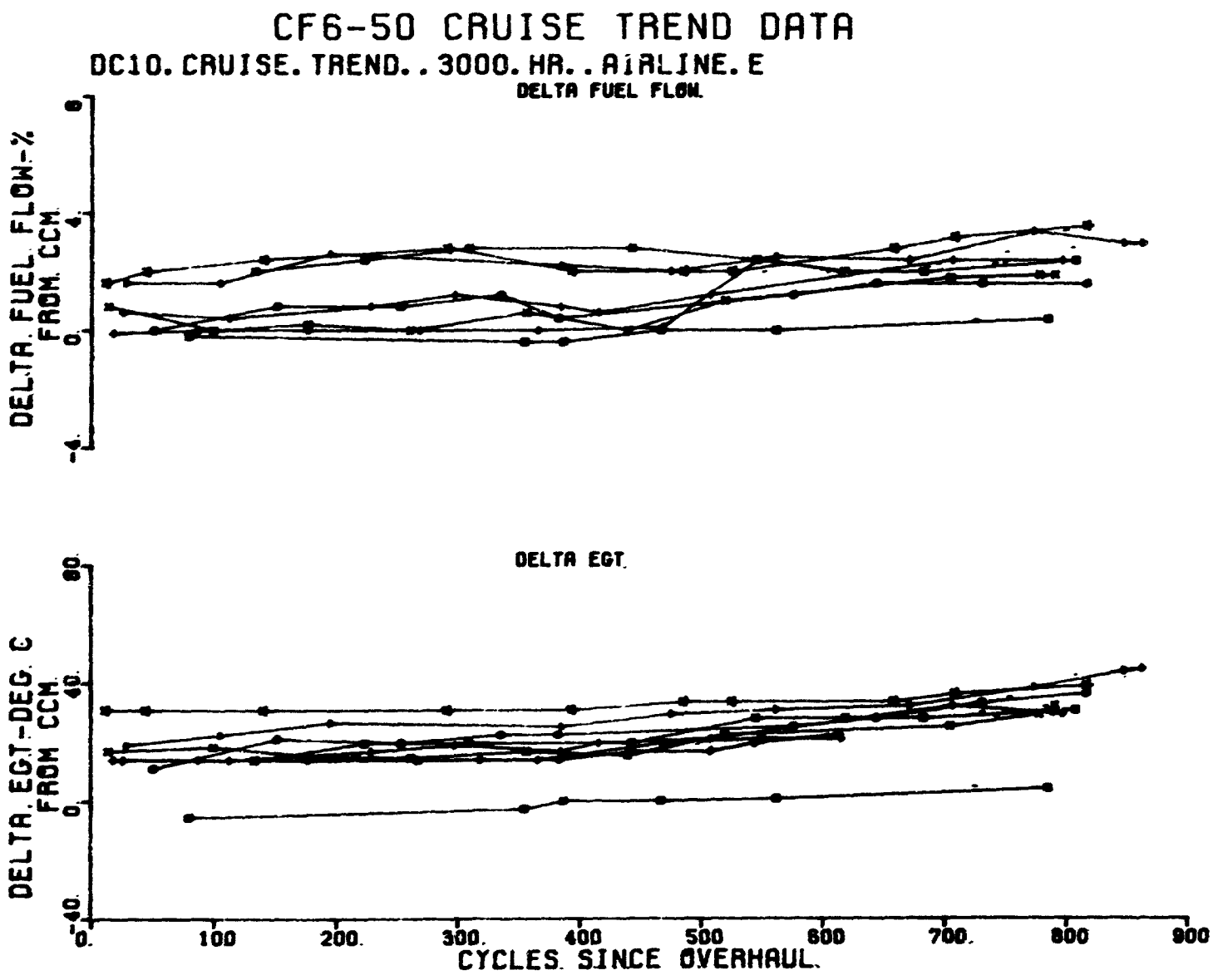

Figure B-16. CF6-50 Cruise Trend Data.

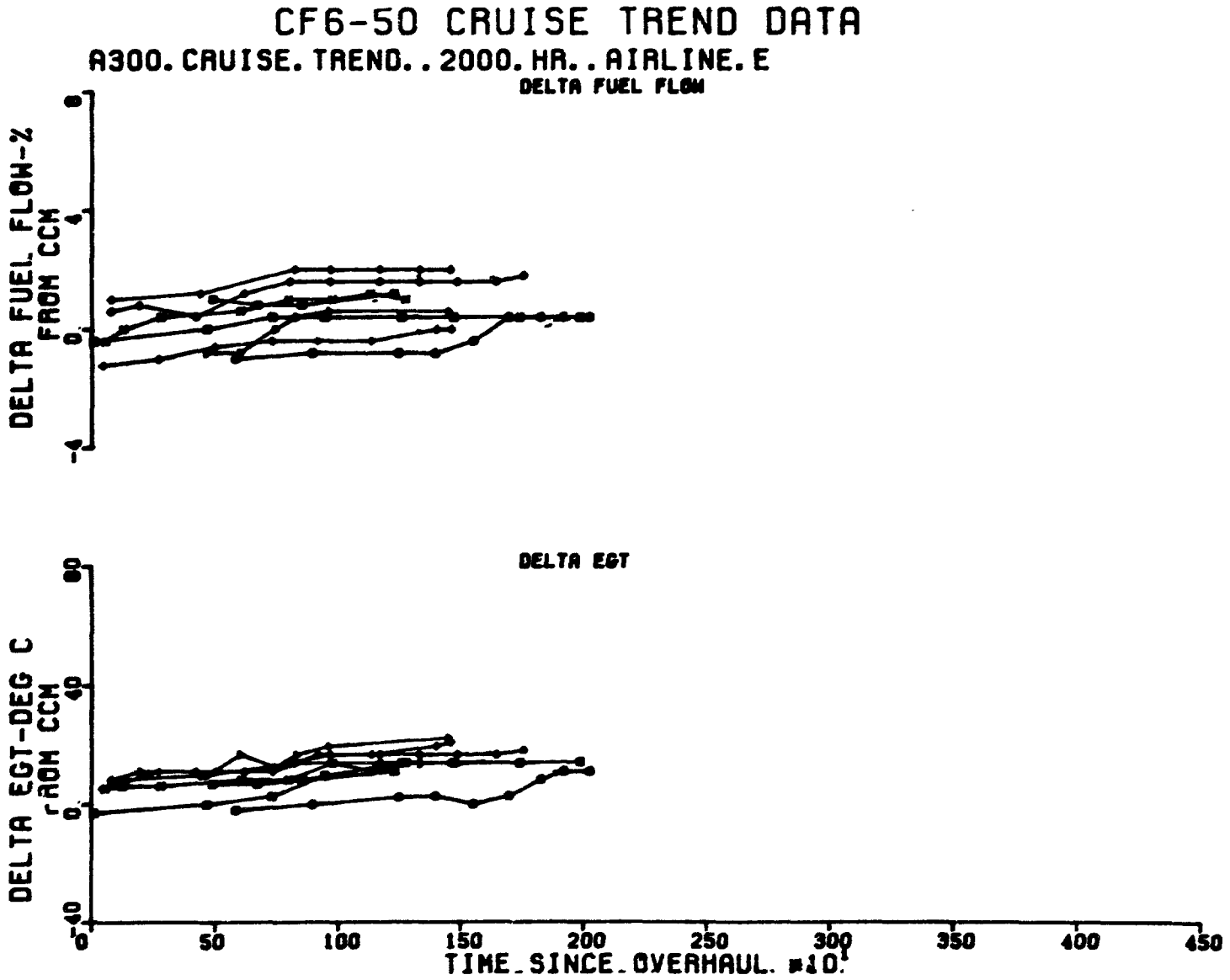

Figure B-17. CF6-50 Cruise Trend Data.

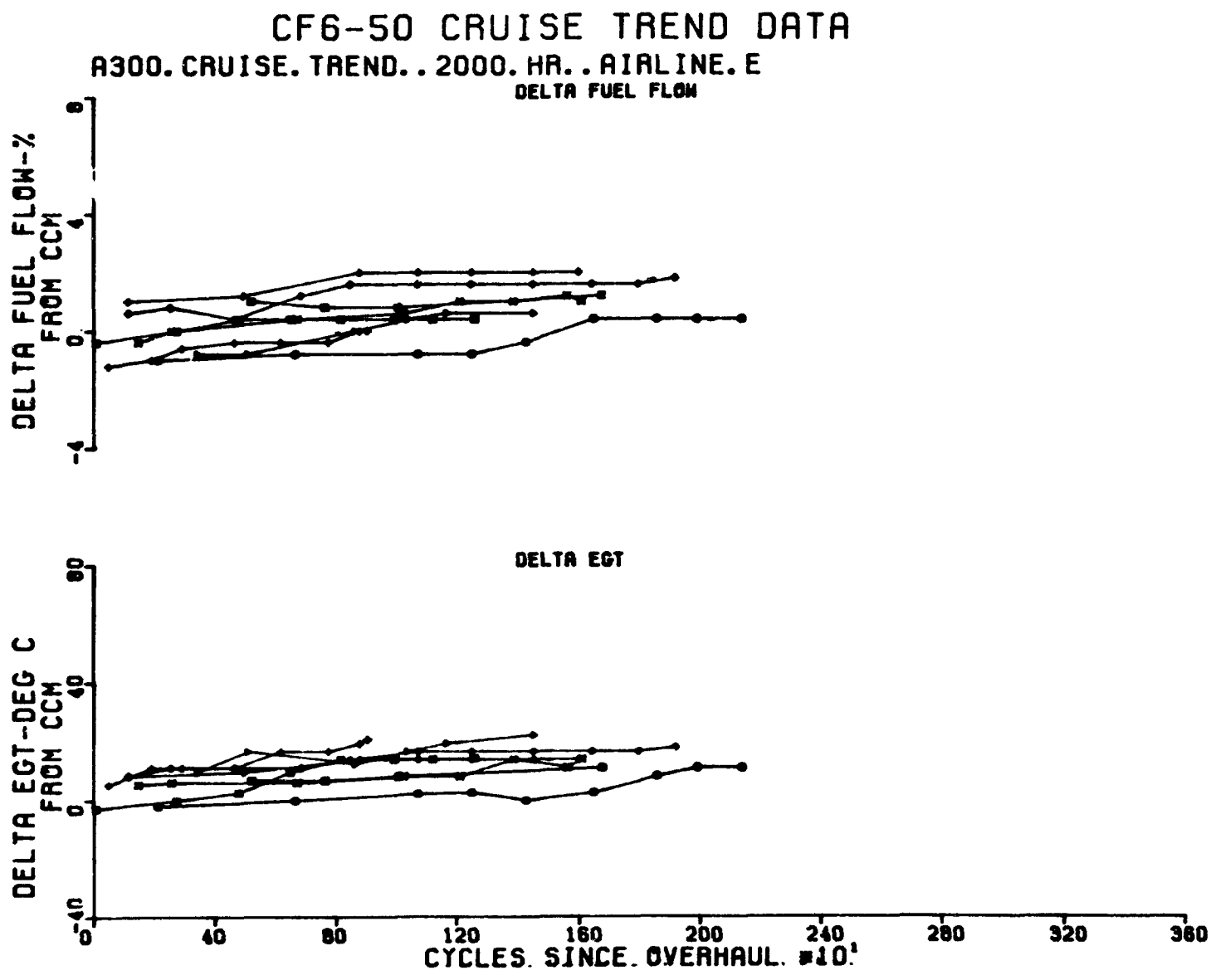

Figure B-18. CF6-50 Cruise Trend Data.

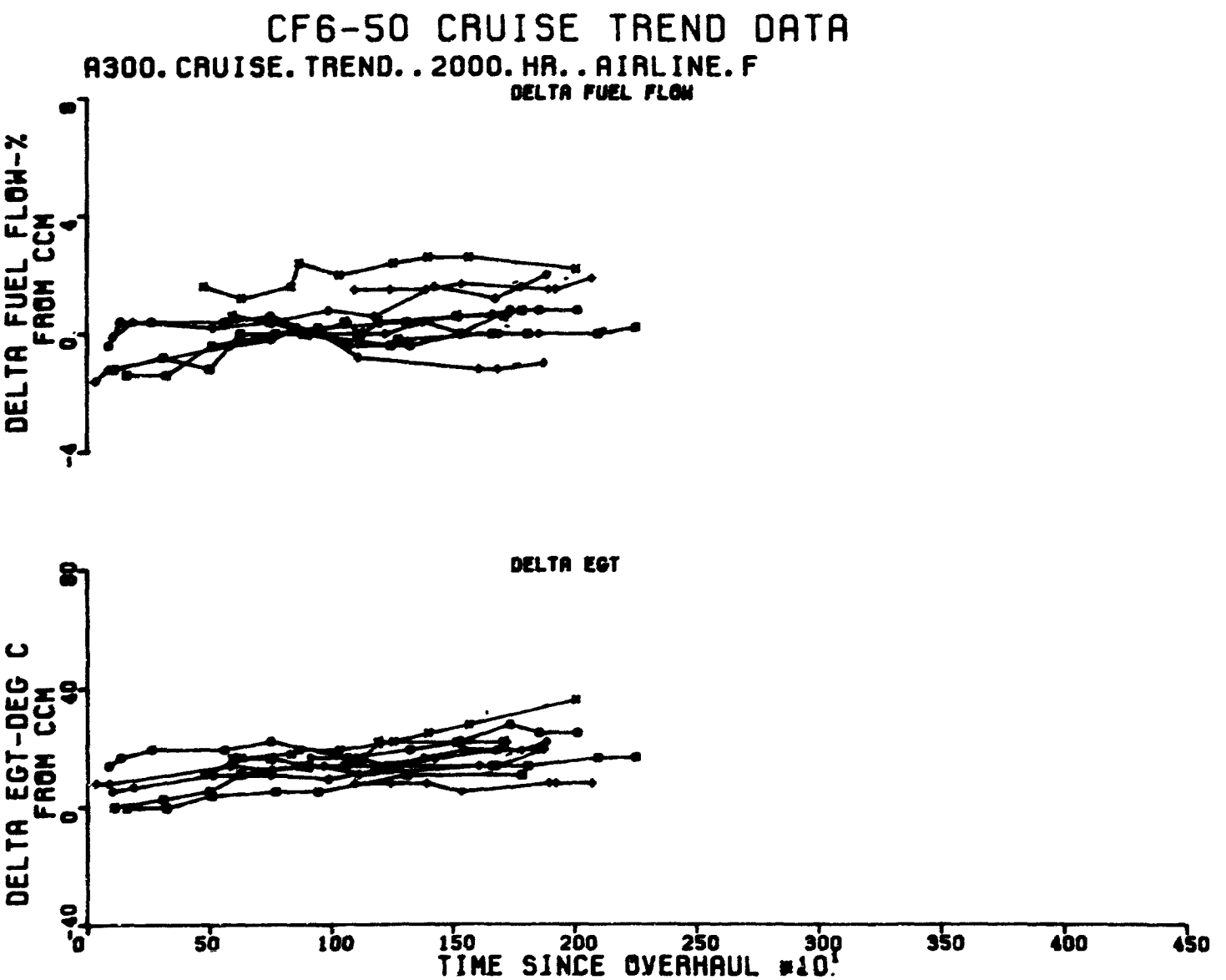

Figure B-19. CF6-50 Cruise Trend Data.

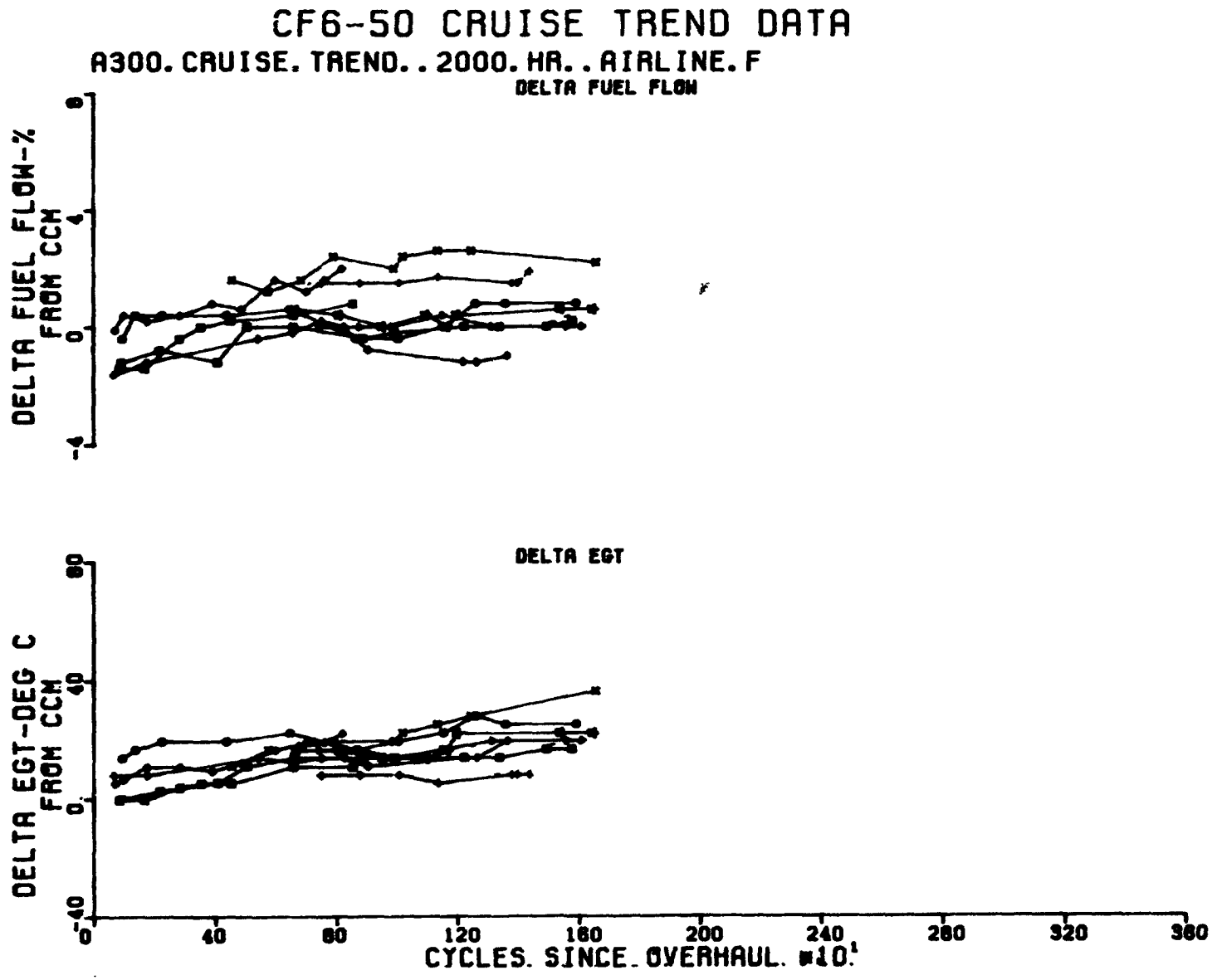

Figure B-20. CF6-50 Cruise Trend Data.

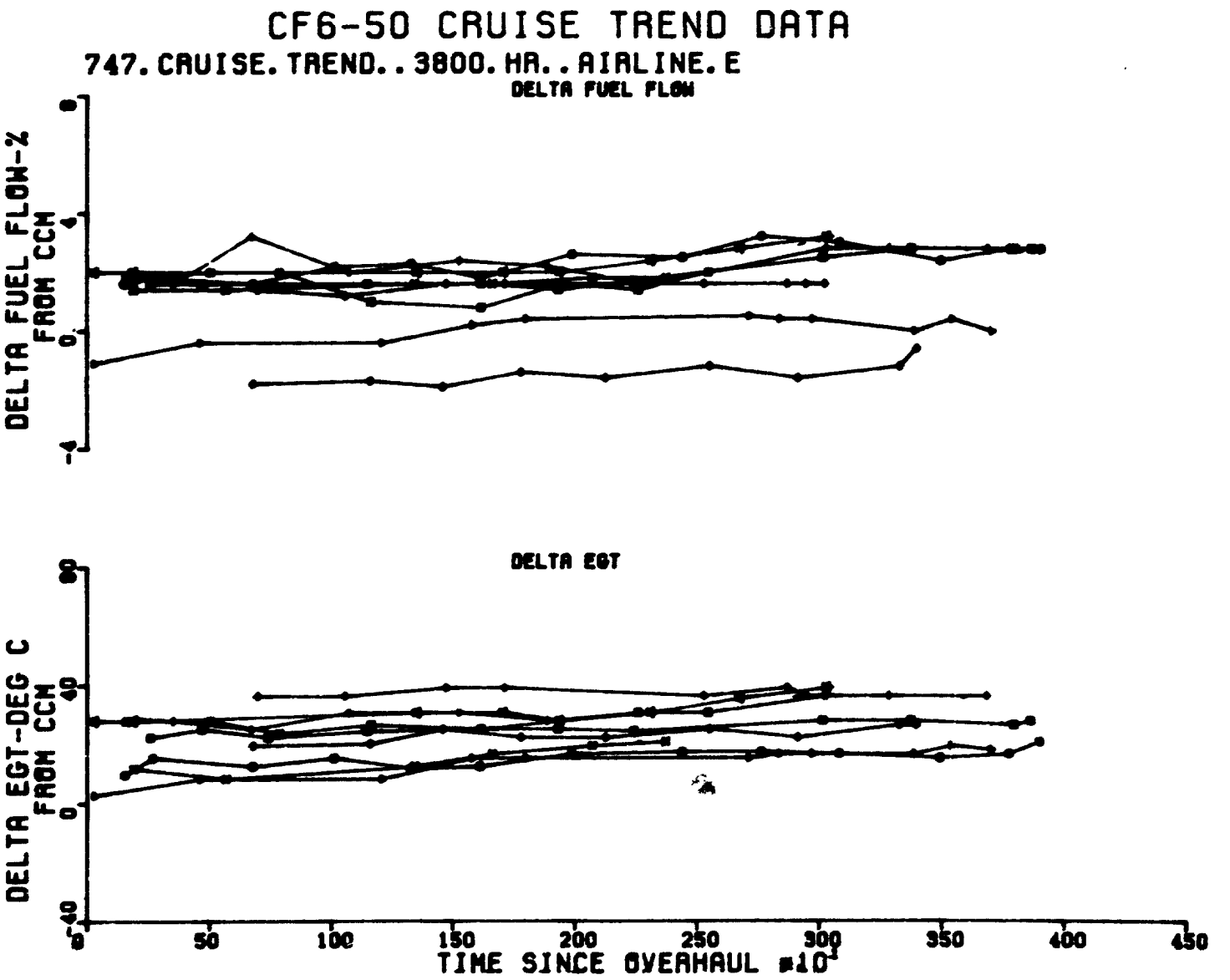

Figure B-21. CF6-50 Cruise Trend Data.

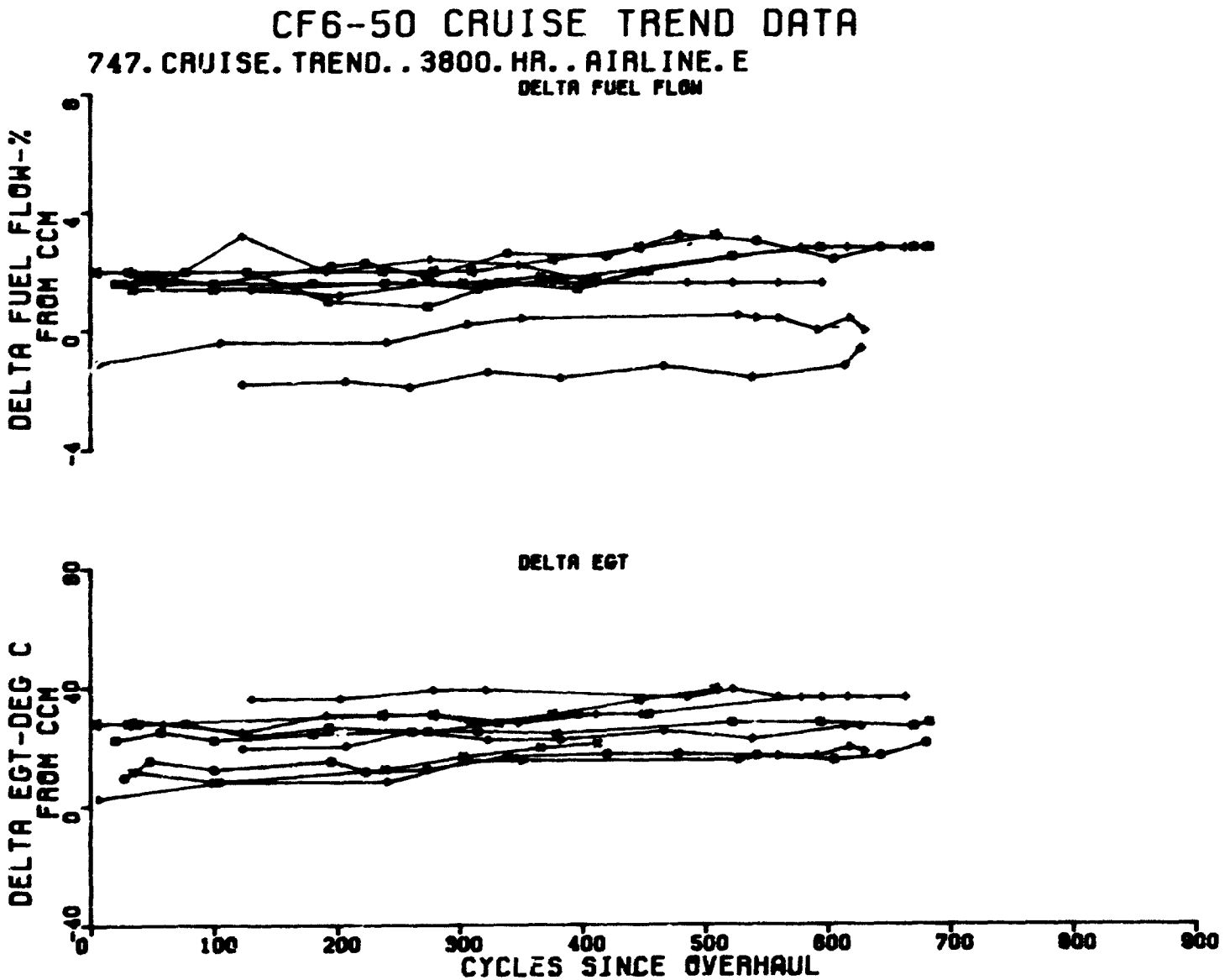

Figure B-22. CF6-50 Cruise Trend Data.

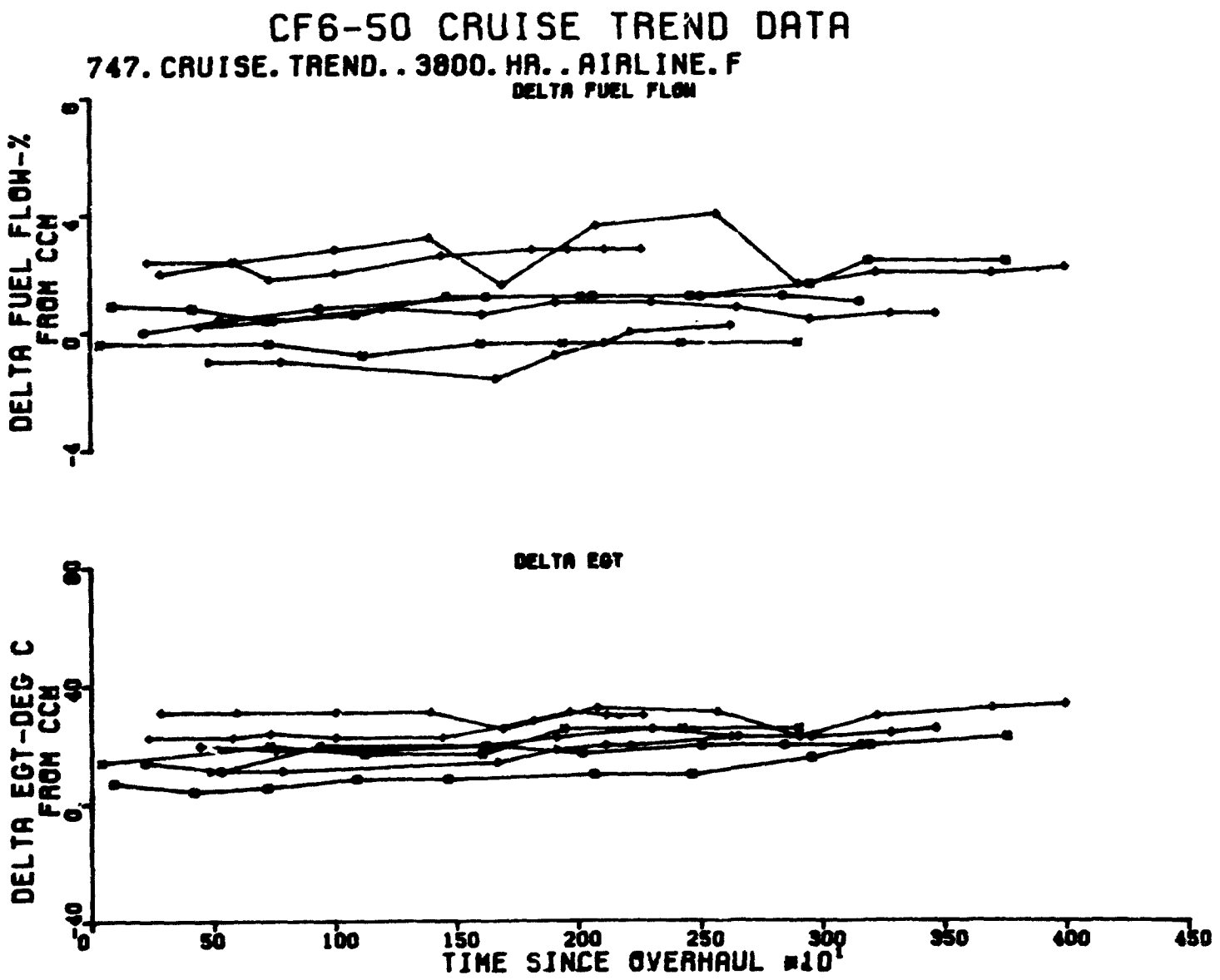

Figure B-23. CF6-50 Cruise Trend Data.

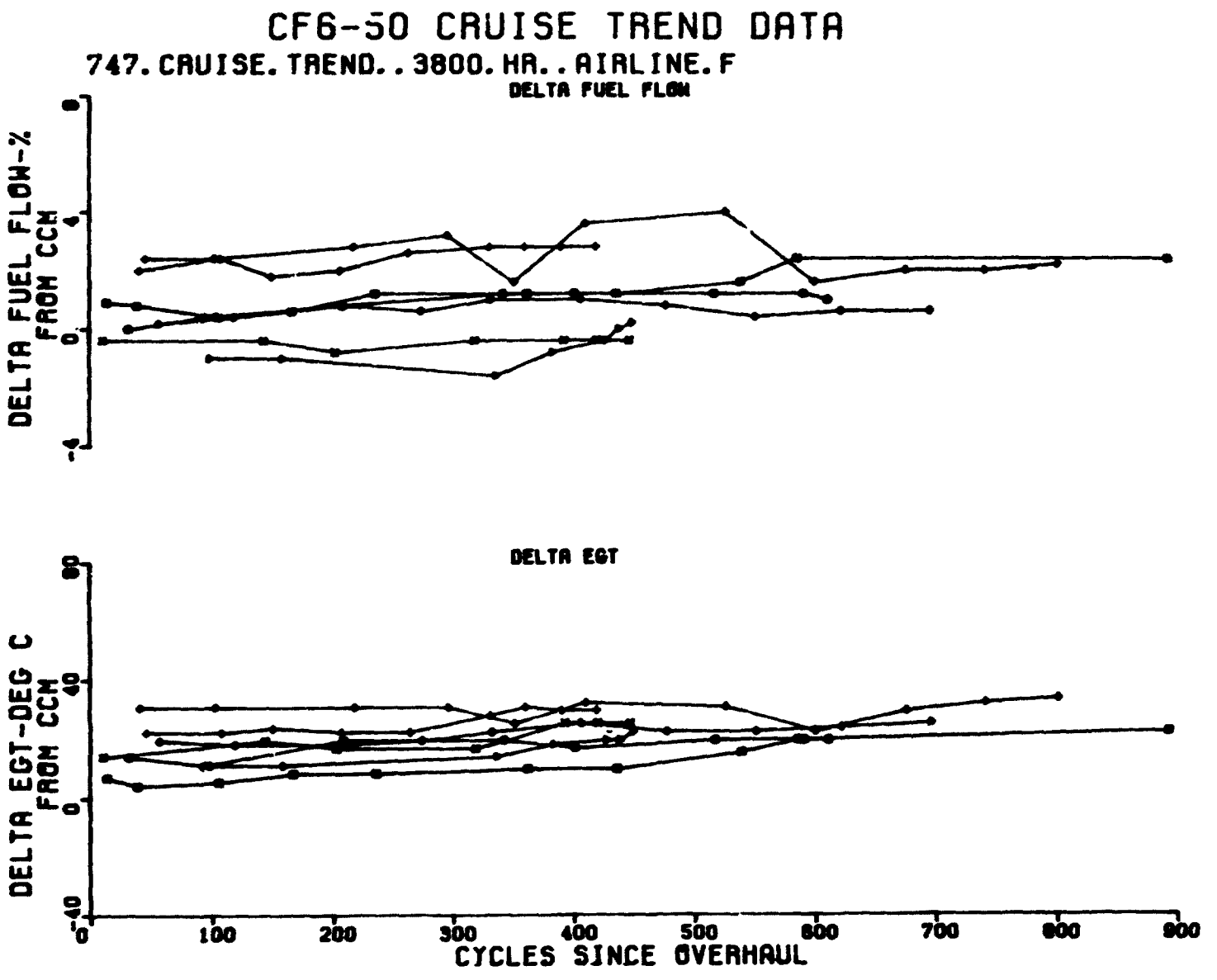

Figure B-24. CF6-50 Cruise Trend Data.

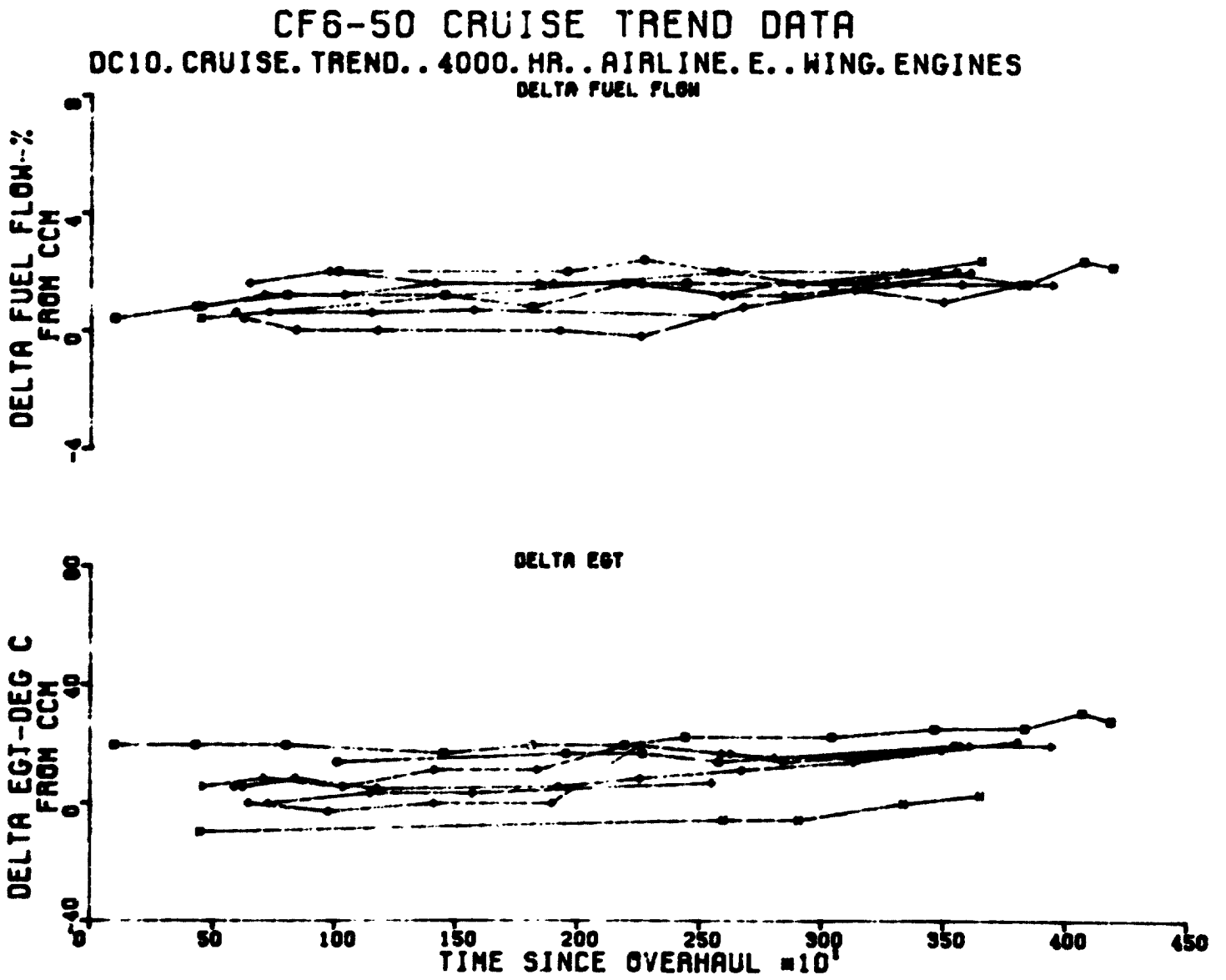

Figure B-25. CF6-50 Cruise Trend Data.

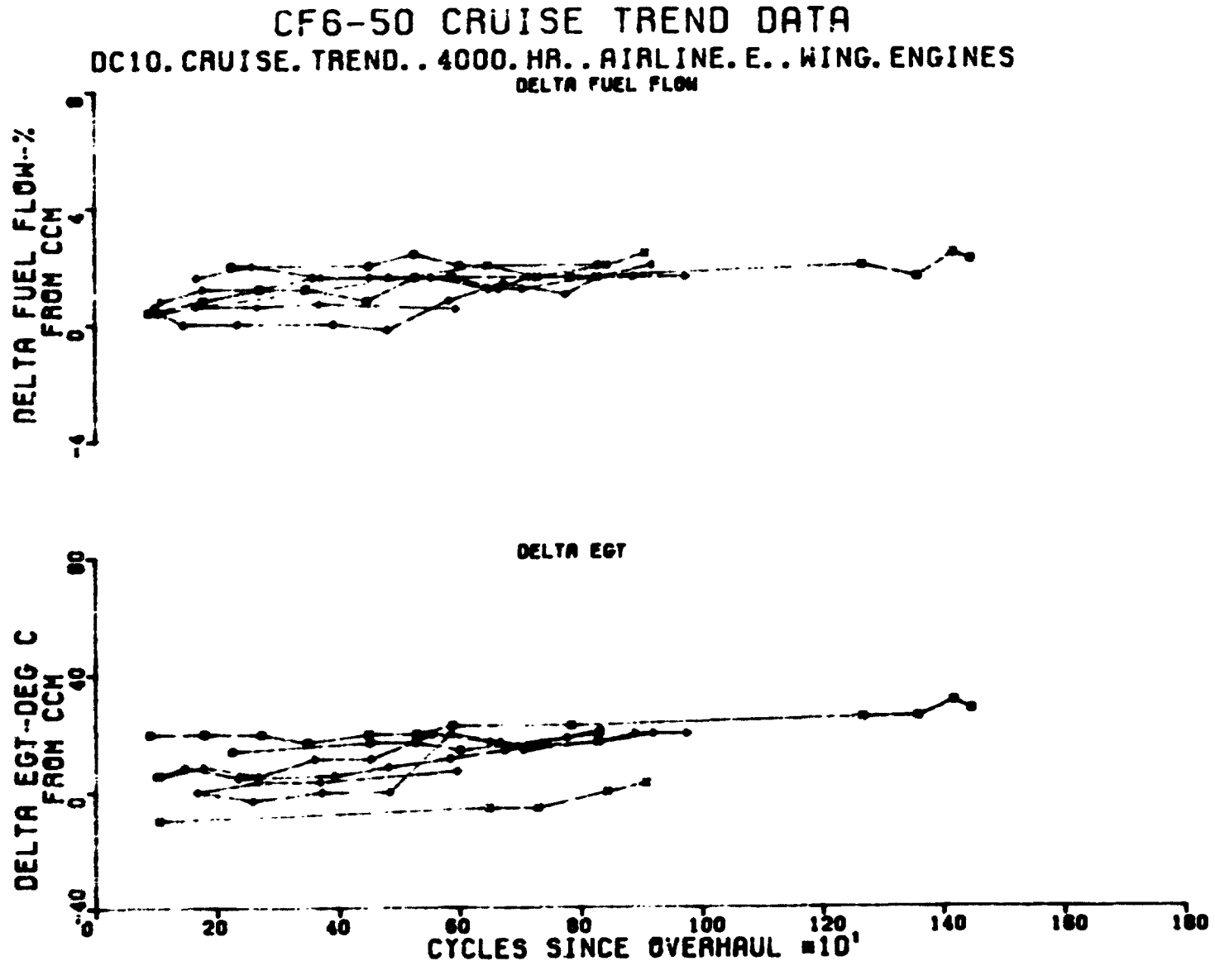

Figure B-26. CF6-50 Cruise Trend Data.

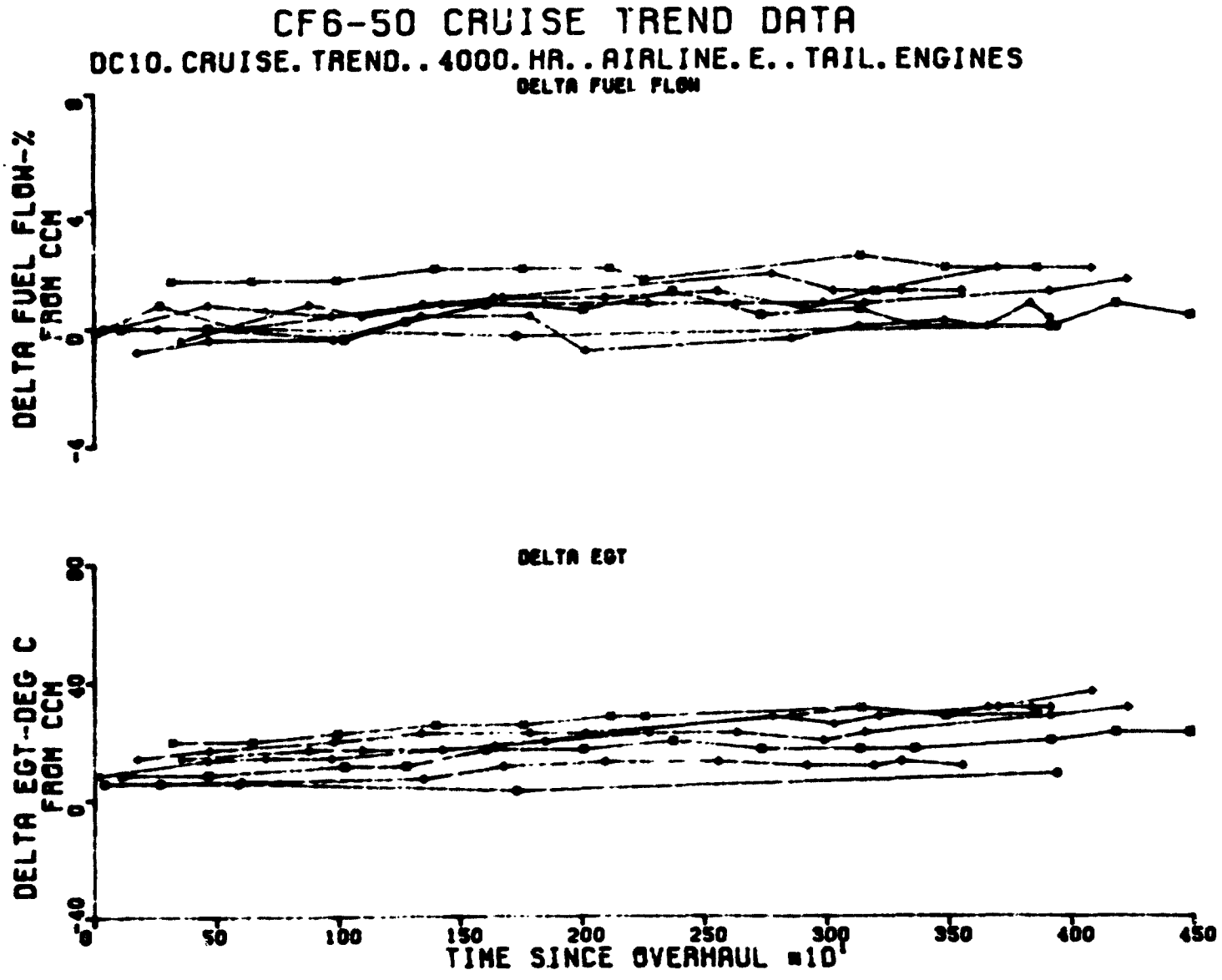

Figure B-27. CF6-50 Cruise Trend Data.

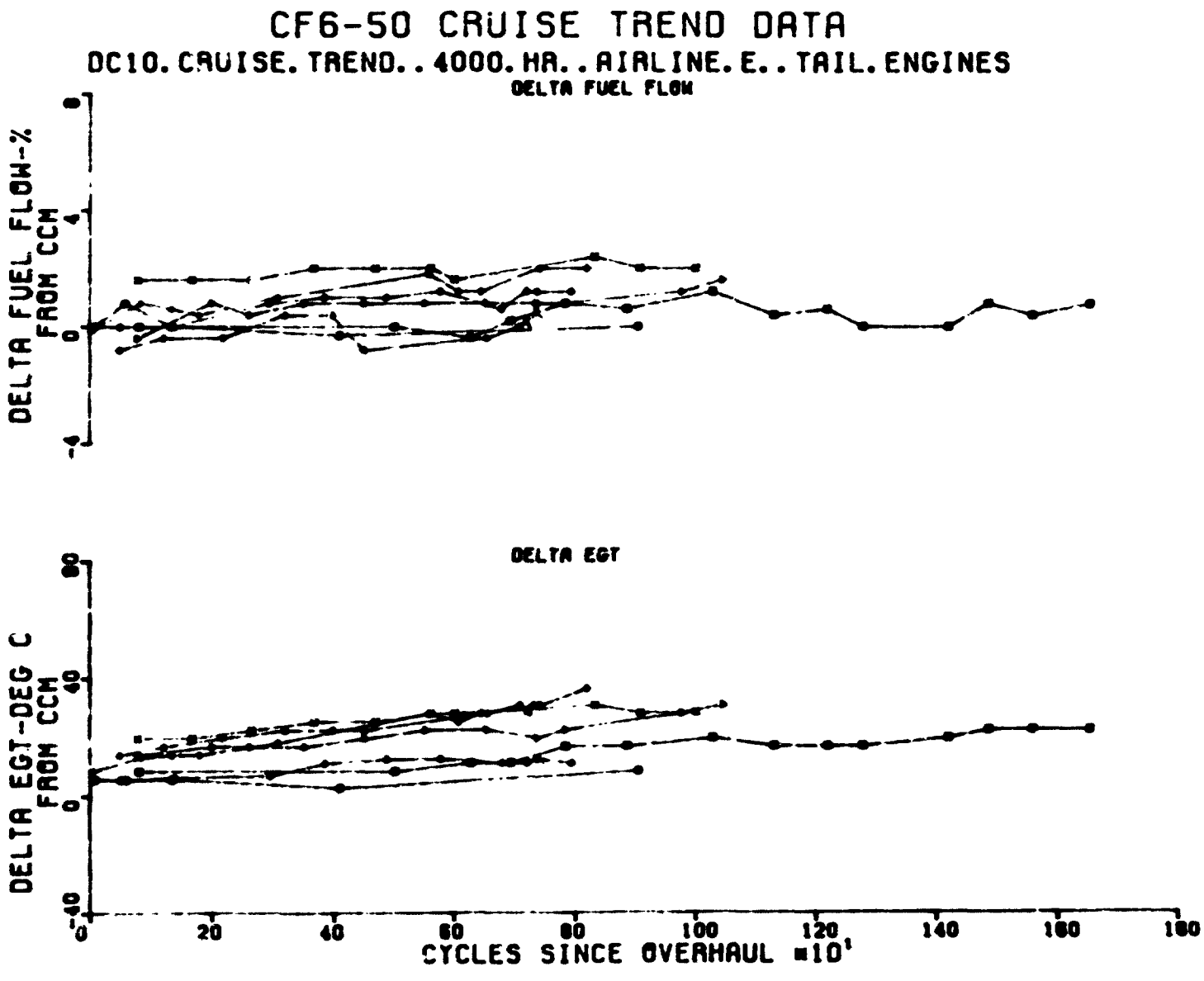

Figure B-28. CF6-50 Cruise Trend Data.

APPENDIX C

LIST OF REFERENCES

1. NASA CR-159786, "CF6-6D Engine Performance Deterioration," R.H. Wulf, January 1980.

2. NASA CR-159830, "CF6-6D Engine Short-Term Performance Deterioration," W.H. Kramer, J.E. Paas, J.J. Smith, and R.H. Wulf, April 1980.

3. NASA CR-159618, "Long-Term CF6-6D Low-Pressure Turbine Deterioration," J.J. Smith, August 1979.

APPENDIX D

SYMBOLS AND ACRONYMS

A4	Stage 1 High Pressure Turbine Nozzle Area
A/C	Aircraft
ACEE	Aircraft Energy Efficiency Program
ALF	Aft Looking Forward
ASE	Airline Support Engineering
ASO	Aviation Service Operation
ASO/O	Aviation Service Operation/Ontario, California
Avg.	Average
B/P	Blueprint
BW	Blade Width
CAL	Continental Airline
CCM	Cruise Control Manual
CDP	Compressor Discharge Pressure
CL	Clearance
CR	Cruise
CRF	Compressor Rear Frame
CSI	Cycles Since Installed
CSN	Cycles Since New
CSO	Cycles Since Overhaul
CW	Clockwise
DAC	Douglas Aircraft Company
DELT	Delta
DETAC	Delta High Pressure Compressor Efficiency
DETALP	Delta Low Pressure System Efficiency

SYMBOLS AND ACRONYMS (Continued)

DETALPS	Delta Low Pressure System Efficiency
DFN1	Delta Net Thrust at Constant Fan Speed
Dia.	Diameter
DPARA	Delta Parasitic
DPARAS	Delta Parasitics
E12, E13	Fan Blade Tip Clearance Locations
ECI	Engine Component Improvement
EGT	Exhaust Gas Temperature
EGTM	Exhaust Gas Temperature Margin
Eff.	Efficiency
EMU	Engine Maintenance Unit
EPR	Engine Pressure Ratio
EROM	Electronic Readout Machine
ESN	Engine Serial Number
ETAC	High Pressure Compressor Efficiency
ETALPS	Low Pressure System Efficiency
ETAT	High Pressure Turbine Efficiency
FAA	Federal Aviation Agency
FBW	Full Blade Width
FIR	Full Indicated Runout
FLA	Forward Looking Aft
Fn	Net Thrust
Fn @ N1	Net Thrust at Constant Fan Speed

SYMBOLS AND ACRONYMS (Continued)

F/N	Fuselage Number
FOD	Foreign Object Damage
FP & CCM	Flight Planning and Cruise Control Manual
FPI	Fluorescent Penetrant Inspection
FWD	Forward
G1,G2,G3 G4,G5,G6	High Pressure Turbine Rotor Forward Shaft, Forward Seal Teeth
GE	General Electric Company
H1,H2,H3 H4,H5,H6	High Pressure Turbine Rotor Forward Shaft - Aft Seal Teeth
HD EGT	Hot Day Exhaust Gas Temperature
HP	High Pressure
HPC	High Pressure Compressor
HPCR	High Pressure Compressor Rotor
HPCS	High Pressure Compressor Stator
HPS	High Pressure System (Core Engine)
HPT	High Pressure Turbine
HPTN	High Pressure Turbine Nozzle
HPTR	High Pressure Turbine Rotor
Hrs	Hours
ID	Inside Diameter
IGB	Inlet Gearbox
IGV	Inlet Guide Vane
In.	Inch

SYMBOLS AND ACRONYMS (Continued)

I/S	Interstage
Dim "K"	Dimension "K", High Pressure Turbine Nozzle Support - Reference Shop Manual, 72-52-00
LE	Leading Edge
LP	Low Pressure
LPS	Low Pressure System (Fan and LPT)
LPT	Low Pressure Turbine
LPTN	Low Pressure Turbine Nozzle
LPTR	Low Pressure Turbine Rotor
Max	Maximum
M/C	Maximum Continuous
Min	Minimum
MM	Maintenance Manual
MRL	Maximum Repairable Limit
MXCR	Maximum Cruise
N1	Fan Speed
N2	Core Speed
N/A	Not Applicable
NAL	National Airline
NASA-Lewis	National Aeronautics and Space Administration - Lewis Research Center
No.	Number
No. 4B	Number 4 Ball Bearing
Noz.	Nozzle

SYMBOLS AND ACRONYMS (Continued)

OD	Outer Diameter
OGV	Outlet Guide Vane
P3	Compressor Discharge Pressure
P49	Low Pressure Turbine Inlet Pressure
QEC	Quick Engine Connect
R	Roundness
Rad.	Radius
Ref.	Reference
RMS	Root Mean Square
RPM	Revolutions Per Minute
RTV	A Room Temperature Vulcanizing Compound
SB	Service Bulletin
SEE	Standard Error of Estimate
Serve Limit	Serviceable Limit
sfc	Specific Fuel Consumption
SI	International System of Units
SLS	Sea Level Static
S/M	Shop Manual
S/N	Serial Number
Stg.	Stage
SWECO	Vibratory Mill Cleaning Process
T3	Compressor Discharge Total Temperature
T5X	Calculated Exhaust Gas Temperature
T/C	Thermocouple

SYMBOLS AND ACRONYMS (Concluded)

TE	Trailing Edge
TMF	Turbine Midframe
T/O	Takeoff
TSI	Time Since Installed
TSN	Time Since New
TSO	Time Since Overhaul
UAL	United Airlines
V1,V2,V3,V4	High Pressure Turbine Rotor Thermal Shield Seal Teeth
VTL	Vertical Turret Lathe
WAL	Western Airlines
WC16	16th Stage Cooling Flow
WFM	Fuel Flow
WK	Corrected Airflow
Δ	Delta
η	Efficiency (Eta)
ηc	High Pressure Compressor Efficiency
ηf	Fan Efficiency
ηt	High Pressure Turbine Efficiency
$\eta 2t$	Low Pressure Turbine Efficiency
σ	Standard Deviation
μ in./in. AA	Microinch per inch, Arithmetic Average

APPENDIX E

SPECIAL TERMINOLOGY

Analytical Teardown

The disassembly of an engine specifically to provide hardware inspection data to determine the sources and mechanisms for performance deterioration.

Coefficient of Determination (R^2)

A numerical measure of the proportion of variation accounted for by the multiple linear regression fit, where a value of "1" indicates a perfect fit while a value of "0" indicates lack of fit.

Deteriorated Engine (or Module)

An engine (or module) as removed from wing for induction into the shop, but prior to any repairs.

Deterioration Model

Two models are utilized in this report. The "Performance Deterioration Model" is based on performance data and describes the magnitude and rate at which deterioration occurs with time. The "Hardware Deterioration Model" assigns the performance deterioration to the individual parts and damage mechanisms, and is based on hardware inspection data and influence coefficients.

Engine Derivatives

Computer cycle model factors which equate changes in component efficiencies, flows, and areas to changes in engine cycle parameters.

Fuel Burn

Fuel consumed (sfc at constant thrust) during the cruise portion of a revenue flight.

Influence Coefficients

Empirically or analytically derived factors which equate a change in hardware condition to a change in performance.

Initial Installation

The portion of long-term deterioration which occurs during the revenue service operation of a production new engine prior to the first shop visit.

Long-Term Deterioration

This broad category defines all performance losses which occur during revenue service operation for the life of the engine.

Modular Maintenance

The maintenance concept that concentrates on repairing modules as opposed to the engine as a whole. This concept is utilized as part of the on-condition maintenance concept to achieve optimum repair costs.

Multiple-Build Installation

The revenue service operation of an engine following the first shop visit. This category includes all long-term deterioration except that which occurs during the initial installation.

Parasitics

The internal leakage of gas flow that bypasses a stage or stages of airfoils. An example of a parasitic leakage is any excess (beyond design) turbine mid-frame liner purge air which bypasses the high pressure turbine.

Refurbished Engine (or Module)

An engine (or module) that has been restored for mechanical and performance reasons. This designation implies that performance losses were restored in addition to the minimum mechanical repair required to satisfy the serviceable classification.

Serviceable Engine (or Module)

An engine that meets the minimum inspection requirements for the particular maintenance concept being utilized so that it is eligible for additional revenue service. The engine (or module) may or may not be completely refurbished.

Shop Visit

When the engine is inducted into the maintenance shop for repair after removal from the aircraft.

Short-Term Deterioration

Performance losses which occur at the aircraft manufacturer during airplane acceptance test flights prior to initiation of revenue service.

Standard Deviation

The root-mean-square of deviations from a mean, used as the measure of the spread of a sample or population.

Standard Error of Estimate (SEE)

The root-mean-square of deviations about a fitted curve, used as the measure of the spread of a sample or population about that fitted curve.

Unrestored Performance (Unrestored Losses)

The difference between the production new performance levels and those for a revenue service engine after a shop visit.

APPENDIX F

QUALITY ASSURANCE REPORT

INTRODUCTION

It is the fundamental precept of the Aircraft Engine Group to provide products and services that fulfill the Product Quality expectations of customers and maintain leadership in product quality reputation, in conformance to the policy established by the Executive Office.

The Quality System as documented in Aircraft Engine Group Operating Procedures provides for the establishment of Quality assurance requirements through the design, development, manufacture, test, delivery, application, and postdelivery servicing of the product. These instructions and Operating Procedures clearly delineate the cross-functional responsibilities and procedures for implementing the system, which includes coordination with cognizant FAA/AFPRO functions prior to issue and implementation.

The Quality Organization implements the Quality System requirements in each of their assigned areas of responsibility, providing design review participation, quality planning, quality input to Manufacturing planning, quality assurance and inspection, material review control, production testing, and instrument calibration.

The Aircraft Engine Group has additional Manufacturing facilities, and Overhaul/Service Shops such as the one at Ontario, California. These various facilities are termed "satellite" plants or locations. They are not considered vendors or suppliers for quality control purposes and have the same status and requirements they would have if located in the Evendale Manufacturing Facility.

The specific requirements for this contract were accomplished at the following locations:

- Production Assembly and Engine Test - Evendale
- Ontario Service Shop - Ontario

A summary of activities for each location is included in this report.

QUALITY SYSTEMS

Quality Systems for Evendale and Ontario are constructed to comply with Military Specifications MIL-Q-9858A, MIL-I-45208A, and MIL-C-45662A, and with Federal Aviation Regulations FAR-145 and (where applicable) FAR-21. The total AEG Quality System has been accepted by NASA-LeRC for fabrication of engines under prior contracts.

Inherent in the system is the assurance of conformance to the quality requirements. This includes the performance of required inspections and tests. In addition, the system provides change control requirements which ensure that design changes are incorporated into manufacturing, procurement, and quality documentation, and into the products.

Engine parts are inspected to documented quality plans that define the characteristics to be inspected, the gages and tools to be used, the conditions under which the inspection is to be performed, the sampling plan, laboratory and special process testing, and the identification and record requirements.

Work instructions are issued for compliance by operators, inspectors, testers, and mechanics. Component part manufacture provides for laboratory overview of all special and critical processes, including qualification and certification of personnel, equipment, and processes.

When work is performed in accordance with work instructions, the operator/inspector records that the work has been performed. This is accomplished by the operator/inspector stamping or signing the operation sequence sheet to signify that the operation has been performed.

Control of part handling, storage, and delivery is maintained through the entire cycle. Engines and assemblies are stored in special dollies and transportation carts. Finished assembled parts are stored to preclude damage and contamination, openings are covered, lines are capped, and protective covers are applied as required.

A buildup record and test log is maintained for the assembly, inspection, and test of each major component or engine. Component and engine testing is performed according to documented test instructions, test plans, and instrumentation plans. Test and instrumentation plans were submitted to NASA for approval prior to the testing.

Records essential to the economical and effective operation of the Quality Program are maintained, reviewed, and used as a basis for action. These records include inspection and test results, nonconforming material findings, laboratory analysis, and receiving inspection.

Nonconforming hardware is controlled by a system or material review at the component source. Both a Quality representative and an Engineering representative provide the accept (use-as-is or repair) decision. Nonconformances are documented, including the disposition and corrective action if applicable to prevent recurrence.

CALIBRATION

The need for product measurement is identified and the design, procurement and application of measuring equipment specified at the start of the product cycle. Measuring devices used for product acceptance and instruments used to control, record, monitor, or indicate results of, or readings during, inspection and test are initially inspected, calibrated, and periodically reverified or recalibrated.

Documented procedures are used to define methods of calibration and verification of characteristics which govern the accuracy of the gage or instrument. Provisions are made for procurement of instrument calibration capability as a part of instrument system acquisition.

Frequency of recalibration is specified and measuring gages and instruments are labeled to indicate the period of use before recalibration is necessary. Records are maintained for each gage or instrument which lists the identification, serial number, calibration frequency, procedure, and results of each calibration.

Recalibration periods (frequency of calibration) are prescribed on the basis that the gages and instruments are within calibration tolerance limits at the end of the recalibration period. The results of recalibration are analyzed to determine the effectiveness of the recalibration period, and adjustments are made to shorten or lengthen the cycle when justified.

Standards used to verify the gages and instruments are traceable to the National Bureau of Standards.

QUALITY ASSURANCE FOR INSTRUMENTATION

Items defined as Standard Instrumentation (items appearing on the engine parts lists) will have Quality Assurance Control to the same degree as other engine components. Instrumentation on engines for Revenue Service will be subject to the test and inspection criteria identified in the applicable Shop Manual.

Items defined as "Test Instrumentation" (standard test instrumentation as identified in the applicable engine manual GEK 9266 for CF6 Test Section 72-00) will be subject to the same controls required for measuring and test equipment. This instrumentation is periodically reverified by the technician and recalibrated, at a prescribed frequency, against standards traceable to the National Bureau of Standards.

Items identified as "Special Instrumentation" (non-parts list or non-Tech Manual instrumentation supplied for this program) will have Quality Assurance Control consistent with the stated objectives of this program.

The instrumentation used for obtaining data for this contract fulfillment has not affected the engine operations or performance.

ACTIVITY SUMMARY BY LOCATION

PRODUCTION ASSEMBLY

In Production Assembly, the standard engine build procedures were used to ensure compliance to Quality Systems. These procedures and practices are approved under FAA Production Certificate 108. The operating procedures utilize an Engine Assembly Build Record (EABR) and an Engine Assembly Configuration Record (EACR). These documents, incorporated into an Engine Record Book, serve as an historical record of the compliance to the Assembly Procedure, a record of critical assembly dimensions, and a record of the engine configuration. Work performed is claimed by the applicable inspector or assembler. (Samples of the EABR and EACR cards are provided in Figures C-1 and C-2, respectively.)

Production Assembly releases the engine to Test and upon successful completion of the required test, performs the necessary work and inspection in preparation for shipment to the customer.

PRODUCTION ENGINE TEST

In Production Engine Test, the engine is inspected and prepared for test per Engine Test Instruction (ETI) Number C-15.

Limits and restrictions of Production Test Specifications were applied during the testing of engines under this contract. The safety of the test crew and engine is ensured by conducting ETI C-18 CF6 cell check sheets prior to the performance of the test.

The engine performance data and safety parameters are recorded by automatic data recording (ADR). The data systems, test cell, thrust frame, and fuel measuring systems are calibrated on a periodic basis by specialized technicians. During testing, the ADR system is continually monitored by test engineers to ensure the quality of the data being recorded.

ONTARIO SERVICE SHOP

At the Ontario facility, a Quality Control Work Instruction (QCWI DF015) was written and coordinated with NASA LeRC. The QCWI provided instructions on these specific items as applicable to the CF6 Diagnostic Program.

Assembly/Disassembly Control

Rework Control

Workscope Definition

Nonconformance

GT 6531 10/73

ENGINE ASSEMBLY BUILD-UP RECORD

DATE ISSUED _____ ENGINE SERIAL NO 450567 ASSEMBLY SERIAL NO. _____ PAGE 02 OF 04

WORK STAT.	ENGINE MODEL	ASSEMBLY DWG. NO.	ASSEMBLY NAME	PROCEDURE TITLE	PROCEDURE DATE	REV. NO.
MSGSB	CF6-80			FAN FRAME SUB-ASSY	02-14-77	

DATA IDENTIFICATION	OPER NO	OPERATION INSTRUCTIONS	GREEN	FINAL	EPR	C/I
	036	TORQUE INLET GEARBOX MOUNTING BOLTS	A 4245	A		0
	037	DROP C / / / REF DIM 1.200	I J-38			0
		1.193 / 1.193 / 1.193				
		DIFF / / / REF LIMIT B- .002	I J-38			0
		.001 / .002 / .001				
		DROP C / / / REF DIM 1.200		I		0
		DIFF / / / REF LIMIT B- .002		I		0
NO2BHBF	038	FIR OF NO 2 BRG HOUSING BORE LIMIT MAX .010	I J-38	I		0
		.008				
NO3RHBF	041	FIR OF NO 3 BRG HOUSING BORE LIMIT MAX .008	I J-38	I		0
		.006				
	043	ASSURE PROPER NO 3 BRG AND RECORD BRG S/N SKF C1833	A 4245			0
	047	TORQUE NO 3 BRG BOLTS	A 4245			0
	056	TORQUE 2 SCREWS TO 25 IN LB AND ASSURE SCREW HEADS ARE				0
		.001-.020 BELOW FLANGE	A 4245			0
	059	CHECK NO 2 BRG HOUSING SEATING	A N/D			0
	061	PLUG GAGE INTO ID OF SEAL NUT	A N/D			0
	064	TORQUE NO 1 BRG HOUSING BOLTS	A N/D			0
NO2FIR	065	RECORD MAX FIR LIMIT .010 FIR MAX	A N/D			1
	071	CHECK FOR .060 CLEARANCE BETWEEN TUBES AND FRAME	A N/D			0
	078	CHECK NO 2 BRG SEATING	A N/A	A		0
	074	TORQUE NO 2 BRG BOLTS	A N/A	A		0

Figure C-1. EMBR Card.

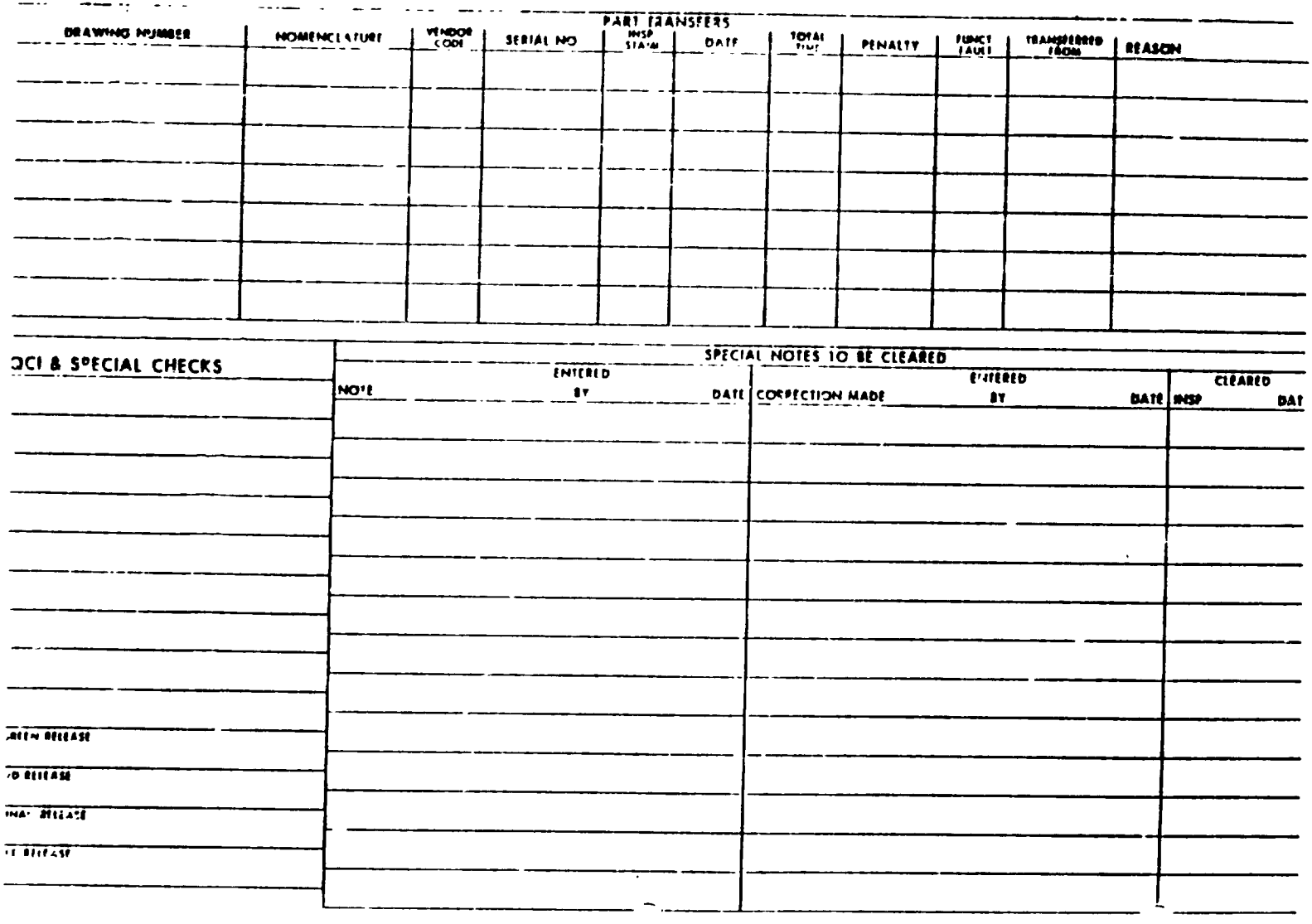

Figure C-1. EABR Card (Concluded).

1556

ENGINE ASSEMBLY CONFIGURATION RECORD

BOOK/END NUMBER	WORK STATION	DATE ISSUED	WORK STATION DESCRIPTION	MODEL	SUB ASSY	DRAWING NO	S/A SERIAL NO	PAGE
491-507	MGG56	09-02-77	FAN FRAME S/A	CF6-6				1

SOS DATA	G E DRAWING NUMBER	A I	R W	NOMENCLATURE	PART POSITION NUMBER	QTY	V S I	VENDOR CODE	E O D	PART SERIAL/HEAT LOT NO	E O D	CURE DATE
BR	MIL-L-25681C			SO-SO MOLY	00000025 B	A/R		XXXXX		XXXXXXXX		
NEW MAT	9155M87P01			NO 3 BEARING	01100	1	•	52676 SGA	S	SGA 01833		
BR	MS9217-06			BOLT-STA 3	01121	17		XXXXX		XXXXXXXX		
BR	MS84P09SL			BOLT BRG 3+4	01122	12		XXXXX		XXXXXXXX		
BR	MS9208-10			BOLT STA 3	01123	20		XXXXX		XXXXXXXX		
BR	MS9321-09			WASHER	01130	20		XXXXX		XXXXXXXX		
BR	9807M09P08			PKG PREFOR	01152	1		XXXXX		XXXXXXXX		
••• MAT	9694M23P04			NO 3 BRG SEAL	01153	1	•	11512 LAM	S	LAM 01269		
							•	19714 BER	S			
BR	R149P09A			PKG PREFOR	01155	1		XXXXX		XXXXXXXX		
•••	9654M03G05			SEAL COMP INLE	01156	1	•	07497 PMB	S	PMB #c502		
NEW	9009M78G27			G/B ASSY INLET	03000	1		XXXXX	S	FIA 08203		
BR	A1174P015			BOLT	03020	12		XXXXX		XXXXXXXX		
BR	AN960C416L			WASHER	03030	12		XXXXX		XXXXXXXX		
	9065M44G01			TUBE LUBE	44900	1		XXXXX		XXXXXXXX		
	9064M10G01			MANFD LUBE	44901	1	•	06593 TUPR		XXXXXXXX		
	9065M45G02			MANIFOLD	44902	1		XXXXX		XXXXXXXX		
BR	9064M12P01			BRACKET	44910	1		XXXXX		XXXXXXXX		
BR	MS9208-07			BOLT	44921	1		XXXXX		XXXXXXXX		
	CONTINUED ON NEXT PAGE WORKSTATION MGG56											

Figure C-2. EACR Card.

OPERATION RECORD

START	FINISH	ASSY BADGE	ASSEMBLER NAME	DATE	REMARKS
1	29	4245	P.E. Jones	23 Sept 77	Various Operations
30	100	4245	P.E. Jones	24 Sept 77	not Detailed
					See Insp. Bk. Sht
					P.E.J. 9-24-77
101	120	4245	P.E. Jones	26 Sept 77	

SIGN OUT LAST OPERATION IN HEAVY BLACK LINES

INSPECTION OPERATION RECORD

START	FINISH	INSP BADGE	INSPECTOR NAME	DATE	REMARKS

SIGN OUT LAST OPERATION IN HEAVY BLACK LINES

Figure C-2. BACR Card (Concluded).

Quality Planning

Auditing

Instrumentation Control (Safety)

Measuring and Test Equipment

Engine Test

Witnessing

Records

Failure Recording

To document the condition of the engine hardware, photographs were taken of the LPT shrouds and seals, representative HPT blades, LPT blades, compressor rotor, stator case, fan inlet guide vanes, CDP seal, HPT seals and shroud, HPT rotor, HP nozzles. These photographs were of high quality and are available for review.

Work orders were written to provide work direction for Engine Test, Prep-to-Test inspections, and for assembly and disassembly instructions. Inspections as requested were witnessed by the designated DCAS representative.

Examples of the work documents as issued to the Test and Assembly personnel are presented in the following figures:

- Figure C-3 - Test Operating Requirements Document
- Figure C-4 - Prep-to-Test and Test Check-Off Sheet
- Figure C-5 - Instrumentation Check Sheet
- Figure C-6 - Inspection Check List
- Figure C-7 - Work Order Sample
- Figure C-8 - HPTR Blade Inspection Sheet

General Electric Company
Aviation Service Operation/Ontario
Work Order

PERFORMANCE TESTS

5.1 INBOUND TEST

The following sequence of testing is required for the CF6-6 Task III Engine. The testing will be conducted in the ASO-Ontario CF6 test cell with a lightweight bellmouth and the standard CF6-6 acceptance test cowling configuration.

1. Install Engine in the CF6 test cell and set up per CF6 Shop Manual, 72-00-00 Testing.

2. Check variable stator vanes cold rig, but do not adjust unless VSV tracks outside of the open limit by more than one degree during engine operation. No adjustment is to be made without the concurrence of ASE engineering.

3. Install instrumentation as defined by the Instrumentation Plan for the Task III engines.

4. Conduct the following performance test:

   a. Perform normal prefire checks including a leak check.

   b. Start engine and stabilize for five minutes at ground idle.

   c. Set the following two steady-state data points and take full data readings after four minutes stabilization:

Power Setting	Corrected Fan Speed
50%	76.42% (2623 rpm)
75%	90.11% (3093 rpm)

Note: Perform full functional test

   d. Slow decel to ground idle, and analyze the two points to determine if the engine can be safety operated to takeoff power without exceeding any limits (N2, EGT, VSV). Also ascertain that all instrumentation, including the recorder, is functioning properly.

   e. Set the following steady-state data points and take two back-to-back data readings after four minutes stabilization. The engine should be operated at maximum continuous power for a minimum of six minutes prior to setting the following points. Take one data reading after six minutes.

Figure C-3. Test Operating Requirements Document.

POWER SETTING	CORRECTED FAN SPEED
TAKEOFF	100.30% (3443 rpm)
MAXIMUM CONTINUOUS	98.70% (3388 rpm)
MAXIMUM CRUISE	95.85% (3.90 rpm)
75%	90.11% (3093 rpm)

f. SHUT DOWN FOR A MINIMUM OF 30 MINUTES AND THEN REPEAT STEPS b AND e.

5.2 SPECIAL INSTRUCTIONS:

THE FOLLOWING SPECIAL INSTRUCTIONS APPLY FOR TESTING THE CF6-6D TASK III ENGINE:

1. GENERAL ELECTRIC-EVENDALE PERSONNEL WILL BE ON SITE AND WILL ASSURE DATA QUALITY BEFORE THE ENGINE CAN BE RELEASED FROM THE TEST CELL.
2. OBTAIN A FUEL LHV SAMPLE BETWEEN THE DUAL-PERFORMANCE POWER CALIBRATIONS. A BOMB CALORIMETER WILL BE USED TO OBTAIN THE LHV.
3. NO PERFORMANCE DATA IS TO BE TAKEN WHEN VISIBLE PRECIPITATION EXISTS OR THE RELATIVE HUMIDITY EXCEEDS [illegible] 85%.
4. PRESSURE TRANSDUCERS, FUEL METERS, AND THE THRUST LOAD CELL MUST BE WITHIN FAA CALIBRATION LIMITS AND THE CALIBRATIONS TRACEABLE TO THE NATIONAL BUREAU OF STANDARDS.
5. AFTER FIRST INBOUND PERFORMANCE RUN, CLEAN FAN BLADES USING MCK. PERFORM ANOTHER SINGLE PERFORMANCE TEST.

RLA:mjs

PRODUCTION

Figure C-3. Test Operating Requirements Document - Concluded

W/O _____

ENGINE S/N _____

CF6
PREP TO TEST
&
TEST CHECKOFF SHEET

FORM NO. CF6-TEST-1
2/3/78
Page 4 Of 9
Revision 21

STEP	OPERATION	MECH. SIGNATURE / DATE	PROD DATE
	TEST CELL		
	Engine mount bolts placed correctly, secured and lockwired. Front mount bolts stretch .000"/ .008".		
	Left bolt stretch .006" 6-22-78		6-22-78
	Right bolt stretch .008"		
2.	Check accessory gearbox customer pads for proper installation of gear shaft plugs.		
3.	Check all engine mounts for proper installation and lockwired.		6-22
4.	Check all required vibration pickups for installation, leads connected to their respective amplifier, lockwire. Check cooling air to T R.F. pickup. Hookup.		6-22
5	Check throttle operation and for positive fuel shutoff in zero position of fuel shutoff lever.		6-22
6.	Check both ignition systems for operation of plug.		6-22
7.	Check air starter piping, secure clamp and lockwire.		6-22
8.	All electrical connections secure and lockwired.		6-22
9.	Check to see that specific gravity setting on M.F.C. for JP4 fuel is used.		6-22
10	Visually check inlet instrumentation shoes/probes for condition and security. Check sensing holes for obstructions.		6-22
X	See engineer rework instruction for steps _____ recorded on back of this page. Void sign-off for steps _____ and modify per instruction on back of this page.		

Figure C-4. CF6 Prep-to-Test and Test Checkoff Sheet.

ENGINE S/N 451-507
W/O 182960

CF6-6D-50
INSTRUMENTATION CHECKLIST

FORM NO. CF6- TEST-3
1/17/73
Page 1 OF 4
Revision 1

ITEM	OPERATION	MECH	INSP	DATE
1.	Check air starter for proper servicing.	[illegible]	[illegible]	6-22-78
2.	Vibrations: 3 pick-ups (Lockwire) A. Compressor rear frame horizontal Location: Aft 2 bolt holes of #8 strut (1st strut below 9/o/c split line)	[illegible]	[illegible]	6-22
	B. Turbine rear frame horz. Location: 9 o/c, second & third bolt holes fwd. of T.R.F. flange "V"	[illegible]	[illegible]	6-22
	C. Fan rear stator case horizontal Location: 3 o/c fourth bolt above the upper ignition exciter.	[illegible]	[illegible]	6-22
	D. No. one bearing - horizontal Location: 4 o/c no. 4 fan exit strut below stator actuator.	[illegible]	[illegible]	6-22
	Variable stator vane position ind. Location: Transducer bracket at approx. 3 o/c on comp. front casing. Check rig marks: Ref. IAARR T.R. #CF6-50/087 Synchronize indicator to read zero ± 0.005 volts full open - record full closed 7.74 ± 0.03 volts. Lockwire.	[illegible]	[illegible]	6-22
4.	Variable bleed valve position ind. Location: Transducer bracket at V.B.V. - Bellcrank at 9 o/c position. Check rig plate alignment bar is centered in shaft cover "V" notch - synchronize indicator to read 5.0 ± 0.02 volts. Record full open_____ Lockwire.	[illegible]	[illegible]	6-22

Figure C-5. CF6-6D,-50 Instrumentation Checklist.

CF6-6D,-50
INSPECTION CHECKLIST

FORM NO. Q.C.-732
3/10/70
Page 2 Of 3
Revision 9

ITEM	AREAS INSPECTED	CLEAN	NORMAL	CONTAMINATED	INCOMING INSP/DATE	PREP TO TEST INSP/DATE	PREP TO SHIP INSP/DATE
2.	Starter magnetic plug						
	Starter valve filter					NA	
	Explain on squawk sheet, the condition of any filter that is contaminated. All filters are to be clean prior to re-installation. Report any abnormal contamination to Q.C. Engineering.						
3.	Inlet area for "FOD" & loose or missing hardware, overall condition.						
R 4.	Incoming check blocker doors; open ☐ closed ☐ (check one). If received with blocker doors open, close them.						
5.	Fan stator case & frame not including accessory gearbox area.						
6.	High pressure compressor stator & related plumbing - right hand side.						
7.	High pressure compressor stator & related plumbing - left hand side.						
8	Compressor rear frame - right half to forward side of fireseal.						
9.	Compressor rear frame - left half to forward side of fireseal.						
10.	Compressor rear frame - right half aft of fireseal.						
11.	Compressor rear frame - left half aft of fireseal.						
12.	Low pressure turbine module - right half.						
13.	Low pressure turbine module - left half.						
14.	Low pressure exhaust including turbine reverser or conical nozzle.						
15. R	Prep to ship; if received with blocker doors open, close them.						

Figure C-6. CF6-6D,-50 Inspection Checklist.

RCA. 5/12/78

REASSEMBLY

After all inspection checks are completed, rebuild the LPT module per the SM.

3. CORE ENGINE INSPECTIONS

Disassemble the engine as necessary to obtain the required data on the noted EMU's. Disassembly will be performed per the following sequence of events; visually inspect- EMU's to H.M.M.

NOTE 1: Photographs (detailed and overall) will be taken of each sub-assembly prior to its disassembly, with particular emphasis on deteriorated parts, or any unique condition. PHOTOGRAPHS NOT REQUIRED RCA 5/12/78

NOTE 2: Prior to removal of the Stage 1 HPTN assembly, obtain drop checks from the aft face of the CRF outer flange to the aft face of Stage 1 HPTN vane outer platforms in 8 equally spaced locations. At each location, obtain drops to both ends of each segment (16 individual readings). DCAS Insp.

NOTE 3: Record inspection requirements on sheets supplied by Evendale engineer.

B. Split core engine away from fan module and route core to S/N Remove HPT module.

C. Position-mark and remove Stage 2 HPTR blades. Remove [redacted] stage nozzle.

D. Remove second stage nozzle, preserve the stage 2 blade retainer seal wire for engineering inspection.

E. Comply with Note 2 above (drop checks). Then remove the Stage 1 HPTN assembly.

F. Position-mark, then remove the 4B pressure balance seal (mini-nozzle).

G. Remove the CRF.

H. Remove the HPCS cases.

I. Send the HPC rotor to the rotor area.

4. HIGH PRESSURE TURBINE ROTOR (REFERENCE 72-53-00)

A. Install the rotor in the Runout Fixture. Shim the blades per the SM, and measure each Stage 1 and 2 blade tip at 0.1 inch from the leading and trailing edges as follows:

1. Measure and record the radius of blade No. 1 0.1 inch from the LE of each stage. DCAS Insp.

PRODUCTION

Figure C-7. Example of Work Order.

ESN 451507

DATE ________

STAGE 1 HPTR BLADE RUNOUT DATA

RUN WITH [illegible] AT .100" [illegible] LE AND TE OF EACH BLADE

No	FWD	AFT	No	FWD	AFT	No	FWD	AFT	No	FWD	AFT
1	.003	000	28	-.003	+.005	55	-.001	000	82	+.003	+.007
2	+.002	+.003	29	-.003	+.001	56	-.002	+.001	83	+.001	+.005
3	-.003	+.001	30	000	+.005	57	000	+.003	84	000	+.006
4	+.001	+.006	31	-.004	+.003	58	-.001	+.006	85	-.001	+.005
5	-.002	-.001	32	000	+.008	59	-.001	+.002	86	+.001	+.007
6	+.003	+.005	33	-.004	-.001	60	-.002	+.004	87	+.001	+.007
7	-.002	-.001	34	000	+.004	61	-.002	+.007	88	-.001	+.006
8	+.002	+.005	35	-.002	+.001	62	000	+.003	89	-.002	+.008
9	-.003	-.001	36	000	+.005	63	000	+.003	90	-.003	+.006
10	-.001	+.005	37	-.006	-.003	64	+.001	+.005	91	+.001	[illegible]
[illegible]	-.004	-.002	38	-.002	+.004	65	000	+.001	92	+.002	[illegible]
[illegible]	000	+.005	39	-.004	000	66	-.001	+.005	93	+.003	+.003
[illegible]	-.002	-.003	40	-.002	+.006	67	000	-.001	94	000	+.002
14	+.001	+.004	41	-.004	+.002	68	-.001	+.004	95	000	+.006
15	-.002	000	42	-.001	+.007	69	000	-.001	96	-.002	+.007
16	+.001	+.004	43	[illegible]	-.002	70	+.002	+.004	97	-.001	+.006
17	-.004	-.002	44	-.001	+.005	71	-.001	000	98	-.006	+.007
18	+.002	+.003	45	-.006	+.002	72	+.002	+.005	99	-.001	+.006
19	-.004	-.001	46	[illegible]	+.004	73	000	+.001	100	-.004	-.006
20	+.002	+.007	47	[illegible]	+.003	74	+.003	+.006	101	000	+.010
21	-.002	[illegible]	48	[illegible]	-.005	75	+.001	-.001	102	-.003	+.009
22	+.001	+.002	49	-.003	+.002	76	+.003	+.005	103	-.003	+.006
23	-.002	-.001	50	+.002	+.006	77	000	000	104	-.004	[illegible]
24	+.002	+.004	51	-.002	000	78	+.002	+.007	105	-.005	+.006
25	-.002	+.001	52	+.002	+.006	79	+.002	+.001	106	-.005	-.006
26	000	+.005	53	+.001	+.001	80	+.002	+.006	107	-.006	000
27	-.004	+.001	54	000	+.005	81	+.001	+.001	108	-.009	+.003

READINGS ARE IN MILS [illegible]
RADIUS AT #1 = 16.560 AFT = 16.566

FWD. MAX = 16.563 MIN = 16.552 AVG = 16.559
AFT MAX = 16.576 MIN = 16.562 AVG = 16.570

Figure C-8. **HPTR Blade Inspection Sheet**